Activity Studies of Indoleamine 2,3-Dioxygenase 1 Enzyme

A thesis submitted to the
Indian Institute of Technology Guwahati
as partial fulfilment for the degree of
Doctor of Philosophy in Chemistry

Submitted

by

Ashalata Roy

Department of Chemistry
Indian Institute of Technology Guwahati
Guwahati 781039, Assam, India

Dedicated

To

My Parents and Family

Table of Contents

INDIAN INSTITUTE OF TECHNOLOGY GUWAHATI

Department of Chemistry

STATEMENT

I do hereby declare that the matter embodied in this thesis is the result of investigations carried out by me in the Department of Chemistry, Indian Institute of Technology Guwahati, India, under the supervision of associate professor Dr. Debasis Manna. This thesis has been submitted by me to the Department of Chemistry, Indian Institute of Technology Guwahati, for the award of the degree of Doctor of Philosophy.

In keeping with the general practice of reporting scientific observations, due acknowledgements have been made wherever the work described is based on the findings of other investigators.

Date **Ashalata Roy**

IIT Guwahati

INDIAN INSTITUTE OF TECHNOLOGY GUWAHATI

Department of Chemistry

CERTIFICATE

This is to certify that Ashalata Roy (Roll No. 146122027) has been working under my supervision since July, 2014 as a regular registered Ph. D. student. I am forwarding her thesis entitled **"Activity Studies of Indoleamine 2,3-dioxygenase 1 enzyme"** being submitted for the Ph. D. (Science) degree of this Institute. I certify that this work is an authentic record of the results obtained from the research work and she has fulfilled all the requirements according to the rules of this Institute regarding the investigations embodied in her thesis and this work has not been submitted elsewhere for a degree.

Date

IIT Guwahati

Dr. Debasis Manna
(Thesis Supervisor)
Department of Chemistry
IIT Guwahati

Acknowledgements

First, I would like to deeply thank my thesis supervisor Dr. Debasis Manna for his incisive guidance, precious suggestion, support and decisive insights throughout my Ph. D. journey. I am also thankful to him for giving me an opportunity for such a very interesting and leading edge project and I feel that my project has contributed to science and provided vital information for the study of some human diseases. His help to me in research was priceless. I have learned a lot of new ideas and gained knowledge from him. My sincere everlasting gratitude goes towards him.

I would like to acknowledge my sincere gratitude to all my doctoral committee members, Prof. Biplab Mondal, Dr. Bhubaneswar Mandal and Dr. Krishna Pada Bhabak for their insightful advices, valuable suggestions and support during my entire research work. My honest regards to all the faculty members of the Department of Chemistry for their motivation and encouragements. I am also grateful to Dr. Vishal Trivedi (Department of BSBE, IIT Guwahati) for his collaborative support in carrying out the in vivo cellular studies during my research work.

I wish to acknowledge my sincere gratitude to the IIT Guwahati for the financial support and facilities that were made available to me. I am also thankful to the Central Instrument Facility (CIF), IIT Guwahati for providing the instrument facility and to all the official staff members of the Department of Chemistry for their generous help and support.

I would like to thank my former group members Dr. Sukhamoy Gorai, Dr. Rituparna Borah, Mr. Saurav Paul and all my labmates namely Mr. Dipjyoti Talukdar, Mr. Subhankar Panda, Mr. Abhishek Saha, Mr. Nirmalya Pradhan, Mr. Nasim Akhtar, Ms. Oindrilla Biswas, Mr. Subhasis Dey, and Dr. Sreeparna Das with whom I have shared hours of lab time and without their great support and help my project would not have been completed. I extend my sincere thanks especially to Mr. Saurav Paul and Mr. Subhankar Panda for their collaborative effort in carrying out the synthesis work as well as to Mr. Nirmalya Pradhan for his contribution during my entire research work. I am also thankful to Dr. Suman Joyti Deka (Department of BSBE, IIT Guwahati) for his collaborative support in carrying out the in vivo cellular studies during my research work.

I also take this opportunity to thank all my Ph.D. batchmates (July, 2014), the other research scholars in the Department of Chemistry and all my friends, who have shared their thoughts and views with me. I am very much thankful to most of my batchmates for their supportive nature and frequent help in many aspects.

Most importantly, my Ph. D. endeavours would not have been completed without the endless love, unending support, tolerance and blessing from my family members. I wish to express my sincere gratitude to my parents and family for their trust and support throughout the period of my stay here. They are the main soul and inspiration for each and every step that I have achieved in my life.

And finally I express my humble gratitude and prayers to the Almighty God for guiding me through and blessing me with the necessary patience and strength to carry out my work and responsibilities so far.

Ashalata Roy

List of Abbreviations

5-HT	5-hydroxytryptamine
AcOH	Acetic acid
AIDS	Acquired immunodeficiency syndrome
ALA	5-Aminoleuvunilic acid
Amp	Ampicillin
AA	Ascorbic acid
CD	Circular dichroism
cDNA	Complementary deoxyribonucleic acid
CSF	Cerebral spinal fluid
D-1MT	D-1-methyltryptophan
DCM	Dichloromethane
DMF	Dimethyl formamide
DMSO	Dimethylsulfoxide
DNA	Deoxyribonucleic acid
DTT	Dithiothreitol
EDC.HCl	1-ethyl-3-(3-dimethylaminopropyl)carbodiimide hydrochloride
E. coli	Escherichia coli
EDTA	Ethylene diamine tetraacetic acid
ESI	Electrospray ionisation
Et_3N	Triethylamine
EtOAc	Ethyl acetate
EtOH	Ethanol
HeLa	Henrietta Lacks
HEPES	4-(2-hydroxyethyl)-1-piperazineethanesulfonic acid
hIDO1	Human Indoleamine 2,3-dioxygenase 1
HIV	Human immunodeficiency virus
HOBt	1-Hydroxybenzotriazole
HPLC	High performance liquid chromatography
HRMS	High resolution mass spectrometry
HTS	High throughput screening

HuIFN-γ	Human interferon gamma
IFN-γ	Interferon gamma
IR	Infrared
IPTG	Isopropyl-β-D-1-thiogalactopyranoside
Kan	Kanamycin
K_2CO_3	Potassium carbonate
Kyn	Kynurenine
L-1MT	L-1-methyltryptophan
L-Trp	L-tryptophan
m/z	Mass to charge ratio
MB	Methylene blue
$MgCl_2$	Magnesium chloride
MeOH	Methanol
mL	Milliliter
mM	Millimolar
mp	Melting point
MVD	MoleGro. virtual docking
Na_2CO_3	Sodium carbonate
Na_2SO_4	Sodium sulphate
NAD^+	Nicotineamide adenine dinucleotide
NADPH	Nicotinamide adenine dinucleotide phosphate
$NaHCO_3$	Sodium hydrogen carbonate
NaOH	Sodium hydroxide
NFK	*N*-formylkynurenine
NH_4Cl	Ammonium chloride
Ni-NTA	Nickel-nitrilotriacetic acid
nm	Nanometer
nM	Nanomolar
NMR	Nuclear magnetic resonance
ORF	Open reading frame
PBS	Phosphate buffer saline
PDB	Protein data bank
Pd-C	Palladium on activated charcoal

*p*DMAB	*para*-dimethylaminobenzaldehyde
PMSF	Polymethylsulfonylfluoride
PEG	Polyethylene Glycol
ppm	Parts per million
PIM	4-Phenolimidazole
PTSA	*p*-Toluenesulfonic acid
r.t.	Room temperature
RNA	Ribonucleic acid
SAR	Structure activity relationship
SDS	Sodium dodecyl sulphate
TCA	Trichloroacetic acid
TDO	Tryptophan 2,3-dioxygenase
THF	Tetrahydrofuran
TLC	Thin layer chromatography
TMS	Trimethylsilane
Tris	Tris(hydroxymethyl)aminomethane
UV	Ultra violet

Amino Acid	**3-letter symbol**	**1-Letter symbol**	**Amino Acid**	**3-letter symbol**	**1-Letter symbol**
Alanine	Ala	A	Leucine	Leu	L
Arginine	Arg	R	Lysine	Lys	K
Aspargine	Asn	N	Methionine	Met	M
Aspartic acid	Asp	D	Phenylalanine	Phe	F
Cysteine	Cys	C	Proline	Pro	P
Glutamic acid	Glu	E	Serine	Ser	S
Glutamine	Gln	Q	Threonine	Thr	T
Glycine	Gly	G	Tryptophan	Trp	W
Histidine	His	H	Tyrosine	Tyr	Y
Isoleucine	Ile	I	Valine	Val	V

Abbreviations for intensities of ^{1}H-NMR signals			
s	singlet	m	multiplet
d	doublet	brs	broad signal
dd	doublet of doublet	Hz	Hertz
t	Triplet	MHz	Mega-Hertz

Abbreviations for units/symbols			
A	Absorption	min	Minutes
ε	Absorption coefficient	mV	miliVolts
Å	Angström	M	Molar
bp	Base pairs	OD	Optical density
°C	Degree celcius	rpm	Revolutions per minute
g	Grams	s	Seconds
h	Hours	v/v	Volume to volume
kb	Kilobases	ʎ	Wavelength
kDa	Kilo Daltons	w/v	Weight per volume
l	Litres	µM	Micromolar

Compounds and inhibitor constant parameters

EC_{50}	The concentration of an compound which causes 50% of a maximal effect
IC_{50}	The concentration of an inhibitor which causes 50% inhibition of a maximal activity
K_i	Inhibitor dissociation constant
K_M	Michaelis-Menten constant
K_{cat}	Turnover number
V_{max}	Maximum rate
K_{cat}/K_M	Catalytic efficiency
L. E.	Ligand efficiency

Abstract

Immunosuppressive enzyme, indoleamine 2,3-dioxygenase 1 (IDO1) plays a pivotal role in regulating the metabolism of L-tryptophan (L-Trp) through kynurenine pathway, which is a well-established therapeutic target for the treatment of diseases associated with immunosuppression. Under pathophysiological conditions the expression of IDO1 enzyme from its mRNA gets highly up-regulated in response to inflammatory signals (like interferon-γ) within the immune system. Up-regulation of the IDO1 enzyme is directly related with several diseases including cancer, neurodegenerative disorders (Alzheimer's disease), Huntington's disease, schizophrenia, depression, age-related cataract, and HIV-1 encephalitis. Hence, proper understanding of the IDO1 activity will be helpful for the development of novel IDO1 inhibitors as emerging immuno-oncology agents.

On the basis of the experimental works performed during the research period, the content of the thesis entitled **"*Activity Studies of Indoleamine 2,3-Dioxygenase 1 Enzyme*"** have been divided into five chapters. **Chapter 1** of the thesis provides an overview of IDO1 enzyme and demonstrates the activity and regulation of this immunosuppressive enzyme in medicine, life science and other related research fields. These enzymes are responsible for the degradation of an essential amino acid L-Trp, which is required for the protein synthesis and other important metabolic functions. IDO1 mediated depletion of the local L-Trp concentration and accumulation of the kynurenine metabolites regulate the local immunosuppression. High levels of various L-Trp metabolites cause a variety of diseases, such as rheumatoid arthritis, tuberculosis, leukemia, Hodgkins disease, bladder cancer, and prostate disorders. On-going pre-clinical and clinical studies with different cancer models suggest that the IDO1 enzyme assists cancer progression and metastasis. The immunomodulatory role of IDO1 suggests that its inhibition might results in the rejuvenation of the normal immune responses and would enhance the efficacy of cancer treatment. Therefore, key challenges in advancing immunotherapies are the development of specific IDO1 inhibitors and exploration of their mechanism of action.

Chapter 2 describes the optimization of an efficient bacterial expression and purification system for the production of recombinant human IDO1 and TDO enzymes. Purified IDO1 enzyme will greatly assist in screening the synthesized inhibitors. Bacterial

expression conditions and purification system for the production of rhIDO1 and rhTDO enzymes were optimised in our laboratory by varying the incubation temperature, IPTG, ALA concentrations and buffer composition with high concentration of imidazole using Ni^{2+} affinity chromatography, respectively. The purity of the enzyme was assessed by Coomassie-blue stained SDS-PAGE analysis. The UV-visible spectra of IDO1 and TDO enzymes displayed the characteristic Soret and Q band in two different state of iron. The circular dichroism (CD) spectral data in the region of 190-260 nm showed that the secondary structure of rhIDO1 consists of 30.2% alpha helical, 7.9% beta sheet and 64.2% random coil. The thermal denaturation temperature of IDO1 enzyme was found to be 55 ºC. The enzyme activity studies were performed by spectroscopic and HPLC methods. The other enzyme kinetics parameters including K_M, k_{cat}, V_{max} and k_{cat}/K_M were also calculated from spectroscopic measurements. Overall findings suggest that the access of this enzyme assisted in the design of IDO1 inhibitors.

Chapter 3 demonstrates the rational design and synthesis of a series of nitrobenzofurazan derivatives of *N'*-hydroxyamidines and their inhibitory activity against purified IDO1 enzyme under *in vitro* and cellular environments. The optimization leads to the identification of few compounds as potent inhibitors of IDO1 enzyme with IC_{50} value of 39-98 nM. The *in vitro* cellular IDO1 enzyme inhibitory activity of these selected compounds also showed stronger potency (IC_{50} = 50-151 nM) with no/ negligible level of toxicity. The stronger IDO1 enzyme inhibitory properties of these compounds were supported by the molecular modelling studies. The UV-visible spectra showed the direct binding and competitive mode of inhibition of the potent compound with the IDO1 enzyme. The TDO enzyme activity of the potent hydroxyamidine analogues also showed 118 to 1593-fold stronger selectivity for IDO1 enzyme over TDO enzyme. Overall, the experimental results suggest that the compounds with hydroxyamidine and nitrobenzofurazan moieties are potential inhibitors of IDO1 enzyme and can be used as a tool for further development of IDO1-based inhibitors.

To identify a new structural class of IDO1 inhibitors, in the **Chapter 4** a series of pyridopyrimidine, pyrazolopyranopyrimidine derivatives were synthesized and their inhibitory activities were investigated under *in vitro* and cellular environments. Subsequent modification of the electronic properties of the fused heterocyclic ring and substitution of the phenyl ring directed to the identification of potent inhibitors with low micromolar (IC_{50} = 296-473 nM) inhibitory activities against purified IDO1 enzyme. These compounds also showed EC_{50} value in the nanomolar range with no/negligible

cytotoxicity. Spectroscopic studies suggest that the pyrazolopyranopyrimidine derivatives preferably interact with the deoxy-ferrous-IDO1 enzyme. Molecular model structure propose that the electronic properties of pyridopyrimidines and pyrazolopyranopyrimidines ring and halogen substituted phenyl ring assist these compounds to interact with the IDO1 through hydrogen bonding, pi-stacking and hydrophobic interactions. Counter screening against TDO enzyme show the stronger selectivity of the potent compounds (100-300 fold) for IDO1 over TDO enzyme. Overall, these observations suggest that further development of fused heterocyclic compounds could lead to a new class of potent inhibitors of IDO1 enzyme.

IDO1-based drug development has been hindered due to the use of idealized dilute buffer solution media during the screening and optimization of inhibitors, which do not reflect the highly crowded intracellular environment. **Chapter 5** describes the efficacy of external crowding agents in mimicking the cell-like environment for IDO1 activity assay. To mimic the intracellular environment under *in vitro* conditions, chemically inert, non-charged, hydrophilic synthetic polymers polyethylene glycol (PEG) and ficoll were selected as crowding agents. A non-linear relationship between the size and volume of the crowding agent with enzyme kinetics parameters was observed. The results suggest that judicious use of size and volume of the crowding agent could provide cellular mimetic environment. The inhibitory activity study under the optimized crowding conditions showed a similar IDO1 inhibitory potency of the selected potent compounds as in the presence of cellular environment. The circular dichroism (CD) analysis of the IDO1 enzyme showed almost no change in the secondary structure content of the protein. The temperature-dependent CD measurements revealed that the presence of crowding agent increases the thermal perturbation temperature of IDO1 enzyme, indicating the improved stability of the enzyme under the experimental conditions. Overall our findings suggest that IDO1 enzyme activity under *in vitro* crowding environments will be helpful in understanding its enzymatic activity under complex media such as biological fluids.

Our attempt to design small molecules inhibitors for IDO1 enzyme in order to achieve higher selectivity and specificity, led to the development of nitrobenzofurazan derivatives of *N*′-hydroxyamidines and pyridopyrimidine, pyrazolopyranopyrimidine derivatives which showed stronger inhibitory potency for IDO1 enzyme. The development of new IDO1 enzyme activity assay mimicking the intracellular environment was also helpful for designing and screening of the synthesized IDO1 inhibitors. Overall, our findings suggest that structural simplicity, low cytotoxicity,

inactivity for TDO enzyme, similar catalytic efficiency and secondary structural contents of the IDO1 enzyme under *in vitro* crowded conditions helps to understand the therapeutic applicability of the selected crowding agents as well as the inhibitors.

CHAPTER 1

Introduction

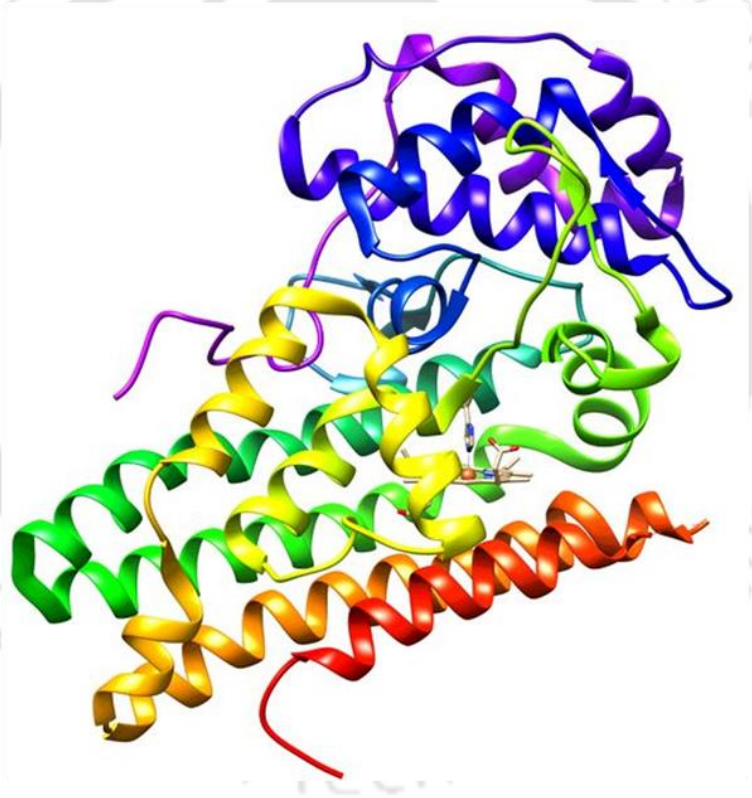

This chapter provides an overview to heme-containing enzyme namely, indoleamine 2,3-dioxygenase 1 (IDO1) and demonstrate the activity and regulation of these dioxygenase enzyme in medicine, life science and other related research fields.

1.1. Enzymes and life processes

Life is characterized by all biochemical activities such as development of new tissue, substitution of old tissue, transformation of food to energy, removal of waste materials, and reproduction. The majority of these biochemical reactions are regulated by catalysts, which are necessary for all life processes but it undergoes no permanent chemical changes. Enzymes act as a catalyst for regulating almost all of the biochemical reactions in living organisms. Primarily enzymes are proteins, formed by the amino acids chain through peptide bonds. They are important in diagnostic and research tools due to their specificity and selectivity. On the basis of their catalytic reactions, enzymes are classified as oxidoreductases, transferases, hydrolases, lyases, isomerases and ligases.

1.2. Biological role of dioxygen molecule

Oxygen is one of the most abundant elements in the universe and involves in the respiration of all living organisms. Initially, it is thought that the origin of oxygen in organic substances is water. It is also considered that in biological systems, dioxygen act only as an electron acceptor in oxidase or dehydrogenase mediated reactions. But, it is independently established that incorporation of either one or both ^{18}O into organic compounds directly come from $^{18}O_2$.[1] Hence, dioxygen (O_2) serves as a terminal electron acceptor (e.g. in the respiratory chain, in the transfer of electrons from cytochrome c to molecular oxygen, catalysed by cytochrome oxidase) as well as a biosynthetic reagent, both the functions are essential in aerobic life. In the latter role, either one or both oxygen atoms of dioxygen get incorporated into the organic substrates by cleaving the oxygen-oxygen bond which is an energetically very favourable process.

The enzyme, involved in the incorporation of oxygen atoms from dioxygen is designated as oxygenase enzyme. These oxygenase enzymes are widely distributed in nature throughout the microorganism, plant and animal kingdoms. Now-a-days, functions of some bewildering variety of oxygenase are recognized which form essential metabolites including, active derivatives of vitamin D, amino acids, sterols and prostaglandins. The oxygenase enzymes are divided into two classes, monooxygenase and dioxygenase, depending on the incorporation of oxygen atom into the substrate.[2] Monooxygenase enzymes involve in the incorporation of one oxygen atom into organic substance and are subdivided into external and internal monooxygenase. Dioxygenase enzymes are also subdivided into two separate classes based on the incorporation of two

oxygen atoms into two separate substrates (intermolecular) or into a single substrate (intramolecular).

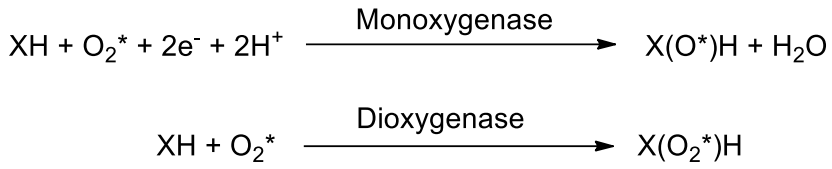

1.3. Biological role of metal ions

Most of the organic compounds are stable in their singlet ground state in comparison to that of dioxygen which has a triplet ground state. Formation of product with singlet state through the transition from triplet to singlet state is spin-forbidden and can be spin-allowed via the formation of a high energy unstable triplet intermediate and a slow spin inversion rates.[3] Formation of such high kinetic barrier, characteristic to the reactions of triplet O_2 is overcome by the assistance of transition metals including, iron or copper. Most of the dioxygenase enzymes require transition metal ion as cofactor for carrying out such biological oxidations. Transition metal ions in its appropriate oxidation states show ability to react directly with triplet O_2 to form dioxygen adducts. The participation of dioxygen adducts within reaction pathways either incorporate the oxygen atoms into substrates or oxidize the substrates.

Nature has preferred transition metal ions to transport, activate, and reduce O_2 for the following reasons. First, availability of unpaired electrons allows most of the transition metals to react with triplet O_2. Second, the comparatively heavy atomic weight of transition metals allow them to alter the spin-state of an electron by increasing their spin-orbit coupling (SOC) efficiency, and offer a quantum mechanical pathway to alter the electron's spin-state. However, the SOC for the first-row transition metals are too small to allow spin transitions. Third, the excited states of transition metals with unpaired electrons whose energies are in close proximity to the ground-state, can be used to increase the spin inversion probability.[3] Transition metals with 3d-unpaired electrons also use three pathways for the activation of dioxygen. First of all, when dioxygen is complexed with a transition metal ion, the unpaired electrons in the dioxygen π^* orbitals have the ability to overlap with the unpaired 3d-orbital electrons of the metal ion.[4] Then such transition metal-dioxygen complex is allowed to react with a singlet organic compound providing the overall fixed number of unpaired-electrons in the complex.

Next, the transition metals present in metallo-enzymes contain two consecutive oxidation states (e.g. Fe^{2+}/Fe^{3+}, Cu^{+}/Cu^{2+}) and shows the ability to allow single electron transfer process to the bound dioxygen. The acceptance of a single electron by the triplet oxygen ground state to form superoxide is the other probable way for oxygen activation. Participation of superoxide in a range of 1- or 2-electron transfer-based chemical reactions causes activation of dioxygen.[5] Finally, the probable mechanism for α non-heme dioxygenase enzyme could be the reaction of dioxygen through a radical pathway. In this pathway, a stable radical is formed due to the attack of a bound intermediate, a substrate radical to dioxygen.[6]

1.4. Biological role of heme-containing proteins

Heme-containing proteins are one of the most important metallo-proteins present in prokaryotes and eukaryotes. They are involved in several biologically important function such as electron transfer (e.g. cytochrome-c), catalysis (e.g. catalase), oxygen transport and storage (e.g. hemoglobin and myoglobin) and signal transduction (e.g. nitric oxide synthase). Inspite of their different functions, they contain same chromophore, a porphyrin moiety with an iron atom at the centre. The iron protoporphyrin-IX system is also known as heme-b and it has a square planar structure with iron (Fe^{3+}) at the centre containing six coordination sites (Figure 1.1). Among those six coordination sites of iron, four coordination positions are occupied by the four nitrogen atoms of porphyrin, the fifth and sixth coordination sites remain free so that a ligand such as oxygen (O_2), nitric oxide (NO) and carbon monoxide (CO) can interact with the active site of the given protein. This fifth and sixth axial bond is also called the proximal and distal coordination sites. In most cases the proximal site is filled by the histidine residue. The imidazole nitrogen of histidine, sulfur of methionine and cysteine, phenoxide group of tyrosine and carboxylate group of glutamic acid and aspartic acid are commonly involved in the coordination with the heme-group. In general, heme-containing proteins contain the iron atom in two oxidation states, the ferric (Fe^{3+}) and the ferrous (Fe^{2+}) state. Sometimes iron can be in ferryl (Fe^{4+}) state transiently, to maintain the enzyme's catalytic circle (e.g. cytochrome P450 and indoleamine 2,3-dioxygenase).[2, 7]

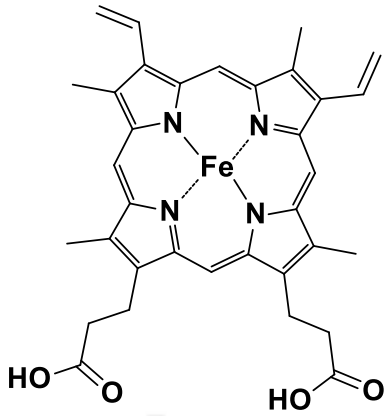

Figure 1.1. Iron protoporphyrin-IX (heme-b).

1.5. Significance of L-tryptophan (L-Trp) metabolism

About 2000 enzymes having specific functions are known and around 20 amino acids have been identified. Among those amino acids, 12 amino acids can be synthesized by human body but the others must be acquired through diet. These amino acids are called the essential amino acids. L-tryptophan (L-Trp) is one of the essential amino acid for human beings. The presence of an indole functional group confers its unique properties such as high hydrophobicity and aromaticity. Apart from biosynthesis of protein, majority of dietary intake of L-Trp is metabolised by serotonin and kynurenine pathways (Figure 1.2). In healthy human body the L-Trp level is properly balanced between protein synthesis and two different enzymatic cascade pathways.[8] Metabolism of L-Trp through this enzymatic cascade pathway plays a vital role in physiology. Nervous system related diseases including Alzheimer's disease, Huntington's disease and schizophrenia, and infectious diseases including, microbial and human immunodeficiency viral (HIV) infections are caused by the dysregulation of L-Trp metabolism.[8] Also the high levels of various L-Trp metabolites causes a variety of diseases, such as rheumatoid arthritis, tuberculosis, leukemia, Hodgkins disease, bladder cancer, and prostate disorders.[9] Deficiency of L-Trp in the diet causes vitamin-deficiency disease called pellagra.

1.5.1. The serotonin pathway

In this pathway, L-Trp is first hydrolysed to 5-hydroxytrytophan (5-HTP) by tryptophan hydroxylase. 5-HTP is then metabolised to serotonin or 5-hydroxytryptamine (5-HT) by aromatic amino acid decarboxylase enzyme. The neurotransmitter, serotonin is involved in regulating mood and sleep and it promotes feelings of calm and relaxation. Deficiency of serotonin level causes belligerence and impulsivity in children and adults.[10] Serotonin

is finally metabolised to melatonin through 5-hydroxyindole acetaldehyde (5-HIA) and 5-hydroxyindoleacetic acid (5-HIAA) intermediates. Neurohormone, melatonin has strong antioxidant properties and plays a crucial role in defending mitochondrial and nuclear DNA. Melatonin regulates the circadian rhythms of several biological activities (Figure 1.3).[11]

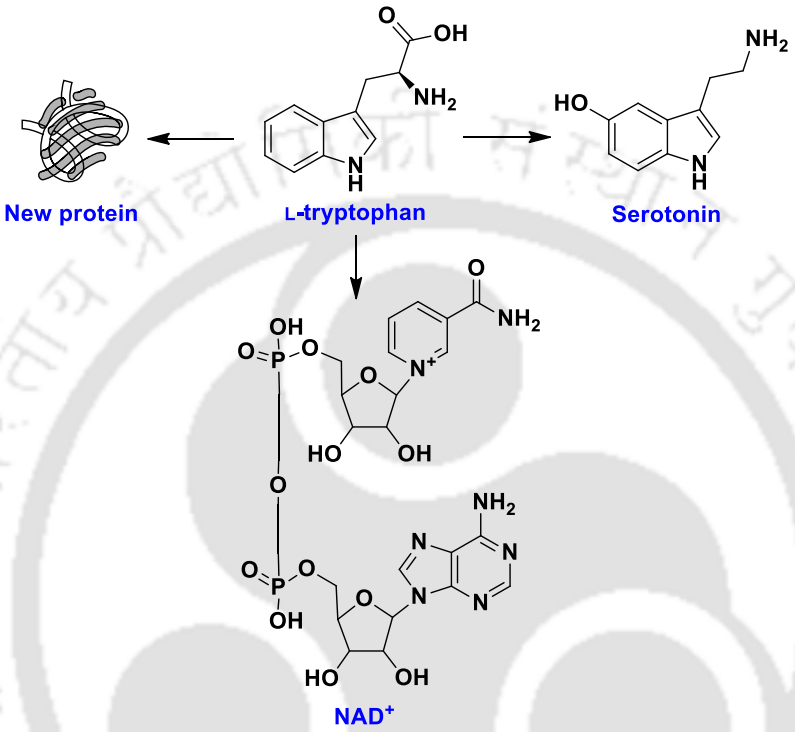

Figure 1.2. L-Trp metabolism leads to three possible products nicotinamide adenine dinucleotide (NAD^+), serotonin or the biosynthesis of a new protein.

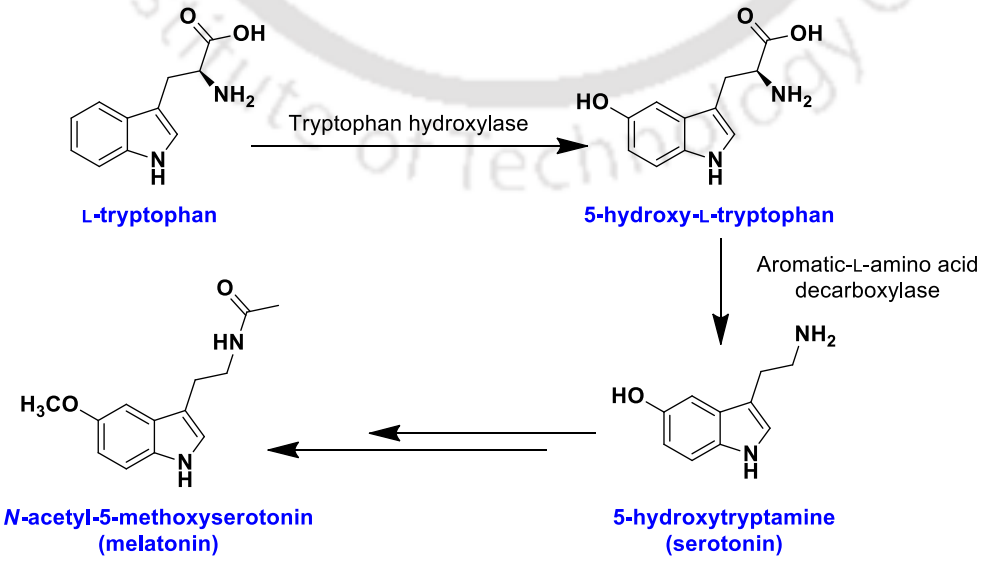

Figure 1.3. Serotonin pathway of L-Trp metabolism.

1.5.2. The kynurenine pathway

The majority (~ 95%) of dietary L-Trp is catabolised in the kynurenine pathway. In this pathway, a number of bioactive metabolites and a co-enzyme nicotinamide adenine dinucleotide (NAD^+) are produced.[12] Some of the kynurenine pathway metabolites are neurotoxic e.g. 3-hydroxyanthranilic acid (3-HAA), 3-hydroxykynurenine (3-HK) and quinolinic acid (QA) and some metabolites are neuroprotective e.g. kynurenic acid (KA) and picolinic acid (PA).[13] The excitotoxic QA selectively triggers *N*-methyl-D-aspartate (NDMA) receptors, produces powerful, reactive oxygen species (ROS) by complexion with iron.[14] Similarly, harmful free radicals are produced by 3-HK and 3-HAA.[15] On the other hand, KA acts as a scavenger for free radicals including superoxide anion, hydrogen peroxide or peroxynitrite, produced by other kynurenine pathway metabolites and nitric oxide synthases.[16] KA also acts as an NMDA receptors antagonist.[17] Reduction of L-Trp level and accumulation of kynurenine pathway metabolites are found to be immune-suppressive and plays an important role in pregnancy and tumoural immune escape.[18] Decrease in L-Trp level also showed important resistance mechanism against certain microbes and intracellular parasites auxotrophic for L-Trp.[19] The kynurenine pathway metabolites also showed an important role in brain function. QA caused convulsion and excitotoxicity, 3-HAA and 3-HK caused neuronal damage (necrosis and apoptosis) in cell cultures. Whereas KA reduced excitotoxin-induced neuronal death by antagonising ionotropic glutamate receptors.[12] Elevated levels of kynurenine concentration and up regulation of IDO1 activity were associated with Crohn's disease, multiple sclerosis, rheumatoid arthritis or AIDS.[20] Apart from this, kynurenine pathway metabolites kynurenine and 3-HK contributes to the development of cataract formation by covalently modifying human lens proteins.[21] Niacin produced through kynurenine pathway is a precursor to NAD and plays a crucial role with cells by repairing DNA and producing steroid hormones. A deficiency disease called pellagra is happened due to the deficiency of niacin in the body (Figure 1.4).[22]

1.6. The controller of the kynurenine pathway (TDO, IDO1 and IDO2 enzymes)

L-Trp metabolism through the oxidation of L-Trp to *N*-formylkynurenine and then rapid conversion of *N*-formylkynurenine to kynurenine is known as kynurenine pathway (Figure 1.4). The first and rate-limiting step of this kynurenine pathway is catalysed by three heme-containing enzymes indoleamine 2,3-dioxygenase 1 (IDO1), indoleamine 2,3-dioxygenase 2 (IDO2) and tryptophan 2,3-dioxygenase (TDO).[23] All these three enzymes

catalyse the same biochemical reaction even though they have distinct physicochemical properties, structures, and biological roles. Native human IDO1 is a monomeric protein of 403 amino acids residues with a molecular weight of 45 kDa and a pI of 7.1.[24] But TDO is a tetrameric protein of 406 amino acid residues with molecular weight of 167 kDa.[25]

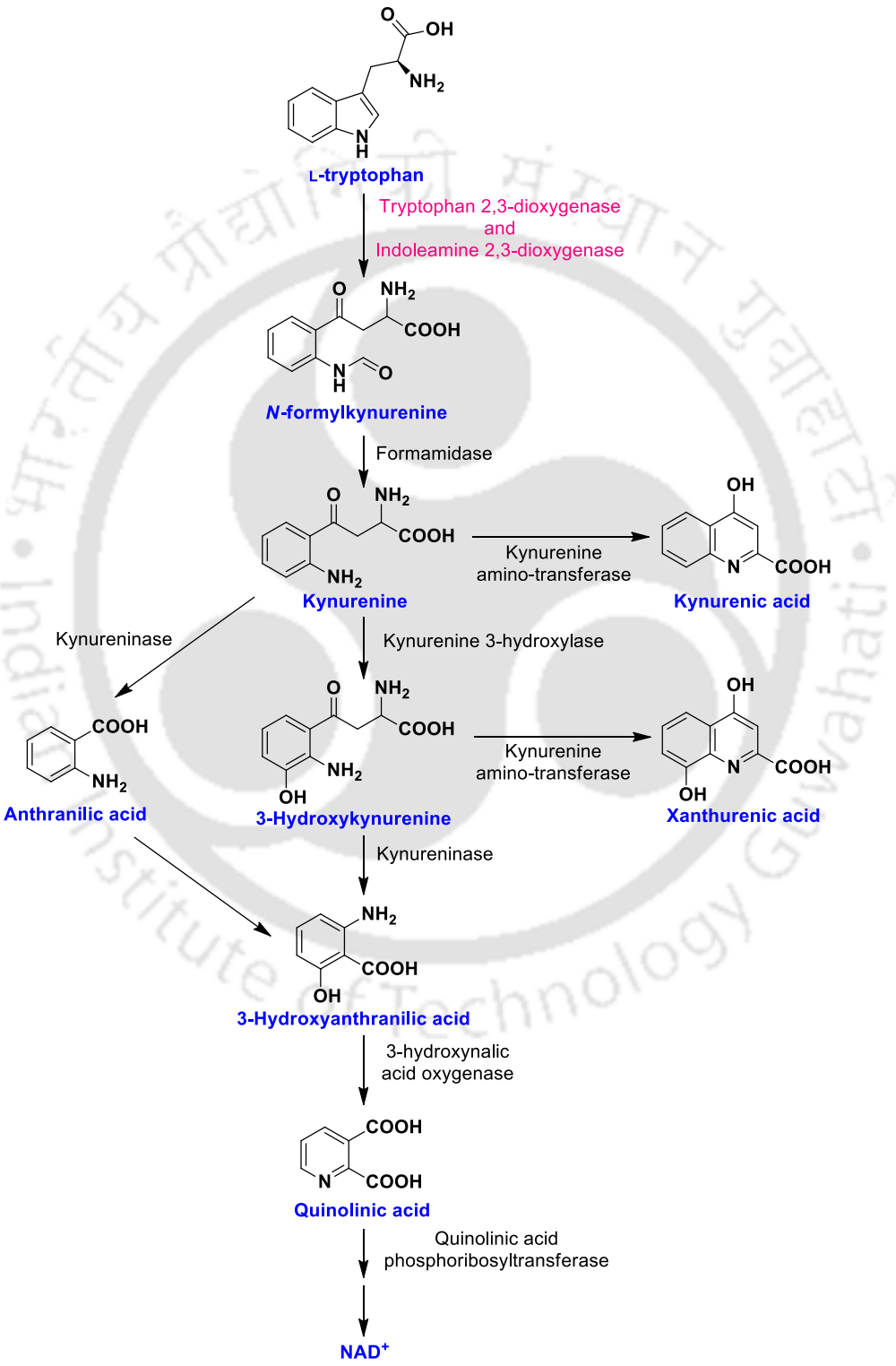

Figure 1.4. Kynurenine pathway of L-Trp metabolism.[23a]

The contribution of the monomers of TDO and IDO1 to the amino acid sequence identity is only 10% excluding its alike active site topology. It is an indication to their binding with similar substrates and catalytic mechanism. The TDO enzyme is primarily located in the liver, whereas IDO1 is dispersed in nonhepatic organs of mammals.[26] Moreover, the expression of IDO1 and TDO is controlled by several inflammatory cytokines like IFN-γ and glucocorticoids, respectively. Furthermore, TDO activity is specific to L-Trp substrate, whereas IDO1 has broad substrates specificity i.e. it has ability to metabolize indole derivatives such as L- and D-tryptophan, tryptamine, melatonin and serotonin.[27] Human IDO2 is a full length protein with 420 amino acids residues and shares 72% identity with mouse IDO2, 45% identity with mouse IDO1 and 44% identity with human IDO1.[28] IDO2 is mostly expressed in mammalian liver, kidney, epididymis and brain. In comparison with IDO1, IDO2 shows very weak or imperceptible catalytic activity for L-Trp metabolism in both *in vitro* and *in vivo*.[29]

1.7. Crystal structure of IDO1 enzyme

Recently three co-crystal structures of IDO1 enzyme complexes with different ligands have been reported. The crystal structures of human IDO1 enzyme suggests that the human IDO1 contains a large (*C*-terminal) domain which comprises the catalytic site and a small (*N*-terminal) domain (Figure 1.5A).[30] The large domain of hIDO1 is composed of 13 α-helices and two 3_{10} helices whereas the small domain consists of six α-helices, three 3_{10} helices and two β-sheets. One of the 15 α-helices of large domain contains histidine 346 (H346) residues that act as the endogenous proximal ligand. The small domains are connected by a flexible loop of 17 residues. These residues also play an important role within the catalytic site of the enzyme. The catalytic site of IDO1 contains porphyrin group heme-b. The heme-prosthetic group is placed in a plane parallel to the loop in between the two domains. It is associated with the large domain by H346 residue at the fifth coordination position. The crystal structure reveals that the requisite active site residues for binding with the L-Trp are R231, F226, F163, S167, H364 (Figure 1.5B). The presence of active sites residue S167 is found on the distal site and close to the heme-group. This active site residue S167 plays a crucial role in the reaction mechanism by H-bonding to the indole nitrogen of the L-Trp.[31] The crystal structures also display that there are specific interactions between the carboxyl group of L-Trp and the active site residues. The interactions are ion-pair interaction with R231. The NH_2 group of L-Trp form H-bonds with the 7-propionate group of the heme. The N-atom of the indole ring form H-

bond with S167. Also, there are van der Waals interactions between the indole-ring and hydrophobic residues.

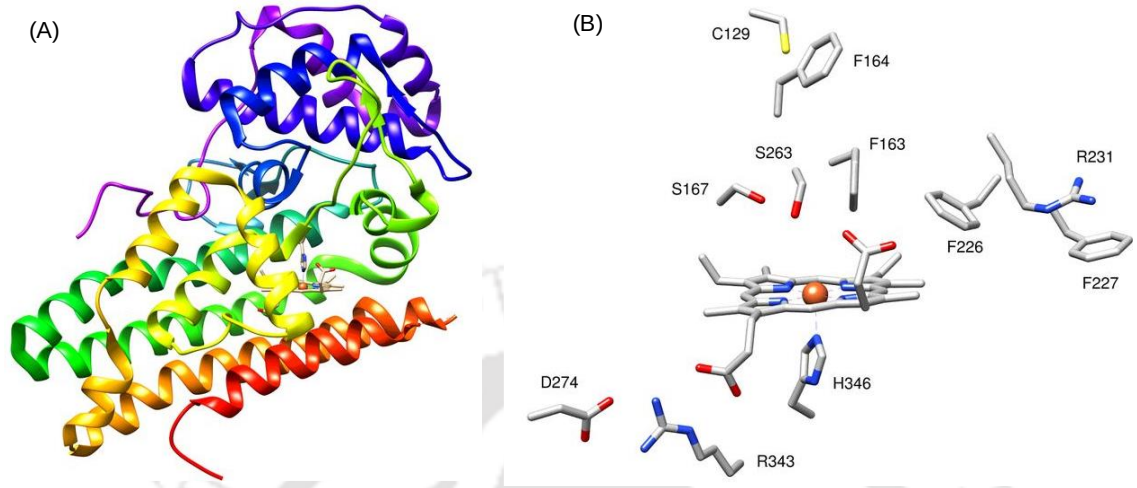

Figure 1.5. Crystal structure of IDO1 (A) and active site residues of IDO1 (B).[30-31]

1.8. Catalytic properties of IDO1 enzyme

The UV-visible spectrum of IDO1 have a Soret band centred at 405 nm along with bands at 530 nm and 565 nm which are a prominent characteristic peaks of a high-spin ferric (Fe^{3+}) heme-protein. The inactive hIDO1 enzyme is found to be in the ferric state (Fe^{3+}). However, IDO1 mediated L-Trp metabolism through the kynurenine pathway requires the heme iron of IDO1 to be in the ferrous state (Fe^{2+}) i.e. the active state. For the reductive activation of IDO1, the reduction equivalent is required. Methylene blue/ascorbic acid (MB/AA) system as well as the superoxide anion provides reduction equivalent for *in vitro* enzyme assays. Whereas cytochrome b_5 and either NADH/cytochrome b_5 reductase or NADPH/cytochrome P450 reductase systems acts as an efficient IDO1 activators *in vivo*.[32]

The active catalytic site of IDO1 is reduced ferrous (Fe^{2+}) form. It has been proposed that the catalytically-active IDO1 ternary complex (Trp-Fe^{2+}-O_2) is formed by binding with L-Trp and dioxygen. IDO1 can form two different stable binary complexes by binding with either L-Trp or dioxygen. The ternary complex is then formed by subsequent binding of dioxygen or L-Trp. After that the ternary complex gets decomposed to yield the ferrous enzyme and product. After completion of each catalytic cycle, IDO1 shows tendency to auto-oxidise. Therefore re-reduction of IDO1 for activity is a prerequisite and to be continued (Figure 1.6).[33]

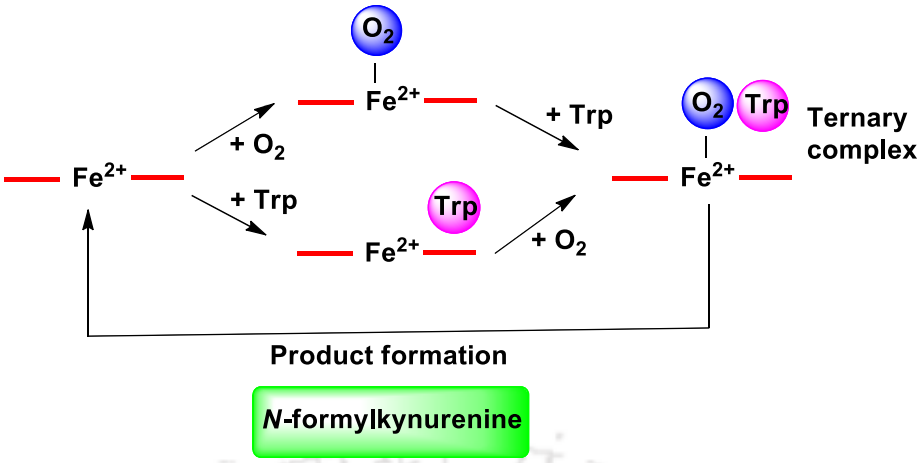

Figure 1.6. Ternary complex formation.[33]

1.9. Proposed catalytic mechanism of IDO1 enzyme

Based on the crystal structures of IDO1 enzyme it was initially proposed that the catalytic mechanism for the oxidative cleavage of C_2-C_3 double bond of the indole ring follows an ionic mechanism. The proposed ionic mechanism precedes through first a base-catalysed deprotonation of N-H proton of the indole ring. The active site residue like histidine or a water molecule can act as a base or a nucleophile. Then, the electron-rich indole-C_3 triggers the nucleophilic attack on the distal oxygen of the dioxygen containing heme-group leading to the formation of 3-indolenylperoxy-Fe^{2+} intermediate. The conversion of this intermediate to *N*-formylkynurenine occurs in one of two ways Criegee-rearrangement and Dioxetane-rearrangement (Figure 1.7). Although both of this rearrangement is feasible there is a doubt about their happening *in vivo* due to highly distorted transition state and high energy barrier. The unfeasibility of this mechanism is supported by density functional theory (DFT) calculations. In addition, from the crystal structure of IDO1, it has been shown that amino acid residues S167 are in an appropriate position of IDO1. These amino acid residues play the role as a base. But, single point mutation of S167 in IDO1 shows their unnecessity for catalytic activity. Hence, active site base-catalysed ionic mechanism is doubtful.[34]

Based on the DFT calculations, a newly proposed mechanism for the activation of dioxygen in these heme systems describes a direct electrophilic addition of the Fe^{2+}-bound oxygen to the C_2 /C_3 position of the indole ring in the singlet state. This mechanism also proposed a direct radical reaction of the Fe^{3+}-superoxide species to the C_2 position of the indole in the triplet state. The direct electrophilic addition of dioxygen to the indole ring can be initiated by the lone pair electrons of nitrogen. This reaction is

found to be thermodynamically favourable due to the lower activation energy than the base-catalyzed deprotonating mechanism.

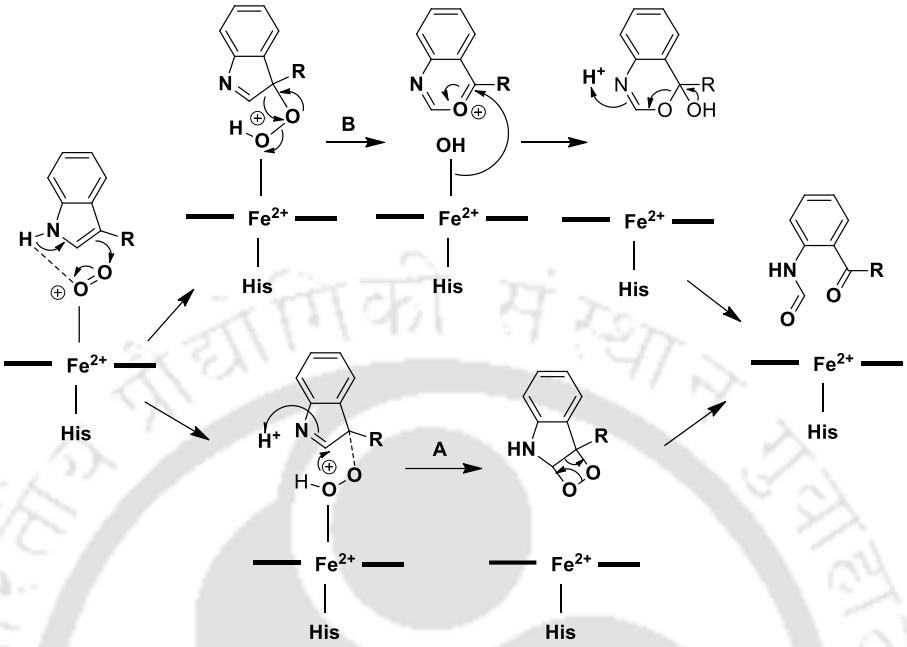

Figure 1.7. Conversion of 3-indolenylperoxy-Fe^{2+} intermediate to *N*-formylkynurenine via two ways Dioxetane rearrangement (A) and Criegee rearrangement (B).

In the radical mechanism, the 3-indolenylperoxy-Fe^{2+} complex intermediate are also formed. A radical-recombination or closely barrier less charge-recombination step from the subsequent diradical or zwitterionic intermediates, respectively, continues to provide the metastable dioxetane intermediates. Otherwise, homolytic cleavage of O-O bond from the diradical intermediate and subsequent oxo-attack and C_2-C_3 bond cleavage could contest with the dioxetane generation pathway. Both of electrophilic and radical addition mechanisms are the most possible to happen, but none is well established (Figure 1.8).[35]

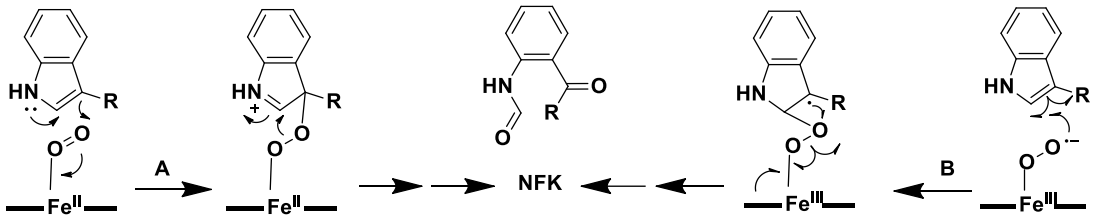

Figure 1.8. The proposed reaction mechanism for heme dioxygenases. Electrophilic addition (A) and radical addition (B).

The most recently proposed mechanism describe that the insertion of dioxygen into L-Trp occurs stepwise instead of incorporation of both oxygen atoms concurrently. Both electrophilic and radical mechanisms are consistent with this proposed mechanism. In this mechanism, a ferryl heme species with an epoxide intermediate species is formed by either electrophilic or radical routes. The ring-opening of the epoxide intermediate is occurred by the inserting the second oxygen atom into the indole ring. The ring cleavage then produces *N*-formylkynurenine (Figure 1.9).[36] Formations of epoxide intermediate species and ferryl heme species is supported by the recent theoretical studies and resonance Raman method respectively. Ring opening of the proposed epoxide intermediate is supported by various computational studies. Hence, the formation of *N*-formylkynurenine via epoxide intermediate step is favourable.

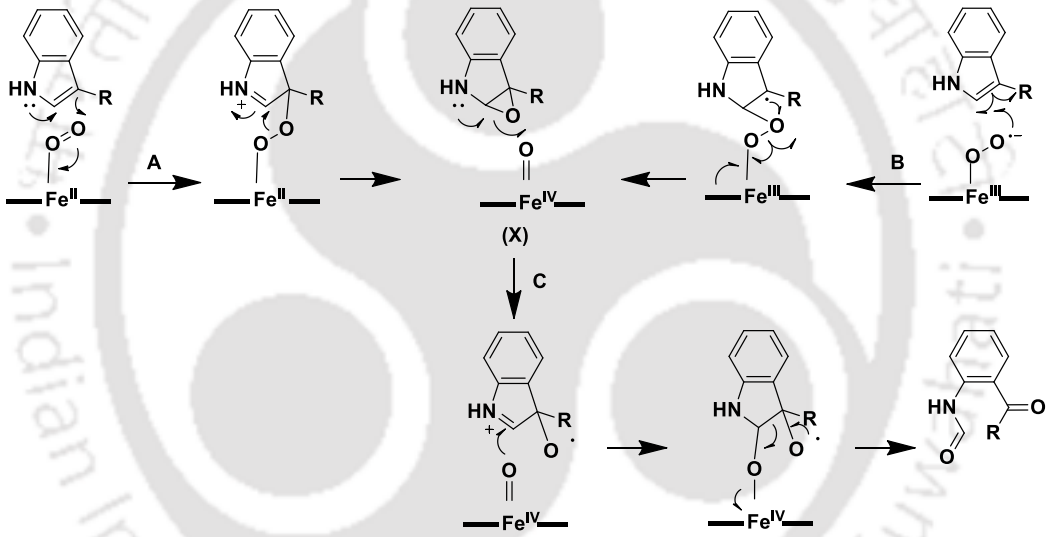

Figure 1.9. Electrophilic addition (A) and radical addition (B). Epoxide species (X) and most recently proposed catalytic mechanism for *N*-formylkynurenine formation (C).

1.10. The immunomodulatory role of IDO1

In antigen presenting cells (APCs), stromal cells, tumour cells or tumor infiltrating lymphocytes, the local concentration of L-Trp can be effectively depleted by the active IDO1. The IDO1 mediated kynurenine pathway of L-Trp depletion leads to the suppression of T cell proliferation following two proposed mechanism (i) the mTOR kinase pathway or (ii) the GCN2 stress kinase pathway. Mammalian target of rapamycin (mTOR) is a kinase and inhibited by rapamycin. During the L-Trp starvation, mTOR kinase is inhibited which arrests cell cycle progression of activated T cells. As a result, T

cell proliferation is repressed and the number of effector T cells is reduced.[37] The effector T cell is important for proliferation and survival of several natural mammalian tumours and promotes angiogenesis in a numeral cancer cell lines.[37] Recently published an inflammatory carcinogenesis mouse model studies shows that IDO1-mediated L-Trp depletion acts as a inhibitor of mTOR kinase.[38] Another pathway through which L-Trp starvation suppresses T cells proliferation is the integrated stress response kinase General control non-derepressible 2 (GCN2) pathway. During the L-Trp starvation, uncharged tRNAs activate the GCN2 kinase which then phosphorylates serine-51 in the α-subunit of eukaryotic translation initiation factor 2 (eIF2α). Consequently most mRNA translation in the cell is inhibited and total protein biosynthesis is shutdown. The mouse models study confirms the important role of GCN2 for tumour proliferation.[39]

On the other hand, IDO1-mediated kynurenine pathway of L-Trp metabolites has been identified as an activator of aryl hydrocarbon receptor (AhR). AhR is a ligand-activated transcription factor and play a number of functions along with the differentiation between the two opposing populations of T cells, Tregs and Th17 cells. Tregs are immunosuppressive and Th17 cells cause's autoimmunity.[40] The differentiation of Tregs triggered by kynurenine-activated AhR suggests an immunosuppressive mechanism of IDO1. Hence, kynurenine-mediated AhR can directly induce apoptosis in lymphocytes and appears to suppress the activated T cells. Thus, IDO1 play a crucial role in diseases related to immune responses including, T cell suppression, maternal tolerance to allogenic foetus, production of quinolinic acid as a neurotoxin and cancers.[41] For this reason IDO1 is a target for drug discovery against cancer.

1.11. Regulation of IDO1 expression and activity

It is well documented that the excessive catabolism of L-Trp is toxic to cells; hence a tight regulation of IDO1 expression and activity is required. The mRNA of IDO1 is absent in most tissues, which is considered as a natural controller of IDO1 over-expression and also represent a major mechanism for the regulation of IDO1.[41] Therefore, IDO1 gene knockdown could be considered as an alternative approach to regulate the IDO1 expression and activity. However, the other heme-dependent proteins will be affected by the regulation of the biosynthesis of heme-b and reductive cofactors such as cytochrome-b_5 or NADH, necessary for IDO1 activity. Hence, it is not emerged as a specific IDO1 regulatory mechanism. The IDO1 activity is also regulated by nitric oxide significantly. The enzyme activity is inhibited by the binding of nitric oxide to the IDO1 active site and

its proteasomal degradation is also accelerated. In addition, nitric oxide forms peroxynitrite by reacting with superoxide anions, consequently it inactivates IDO1 by nitrating with the three tyrosine residues (Y15, Y315 and Y353).[42] Similarly, oxidation of surface exposed cysteine residues of IDO1 is irreversibly inactivated by hydrogen peroxide.[43] These findings suggest that the regulation of IDO1 activity is also involved in the oxidative stress in the cell. The oxidative stress in human macrophages is augmented by the catalytic activity of IDO1, which correlates well with this idea. The expression of IDO1 mRNA is also reduced due to the presence of antioxidants such as 2-mercaptoethanol.[44] The up regulation of IDO1 expression may be due to the oxidative stress that can be harmful to IDO1. The oxidative stress for the regulation of IDO1 activity through the signalling pathways is so far not well recognized.

1.12. Therapeutic objectivity and validity of IDO1 in cancer therapy

The expression of IDO1 in a broad range of human tumours is correlated with a poor prognosis. There are compelling evidences that IDO1 plays a major role in suppressing the immune system during cancer progression.[45] IDO1 is associated with higher rates of metastasis and poor prognosis. In pregnant model mice the inhibition of IDO1 by L-1MT showed reverse immune-suppressive activity suggests that the reverse tumour-mediated immune suppression could be by the inhibition of IDO1. The growth of IDO1-transfected mastocytoma cells (P815B) in mice is significantly suppressed by the IDO1 inhibitor L-1MT.[46] Other mouse models of cancer, melanoma and orthotopic glioblastoma also produce the similar results.[47] Hence the inhibition of IDO1 might be a promising target for cancer treatment. Thus the search for IDO1 inhibitors has become a very active area of research.

1.13. IDO1 inhibitors

The discovery of IDO1 inhibitors is challengeable due to various reasons. First of all, due to the relatively small size of IDO1, the binding of large inhibitor molecules is hindered. Secondly, the competitive or non-competitive mode of inhibition kinetics of some reported IDO1 inhibitors are not completely understood.[48] The third and main challenge in developing a promising IDO1 inhibitor is the bioavailability, low toxicity profile and no/minimal side effects of compound.[49] Therefore, a better understanding of IDO1 inhibition kinetics and use of small-molecule as IDO1 inhibitors are required to design better drug. Small-molecules are used as IDO1 inhibitors for the therapeutic inhibition

over monoclonal antibodies which have targeted on "immune checkpoints" following several reasons. First, cost of production and formulation of small molecules is significantly lower as compared with monoclonal antibodies or cell-based therapies. Next, the quantification of the kyn/trp ratio in blood serum of animals or human patients in the laboratory can easily determine the pharmacodynamics of IDO1 inhibitors. Studies with model mice having genetically deficient IDO1 enzyme shows healthy behaviour and no natural autoimmunity, indicates that pharmacological inhibition of IDO1 is reasonably protected. IDO1 activity in most of the healthy tissues is very low, but it's abundance in a broad range of tumours highlights that IDO1 is an ideal target for a therapeutic blockade.[50]

Already three major companies have started to develop the IDO1 inhibitors. Newlink Genetics has produced a number of phenyl-imidazole-derived compounds as IDO1 inhibitors with activities in the nanomolar range. The Ludwig Institute for Cancer Research (LICR) works mainly on PIM analogues such as phenyl-trizoles and a series of amino-hydroxyquinolines, and Incyte Corporation has discovered a series of hydroxyamidines as an active IDO1 inhibitors with activity in the nanomolar range.[51] Recently, two compounds hydroxyamidine INCB024360 (epacadostat) and imidazole NLG919, combined with pembrolizumab and ipilimumab antibodies are under phase I/II clinical trials for the treatment of cancer and other diseases. Even though D-1MT is under clinical trials as kynurenine pathway inhibitor, but its mechanism of action is doubtful (Figure 1.10).[52]

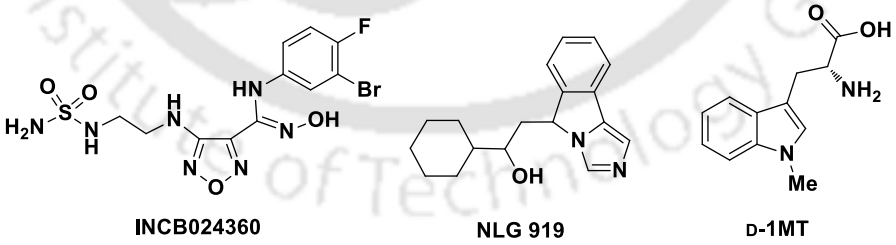

Figure 1.10. Structure of INCB024360, NLG919, and D-1MT.

The first known IDO1 inhibitors with inhibitory activity in the range of micro molar are β-carbolines and tryptophan derivatives. β-carbolines and its derivatives are one among the first natural inhibitors to be investigated and are widely found in plants and animals. One such derivative is 'Norharmane' that inhibits competitively by binding with the heme-iron of the IDO1 (Figure 1.11).

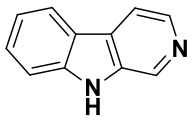

Norharmane

Figure 1.11. Structure of Norharmane.

Several indole-based IDO1 inhibitors have been developed. Among those compounds, the indole derivative 5-(1*H*-indol-3-yl)-3-methyl-2-thioxoimidazolidin-4-one, known as necrostatin 1 showed IDO1 inhibitory potency with K_i value, 12 µM and cellular IC_{50} value, 0.5 µM.[52-53] The other indole derivatives IDO1 inhibitors are dithiocarbamates, 1-methyltryptophantirapazamine, keto indoles, tryptoline derivatives and tryptamine derivatives (Figure 1.12).

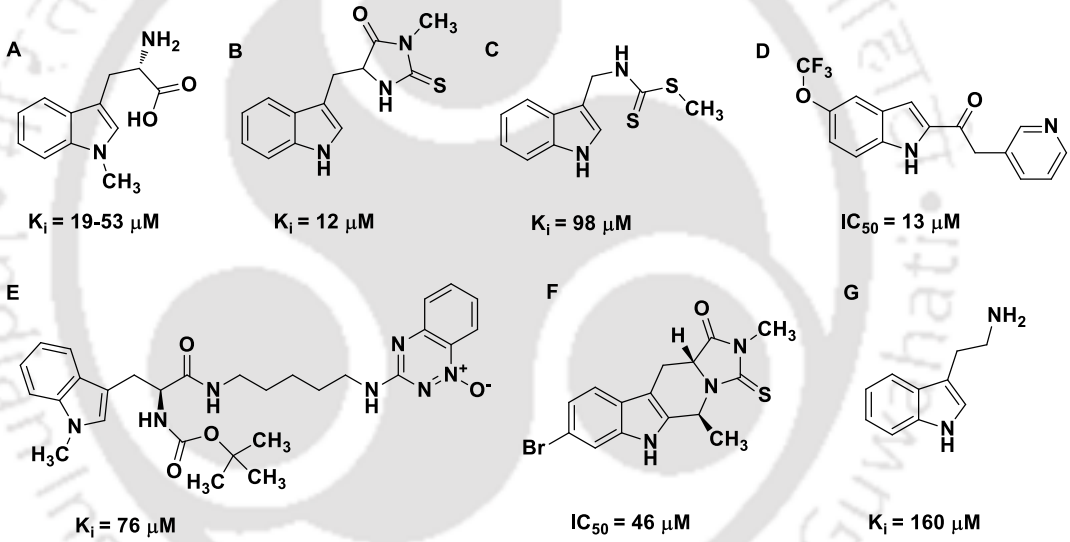

Figure 1.12. Structure of tryptophan and indole based inhibitors.

Pharmacophore modelling discovered 4-Aryl-1,2,3-triazoles. Among those substituted triazole derivatives, MMG-0358 showed IC_{50} value of 0.33 µM and also exhibited cellular IC_{50} value in nanomolar range. In addition, this compound demonstrated lower cytotoxicity and higher selectivity for IDO1 over TDO enzyme.[52, 54] Also the *N*-phenyl-1,2,3-triazol-4-amine compounds showed cellular IC_{50} value of <1 µM (Figure 1.13).

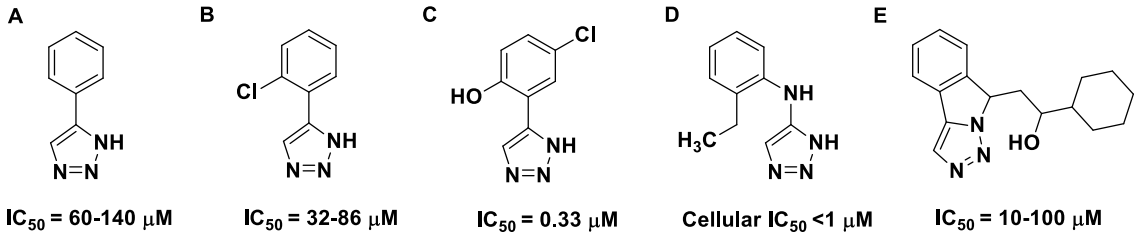

Figure 1.13. Structure of 4-aryl-1,2,3-triazole based inhibitors.

Among phenyl substituted imidazole derivatives, it was shown that 4-PI derivatives is more than 10-fold potent than the compound, 4-PI. Fungistatic agents containing imidazole moiety such as econazole and miconazole were identified as IDO1 active. However, 1,2,4-triazole-based fungistatic agent fluconazole was IDO1 inactive (Figure 1.14).[52, 55]

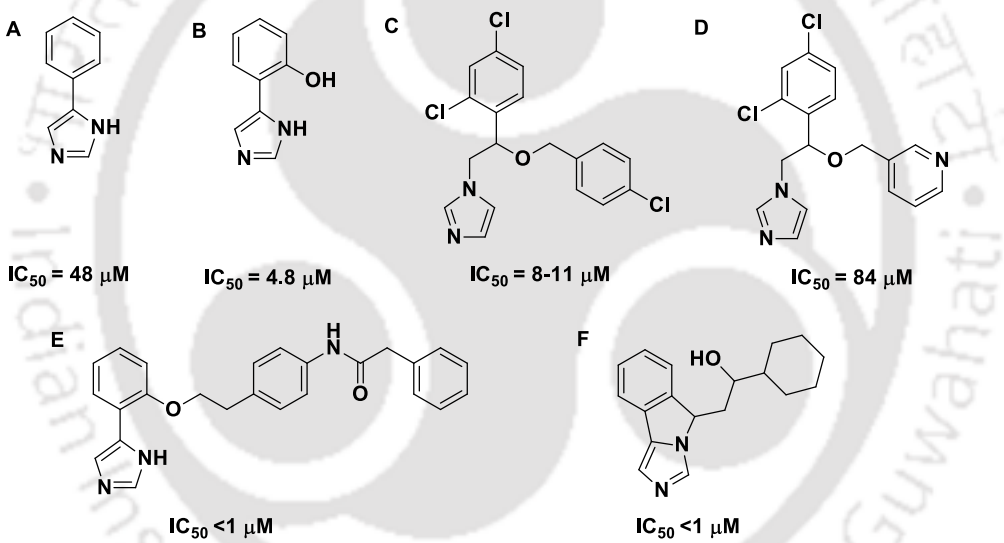

Figure 1.14. Structure of imidazole based inhibitors.

1.14. Conclusion

The immune regulatory molecule IDO1 plays an important role in immune evasion and metastasis of cancer cells. To date, a large number of inhibitors targeting the IDO1 enzymatic function not its signalling function have been reported but only few of them has been used in clinical trials. Most of them showed moderate IDO1 inhibitory potency. Hence, there is a demand for potent IDO1 inhibitors which can actively and specifically inhibits IDO1 compared to other heme-containing enzymes. The present approach for the identification of novel inhibitors for IDO1 is based upon a ligand based methodology. Previous studies and the recently available structural knowledge of IDO1 help in the

screening and characterisation of a series of potential inhibitors. It also helps in calculating the inhibitory constants and gaining the structural related information using various computer aided molecular techniques against purified IDO1 enzyme. Therefore, this is an important approach for the development of a pharmacophore as well as rational ligand-based drug design. Hence, an access of this enzyme will greatly assist in the design of IDO1 inhibitors as well as in the elucidation of the role of IDO1 in humans.

1.15. Aim of the research work

The major objectives of this thesis were

1. Optimization of an expression and purification system for rhIDO1 and rhTDO enzymes.
2. Characterisation of the enzyme by spectroscopic and kinetic method.
3. To gain inhibition information for rhIDO1.
4. Search for cellular mimicking environment for IDO1 activity study under *in vitro* condition.

1.16. References

1. Mason, H.; Fowlks, W.; Peterson, E., Oxygen transfer and electron transport by the phenolase complex 1. *J. Am. Chem. Soc.* **1955,** *77* (10), 2914-2915.

2. Sono, M.; Roach, M. P.; Coulter, E. D.; Dawson, J. H., Heme-containing oxygenases. *Chem. Rev.* **1996,** *96* (7), 2841-2888.

3. Jensen, K. P.; Ryde, U., How O_2 binds to heme reasons for rapid binding and spin inversion. *J. Biol. Chem.* **2004,** *279* (15), 14561-14569.

4. Jones, R. D.; Summerville, D. A.; Basolo, F., Synthetic oxygen carriers related to biological systems. *Chem. Rev.* **1979,** *79* (2), 139-179.

5. Lee-Ruff, E., The organic chemistry of superoxide. *Chem. Soc. Rev.* **1977,** *6* (2), 195-214.

6. Que, L.; Ho, R. Y., Dioxygen activation by enzymes with mononuclear non-heme iron active sites. *Chem. Rev.* **1996,** *96* (7), 2607-2624.

7. (a) Wong, L.-L., Cytochrome P450 monooxygenases. *Curr. Opin. Chem. Biol.* **1998,** *2* (2), 263-268; (b) Millett, E. S.; Efimov, I.; Basran, J.; Handa, S.; Mowat, C. G.; Raven, E. L., Heme-containing dioxygenases involved in tryptophan oxidation. *Curr. Opin. Chem. Biol.* **2012,** *16* (1-2), 60-66.

8. (a) Ruddick, J. P.; Evans, A. K.; Nutt, D. J.; Lightman, S. L.; Rook, G. A.; Lowry, C. A., Tryptophan metabolism in the central nervous system: medical implications. *Expert Rev. Mol. Med.* **2006,** *8* (20), 1-27; (b) Widner, B.; Leblhuber, F.; Walli, J.; Tilz, G.; Demel, U.; Fuchs, D., Tryptophan degradation and immune activation in Alzheimer's disease. *J. Neural. Transm.* **2000,** *107* (3), 343-353. (c) Peters, J. C., Tryptophan nutrition and metabolism: an overview. *Adv. Exp. Med. Biol.* **1991**, *294*, 345-358.

9. Bett, I. M., Metabolism of tryptophan in rheumatoid arthritis. *Ann. Rheum. Dis.* **1962,** *21* (1), 63-69.

10. Berger, M.; Gray, J. A.; Roth, B. L., The expanded biology of serotonin. *Annu. Rev. Med.* **2009,** *60*, 355-366.

11. (a) Hardeland, R., Atioxidative protection by melatonin. *Endocrine* **2005,** *27* (2), 119-130; (b) Altun, A.; Ugur-Altun, B., Melatonin: therapeutic and clinical utilization. *Int. J. Clin. Pract.* **2007,** *61* (5), 835-845.

12. (a) Botting, N. P., Chemistry and neurochemistry of the kynurenine pathway of tryptophan metabolism. *Chem. Soc. Rev.* **1995,** *24* (6), 401-412. (b) Moroni, F., Tryptophan metabolism and brain function: focus on kynurenine and other indole metabolites. *Eur. J. Pharmacol.* **1999**, *375* (1-3), 87-100.

13. Stone, T. W.; Darlington, L. G., Endogenous kynurenines as targets for drug discovery and development. *Nat. Rev. Drug Discov.* **2002,** *1* (8), 609-620.

14. Stone, T.; Perkins, M., Quinolinic acid: a potent endogenous excitant at amino acid receptors in CNS. *Eur. J. Pharmacol.* **1981,** *72* (4), 411-412.

15. Goldstein, L. E.; Leopold, M. C.; Huang, X.; Atwood, C. S.; Saunders, A. J.; Hartshorn, M.; Lim, J. T.; Faget, K. Y.; Muffat, J. A.; Scarpa, R. C., 3-Hydroxykynurenine and 3-hydroxyanthranilic acid generate hydrogen peroxide and promote α-crystallin cross-linking by metal ion reduction. *Biochemistry* **2000,** *39* (24), 7266-7275.

16. Lugo-Huitrón, R.; Blanco-Ayala, T.; Ugalde-Muniz, P.; Carrillo-Mora, P.; Pedraza-Chaverri, J.; Silva-Adaya, D.; Maldonado, P.; Torres, I.; Pinzon, E.; Ortiz-Islas, E., On the antioxidant properties of kynurenic acid: free radical scavenging activity and inhibition of oxidative stress. *Neurotoxicol. Teratol.* **2011,** *33* (5), 538-547.

17. Guidetti, P.; Schwarcz, R., 3-Hydroxykynurenine potentiates quinolinate but not NMDA toxicity in the rat striatum. *Eur. J. Neurosci.* **1999,** *11* (11), 3857-3863.

18. Uyttenhove, C.; Pilotte, L.; Théate, I.; Stroobant, V.; Colau, D.; Parmentier, N.; Boon, T.; Van den Eynde, B. J., Evidence for a tumoral immune resistance mechanism based on tryptophan degradation by indoleamine 2, 3-dioxygenase. *Nat. Med.* **2003,** *9* (10), 1269-1274.

19. Yeung, A. W.; Terentis, A. C.; King, N. J.; Thomas, S. R., Role of indoleamine 2, 3-dioxygenase in health and disease. *Clin. Sci.* **2015,** *129* (7), 601-672.

20. (a) Gupta, N. K.; Thaker, A. I.; Kanuri, N.; Riehl, T. E.; Rowley, C. W.; Stenson, W. F.; Ciorba, M. A., Serum analysis of tryptophan catabolism pathway: correlation with Crohn's disease activity. *Inflamm. Bowel. Dis.* **2011,** *18* (7), 1214-1220; (b) Hartai, Z.; Klivényi, P.; Janáky, T.; Penke, B.; Dux, L.; Vécsei, L., Kynurenine metabolism in multiple sclerosis. *Acta Neurol Scand.* **2005,** *112* (2), 93-96.

21. Aquilina, J. A.; Carver, J. A.; Truscott, R. J., Oxidation products of 3-hydroxykynurenine bind to lens proteins: relevance for nuclear cataract. *Exp. Eye Res.* **1997,** *64* (5), 727-735.

22. Pitche, P. T., Pellagre et érythèmes pellagroïdes. *Sante.* **2005,** *15* (3), 205-208.

23. (a) Kotake, Y.; Masayama, I., The intermediary metabolism of tryptophan. XVIII. The mechanism of formation of kynurenine from tryptophan. *Z. physiol. Chem.* **1936,** *243*, 237-244; (b) Yamamoto, S.; Hayaishi, O., Tryptophan pyrrolase of rabbit intestine D-and L-tryptophan-cleaving enzyme or enzymes. *J. Biol. Chem.* **1967,** *242* (22), 5260-5266; (c) Metz, R.; DuHadaway, J. B.; Kamasani, U.; Laury-Kleintop, L.; Muller, A. J.; Prendergast, G. C., Novel tryptophan catabolic enzyme IDO2 is the preferred biochemical target of the antitumor indoleamine 2, 3-dioxygenase inhibitory compound D-1-methyl-tryptophan. *Cancer Res.* **2007,** *67* (15), 7082-7087.

24. Yamazaki, F.; Kuroiwa, T.; Takikawa, O.; Kido, R., Human indolylamine 2, 3-dioxygenase. Its tissue distribution, and characterization of the placental enzyme. *Biochem. J.* **1985,** *230* (3), 635-638.

25. Schutz, G.; Feigelson, P., Purification and properties of rat liver tryptophan oxygenase. *J. Biol. Chem.* **1972,** *247* (17), 5327-5332.

26. Batabyal, D.; Yeh, S.-R., Human tryptophan dioxygenase: a comparison to indoleamine 2, 3-dioxygenase. *J. Am. Chem. Soc.* **2007,** *129* (50), 15690-15701.

27. Pantouris, G.; Serys, M.; Yuasa, H. J.; Ball, H. J.; Mowat, C. G., Human indoleamine 2, 3-dioxygenase-2 has substrate specificity and inhibition characteristics distinct from those of indoleamine 2, 3-dioxygenase-1. *Amino Acids* **2014,** *46* (9), 2155-2163.

28. Murray, M. F., The human indoleamine 2, 3-dioxygenase gene and related human genes. *Curr. Drug Metab.* **2007,** *8* (3), 197-200.

29. Meininger, D.; Zalameda, L.; Liu, Y.; Stepan, L. P.; Borges, L.; McCarter, J. D.; Sutherland, C. L., Purification and kinetic characterization of human indoleamine 2, 3-dioxygenases 1 and 2 (IDO1 and IDO2) and discovery of selective IDO1 inhibitors. *Biochim. Biophys. Acta* **2011,** *1814* (12), 1947-1954.

30. Sugimoto, H.; Oda, S.-i.; Otsuki, T.; Hino, T.; Yoshida, T.; Shiro, Y., Crystal structure of human indoleamine 2, 3-dioxygenase: catalytic mechanism of O_2 incorporation by a heme-containing dioxygenase. *Proc. Natl. Acad. Sci. U.S.A.* **2006,** *103* (8), 2611-2616.

31. Chauhan, N.; Basran, J.; Efimov, I.; Svistunenko, D. A.; Seward, H. E.; Moody, P. C.; Raven, E. L., The role of serine 167 in human indoleamine 2, 3-dioxygenase: a comparison with tryptophan 2, 3-dioxygenase. *Biochemistry* **2008,** *47* (16), 4761-4769.

32. (a) Hirata, F.; Ohnishi, T.; Hayaishi, O., Indoleamine 2, 3-Dioxygenase. *J. Biol. Chem.* **1977,** *252*, 4637; (b) Pearson, J. T.; Siu, S.; Meininger, D. P.; Wienkers, L. C.; Rock, D. A., In vitro modulation of cytochrome P450 reductase supported indoleamine 2, 3-dioxygenase activity by allosteric effectors cytochrome b_5 and methylene blue. *Biochemistry* **2010,** *49* (12), 2647-2656.

33. (a) Bugg, T. D., Dioxygenase enzymes: catalytic mechanisms and chemical models. *Tetrahedron* **2003,** *59* (36), 7075-7101. (b) Ishimura, Y.; Nozaki, M.; Hayaishi, O. The oxygenated form of Ltryptophan 2,3-dioxygenase as reaction intermediate. *J. Biol. Chem.* **1970**, *245* (14), 3593-3602.

34. Efimov, I.; Basran, J.; Thackray, S. J.; Handa, S.; Mowat, C. G.; Raven, E. L., Structure and reaction mechanism in the heme dioxygenases. *Biochemistry* **2011,** *50* (14), 2717-2724.

35. Basran, J.; Efimov, I.; Chauhan, N.; Thackray, S. J.; Krupa, J. L.; Eaton, G.; Griffith, G. A.; Mowat, C. G.; Handa, S.; Raven, E. L., The mechanism of formation of N-formylkynurenine by heme dioxygenases. *J. Am. Chem. Soc.* **2011,** *133* (40), 16251-16257.

36. Lewis-Ballester, A.; Batabyal, D.; Egawa, T.; Lu, C.; Lin, Y.; Marti, M. A.; Capece, L.; Estrin, D. A.; Yeh, S.-R., Evidence for a ferryl intermediate in a heme-based dioxygenase. *Proc. Natl. Acad. Sci. U.S.A.* **2009,** *106* (41), 17371-17376.

37. (a) Terada, N.; Lucas, J. J.; Szepesi, A.; Franklin, R. A.; Domenico, J.; Gelfand, E. W., Rapamycin blocks cell cycle progression of activated T cells prior to events

characteristic of the middle to late G1 phase of the cycle. *J. Cell. Physiol.* **1993,** *154* (1), 7-15. (b) Facciabene, A.; Gregory T. Motz, G. T.; Coukos, G., T regulatory cells: key players in tumor immune escape and angiogenesis. *Cancer Res.* **2012,** *72* (9), 2162-2171.

38. Metz, R.; Rust, S.; DuHadaway, J. B.; Mautino, M. R.; Munn, D. H.; Vahanian, N. N.; Link, C. J.; Prendergast, G. C., IDO inhibits a tryptophan sufficiency signal that stimulates mTOR: a novel IDO effector pathway targeted by D-1-methyl-tryptophan. *Oncoimmunology* **2012,** *1* (9), 1460-1468.

39. Munn, D. H.; Sharma, M. D.; Baban, B.; Harding, H. P.; Zhang, Y.; Ron, D.; Mellor, A. L., GCN2 kinase in T cells mediates proliferative arrest and anergy induction in response to indoleamine 2, 3-dioxygenase. *Immunity* **2005,** *22* (5), 633-642.

40. Quintana, F. J.; Basso, A. S.; Iglesias, A. H.; Korn, T.; Farez, M. F.; Bettelli, E.; Caccamo, M.; Oukka, M.; Weiner, H. L., Control of T reg and TH 17 cell differentiation by the aryl hydrocarbon receptor. *Nature* **2008,** *453* (7191), 65-71.

41. (a) Takikawa, O., Biochemical and medical aspects of the indoleamine 2, 3-dioxygenase-initiated L-tryptophan metabolism. *Biochem. Biophys. Res. Commun.* **2005,** *338* (1), 12-19. (b) Taylor, M. W.; Feng, G. S., Relationship between interferon-gamma, indoleamine 2,3-dioxygenase, and tryptophan catabolism. *FASEB J.* **1991**, *5* (11), 2516-2522.

42. Fujigaki, H.; Saito, K.; Lin, F.; Fujigaki, S.; Takahashi, K.; Martin, B. M.; Chen, C. Y.; Masuda, J.; Kowalak, J.; Takikawa, O., Nitration and inactivation of IDO by peroxynitrite. *J. Immunol.* **2006,** *176* (1), 372-379.

43. Poljak, A.; Grant, R.; Austin, C. J.; Jamie, J. F.; Willows, R. D.; Takikawa, O.; Littlejohn, T. K.; Truscott, R. J.; Walker, M. J.; Sachdev, P., Inhibition of indoleamine 2, 3 dioxygenase activity by H_2O_2. *Arch. Biochem. Biophys.* **2006,** *450* (1), 9-19.

44. Thomas, S. R.; Salahifar, H.; Mashima, R.; Hunt, N. H.; Richardson, D. R.; Stocker, R., Antioxidants inhibit indoleamine 2, 3-dioxygenase in IFN-γ-activated human macrophages: posttranslational regulation by pyrrolidine dithiocarbamate. *J. Immunol.* **2001,** *166* (10), 6332-6340.

45. Godin-Ethier, J.; Hanafi, L.-A.; Piccirillo, C. A.; Lapointe, R., Indoleamine 2, 3-dioxygenase expression in human cancers: clinical and immunologic perspectives. *Clin. Cancer Res.* **2011,** *17* (22), 6985-6991.

46. Löb, S.; Königsrainer, A.; Rammensee, H.-G.; Opelz, G.; Terness, P., Inhibitors of indoleamine-2, 3-dioxygenase for cancer therapy: can we see the wood for the trees? *Nat. Rev. Cancer* **2009,** *9* (6), 445-452.

47. Wainwright, D. A.; Chang, A. L.; Dey, M.; Balyasnikova, I. V.; Kim, C. K.; Tobias, A.; Cheng, Y.; Kim, J. W.; Qiao, J.; Zhang, L., Durable therapeutic efficacy utilizing combinatorial blockade against IDO, CTLA-4, and PD-L1 in mice with brain tumors. *Clin. Cancer Res.* **2014,** *20* (20), 5290-5301.

48. Eguchi, N.; Watanabe, Y.; Kawanishi, K.; Hashimoto, Y.; Hayaishi, O., Inhibition of indoleamine 2, 3-dioxygenase and tryptophan 2, 3-dioxygenase by β-carboline and indole derivatives. *Arch. Biochem. Biophys.* **1984,** *232* (2), 602-609.

49. Muller, A. J.; Scherle, P. A., Targeting the mechanisms of tumoral immune tolerance with small-molecule inhibitors. *Nat. Rev. Cancer* **2006,** *6* (8), 613-625.

50. Mellor, A. L.; Baban, B.; Chandler, P.; Marshall, B.; Jhaver, K.; Hansen, A.; Koni, P. A.; Iwashima, M.; Munn, D. H., Cutting edge: induced indoleamine 2, 3 dioxygenase expression in dendritic cell subsets suppresses T cell clonal expansion. *J. Immunol.* **2003,** *171* (4), 1652-1655.

51. Dolušić, E.; Frédérick, R., Indoleamine 2, 3-dioxygenase inhibitors: a patent review (2008–2012). *Expert Opin. Ther. Pa.t* **2013,** *23* (10), 1367-1381.

52. Röhrig, U. F.; Majjigapu, S. R.; Vogel, P.; Zoete, V.; Michielin, O., Challenges in the discovery of indoleamine 2, 3-dioxygenase 1 (IDO1) inhibitors. *J. Med. Chem.* **2015,** *58* (24), 9421-9437.

53. Dolušić, E.; Larrieu, P.; Blanc, S.; Sapunaric, F.; Pouyez, J.; Moineaux, L.; Colette, D.; Stroobant, V.; Pilotte, L.; Colau, D., Discovery and preliminary SARs of keto-indoles as novel indoleamine 2, 3-dioxygenase (IDO) inhibitors. *Eur. J. Med. Chem.* **2011,** *46* (7), 3058-3065.

54. Huang, Q.; Zheng, M.; Yang, S.; Kuang, C.; Yu, C.; Yang, Q., Structure–activity relationship and enzyme kinetic studies on 4-aryl-1*H*-1, 2, 3-triazoles as indoleamine 2, 3-dioxygenase (IDO) inhibitors. *Eur. J. Med. Chem.* **2011,** *46* (11), 5680-5687.

55. Kumar, S.; Jaller, D.; Patel, B.; LaLonde, J. M.; DuHadaway, J. B.; Malachowski, W. P.; Prendergast, G. C.; Muller, A. J., Structure based development of phenylimidazole-derived inhibitors of indoleamine 2, 3-dioxygenase. *J. Med. Chem.* **2008,** *51* (16), 4968-4977.

CHAPTER 2

Bacterial expression and purification of rhIDO1 and rhTDO enzymes

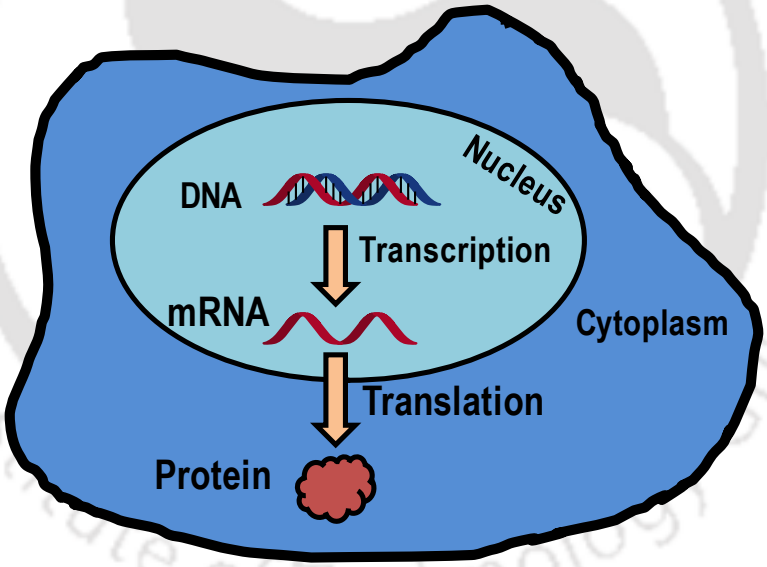

In this chapter an expression and purification system for recombinant human indoleamine 2,3-dioxygenase 1 (IDO1) and tryptophan 2,3-dioxygenase (TDO) enzymes is described and the enzymes is characterized by spectroscopic and HPLC methods.

2.1. Background and focus of the present work

The kynurenine pathway of L-tryptophan (L-Trp) metabolism has been recognized as an important mechanism in immune escape.[1] The heme-containing enzyme indoleamine 2,3-dioxygenase 1 (IDO1) and tryptophan 2,3-dioxygenase (TDO) catalyzes the first and rate-limiting step of the kynurenine pathway through the oxidative cleavage of the 2,3-double bond of the indole ring of L-Trp.[1b] Although both the dioxygenases catalyse the same reaction, their physicochemical structures, properties and biological roles are different. Tetrameric enzyme TDO is primarily expressed in the liver and regulates the L-Trp level in response to dietary intake, whereas monomeric enzyme IDO1 is ubiquitously distributed throughout the body apart from the liver.[2]

In healthy human body, the activity of IDO1 enzyme is low and has trivial physiological effects.[3] However within the immune system, IDO1 activity is up regulated by the cytokines like interferon-ɤ, interleukin 1,2 and tumour necrosis factor.[4] Up regulation of IDO1 activity in tumours is interconnected with the reduction of local L-Trp concentration and the accumulation of kynurenine metabolites. Hence the up regulation of IDO1 activity is related with a variety of diseases, including inflammation, cancer, schizophrenia and Huntington's disease. Moreover, high level of the kynurenine pathway metabolites are implicated in various diseases including AIDS, dementia complex, cerebral malaria, age-related cataract, Parkinson's and Alzheimer's disease.[5] Starvation of L-Trp leads to an increase in the differentiation and activation of immune-suppressive regulatory T cells, and inactivation of tumor-specific immune T cells.[6] High level of IDO1 expression in tumours is also related with poor prognosis for survival in different types of cancer.[7] Recent *in vivo* studies have established that IDO1 promotes immune tolerance via suppression of local T cell responses under various physiological and patho-physiological conditions, including mammalian pregnancy, tumor resistance, autoimmunity, chronic inflammation and chronic infections.[4, 8]

The *in vitro* and *in vivo* studies with small molecule IDO1 inhibitor showed the improvement of the efficacy of therapeutic vaccination or chemotherapy.[9] Several classes of IDO1 inhibitors are reported. Most of them show IDO1 inhibitory potency in micromolar range. One of the hydroxyamidine based compound INCB024360 is a potent IDO1 inhibitors and presently under phase II clinical trials as a single agent in ovarian cancer and in combination with the CTLA-4 antagonist ipilimumab in metastatic melanoma.[10] Hence, IDO1 is considered as an attractive target for the development of inhibitors.

All these findings emphasized to the importance of IDO1 in human physiology and disease. Hence, the access of large quantities of pure human IDO1 and TDO enzymes will be highly advantageous for the study of structure, mechanism of action and for the development of more potent IDO1 inhibitors. Although the expression and purification protocol of IDO1 and TDO was already developed,[11] in this chapter we tried to optimise an improved expression and purification system for the production of recombinant human IDO1 and TDO enzymes in our laboratory conditions. This chapter also describes the characterization of these enzymes by spectroscopic, HPLC and kinetic methods.

2.2. Result and discussion

2.2.1. Amplification of rhIDO1 and rhTDO

For the amplification of the cDNA of rhIDO1 and rhTDO gene, a generous gift from Professor Emma L. Raven (University of Leicester) we performed transformation in *E. coli* DH5α cell with the vector pQE30 and pET28a, respectively. The purity and size of the amplified DNA of rhIDO1 and rhTDO was checked with respect to the DNA ladder of known size by the agarose gel electrophoresis (Figure 2.1).

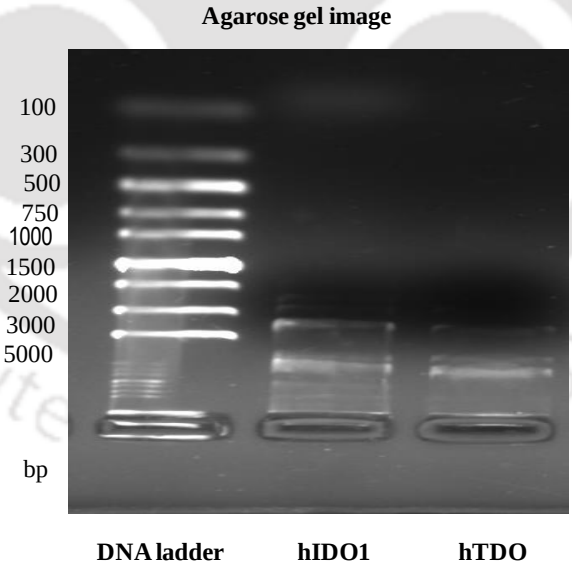

Figure 2.1. Agarose gel image of IDO1 and TDO

2.2.2. Optimal conditions for expression and purification of rhIDO1 and rhTDO

The optimized IPTG concentration at the induction stage of IDO1 expression was 1 mM recommended by Qiagen,[12] the manufacturer of the expression vector pQE30 and 10 µM performed at 37 °C by Littlejohn and 100 µM performed at 30 °C by Austin.[11a, 11b] Hence,

for the expression of rhIDO1, a single colony of *E. coli* M15 cells containing pREP4 and pQE30-IDO1 was regularly grown according to the general method as described above. However, during the bacterial expression of genetically engineered protein especially in *E. coli* cells, insoluble protein gets aggregate, known as inclusion bodies.[13] Therefore, 10 µM concentrations of IPTG and 37 °C growth temperature may not be the optimised condition for total rhIDO1 production as described by Littlejohn. For the production of more soluble active protein from inclusion bodies, growth temperature was generally reduced.[14] The formation of inclusion bodies was examined by growing the *E. coli* (EC538, pREP4, and pQE30-IDO1) at 37 °C, 30 °C and 25 °C temperature. Then the soluble protein was removed by incubating the cell pellets with lysozyme after initial lysing. SDS-PAGE analysis showed the formation of inclusion bodies at 37 °C, 30 °C and 25 °C (Figure 2.2). At 1 mM IPTG concentration, 30 °C temperature showed reduced inclusion body formation compared to 37 °C and 25 °C. Hence, the optimal conditions required for soluble, active 6His-IDO1 expression in EC538 cells was 1 mM IPTG concentration and 30 °C.

The first purification trials performed by Littlejohn[11a-c] showed that the heme (protoporphyrin IX) content of 6His-IDO1, as observed on SDS-PAGE, was low which indicated the formation of apoenzyme. Exogenous heme cannot be added to the purified protein as the exogeneous heme nonspecifically binds to the enzyme resulting in inactivation of the 6His-IDO protein. The supplementation of 7 µM hemin to the culture medium in the induction phase increased the heme content but, not sufficiently increased the rate of synthesis of heme in the induction phase of the IDO1 protein. There was a report on a similar shortage of heme when a recombinant hemoprotein, nitric oxide synthase, was over-expressed in a baculovirus expression system.[15] For further improvement of the heme content, ALA was trialled as an alternative to hemin supplementation. ALA is the natural biosynthetic precursor to heme and has been used for increasing heme content of other hemoproteins.[16] ALA is more soluble than hemin and is less toxic to bacteria.[17] Therefore, various concentration of ALA (0.1-0.5 mM) was used for the expression with 1 mM IPTG and 30 °C. SDS-PAGE analysis showed the higher IDO1 expression at 0.5 mM (Figure 2.2).

Similarly the optimal conditions at the induction stage of TDO expression in EC538 cells was 1 mM IPTG concentration and 37 °C recommended by Ren and Schutz.[11d, 11e]. Hence for the expression of rhTDO, a single colony of *E. coli* Rosetta (DE3) plysS cells containing pET28a-TDO was regularly grown according to the general

method as described earlier. But the SDS-PAGE analysis showed a protein band comigrating with purified rat liver cytosolic TDO. For further improvement of the production of soluble, active rhTDO protein, we have varied the incubation temperature 37 ºC, 30 ºC and 22 ºC and the concentration of ALA 0.1-0.5 mM at 0.5 mM IPTG concentration. SDS-PAGE analysis showed the higher TDO expression at 22 ºC and 0.5 mM ALA concentration (Figure 2.2). As TDO is a heme-containing protein, addition of hemin might also stabilize the nascent apoprotein in culture.

During the induction phase, the addition of PMSF (1 mM), serine protease inhibitor to the culture assists in the prevention of cleavage by an endogenous trypsin-like protease present in *E.coli* host cells without affecting the IDO1 expression. The addition of EDTA, a metalloprotease inhibitor to the cultures at the end of the induction, helps to further reduce protein degradation during harvesting, storage and lysis of cells. Then the fractions were purified by Ni^{2+} affinity chromatography, followed by Sephadex G25 and the final sample gave a single band on SDS-PAGE (Figure 2.2).[11a-c]

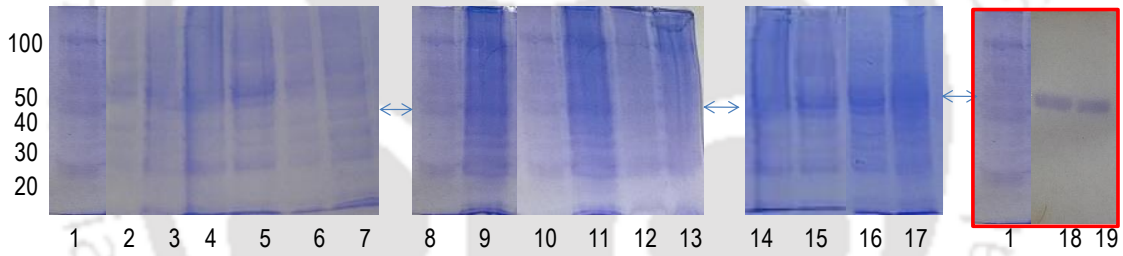

Figure 2.2. SDS gel image for IDO1 and TDO enzyme. (1) protein ladder, (2-4) 37 ºC, 25 ºC, 30 ºC and (5-7) 0.5 mM, 0.25 mM, 0.1 mM (ALA), respectively for hIDO1. (8-10) 37 ºC, 22 ºC, 30 ºC and (11-13) 0.5 mM, 0.25 mM, 0.1 mM (ALA), respectively for hTDO. (14-15) insoluble and soluble at 30 ºC respectively for hIDO1. (16-17) soluble and insoluble at 22 ºC, respectively for hTDO. (18) and (19) pure TDO and IDO1 enzyme, respectively.

2.2.3. Characterization of IDO1 and TDO enzymes by UV-Vis spectroscopy

Optical absorption spectra of purified rhIDO1 and rhTDO enzymes were recorded in UV-Vis spectroscopy.[11d, 18] The spectrum of the ferric form of rhIDO1 has maxima at 404 nm and 409 nm, respectively. Reduction of ferric rhIDO1 and rhTDO results in a red shift in the Soret band (from 404 to 421 nm) and (from 409 to 424 nm), respectively with the formation of a Q band in the visible region (531 nm, 559 nm and 603 nm) and (533 nm,

561 nm and 627 nm), respectively which is consistent with the formation of a high-spin species seen by all rhIDO1 and rhTDO enzymes (Figure 2.3).

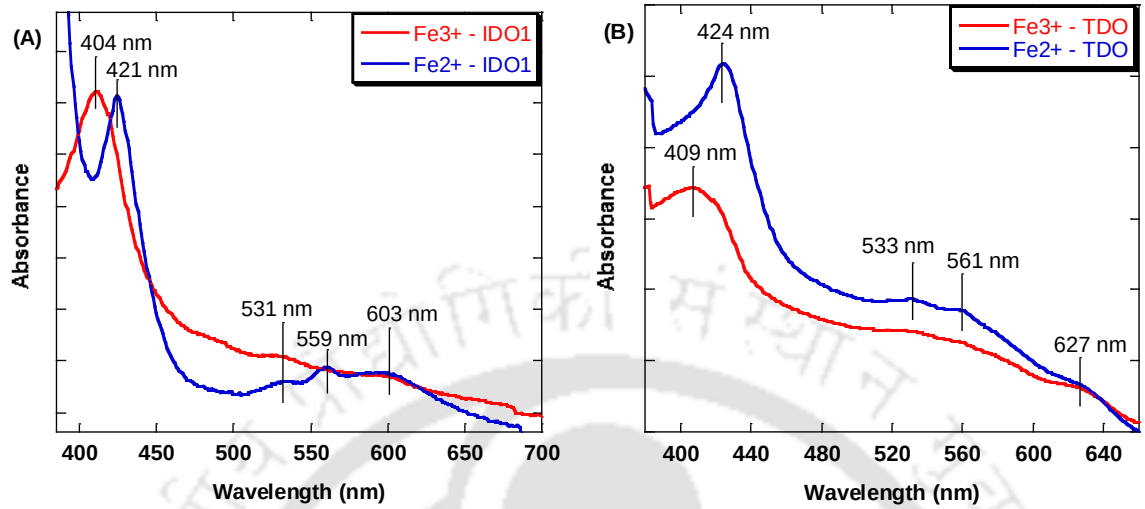

Figure 2.3. Absorption spectra of ferric-IDO1 and deoxy-ferrous-IDO1 enzyme (A), absorption spectra of ferric-TDO and deoxy-ferrous-TDO enzyme (B) in 50 mM potassium phosphate buffer at pH 6.5. IDO1 and TDO enzyme concentration = 5 μM. Ferrous-deoxy reaction environment was generated by adding $Na_2S_2O_4$ under N_2 atmosphere. Y-axis was not same for both cases.

2.2.4. Characterization of IDO1 enzyme by CD spectroscopy

The secondary structure contents of IDO1 enzyme was determined by far-UV circular dichroism (CD) measurements.[18b, 19] CD spectroscopy showed that the secondary structure of 6His-IDO1 consists of 30.2% alpha helical, 7.9% beta sheet and 64.2% random coil (Figure 2.4A). The temperature-dependent CD measurements were also performed. The results showed that the thermal perturbation temperature of IDO1 enzyme was 55 °C (Figure 2.4B).

2.2.5. Measurement of IDO1 and TDO enzyme activity

IDO1 and TDO enzyme activity was performed in HPLC method.[20-21] The amount of kynurenine generated due to the catabolism of L-Trp was directly quantified by HPLC analysis. The area under the curve in HPLC method corresponds to the kynurenine concentration (Figure 2.5A). IDO1 and TDO enzyme activity were also evaluated by measuring the changes in absorbance values of the product produced from kynurenine

and *p*-DMAB at 480 nm in acidic medium in UV-Vis spectroscopy (Figure 2.5B).[11a, 11b, 20].

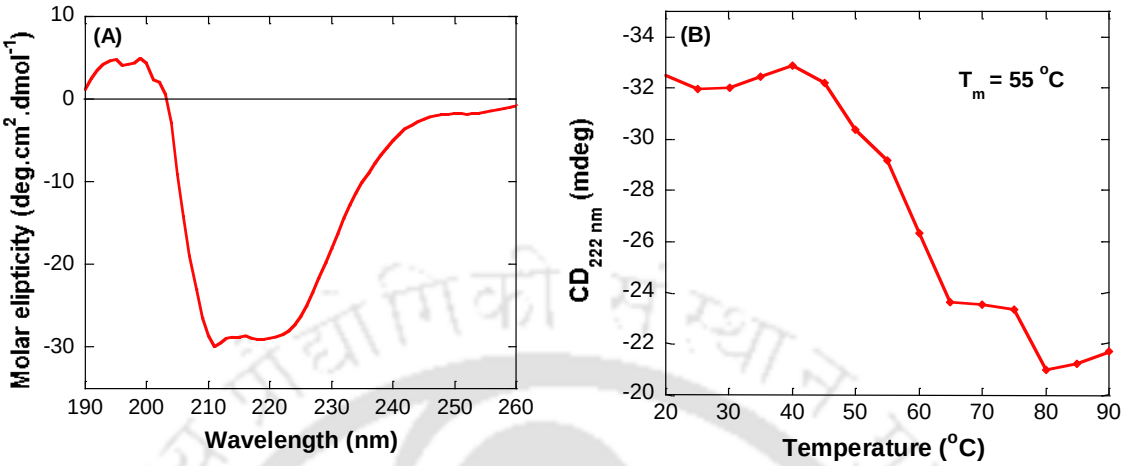

Figure 2.4. Far-UV CD spectra of IDO1 in 50 mM potassium phosphate buffer at pH 6.5 (A). IDO1 enzyme concentration = 2 μM. Thermal perturbation of IDO1 enzyme as probed by changes in CD $_{222\ nm}$.(B).

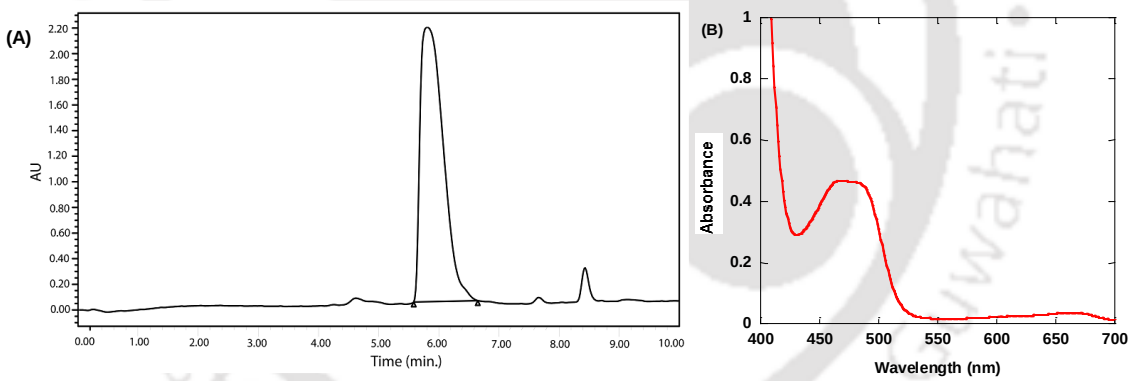

Figure 2.5. IDO1 enzyme activity measurement by HPLC method (A) and UV-Vis spectroscopy (B).

2.2.6. Determination of kinetic parameters of IDO1 enzyme by UV-Vis spectroscopy

The kinetic parameters of the IDO1 enzyme catalyzed reaction were determined by measuring the initial rate of *N*-formylkynurenine formation in UV-Vis spectroscopy (Figure 2.6).[22] The values of K_M, k_{cat} and V_{max} were calculated by using Burk equation and these values were 47.8 ± 2.5 μM, 3.7 ± 0.1 s^{-1} and 8.9 ± 0.4 μM/min, respectively.

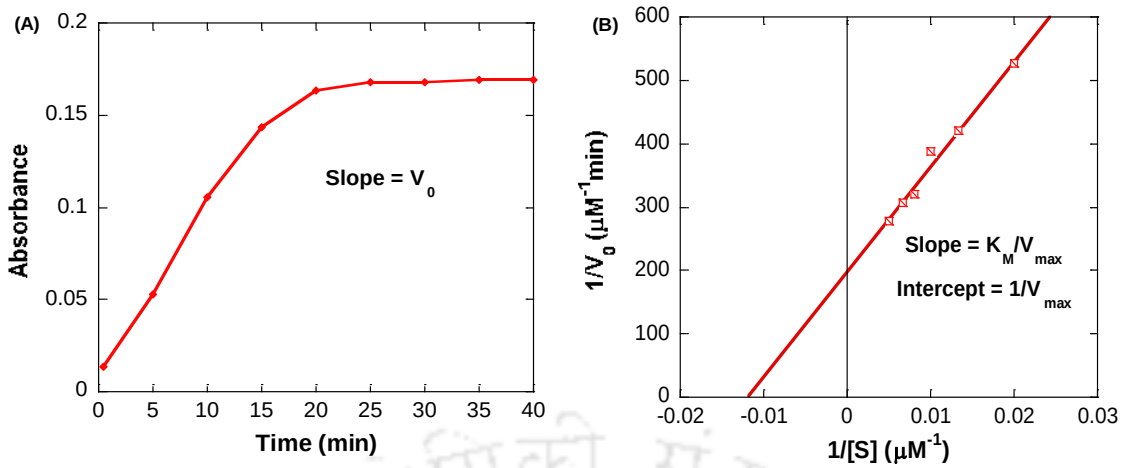

Figure 2.6. Absorbance of product NFK at 321 nm *vs* time (min) plot (A). 1/initial rate *vs* 1/substrate concentration (B).

In summary, after transfection of M15 and Rosetta (DE3) plysS *E. coli* cells with the corresponding engineered pQE30-IDO1 and pET28a-TDO vector, a functionally active IDO1 and TDO protein was expressed. The expressed enzyme was isolated, purified and characterized in term of its electronic absorption spectra, CD spectra and catalytic activity. These properties of the expressed IDO1 and TDO protein were identical to those of the native IDO1 and TDO. Hence, the accessibility of this enzyme will be helpful for the screening of the compounds developed as inhibitor of IDO1.

2.3. Conclusion

In this study, we have tried to optimise an efficient bacterial expression and purification system for the production of rhIDO1 and rhTDO enzymes in our laboratory conditions. During protein expression, inclusion body is formed by EC538 of 6His-IDO1. This was considerably lowered by reducing the incubation temperature from 37 °C to 30 °C for IDO1. Similarly, the improved expression level of soluble, active TDO protein was achieved by reducing the incubation temperature from 37 °C to 22 °C for TDO. The use of optimised concentration of IPTG and ALA, the biosynthetic precursor of protoporphrin IX and coupled with Ni^{2+}-affinity chromatography produced a reliable source of 6His-IDO1 and TDO enzymes. The characterization of these enzymes showed the protein to heme ratio of 1:1.4 and 1:1.2, respectively identical to the previously reported rhIDO1 and rhTDO enzymes in terms of spectroscopic properties and enzyme activity. Therefore, this recombinant IDO1 and TDO will be useful for the rational design of inhibitors, which

could prevent undesirable reactions caused by tryptophan metabolites in the kynurenine pathway.

2.4. Experimental section

2.4.1. General information

All reagents were purchased from different commercial sources and used directly without further purification.

2.4.2. Bacterial strains and plasmids

The bacterial *E. coli* strains used for the expression of pQE30-IDO1 (EC538, pREP4) and (pET28a-TDO) were M15 (Qiagen) and Rosetta (DE3) plysS, respectively and for the DNA amplification was DH5α cell.[23]

2.4.3. Transformation of *E. coli* cells

2.4.3.1. Preparation of competent cells

For long term storage of each expression strain 700 µl of *E. coli* culture media were mixed with 300 µl of sterile glycerol and stored at -80 °C as glycerol stocks. 20 µl of glycerol stocks was inoculated into 5 mL of L.B. media and incubated on a rotary shaker overnight at 37 °C and 180 rpm. Then 100 µl of overnight culture was again incubated in 50 mL of L.B. media on a rotary shaker at 37 °C and 180 rpm until $O.D._{600}$ ~ 0.4. The cells were then cooled in ice for 15 min and centrifuged at 4 °C and 4000 rpm for 10 min. The supernatant was removed and the cell pellet was resuspended in cold TSS and KCM buffer (9:1). The competent cells were then aliquot into 50 µL samples and stored at -80 °C.

2.4.3.2. Transformation of DNA into competent *E. coli* cells

The 50 µL competent *E. coli* cells were thawed and 2 µL of recombinant DNA was added, swirled to mix and left for 30 min on ice. The sample was heat shocked at 42 °C for 90 sec and incubated on ice for 5 min. 700 µL of LB media was added to the reactions and incubated on a rotary shaker at 37 ºC and 180 rpm for 1 h. Cells were pelleted by centrifuging at 4000 rpm and 4 °C for 1 min. Cells were concentrated by dissolving the pellet in 100 µL of the reaction and were streaked on LB agar plates containing appropriate antibiotic. The plates were left inverted at 37 °C overnight. Successfully

transformed cells will grow to form colonies as they express the antibiotic resistance gene.

2.4.4. Characterization of DNA

2.4.4.1. Amplification of DNA

A single colony of transformed DH5α cells from an LB agar plate (containing appropriate antibiotic) was selected and inoculated to 5 mL of LB media with 5 µL of appropriate antibiotic. Then the cells were grown overnight on a rotary shaker at 37 °C and 180 rpm. Bacterial cells (5 mL) were pelleted by spinning down at 10,000 rpm and 4 °C for 1 min. The cells were resuspended in 200 µL of cold alkaline P1 buffer (resuspension buffer) containing RNase. The cells were lysed by using 300 µL of P2 buffer (lysis buffer) and inverting gently 4-6 times. The solution was then neutralised by the addition of 300 µL of P3 buffer (neutralization buffer) and kept in deep freeze for 10 min after inversion of 4-6 times. The cell debris was precipitated by centrifuging at 10,000 rpm and 4 °C for 10 min. To the supernatant, 100% EtOH was added and kept in deep freeze for 30 min. After centrifugation at 10,000 rpm and 4 °C for 15 min, DNA was dried by discarding the supernatant. The bound DNA was eluted into a 1.5 mL of microcentrifuge tube after addition of 30 µL of dd H_2O and centrifuged for 1 min and stored at -20 °C. The DNA was checked by agarose gel electrophoresis.

2.4.4.2. Agarose gel electrophoresis

Agarose gels were cast by dissolving agarose powder (0.8% w/v) in 1x-TAE buffer with 5 µL of 1 mM ethidium bromide. Ethidium bromide binds with DNA and has an intense fluorescence. The gel was placed into a tank of 1x-TAE buffer. Then 5 µL of isolated DNA samples were mixed with 2 µL of loading buffer and loaded into the gel wells. The DNA ladder was loaded on to the gel to identify the size of the DNA bands. An electric current of 60 volt is applied to the gel and after 30 min the DNA was visualised in the gel under UV light on a transilluminator by absorbing UV light near 260 nm.

2.4.5. Expression and purification of IDO1 and TDO enzyme

2.4.5.1. Expression and purification of recombinant human IDO1 enzyme

The expression and purification procedures of recombinant human IDO1 enzyme were carried out as previously described with minor modifications.[11a-c] Human *N*-terminus 6X-histidine tagged IDO1 enzyme was expressed in *E. coli* (EC538) M15 cells (Qiagen)

containing the expression vector pQE30 and pREP4 plasmid. In brief, for the expression of rhIDO1, *E.coli*-M15 cells transformed with both pREP4 and pQE30-hIDO1 was grown on LB agar plate supplemented with 100 µg/mL ampicillin and 50 µg/mL kanamycin. A single colony, picked from a freshly streaked stock plate, was inoculated into 5 mL of LB medium supplemented with 100 µg/mL ampicillin and 50 µg/mL kanamycin. After that the transformed cells were incubated overnight on a rotary shaker at 37 ºC and 180 rpm. The overnight culture was then added to 1 L of LB medium again supplemented with 100 µg/mL ampicillin and 50 µg/mL kanamycin and incubated on a rotary shaker at 37 ºC and 120 rpm to an OD_{600} of 0.6. The culture was cooled in a water/ ice bath and the protein expression was induced by the addition of ALA (0.5 mM), IPTG (1 mM) and PMSF (1 mM). Induced cells were then grown at 30 ºC and 120 rpm for 24 h. Cells were harvested by centrifugation at 5000 rpm for 10 min at 4 ºC. The cell pellets were washed by resuspension with 20 mL of ice-cold 1X PBS buffer (pH 7.4) containing PMSF (1 mM) and EDTA (1 mM) and centrifugation at 15,000 rpm for 15 min at 4 ºC. The cell pellets were then stored at -80 ºC until lysis. Prior to lysis, the cell pellets were resuspended in ice-cold 20 mL of 25 mM Tris-buffer (pH 7.4) containing 150 mM NaCl and 10 mM imidazole. The suspension was then centrifuged at 5000 rpm for 10 min at 4 ºC to remove EDTA. The washed pellets were resuspended in ice-cold 20 mL of 25 mM Tris-buffer (pH 7.4) containing 150 mM NaCl, 10 mM imidazole, 10 mM $MgCl_2$, protease inhibitors (complete EDTA free) and DNase (<1 mg) and the cell membrane was disrupted with an ultrasonic processor UP100H (Hielscher GmbH). The lysate was then centrifuged at 20,000 rpm for 30 min at 4 ºC and the supernatant was filtered through 0.22 µm filter.

To the clear supernatant, 1 mL of Ni-NTA resin (Qiagen) was added and incubated on ice for 1 h with gentle stirring at 80 rpm. Then the mixture was poured into the Ni-NTA agarose column filled with 20 mL of 25 mM Tris-buffer (pH 7.4) containing 150 mM NaCl and 10 mM imidazole. After that the column was sequentially washed with 50 mL of 25 mM Tris-buffer (pH 7.4) containing 150 mM NaCl and 30, 40, 50, 65 and 80 mM imidazole, respectively to remove the nonspecifically bound protein. Finally the protein was eluted with 25 mM Tris-buffer (pH 7.4) containing 150 mM NaCl and 190 mM imidazole. The collected protein was then buffer-exchanged into 50 mM Tris-buffer (pH 7.4) using Sephadex G25 column. The purity of the enzyme was assessed by Coomassie-blue stained SDS-PAGE analysis and it showed 90% purity. The ratio of absorbance of the purified enzyme at 404 nm to that at 280 nm was around 1.4. A purified rhIDO1 enzyme was then mixed with 10% glycerol and stored at -80 °C until required.

2.4.5.2. Expression and purification of recombinant human TDO enzyme

The expression and purification procedures of recombinant human TDO enzyme was carried out as previously described with minor modifications.[20] Human *C*-terminus 6X-histidine tagged TDO enzyme was expressed in Rosetta (DE3) plysS cells containing the expression vector pET28a. In brief, for the expression of rhTDO, Rosetta (DE3) pLysS cells transformed with pET28a-TDO was grown on LB agar plate supplemented with 50 µg/mL kanamycin. A single colony, picked from a freshly streaked stock plate, was inoculated into 5 mL of LB medium supplemented with 50 µg/mL kanamycin. After that the transformed cells were incubated overnight on a rotary shaker at 37 ºC and 180 rpm. The overnight culture was then added to 1 L of LB medium again supplemented with 50 µg/mL kanamycin and incubated on a rotary shaker at 37 ºC and 120 rpm to an OD_{600} of 0.6. The culture was cooled in a water/ ice bath and the protein expression was induced by the addition of ALA (0.5 mM), IPTG (0.5 mM) and bovine hemin (7 µM). Induced cells were then grown at 22 ºC and 120 rpm for 20 h. Cells were harvested by centrifugation at 5000 rpm for 10 min at 4 ºC. The cell pellets were washed by resuspension with 20 mL of ice-cold 1X PBS buffer (pH 7.4) containing PMSF (1 mM) and EDTA (1 mM) and centrifugation at 15,000 rpm for 15 min at 4 ºC. The cell pellets were then stored at -80 ºC until lysis. Prior to lysis, the cell pellets were resuspended in ice-cold 20 mL of 50 mM potassium phosphate buffer (pH 8.0) containing 300 mM KCl and 10 mM imidazole. The suspension was then centrifuged at 5000 rpm for 10 min at 4 ºC to remove EDTA. The washed pellets were resuspended in ice-cold 20 mL of 50 mM potassium phosphate buffer (pH 8.0) containing 300 mM KCl, 10 mM imidazole, 10 mM $MgCl_2$, protease inhibitors (complete EDTA free) and DNase (<1 mg) and the cell membrane was disrupted with an ultrasonic processor UP100H (Hielscher GmbH). The cell debris was then removed by centrifugation at 20,000 rpm for 30 min and filtration on 0.22 µm filter.

To the clear supernatant, 1 mL of Ni-NTA resin (Qiagen) was added and incubated on ice for 1 h with gentle stirring at 80 rpm. Then the mixture was poured into the Ni-NTA agarose column filled with 20 mL of 50 mM potassium phosphate buffer (pH 8.0) containing 300 mM KCl and 10 mM imidazole. After that the column was sequentially washed with 50 mL of 50 mM potassium phosphate buffer (pH 8.0) containing 300 mM KCl and 20, 30 and 50 mM imidazole, respectively to remove the nonspecifically bound protein. Finally the protein was eluted with 50 mM potassium phosphate buffer (pH 8.0) containing 300 mM KCl and 250 mM imidazole. The collected

protein was then buffer-exchanged into 50 mM Tris-buffer (pH 8.0) using Sephadex G25 column. The purity of the enzyme was assessed by Coomassie-blue stained SDS-PAGE analysis and it showed 90% purity. The ratio of absorbance of the purified enzyme at 404 nm to that at 280 nm was around 1.2. A purified rhTDO enzyme was then mixed with 10% glycerol and stored at -80 °C until required.

2.4.6. SDS-PAGE gel electrophoresis

SDS-PAGE gel electrophoresis was performed to confirm the purity and the size of the protein against a marker with known sizes following the method.[24] After assembling the mini Protean SDS gel apparatus (Bio-Rad), the lower gel was made from sealing and stacking buffer and left to polymerise with water which levels the gel. The water was decanted after the bottom gel had set and the top layer of the gel was made from resolving buffer and left to set with combs. The combs were removed and the gel was placed into a tank with 1x-tank buffer. The protein samples (50 µl) were mixed with sample buffer (5 µl) and ddH_2O (10 µl) and boiled for 2-3 minutes. Then 30 µl of protein sample was loaded onto the gel. The protein ladder was also loaded onto the gel to identify the protein size. The gel was run at 120 volt for 2 h and afterwards the apparatus was disassembled. The gels stained with staining buffer which contained the dye Coomassie Brilliant Blue R250 for 4 h and washed with ddH_2O and destained in destaining buffer.

2.4.7. Characterization of IDO1 and TDO enzymes

2.4.7.1. Spectroscopic measurements of IDO1 and TDO enzymes

Absorption spectra of IDO1 and TDO enzyme were measured on PerkinElmer lambda 25 spectrophotometer according to the previously described method.[18a, 25] All experiments were performed in 50 mM potassium phosphate buffer at pH 6.5. Ferrous-deoxy reaction environment was generated by adding molar excess of $Na_2S_2O_4$ under N_2 atmosphere.

2.4.7.2. Secondary structure analysis by circular dichroism spectroscopy

Circular Dichroism (CD) analysis was performed following the procedures as described earlier.[18b, 19] CD spectra were recorded on a Jasco, J-1500 spectropolarimeter with 1 cm path length quartz cuvettes. CD spectra were measured with IDO1 enzyme (2 µM, determined by absorption at 404 nm) in the region of 190 to 260 nm using 1 mL cuvette of a 1-cm cell at 20 °C. CD spectra were recorded with a scan rate of 100 nm/min, a response time of 1 sec, a sensitivity of 100 mdeg with an accumulation of 3 scans. The

190-260 nm regions are an important because it can provide information on the secondary structure of proteins. Absorbance minima at 222 and 208 nm indicated the presence of α-helical structure and β-sheet structure. The spectral data was analyzed with respect to internal Yang's reference. The % of the secondary structures of the IDO1 enzyme was analyzed using the inbuilt software of the instrument. Thermal stability of IDO1 enzyme were determined by heating from 20 to 90 °C at a constant heating rate of 1 °C/min and monitoring the CD signal at 222 nm as a function of temperature. Near-UV CD spectroscopy was also measured in the region of 250 to 400 nm in a 1-cm cell at 20 °C.

2.4.7.3. IDO1 and TDO enzyme activity assay by spectroscopic method

IDO1 and TDO enzyme activity assay was performed as previously described with minor modifications.[11a-c, 20, 26] In brief, IDO1 and TDO enzyme activity was measured in the assay medium (500 µL) containing potassium phosphate buffer (50 mM, pH 6.5), sodium ascorbate (20 mM), methylene blue (10 µM), catalase (240 nM), L-Trp (150 µM), purified hIDO1 enzyme (41 nM) and hTDO enzyme (25 nM), DMSO (0.05%, v/v) and triton-X 100 (0.01%, v/v). The reaction mixture was then incubated at 37 ºC for 1 h. For the hydrolysis of *N*-formylkynurenine into kynurenine, the reaction mixture was further incubated with 100 µL of 30% (w/v) TCA at 50 ºC for 30 min, followed by centrifugation at 10,000 rpm for 10 min. After that, the supernatant was transferred into another tube with 100 µL of *p*-DMAB (Ehrlich's reagent, 2% (w/v) in acetic acid) and incubated for 10 min at room temperature for the generation of Schiff base with kynurenine. Kynurenine concentrations were determined by measuring the absorbance of the yellow pigment formed at 480 nm. A similar assay was performed with pure kynurenine.

2.4.7.4. IDO1 and TDO enzyme activity assay by HPLC method

IDO1 and TDO enzyme activity assay was performed as previously described with minor modifications.[11c, 20-21] In brief, IDO1 and TDO enzyme activity was measured in the assay medium (100 µL) containing potassium phosphate buffer (50 mM, pH 6.5), sodium ascorbate (20 mM), methylene blue (10 µM), catalase (240 nM), L-Trp (150 µM), purified hIDO1 enzyme (41 nM) and hTDO enzyme (25 nM), DMSO (0.05%, v/v) and triton-X 100 (0.01%, v/v). The reaction mixture was then incubated at 37 ºC for 1 h. For the hydrolysis of *N*-formylkynurenine into kynurenine, the reaction mixture was further incubated with 100 µL of 30% (w/v) TCA at 50 ºC for 30 min, followed by centrifugation at 10,000 rpm for 10 min. A 20 µL of supernatant from each reaction mixture was used

for HPLC analyses. The mobile phase for HPLC measurements was 50% sodium citrate buffer (40 mM, pH 2.25) and 50% methanol with 400 μM SDS. The rate of flow through the Ascentis® Express C18, 2.7 μm HPLC column was 0.5 mL/min, and kynurenine was detected at a wavelength of 365 nm. The area under the curve is the amount of kynurenine concentration. A similar HPLC analyses were performed using pure kynurenine.

2.4.7.5. Steady state kinetics measurement of IDO1 enzyme

The IDO1 enzyme kinetics was performed following the procedure as described earlier varying L-Trp concentrations (50-200 μM).[22b, 27] The reaction was initiated by the addition of the purified hIDO1 enzyme (40 nM). The formation of *N*-formylkynurenine at 37 °C was monitored at 5 min interval by UV-Vis spectroscopy in a 1 mL cuvette at 321 nm (ε_{321} = 3.75 mM^{-1} cm^{-1}). The initial rate of *N*-formylkynurenine formation was determined by dividing the change in absorbance from product *N*-formylkynurenine formation at 321 nm by the time. The reciprocal of initial rates of *N*-formylkynurenine formation were plotted against the reciprocal of L-Trp concentrations to obtain the kinetic parameters, K_M, k_{cat} and V_{max} (Lineweaver-Burk plot). Where, K_M, the Michaelis-Menten constant is the concentration at which the reaction rate is half of its maximal value, k_{cat} is the turnover number and V_{max} is the maximal rate, respectively. All kinetic parameters reported are averages of three separate experiments.

2.5. References

1. (a) Austin, C. J.; Rendina, L. M., Targeting key dioxygenases in tryptophan–kynurenine metabolism for immunomodulation and cancer chemotherapy. *Drug discovery today* **2015,** *20* (5), 609-617; (b) Mellor, A. L.; Munn, D. H., IDO expression by dendritic cells: tolerance and tryptophan catabolism. *Nat. Rev. Immunol.* **2004,** *4* (10), 762-774; (c) Röhrig, U. F.; Majjigapu, S. R.; Vogel, P.; Zoete, V.; Michielin, O., Challenges in the discovery of indoleamine 2, 3-dioxygenase 1 (IDO1) inhibitors. *J. Med. Chem.* **2015,** *58* (24), 9421-9437; (d) Uyttenhove, C.; Pilotte, L.; Théate, I.; Stroobant, V.; Colau, D.; Parmentier, N.; Boon, T.; Van den Eynde, B. J., Evidence for a tumoral immune resistance mechanism based on tryptophan degradation by indoleamine 2, 3-dioxygenase. *Nat. Med.* **2003,** *9* (10), 1269-1274.

2. (a) Takikawa, O.; Yoshida, R.; Kido, R.; Hayaishi, O., Tryptophan degradation in mice initiated by indoleamine 2, 3-dioxygenase. *J. Biol. Chem.* **1986,** *261* (8), 3648-3653;

(b) Yamamoto, S.; Hayaishi, O., Tryptophan pyrrolase of rabbit intestine D-and L-tryptophan-cleaving enzyme or enzymes. *J. Biol. Chem.* **1967,** *242* (22), 5260-5266; (c) Sono, M.; Roach, M. P.; Coulter, E. D.; Dawson, J. H., Heme-containing oxygenases. *Chem. Rev.* **1996,** *96* (7), 2841-2888.

3. Stone, T. W.; Darlington, L. G., Endogenous kynurenines as targets for drug discovery and development. *Nat. Rev. Drug Discov.* **2002,** *1* (8), 609-620.

4. (a) Croitoru-Lamoury, J.; Lamoury, F. M.; Caristo, M.; Suzuki, K.; Walker, D.; Takikawa, O.; Taylor, R.; Brew, B. J., Interferon-γ regulates the proliferation and differentiation of mesenchymal stem cells via activation of indoleamine 2, 3 dioxygenase (IDO). *PloS one* **2011,** *6* (2), e14698; (b) Greco, F. A.; Coletti, A.; Camaioni, E.; Carotti, A.; Marinozzi, M.; Gioiello, A.; Macchiarulo, A., The Janus-faced nature of IDO1 in infectious diseases: challenges and therapeutic opportunities. *Future Med. Chem.* **2016,** *8* (1), 39-54.

5. (a) Vazquez, S.; Parker, N. R.; Sheil, M.; Truscott, R. J., Protein-bound kynurenine decreases with the progression of age-related nuclear cataract. *Invest. Ophthalmol. Vis. Sci.* **2004,** *45* (3), 879-883; (b) Wichers, M. C.; Maes, M., The role of indoleamine 2, 3-dioxygenase (IDO) in the pathophysiology of interferon-α-induced depression. *J. Psychiatry Neurosci.* **2004,** *29* (1), 11; (c) Heyes, M.; Saito, K.; Crowley, J.; Davis, L.; Demitrack, M.; Der, M.; Dilling, L.; Elia, J.; Kruesi, M.; Lackner, A., Quinolinic acid and kynurenine pathway metabolism in inflammatory and non-inflammatory neurological disease. *Brain* **1992,** *115* (5), 1249-1273; (d) Sardar, A. M.; Reynolds, G. P., Frontal cortex indoleamine-2, 3-dioxygenase activity is increased in HIV-1-associated dementia. *Neurosci. Lett.* **1995,** *187* (1), 9-12.

6. Prendergast, G. C.; Smith, C.; Thomas, S.; Mandik-Nayak, L.; Laury-Kleintop, L.; Metz, R.; Muller, A. J., Indoleamine 2, 3-dioxygenase pathways of pathogenic inflammation and immune escape in cancer. *Cancer Immunol. Immunother.* **2014,** *63* (7), 721-735.

7. (a) Okamoto, A.; Nikaido, T.; Ochiai, K.; Takakura, S.; Saito, M.; Aoki, Y.; Ishii, N.; Yanaihara, N.; Yamada, K.; Takikawa, O., Indoleamine 2, 3-dioxygenase serves as a marker of poor prognosis in gene expression profiles of serous ovarian cancer cells. *Clin. Cancer Res.* **2005,** *11* (16), 6030-6039; (b) Platten, M.; Wick, W.; Van den Eynde, B. J., Tryptophan catabolism in cancer: beyond IDO and tryptophan depletion. *Cancer Res.* **2012,** *72* (21), 5435-5440; (c) Godin-Ethier, J.; Hanafi, L.-A.; Piccirillo, C. A.; Lapointe,

R., Indoleamine 2, 3-dioxygenase expression in human cancers: clinical and immunologic perspectives. *Clin. Cancer Res.* **2011,** *17* (22), 6985-6991.

8. (a) Uyttenhove, C.; Pilotte, L.; Théate, I.; Stroobant, V.; Colau, D.; Parmentier, N.; Boon, T.; Van den Eynde, B. J., Evidence for a tumoral immune resistance mechanism based on tryptophan degradation by indoleamine 2, 3-dioxygenase. *Nat. Med.* **2003,** *9* (10), 1269-1274; (b) Fallarino, F.; Grohmann, U.; You, S.; McGrath, B. C.; Cavener, D. R.; Vacca, C.; Orabona, C.; Bianchi, R.; Belladonna, M. L.; Volpi, C., The combined effects of tryptophan starvation and tryptophan catabolites down-regulate T cell receptor ζ-chain and induce a regulatory phenotype in naive T cells. *J. Immunol.* **2006,** *176* (11), 6752-6761; (c) Hornyák, L.; Dobos, N.; Koncz, G.; Karányi, Z.; Páll, D.; Szabó, Z.; Halmos, G.; Székvölgyi, L., The role of indoleamine-2, 3-dioxygenase (IDO) in cancer development, diagnostics, and therapy. *Front Immunol.* **2018,** *9*, 151; (d) Greco, F. A.; Coletti, A.; Camaioni, E.; Carotti, A.; Marinozzi, M.; Gioiello, A.; Macchiarulo, A., The Janus-faced nature of IDO1 in infectious diseases: challenges and therapeutic opportunities. *Future Med. Chem.* **2016,** *8* (1), 39-54.

9. (a) Muller, A. J.; DuHadaway, J. B.; Donover, P. S.; Sutanto-Ward, E.; Prendergast, G. C., Inhibition of indoleamine 2, 3-dioxygenase, an immunoregulatory target of the cancer suppression gene Bin1, potentiates cancer chemotherapy. *Nat. Med.* **2005,** *11* (3), 312-319; (b) Hou, D.-Y.; Muller, A. J.; Sharma, M. D.; DuHadaway, J.; Banerjee, T.; Johnson, M.; Mellor, A. L.; Prendergast, G. C.; Munn, D. H., Inhibition of indoleamine 2, 3-dioxygenase in dendritic cells by stereoisomers of 1-methyl-tryptophan correlates with antitumor responses. *Cancer Res.* **2007,** *67* (2), 792-801; (c) Muller, A. J.; Prendergast, G. C., Marrying immunotherapy with chemotherapy: why say IDO? *Cancer Res.* **2005,** *65* (18), 8065-8068.

10. Dolušić, E.; Frédérick, R., Indoleamine 2, 3-dioxygenase inhibitors: a patent review (2008–2012). *Expert Opin. Ther. Pat.* **2013,** *23* (10), 1367-1381.

11. (a) Austin, C. J.; Mizdrak, J.; Matin, A.; Sirijovski, N.; Kosim-Satyaputra, P.; Willows, R. D.; Roberts, T. H.; Truscott, R. J.; Polekhina, G.; Parker, M. W., Optimised expression and purification of recombinant human indoleamine 2, 3-dioxygenase. *Protein Expr. Purif.* **2004,** *37* (2), 392-398; (b) Littlejohn, T. K.; Takikawa, O.; Skylas, D.; Jamie, J. F.; Walker, M. J.; Truscott, R. J., Expression and purification of recombinant human indoleamine 2, 3-dioxygenase. *Protein Expr. Purif.* **2000,** *19* (1), 22-29; (c) Takikawa, O.; Kuroiwa, T.; Yamazaki, F.; Kido, R., Mechanism of interferon-gamma action. Characterization of indoleamine 2, 3-dioxygenase in cultured human cells induced by

interferon-gamma and evaluation of the enzyme-mediated tryptophan degradation in its anticellular activity. *J. Biol. Chem.* **1988,** *263* (4), 2041-2048; (d) Ren, S.; Liu, H.; Licad, E.; Correia, M. A., Expression of Rat Liver Tryptophan 2, 3-Dioxygenase inEscherichia coli: Structural and Functional Characterization of the Purified Enzyme. *Arch. Biochem. Biophys.* **1996,** *333* (1), 96-102; (e) Schutz, G.; Feigelson, P., Purification and properties of rat liver tryptophan oxygenase. *J. Biol. Chem.* **1972,** *247* (17), 5327-5332.

12. (a) Elvert, G.; Kappel, A.; Heidenreich, R.; Englmeier, U.; Lanz, S.; Acker, T.; Rauter, M.; Plate, K.; Sieweke, M.; Breier, G., Cooperative interaction of hypoxia-inducible factor-2α (HIF-2α) and Ets-1 in the transcriptional activation of vascular endothelial growth factor receptor-2 (Flk-1). *J. Biol. Chem.* **2003,***278* (9), 7520-7530; (b) Wu, Q.; Zhang, W.; Pwee, K.-H.; Kumar, P. P., Rice HMGB1 protein recognizes DNA structures and bends DNA efficiently. *Arch. Biochem. Biophys.* **2003,** *411* (1), 105-111.

13. Villaverde, A.; Carrió, M. M., Protein aggregation in recombinant bacteria: biological role of inclusion bodies. *Biotechnol Lett.* **2003,** *25* (17), 1385-1395.

14. (a) Chalmers, J.; Kim, E.; Telford, J.; Wong, E.; Tacon, W.; Shuler, M.; Wilson, D., Effects of temperature on Escherichia coli overproducing beta-lactamase or human epidermal growth factor. *Appl. Environ. Microbiol.* **1990,** *56* (1), 104-111; (b) Schein, C. H.; Noteborn, M. H., Formation of soluble recombinant proteins in Escherichia coli is favored by lower growth temperature. *Nat. Biotechnol.* **1988,** *6* (3), 291.

15. Richards, M. K.; Marletta, M. A., Characterization of neuronal nitric oxide synthase and a C415H mutant, purified from a baculovirus overexpression system. *Biochemistry* **1994,** *33* (49), 14723-14732.

16. Delcarte, J.; Fauconnier, M.-L.; Jacques, P.; Matsui, K.; Thonart, P.; Marlier, M., Optimisation of expression and immobilized metal ion affinity chromatographic purification of recombinant (His) 6-tagged cytochrome P450 hydroperoxide lyase in Escherichia coli. *J. Chromatogr. B* **2003,** *786* (1-2), 229-236.

17. Stojiljkovic, I.; Evavold, B. D.; Kumar, V., Antimicrobial properties of porphyrins. *Expert Opin. Investig. Drugs* **2001,** *10* (2), 309-320.

18. (a) Malachowski, W. P.; Winters, M.; DuHadaway, J. B.; Lewis-Ballester, A.; Badir, S.; Wai, J.; Rahman, M.; Sheikh, E.; LaLonde, J. M.; Yeh, S.-R., O-alkylhydroxylamines as rationally-designed mechanism-based inhibitors of indoleamine 2, 3-dioxygenase-1. *Eur. J. Med. Chem.* **2016,** *108*, 564-576; (b) Terentis, A. C.; Freewan, M.; Sempértegui Plaza, T. S.; Raftery, M. J.; Stocker, R.; Thomas, S. R., The

selenazal drug ebselen potently inhibits indoleamine 2, 3-dioxygenase by targeting enzyme cysteine residues. *Biochemistry* **2009,** *49* (3), 591-600.

19. (a) Sreerama, N.; Venyaminov, S. Y.; Woody, R. W., Estimation of protein secondary structure from circular dichroism spectra: inclusion of denatured proteins with native proteins in the analysis. *Anal. Biochem.* **2000,** *287* (2), 243-251; (b) Austin, C. J.; Kosim-Satyaputra, P.; Smith, J. R.; Willows, R. D.; Jamie, J. F., Mutation of cysteine residues alters the heme-binding pocket of indoleamine 2, 3-dioxygenase-1. *Biochem. Biophys. Res. Commun.* **2013,** *436* (4), 595-600.

20. Wu, J.-S.; Lin, S.-Y.; Liao, F.-Y.; Hsiao, W.-C.; Lee, L.-C.; Peng, Y.-H.; Hsieh, C.-L.; Wu, M.-H.; Song, J.-S.; Yueh, A., Identification of substituted naphthotriazolediones as novel tryptophan 2, 3-dioxygenase (TDO) inhibitors through structure-based virtual screening. *J. Med. Chem.* **2015,** *58* (19), 7807-7819.

21. Röhrig, U. F.; Awad, L.; Grosdidier, A.; Larrieu, P.; Stroobant, V.; Colau, D.; Cerundolo, V.; Simpson, A. J.; Vogel, P.; Van den Eynde, B. t. J., Rational design of indoleamine 2, 3-dioxygenase inhibitors. *J. Med. Chem.* **2010,** *53* (3), 1172-1189.

22. (a) Sono, M.; Cady, S. G., Enzyme kinetic and spectroscopic studies of inhibitor and effector interactions with indoleamine 2, 3-dioxygenase. 1. Norharman and 4-phenylimidazole binding to the enzyme as inhibitors and heme ligands. *Biochemistry* **1989,** *28* (13), 5392-5399; (b) Yang, S.; Li, X.; Hu, F.; Li, Y.; Yang, Y.; Yan, J.; Kuang, C.; Yang, Q., Discovery of tryptanthrin derivatives as potent inhibitors of indoleamine 2, 3-dioxygenase with therapeutic activity in Lewis lung cancer (LLC) tumor-bearing mice. *J. Med. Chem.* **2013,** *56* (21), 8321-8331.

23. (a) Sharma, M.; Dixit, A., Immune response characterization and vaccine potential of a recombinant chimera comprising B-cell epitope of Aeromonas hydrophila outer membrane protein C and LTB. *Vaccine* **2016,** *34* (50), 6259-6266;(b) Gengenbacher, M.; Xu, T.; Niyomrattanakit, P.; Spraggon, G.; Dick, T., Biochemical and structural characterization of the putative dihydropteroate synthase ortholog Rv1207 of Mycobacterium tuberculosis. *FEMS Microbiol. Lett.* **2008,** *287* (1), 128-135.

24. Laemmli, U. K., Cleavage of structural proteins during the assembly of the head of bacteriophage T4. *nature* **1970,** *227* (5259), 680.

25. Terentis, A. C.; Thomas, S. R.; Takikawa, O.; Littlejohn, T. K.; Truscott, R. J.; Armstrong, R. S.; Yeh, S.-R.; Stocker, R., The Heme Environment of Recombinant Human Indoleamine 2, 3-Dioxygenase Structural properties and substrate-ligand interactions.. *J. Biol. Chem.* **2002,** *277* (18), 15788-15794.

26. Ute, F.; Somi, R.; Aurelien, G.; Sylvian, B.; Vincent, S.; Luc, P.; Didier, C.; Pierre, V.; Benoit, J.; Vincent, Z., Rational design of 4-aryl-1, 2, 3-triazoles for indoleamine 2, 3-dioxygenase 1 inhibition. *J. Med. Chem* **2012,** *55*, 5270-5290.

27. Sono, M., Enzyme kinetic and spectroscopic studies of inhibitor and effector interactions with indoleamine 2, 3-dioxygenase. 2. Evidence for the existence of another binding site in the enzyme for indole derivative effectors. *Biochemistry* **1989,** *28* (13), 5400-5407.

CHAPTER 3

Development of N-hydroxyamidine based compounds as IDO1 inhibitors

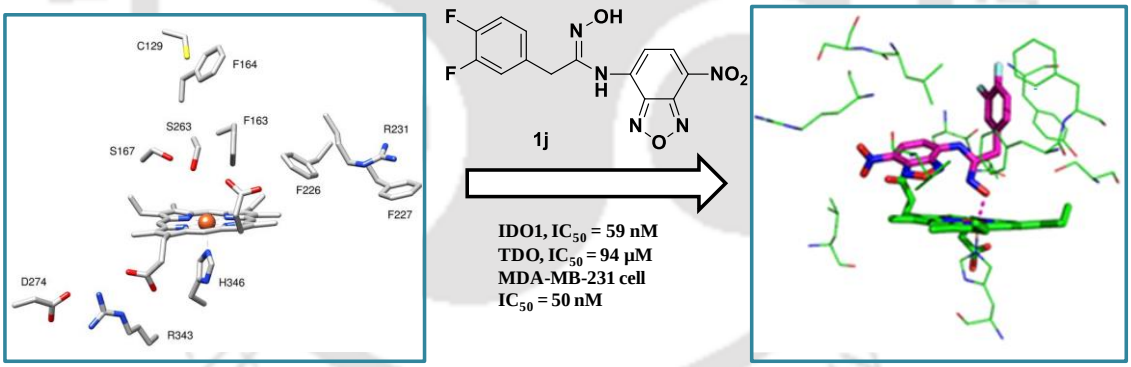

This chapter describes the synthesis and inhibitory activity of *N*-hydroxyamidine based compounds against purified IDO1 enzyme both under *in vitro* and cellular condition.

3.1. Background and focus of the present work

In the last decade, indoleamine 2,3-dioxygenase 1 (IDO1) mediated kynurenine pathway of L-tryptophan (L-Trp) metabolism is recognized as an important immunosuppressive pathway in tumor immuno-editing process. Blockade of this tumor induced immunosuppressive mechanism is regarded as an exciting approach against cancer.[1]

Both IDO1 and TDO catalyzes the initial and rate limiting step in the catabolism of L-Trp by the oxidative cleavage of the indole 2,3-double bond along the kynurenine pathway. TDO enzyme mainly catabolises L-Trp in the liver and systematically regulates L-Trp level in response to dietary intake. But, IDO1 is widely expressed in extra hepatic tissues. In healthy human, the activity of IDO1 is low and has limited physiological effects, but its deregulation has been identified in a variety of human malignancies, including ovarian, colorectal, pancreatic cancers and non-small-cell lung carcinoma.[1c, 2] Depletion of local L-Trp concentrations and the accumulation of the kynurenine pathway metabolites (quinolinic acid, kynurenic acid, 3-hydroxykynurenine, anthranilic acid and 3-hydroxyanthranilic acid) assists IDO1 enzyme to promote immune tolerance by increasing the differentiation and activation of immune-suppressive regulatory T cells under various physiological and patho-physiological conditions, including mammalian pregnancy, tumor resistance, autoimmunity, chronic inflammation, and chronic infections.[1b-d, 2c, 3] Cytokines like interferon-γ (IFN-γ), interleukins (IL-1,2), and tumour necrosis factor alpha (TNF-α) are mainly responsible for the over expression of IDO1 enzyme in the macrophages, epithelial and dendritic cells.[1f, 4] The over expression of IDO1 has been concerned in a variety of diseases, including cancer, neurodegenerative disorders (Alzheimer's disease), age-related cataract, and HIV-1 encephalitis.[1c, 5] Recent *in vivo* studies have established that systematic blockade of IDO1 activity with small molecule inhibitors in different animal models of cancers successfully suppressed the abnormal growth of tumors.[6] Accordingly, the inhibition of IDO1 restores the antitumor immune response and represents an effective adjuvant for chemotherapeutic and immunotherapeutic antitumor strategies.[6a, 7] Hence, IDO1 is a very promising target for cancer immunotherapy.

Several classes of potent IDO1 inhibitors containing the natural products, scaffolds of indole, quinone/iminoquinone, imidazoles, triazoles, hydroxyamidines and others have been reported. Presently, two IDO1 inhibitors, INCB024360 (Epacadostat) developed by Incyt Corporation and GDC-0919 (NLG919) produced by NewLink Genetics are under clinical trials for the treatment of different type of cancer.[8] Incyte

Corporation discovered *N*-hydroxyamidines as reversible, potent inhibitors of IDO1 enzyme. *N*-hydroxyamidine moiety containing compound 4-amino-*N*-(3-chloro-4-fluorophenyl)-*N'*-hydroxy-1,2,5-oxadiazole-3-carboxymidimade (**5l**) showed stronger inhibitory potency of IDO1 enzyme both *in vitro* and *in vivo* enzymatic assay with IC_{50} value of 67 nM and 19 nM, respectively.[9] This potent compound lowered the blood plasma level of kynurenine and restricted tumor growth in a mouse model. Another *N*-hydroxyamidine moiety containing compound CBR703 alter the activity of RNA polymerase from bacteria.[1c, 8c, 10] Hence, due to several biological activities hydroxyamidine based compounds have been found to be a useful drug scaffold.

The present study describes the synthesis, *in vitro* and cellular IDO1 enzyme inhibitory activity of a series of *N'*-hydroxyamidine moiety containing nitrobenzofurazan derivatives. Interestingly, *in vitro* IDO1 enzyme inhibitory activity of the resulting compounds showed stronger inhibitory potency in nanomolar range. Cellular IDO1 enzyme inhibitory activity of the selected compounds in MDA-MB-231 cells also showed stronger inhibitory potency with insignificant amount of cytotoxicity. In addition, they showed stronger selectivity for IDO1 enzyme by counter screening against TDO enzyme.

3.2. Results and discussion

3.2.1. Design and synthesis

Incyte Corporation identified *N*-hydroxyamidines as reversible, potent and competitive inhibitors of IDO1 enzyme through the high throughput screening (HTS).[1c, 9] Hydroxyamidine moiety containing compound INCB024360 in combination with antibody pembrolizumab is now in phase-II clinical trials for the treatment of several types of cancers.[1c] Another hydroxyamidine based potent compound, 4-amino-*N*-(3-chloro-4-fluorophenyl)-*N'*-hydroxy-1,2,5-oxadiazole-3-carboxymidimade (**5l**) showed stronger IDO1 inhibitory potency with enzymatic and cellular IC_{50} values of 67 nM and 19 nM (in Hela cell), respectively and reduce melanoma growth in mouse model.[9] A thorough molecular model studies showed that binding of the oxygen of this hydroxyamidines to the heme-iron is crucial for inhibiting IDO1 activity. The hydrophobic "pocket-A" of IDO1 enzyme was filled with the substituted phenyl ring of INCB024360 or **5l** and the furazan ring interact with the 7-propionate of the heme-group of IDO1 enzyme.[1c, 9] From the detailed mechanistic studies, it was suggested that in extra hepatic tissues the requirement for the IDO1 promoted oxidative cleavage of L-Trp is the addition of ferrous heme iron coordinated molecular oxygen across the C2-C3 double

bond and alkylperoxy transition/intermediate state or dioxetane intermediate state was formed during the transformation of L-Trp to *N*-formylkynurenine.[1c, 8c]

To discover compounds containing hydroxyamidine scaffold with better inhibitory potencies and to mimic the alkylperoxy transition/intermediate state, we synthesized a series of nitrobenzofurazan derivatives of substituted *N*′-hydroxy-2-phenylacetimidamides, with the substitution of one nitrogen atom in place of one oxygen atom of the peroxo-moiety (Figure 3.1). It was assumed that the substituted hydroxy-2-phenylacetimidamides would be positioned by the hydrophobic "pocket A" of IDO1 enzyme and interact with heme iron and can act as a mimic of the alkylperoxy transition/intermediate state during the transformation of L-Trp to *N*-formylkynurenine. Whereas, the benzofurazan moiety may interact with the 7-propionate of the heme group. The synthesis occurred in two steps by condensing phenylacetonitrile with hydroxylamine in basic condition and treating the resulting substituted *N*′-hydroxy-2-phenylacetimidamides with 4-chloro-7-nitrobenzofurazan (NBD-Cl) in the presence of $NaHCO_3$ in ethanolic solution to obtain the target compounds in moderate to good yields (Scheme 3.1).[11]

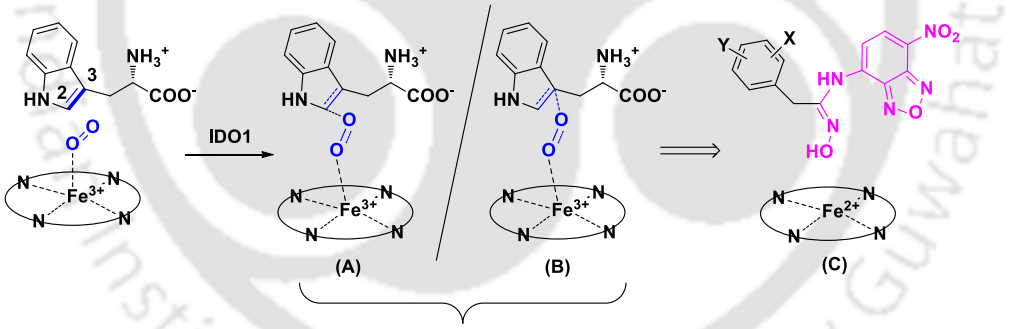

Figure 3.1. Proposed alkylperoxy transition/intermediate state of IDO1 (A and B) and its mimic (C).

Scheme 3.1. Synthesis of nitrobenzofurazan derivatives of *N*′-hydroxy-2-phenylacetimidamides

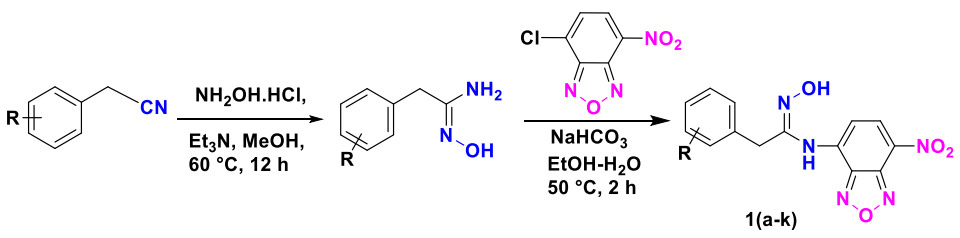

3.2.2. Inhibitory activities of hydroxyamidines against purified IDO1 enzyme

To evaluate the IDO1 enzyme inhibitory potencies of the synthesized nitrobenzofurazan derivatives, we measured the changes in absorbance values of the product produced from kynurenine and *p*-dimethylaminobenzaldehyde (*p*-DMAB) in acidic medium by UV-visible spectroscopy at 480 nm.[12] Spectral properties of the pure compounds (50 nM to 1 μM) showed no or little interference with the activity assay. The kinetic parameters, K_M and k_{cat} of the purified hIDO1 enzyme with L-Trp as substrate were measured by UV-visible spectroscopy and the values were 47.8 ± 2.5 μM and 3.7 ± 0.1 s^{-1}, respectively. To investigate the substitutions effect on the aryl ring for potential interactions with the hydrophobic residues positioned within the "pocket-A", methoxy or halogen groups was incorporated. Several research groups had successfully exploited these hydrophobic interactions in the optimization of the IDO1 inhibition efficacies.[1c, 12a, 13] The kinetic parameters (K_i), IC_{50} and ligand efficiency (L.E.) values of nitrobenzofurazan derivatives of *N*′-hydroxy-2-phenylacetimidamides, **1(a-k)** are shown in Table 3.1.

The structure activity relationship (SAR) studies demonstrated that halogen-substituted benzyl derivatives **1b**, **1f**, **1j** and **1k** were significantly more potent than the original benzyl lead **1a**. Among these tested *N*′-hydroxy-2-phenylacetimidamide derivatives, 3,4-dichloro substituted compound, **1k** showed 8.0-fold (IC_{50} = 39 nM) stronger hIDO1 inhibitory activity than the lead compound **1a** (IC_{50} = 307 nM). 3,4-difluoro substituted compound **1j** showed 5.2-fold (IC_{50} = 59 nM) stronger hIDO1 inhibition potency than unsubstituted parent compound **1a**. A moderate preference for fluoro-substitution at meta-, ortho- and para- positions was also demonstrated by the 2.3-3.1-fold improvement in hIDO1 enzyme inhibition activity. Interestingly 3,4-dichloro-substitution significantly enhances the hIDO1 inhibitory potency by 3.3-5.1-fold than its respective mono substituted derivatives. Similarly, synergistic effect of 3,4-difluoro substitution was also observed. The reported potent compound, 4-amino-*N*-(3-chloro-4-fluorophenyl)-*N*′-hydroxy-1,2,5-oxadiazole-3-carboxymidimade (**5l**) showed IC_{50} value of 91 nM under the experimental conditions, which is in consistent with the reported values.[9]

3.2.3. Inhibitory activities of hydroxyamidines against purified IDO1 enzyme by HPLC method

To confirm the efficacy, the IDO1 activity assay was also performed by HPLC analysis in the presence and absence of the potent compounds.[13a] The inhibitory concentrations of the

compounds were in the nanomolar range (Table 3.2) which was in consistent with the spectroscopic IC_{50} values. The potent compounds **1j** and **1k** showed IC_{50} values of 49 and 53 nM, respectively which were lower than the reported potent compound, **5l** under the similar experimental conditions.[9]

Table 3.1. Inhibitory activity of the nitrobenzofurazan derivatives of *N*′-hydroxy-2-phenylacetimidamides against purified human IDO1 enzyme

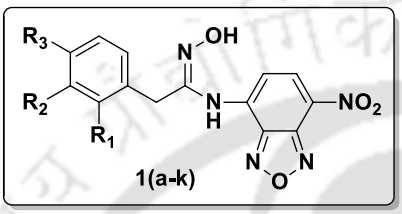

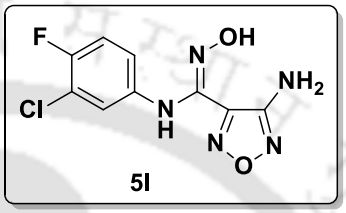

Compound	IDO1 inhibition		Ligand efficiency (LE) = 1.4 × pIC_{50}/HAC[b]
	IC_{50} (nM)[a]	K_i (nM)[a]	
1a; $R_1 = R_2 = R_3 = H$	307 ± 22	74 ± 15	0.396
1b; $R_1 = F, R_2 = R_3 = H$	102 ± 5	24 ± 2	0.408
1c; $R_1 = H, R_2 = F, R_3 = H$	131 ± 4	32 ± 1	0.401
1d; $R_1 = H, R_2 = Cl, R_3 = H$	199 ± 11	48 ± 3	0.391
1e; $R_1 = R_2 = H, R_3 = OCH_3$	128 ± 3	31 ± 0.8	0.386
1f; $R_1 = R_2 = H, R_3 = F$	98 ± 10	24 ± 2	0.409
1g; $R_1 = R_2 = H, R_3 = Cl$	127 ± 1	31 ± 0.2	0.402
1h; $R_1 = R_2 = H, R_3 = Br$	112 ± 7	27 ± 2	0.405
1i; $R_2 = H, R_1 = R_3 = F$	160 ± 12	39 ± 3	0.380
1j; $R_1 = H, R_2 = R_3 = F$	59 ± 5	14 ± 0.4	0.405
1k; $R_1 = H, R_2 = R_3 = Cl$	39 ± 1	9 ± 0.1	0.415
5l[c]	91 ± 2	22 ± 2	0.547

[a] IC_{50} and K_i values are the mean of five independent assays.

[b] HAC = heavy atom count.

[c] Reported compound.

Table 3.2. HPLC based IDO1 inhibition assay of the selected compounds

Compound	IDO1 inhibition IC_{50} (nM)[a]
1a	75 ± 7
1f	73 ± 6
1g	78 ± 7
1j	49 ± 4
1k	53 ± 5
5l[b]	67 ± 5

[a] IC_{50} values are the mean of three independent assays against purified enzymes.

[b] Reported compound.

Most of the compounds showed stronger hIDO1 inhibitory potencies. We hypothesized that the stronger effect of either *N*′-hydroxy or nitrobenzofurazan moiety of the compounds on hIDO1 inhibition could suppress the effect of substitution in *N*′-hydroxy-2-phenylacetimidamide derivatives. Separate inhibitory assay with 4-chloro-7-nitrobenzofurazan and 2-(3,4-difluorophenyl)-*N*′-hydroxyacetimidamide, a precursor for compound **1j** showed very weak or no inhibition of IDO1 enzyme activity under the similar experimental conditions (data not shown here). This signifies the importance of both nitrobenzofurazan and *N*′-hydroxy-2-phenylacetimidamide moiety for stronger inhibition of hIDO1 activity.

3.2.4. Spectroscopic studies for binding analysis of hydroxyamidines with IDO1 enzyme

To understand the ligand/substrate binding ability to IDO1 enzyme we have performed the UV-visible spectroscopic study as the UV-visible absorption properties of the porphyrin-ring are highly sensitive to the changes in the polarity of the heme-surroundings.[13a, 14] The UV-visible absorption spectra of ferric-IDO1 and deoxy ferrous-IDO1 were recorded in the absence and presence of compounds, **1b**, **1f**, **1j**, and **1k** (Figure 3.2A and 3.2B). The absorption spectrum of only ferric-IDO1 showed a Soret band centred at 404 nm, which is in accordance with the reported results.[14a, 14b, 15] In the presence of compound **1j**, this Soret peak showed a slight red shift of 2 nm with increase in intensity under the similar experimental condition (Figure 3.2A).

Figure 3.2B showed that in the absence of any inhibitor the deoxy ferrous-IDO1 enzyme exhibit Soret peak at 424 nm.[14a, 14b, 15] However, in the presence of inhibitors the Soret band shifted to 428 nm and appearance of new Q bands around 530/559 nm (Figure 3.2B). This indicates their probable binding with the Fe^{2+}-IDO1 enzyme possibly via the hydroxyl-oxygen of the *N*′-hydroxy-2-phenylacetimidamides. The absorption spectra of only compounds did not show any peak in this region (spectra not shown here). Although further studies are required to prove the coordination of the hydroxyamidines to heme-group of IDO1, but the results strongly support the proposed mimic of the epoxide intermediate state for the L-Trp oxidation by these hydroxyamidines.

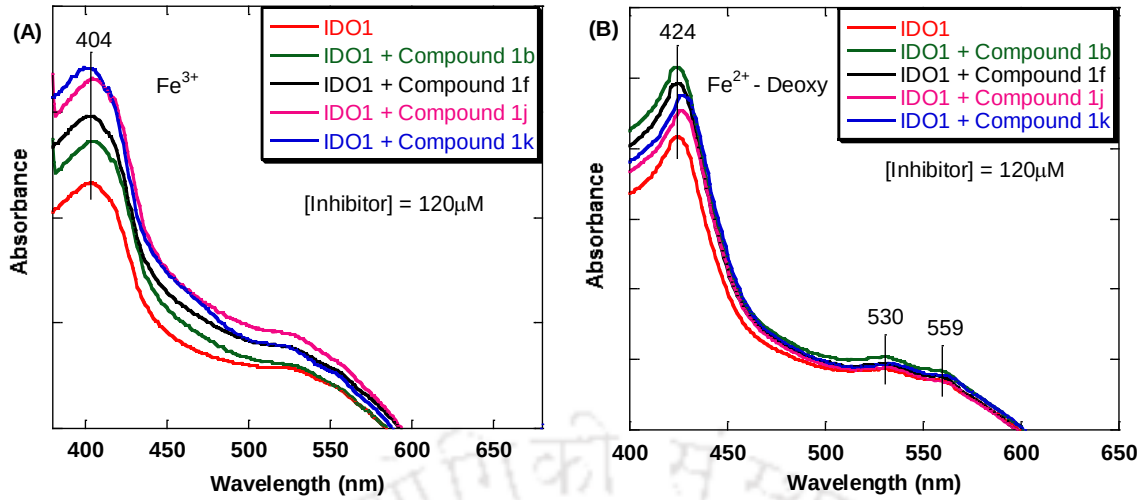

Figure 3.2. Normalized absorption spectra of ferric-IDO1 (A) and deoxy-ferrous-IDO1 enzyme (B) in the absence and presence of the 120 μM compounds in 100 mM potassium phosphate buffer at pH 6.5. Y-axis is not same for both the spectra. IDO1 enzyme concentration = 5.8 μM. The ferrous-deoxy reaction environment was generated by adding $Na_2S_2O_4$ under a N_2 atmosphere.

3.2.5. Cellular IDO1 inhibitory activities of hydroxyamidines

The therapeutic potencies of these hydroxyamidines were examined under the *in vitro* cellular environment using MDA-MB-231 breast cancer cell line. This cancer cell line contains mRNA of native human IDO1 enzyme and express IDO1 enzyme by interferon-γ (IFN-γ) inducer.[16] For this purpose, MDA-MB-231 cells were first incubated with human IFN-γ (20 ng/mL) for 48 h and then in the presence of tested compounds (20, 50, 100 and 500 nM) and L-Trp (150 μM) for additional 9 h. IDO1 enzyme inhibitory activity was estimated by measuring the formation of L-kynurenine using *p*-DMAB by UV-visible spectroscopy (Table 3.3).[12b, 13a, 16] Compound **1j** and **1k** show EC_{50} values of 50 nM and 71 nM respectively in MDA-MB-231 cells. Control compound, 4-amino-*N*-(3-chloro-4-fluorophenyl)-*N*′-hydroxy-1,2,5-oxadiazole-3-carboxymidimade (**5l**) showed EC_{50} values of 58 nM under the similar experimental conditions.[9] Cellular EC_{50} values of the compounds deviate from *in vitro* enzymatic IC_{50} values which could be due to the methylene blue-ascorbate regeneration system to remain IDO1 in active state (Fe^{2+}) or environmental effect on the assay system. In general, a good correlation between these two assays confirmed that these tested hydroxyamidine analogues are potent inhibitors of IDO1 enzyme.

Table 3.3. IDO1 enzyme inhibitory activity of the selected compounds in MDA-MB-231 cells

Compound	IDO1 inhibition in MDA-MB-231 cell[a] IC_{50} (nM)[b]
1b	110 ± 19
1f	151 ± 17
1g	110 ± 19
1j	50 ± 8
1k	71 ± 10
5l[c]	59 ± 4

[a] IDO1 protein expression in MDA-MB-231 cell was induced by human IFN-γ (20 ng/mL).

[b] IC_{50} values are the mean of five independent assays.

[c] Reported compound.

Insignificant level of cytotoxicity of the compounds (concentrations of IC_{50} and 2 × IC_{50} values from the enzymatic assay) in MDA-MB-231 cells was confirmed by MTT assay (Figure 3.3). Data were analyzed by plotting the absorbance of different amount of formazan at 570 nm against the mentioned concentrations of the compounds, obtained from three independent experiments. The more toxicity of the di-chloro substituted compound **1k** over di-fluoro substituted compound **1j** could be one of the reasons for the subtle difference in the IC_{50} values of compound **1j** and **1k** as measured by *in vitro* enzymatic and cellular assay. To investigate the morphological changes of the cells, MDA-MB-231 cells were treated with the compounds (concentrations of 2 × IC_{50} values from the enzymatic assay) for 48 h and morphological changes were observed using cytell imaging system (Figure 3.4). Morphological studies showed that after treatment of MDA-MB-231 cells with the potent compounds, number of cells decreases significantly which indicate the apoptotic cell death. Images were collected from three independent experiments at 10x magnification.

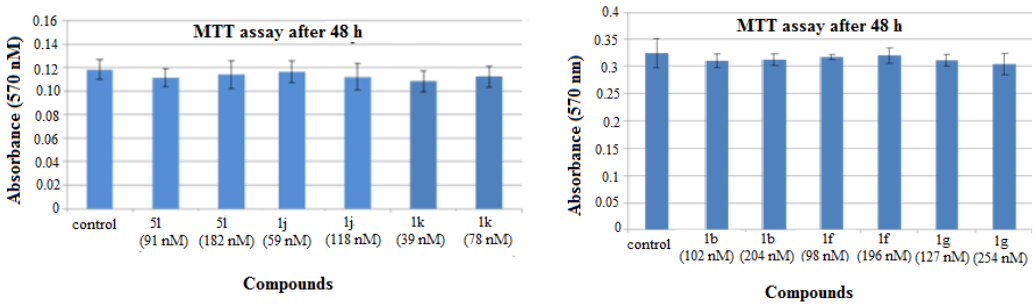

Figure 3.3. Effect of the selected hydroxyamidines on the viability of MDA-MB-231 cells.

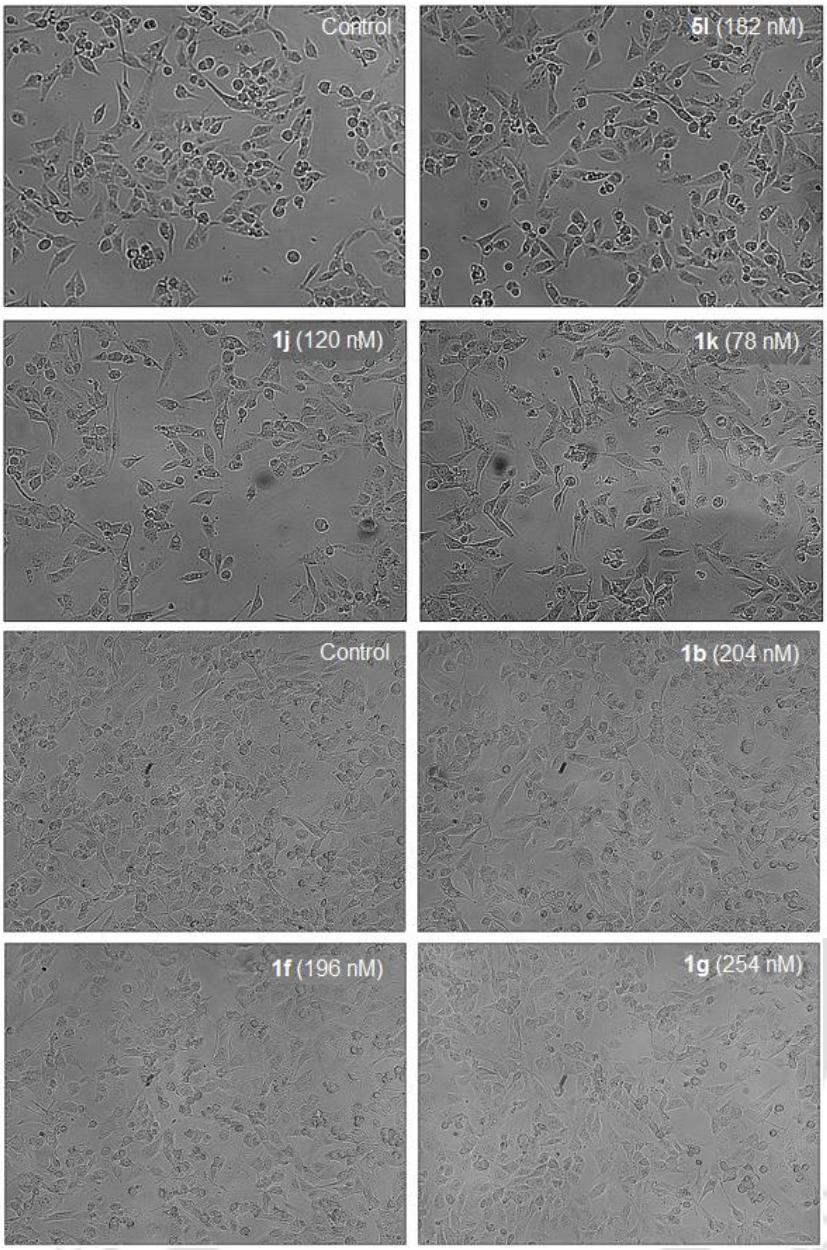

Figure 3.4. Effect of selected hydroxyamidines on the morphological changes of MDA-MB-231 cells.

3.2.6. Mode of IDO1 enzyme inhibition by the potent hydroxyamidines

To find out the mode of inhibition of the potent compounds with the IDO1 enzyme, we have performed kinetic studies with the variation of inhibitor concentration (25 to 150 nM) and L-Trp concentration (50 to 150 µM). [S]/V *vs.* inhibitor concentrations [I] plot showed that, selected compounds **1b, 1f, 1g, 1j** and **1k** exhibited competitive mode of IDO1 enzyme inhibition under the similar experimental conditions (Figure 3.5). [S] and V represent the substrate concentration and initial rate of the reaction, respectively.[17] . Control compound, 4-amino-*N*-(3-chloro-4-fluorophenyl)-*N′*-hydroxy-1,2,5-oxadiazole-

3-carboxymidimade (**5l**) also shows the competitive mode of inhibition of hIDO1 enzyme in our experimental conditions which is in consistent with the reported one.[9]

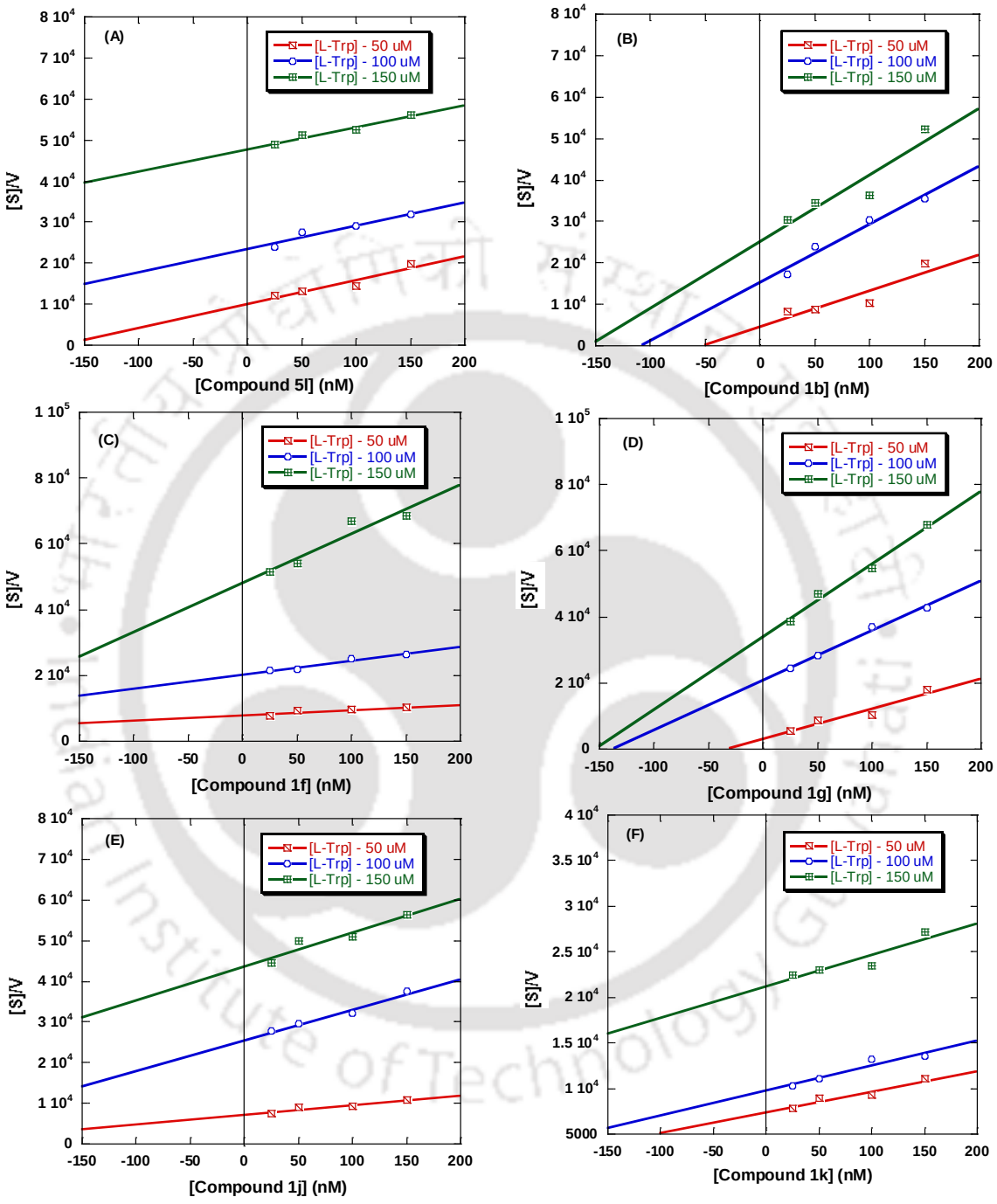

Figure 3.5. Determination of mode of inhibition of the potent compounds. Plot of [S]/V against concentrations of compounds **5l** (A), **1b** (B), **1f** (C), **1g** (D), **1j** (E) and **1k** (F). Concentration of L-Trp was varied from 50 to 150 μM. The concentrations of compounds were varied from 25 to 150 nM.

An important point is that IDO1 is an oxido-reductase enzyme and binding of O_2 to the heme-group is necessary for the transformation of L-Trp to *N*-formylkynurenine. Therefore, although the tested compounds followed competitive mode of IDO1 inhibition with respect to L-Trp but these compounds may follow different mode of inhibition with respect to O_2. Therefore, for thorough understanding, a further kinetic study with respect to O_2 is required, which is beyond the scope of the current study.

3.2.7. Probable mode of interaction of the potent compounds with IDO1 enzyme

The probable mode of interaction of the potent compounds with the IDO1 enzyme was investigated by molecular docking studies to verify the potency of the compounds (PDB code: 4PK5).[18] The docked structures revealed that 'pocket-A' of the IDO1 enzyme was filled with the substituted *N*′-hydroxy-phenylacetimidamide moieties of the compounds (Figure 3.6). Substituted aryl groups interacted with the hydrophobic amino acids present in 'pocket-A' of the IDO1 enzyme by the hydrophobic interaction. *N*′-hydroxy group interacted with Fe-atom and pyrrole ring of the heme-group. The nitrobenzofurazan-ring was placed in 'pocket-B' of the IDO1 enzyme. The nitro group of the nitrobenzofurazan-ring interacted with amino acids present in 'pocket-B' of the IDO1 enzyme. The reported compound, 4-amino-*N*-(3-chloro-4-fluorophenyl)-*N*′-hydroxy-1,2,5-oxadiazole-3-carboxymidimade (**5l**) also showed similar mode of interaction which is consistence with the reported mode of interaction.[9]

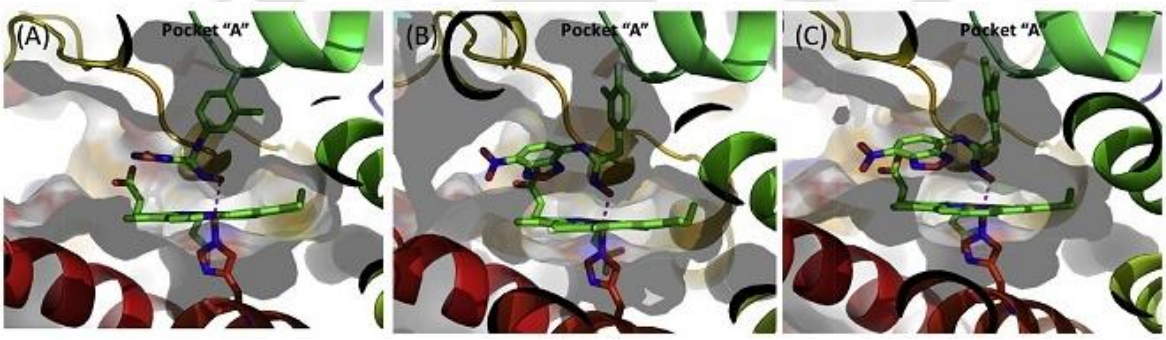

Figure 3.6. Predicted mode of interaction of the compounds, **5l** (A), **1j** (B), **1k** (C) with the active site of the human IDO1 enzyme (4PK5). The modelled structures were generated using MoleGro Virtual Docker (MVD), version 6.0. The oxygen and nitrogen atoms are shown in red and blue, respectively. Interactions are shown using dashed lines (red).

Therefore, both hydrogen bonding and hydrophobic interactions play significant roles in stronger binding of the compounds to the active site of IDO1 enzyme. However, there are no considerable differences in mode of interaction of the compounds from the same series with the IDO1 enzyme. Hence, not only volume and electronic properties of the substituents in the benzene ring but also the presence of nitrobenzofurazan and *N*′-hydroxyamidine moieties to the compound's core structure, are crucial for stronger binding to the IDO1 enzyme. It is also supported by the docking analyses that substituted hydroxy-2-phenylacetimidamides may act as a mimic of alkylperoxy transition/intermediate state of the transformation of L-Trp to *N*-formylkynurenine by IDO1 enzyme.

3.2.8. Inhibitory activities of hydroxyamidines against purified TDO enzyme

To find out the selectivity of the potent compounds for IDO1, we have performed activity assay with another heme containing enzyme TDO. It is well known that TDO enzyme is mainly located to the liver where it regulates the systemic L-Trp level through kynurenine pathway. The potent compounds showed inactivity (IC_{50}> 20 μM) in counter-screening assay against TDO enzyme (Table 3.4). Tested compounds showed significant selectivity (118 to 1593-fold) for IDO1 enzyme in comparison with TDO enzyme.

Table 3.4. Inhibitory activity of the selected compounds against purified human IDO1 and TDO enzymes

Compound	IDO1 inhibition IC_{50} (nM)[a]	TDO inhibition IC_{50} (μM)[a]	Selectivity ratio[b]
1b	102 ± 5	30 ± 2	297
1f	98 ± 10	51 ± 8	520
1g	127 ± 1	43 ± 2	338
1h	112 ± 7	65 ± 12	580
1i	160 ± 12	19 ± 1	118
1j	59 ± 5	94 ± 14	1593
1k	39 ± 1	32 ± 12	820
5l[c]	91 ± 2	24 ± 1	263

[a] IC_{50} values are the mean of five independent assays against purified enzymes.

[b] Selectivity ratio is calculated as (IC_{50} value of TDO)/(IC_{50} value of IDO1).

[c] Reported compound.

The most potent compound, **1j** (based on cellular assay) exhibited over 1500 fold stronger IDO1 inhibitory activity against that of TDO enzyme. TDO activity assay was also performed by HPLC analysis in the absence and presence of the potent compounds. These potent compounds also showed stronger selectivity for IDO1 over TDO enzyme inhibitions (Table 3.5).

Table 3.5. HPLC based IDO1 and TDO inhibition assay of the selected compounds

Compound	IDO1 inhibition IC_{50} (nM)[a]	TDO inhibition IC_{50} (µM)[a]	Selectivity ratio[b]
1b	75 ± 7	13 ± 1	173
1f	73 ± 6	71 ± 4	973
1g	78 ± 7	35 ± 4	449
1j	49 ± 4	89 ± 5	1816
1k	53 ± 5	15 ± 2	283
5l[c]	67 ± 5	11 ± 2	164

[a] IC_{50} values are the mean of five independent assays against purified enzymes.

[b] Selectivity ratio is calculated as (IC_{50} value of TDO)/(IC_{50} value of IDO1).

[c] Reported compound.

In this work, we have designed and synthesized a series of nitrobenzofurazan derivatives of the *N'*-hydroxy-phenylacetimidamides for the rational optimization of IDO1 enzyme inhibitors based on hydroxyamidine moiety. The *in vitro* IDO1 enzyme inhibitory activity studies of the synthesized compounds showed that compounds with suitable substitutions in the benzene ring have stronger potency in the nanomolar (< 100 nM) range. The *in vitro* cellular IDO1 enzyme inhibitory activity of these selected compounds also showed the stronger potency (IC_{50} = 50-151 nM) with no/ negligible level of toxicity and the therapeutic potency of the nitrobenzofurazan derivatives of *N'*-hydroxyamidines. The stronger IDO1 enzyme inhibitory properties of these compounds were supported by the molecular modelling studies. So far, there are limited potent IDO1 inhibitors containing hydroxyamidine moiety.[9] The IDO1 enzyme kinetics studies of the tested compounds showed competitive mode of inhibition. The TDO enzyme activity of the potent hydroxyamidine analogues also showed 118 to 1593-fold stronger selectivity for IDO1 enzyme. Hence the structural simplicity, stronger IDO1 inhibitory potency, low cytotoxicity, and inactivity for TDO enzyme support further development of nitrobenzofurazan derivatives of hydroxyamidines as a potential drug target.

3.3. Conclusion

We prepared a series of *N*′-hydroxyamidine moiety containing nitrobenzofurazan derivatives with good yield. Most of the tested compounds showed strong *in vitro* IDO1 enzyme inhibitory activity which could be due to the stronger effect of either *N*′-hydroxy or nitrobenzofurazan moiety on hIDO1 binding that suppressed the effect of substitution in *N*′-hydroxy-2-phenylacetimidamide moiety. These hydroxyamidine derivatives also exhibited stronger selectivity for IDO1 enzyme over TDO enzyme. The ligand efficiencies of > 0.4 suggests that these hydroxyamidine derivatives are promising therapeutic tools. Cellular EC_{50} values showed that nitrobenzofurazan derivatives of hydroxyamidines **1j** and **1k** have negligible toxicity and stronger potencies. Overall, our findings suggest that compounds with hydroxyamidine and nitrobenzofurazan moieties are potential inhibitor of IDO1 enzyme and can be used as drug target in cancer and other human diseases.

3.4. Experimental section

3.4.1. General information

All reagents were purchased from different commercial sources and used directly without further purification. Column chromatography was performed using 60-120 mesh silica gel. Reactions were monitored by thin-layer chromatography (TLC) on silica gel 60 F254 (0.25 mm). ^{1}H NMR and ^{13}C NMR were recorded at 400 and 100 MHz respectively, with Varian AS400 spectrometer and 600 and 151 MHz respectively, with Bruckner spectrometer, using TMS as an internal standard with $CDCl_3$ and DMSO-d_6. The coupling constant (J values) and chemical shifts (δppm) were described in Hertz (Hz) and parts per million (ppm) respectively. Multiplicities are described as follows: s (singlet), d (doublet), t (triplet), m (multiplet) and br (broadened). High resolution mass spectra (HRMS) were recorded at Agilent Q-TOF mass spectrometer with Z-spray source using built-in software for analysis of the recorded data.

3.4.2. General procedure for the synthesis of substituted hydroxyamidines

To a stirring solution of substituted benzonitrile/ phenylacetonitrile (1 mmol) in anhydrous methanol (20 mL) under N_2 atmosphere was added hydroxylamine hydrochloride (1.2 mmol). Triethylamine (2.5 mmol) was added under continuous stirring condition and the mixture was then heated under reflux condition for overnight at 60 °C and continued until complete consumption of the starting material (monitored by TLC).[9]

The excess solvent was then removed under reduced pressure and the obtained residue was washed successively with water and brine, and extracted with ethylacetate (3 × 10 mL). The organic layer was dried over anhydrous Na_2SO_4 and concentrated under reduced pressure. This reaction mixture was purified using silica gel column chromatography with a gradient solvent system of 10-20% ethylacetate to hexane to obtain the desired product with an average yield of 70-80%.

3.4.3. General procedure for the synthesis of 2-substituted *N'*-hydroxy, *N*- (7 nitro benzoxadiazole) imidamide

Sodium bicarbonate (3.5 mmol) was added to a stirring solution of 2-substituted *N'*-hydroxyimidamide (1.1 mmol) in 20 mL of EtOH/H_2O (9:1) and the solution was stirred for 10 min at room temperature. To this mixture an ethanolic solution of 4-chloro 7-nitrobenzofurazan (1 mmol) was added dropwise under continuous stirring condition and the resulting solution was stirred at 50 °C for another 2-4 hours.[10] After completion of the reaction (monitored by TLC) the excess solvent was removed under reduced pressure and the pH adjusted to 1.5 using 1N HCl solution. Then aqueous layer was extracted with dichloromethane (3 × 20 ml) and the organic layer was dried over anhydrous Na_2SO_4 and concentrated under reduced pressure. The reaction mixture was further purified using silica gel column chromatography using 20-30% ethylacetate to hexane gradient solvent system to afford the desired pure product with 60-90% yield.

3.4.4. Spectroscopic characterization of the synthesized compounds

(Z)-*N'*-hydroxy-*N*-(7-nitrobenzo[c][1,2,5]oxadiazol-4-yl)-2-phenylacetimidamide (1a): As red semi solid (90% yield); ^{1}H NMR (400 MHz, $CDCl_3$ + DMSO-d_6) δppm 8.59 (d, 1H, J = 8 Hz), 7.45 (d, 1H, J = 8 Hz), 7.41-7.34 (m, 5H), 5.10 (br, s, 1H), 3.66 (s, 2H); ^{13}C NMR (151 MHz, $CDCl_3$ + DMSO-d_6) δppm 158.5, 154.4, 144.2, 144.0, 135.1, 134.9, 129.2, 129.0, 127.8, 106.7, 37.2; HRMS (ESI) calcd. for $C_{14}H_{11}N_5O_4$ $[M + H]^+$ 314.0884, found 314.0909.

(Z)-2-(2-fluorophenyl)-*N'*-hydroxy-*N*-(7-nitrobenzo[c][1,2,5]oxadiazol-4-yl)acetimidamide (1b): As yellow solid (85 % yield; mp:148-150 °C); ^{1}H NMR (600 MHz, $CDCl_3$ + DMSO-d_6) δppm 8.48-8.45 (m, 1H), 7.29-7.25 (m, 2H), 7.20-7.18 (m, 1H), 7.06-7.04 (m, 1H), 7.01-6.99 (m, 1H), 5.69 (br, s, 1H), 3.57 (s, 2H); ^{13}C NMR (100 MHz, $CDCl_3$ + DMSO-d_6) δppm 157.9, 154.4, 144.2, 144.0, 135.2, 131.1, 129.6, 129.6,

127.2, 124.8, 119.7, 115.6, 106.6, 30.5; HRMS (ESI) calcd. for $C_{14}H_{10}FN_5O_4$ $[M + H]^+$ 332.0790, found 332.0789.

(Z)-2-(3-fluorophenyl)-*N'*-hydroxy-*N*-(7-nitrobenzo[c][1,2,5]oxadiazol-4-yl)acetimidamide (1c): As yellow solid (70 % yield; mp:140-142 °C); ^{1}H NMR (600 MHz, $CDCl_3$ + DMSO-d_6) δppm 8.61-8.54 (m, 1H), 7.38-7.31 (m, 3H), 7.20-6.93 (m, 2H), 5.84 (s, 1H), 3.55 (s, 2H); ^{13}C NMR (151 MHz, $CDCl_3$ + DMSO-d_6) δppm 163.9, 162.3, 158.3, 154.5, 144.2, 144.0, 137.8, 135.2, 130.5, 124.7, 116.1, 114.6, 106.6, 36.9; HRMS (ESI) calcd. for $C_{14}H_{10}FN_5O_4$ $[M + H]^+$ 332.0790, found 332.0791.

(Z)-2-(3-chlorophenyl)-*N'*-hydroxy-*N*-(7-nitrobenzo[c][1,2,5]oxadiazol-4-yl)acetimidamide (1d): As orange solid (87% yield; mp: 152-154 °C); ^{1}H NMR (400 MHz, $CDCl_3$ + DMSO-d_6) δppm 8.59 (d, 1H, J = 8 Hz), 7.44 (d, 1H, J = 8 Hz), 7.36-7.32 (m, 3H), 7.26-7.24 (m, 1H), 5.14 (br, s, 1H), 3.64 (s, 2H); ^{13}C NMR (151 MHz, $CDCl_3$ + DMSO-d_6) δppm 158.0, 154.0, 143.5, 143.4, 137.3, 134.8, 129.5, 128.4, 126.8, 126.6, 106.0, 36.1; HRMS (ESI) calcd. for $C_{14}H_{10}ClN_5O_4$ $[M + H]^+$ 348.0494, found 348.0525.

(Z)-*N'*-hydroxy-2-(4-methoxyphenyl)-*N*-(7-nitrobenzo[c][1,2,5]oxadiazol-4-yl)acetimidamide (1e): As orange solid (80 % yield; mp: 166-168 °C); ^{1}H NMR (400 MHz, $CDCl_3$ + DMSO-d_6) δppm 8.45 (d, 1H, J = 8 Hz), 7.26 (d, 1H, J = 8 Hz), 7.13-7.08 (m, 1H), 6.72 (d, 2H, J = 8 Hz), 3.61 (s, 3H), 3.36 (s, 2H); ^{13}C NMR (151 MHz, $CDCl_3$ + DMSO-d_6) δppm 158.8, 154.3, 143.8, 143.7, 135.0, 129.7, 126.8, 114.0, 106.3, 55.1, 36.0; HRMS (ESI) calcd. for $C_{15}H_{13}N_5O_5$ $[M + H]^+$ 344.0989, found 344.1020.

(Z)-2-(4-fluorophenyl)-*N'*-hydroxy-*N*-(7-nitrobenzo[c][1,2,5]oxadiazol-4-yl)acetimidamide (1f): As yellow solid (85 % yield; mp: 170-172 °C); ^{1}H NMR (600 MHz, $CDCl_3$ + DMSO-d_6) δppm 8.43 (d, 1H, J = 12 Hz), 7.26-7.18 (m, 3H), 6.89-6.85 (m, 2H), 5.81 (br, s, 1H), 3.42 (s, 2H); ^{13}C NMR (100 MHz, $CDCl_3$ + DMSO-d_6) δppm 162.8, 160.3, 158.5, 154.1, 143.6, 143.5, 135.0, 130.9, 130.1, 130.1, 128.2, 115.2, 106.1, 35.8; HRMS (ESI) calcd. for $C_{14}H_{10}FN_5O_4$ $[M + H]^+$ 332.0790, found 332.0789.

(Z)-2-(4-chlorophenyl)-*N'*-hydroxy-*N*-(7-nitrobenzo[c][1,2,5]oxadiazol-4-yl)acetimidamide (1g): As yellow solid (85% yield; mp: 163-165 °C); ^{1}H NMR (400 MHz, $CDCl_3$ + DMSO-d_6) δppm 8.59 (d, 1H, J = 8 Hz), 7.43 (d, 1H, J = 8 Hz), 7.38-7.36

(m, 2H), 7.30-7.28 (m, 2H), 5.12 (br, s, 1H), 3.63 (s, 2H); ^{13}C NMR (151 MHz, $CDCl_3$ + DMSO-d_6) δppm 158.2, 154.1, 143.6, 143.4, 134.8, 133.7, 132.5, 129.9, 128.3, 106.1, 35.9; HRMS (ESI) calcd. for $C_{14}H_{10}ClN_5O_4$ $[M + H]^+$ 348.0494, found 348.0521.

(Z)-2-(4-bromophenyl)-*N'*-hydroxy-*N*-(7-nitrobenzo[c][1,2,5]oxadiazol-4-yl)acetimidamide (1h): As brown solid (75 % yield; mp: 185-187 °C); ^{1}H NMR (600 MHz, MeOD-d_4 + $CDCl_3$ + DMSO-d_6) δppm 8.70 (d, 1H, J = 9 Hz), 7.52 (d, 2H, J = 8.4 Hz), 7.43 (d, 1H, J = 8.4 Hz), 7.36 (d, 2H, J = 8.4 Hz), 3.55 (s, 2H); ^{13}C NMR (100 MHz, $CDCl_3$ + DMSO-d_6) δppm 161.6, 155.6, 145.4, 136.6, 132.6, 132.4, 131.6, 128.7, 126.9, 117.4, 112.3, 107.4, 37.1; HRMS (ESI) calcd. for $C_{14}H_{10}BrN_5O_4$[M + H]$^+$ 391.9989, found 391.9989.

(Z)-2-(2,4-difluorophenyl)-*N'*-hydroxy-*N*-(7-nitrobenzo[c][1,2,5]oxadiazol-4-yl)acetimidamide (1i): As yellow solid (70 % yield; mp:174-176 °C); ^{1}H NMR (600 MHz, $CDCl_3$ + DMSO-d_6) δppm 8.59-8.58(m, 1H), 7.39-7.35 (m, 3H), 6.91-6.87 (m, 1H), 5.87 (br, s, 1H), 3.65 (s, 2H); ^{13}C NMR (151 MHz, $CDCl_3$ + DMSO-d_6) δppm 157.5, 154.2, 144.0, 143.8, 135.0, 131.7, 128.9, 120.7, 111.8, 106.5, 103.8, 29.8; HRMS (ESI) calcd. for $C_{14}H_9F_2N_5O_4$ $[M + H]^+$ 350.0695, found 350.0692.

(Z)-2-(3,4-difluorophenyl)-*N'*-hydroxy-*N*-(7-nitrobenzo[c][1,2,5]oxadiazol-4-yl)acetimidamide (1j): As yellow solid (65% yield; mp: 165-167 °C); ^{1}H NMR (600 MHz, $CDCl_3$ + DMSO-d_6) δppm 8.30-8.26 (m, 1H), 7.13-7.06 (m, 2H), 6.96-6.93 (m, 1H), 6.82 (s, 1H), 5.86 (br s, 1H), 3.25 (s, 2H); ^{13}C NMR (151 MHz, $CDCl_3$ + DMSO-d_6) δppm 158.1, 154.2, 143.9, 143.7, 135.0, 132.3, 128.7, 124.9, 117.8, 117.7, 117.3, 117.2, 106.4, 36.1; HRMS (ESI) calcd. for $C_{14}H_9F_2N_5O_4$ $[M + H]^+$ 350.0695, found 350.0695.

(Z)-2-(3,4-dichlorophenyl)-*N'*-hydroxy-*N*-(7-nitrobenzo[c][1,2,5]oxadiazol-4-yl)acetimidamide (1k): As yellow solid (88 % yield; mp:183-185 °C); ^{1}H NMR (600 MHz, $CDCl_3$ + DMSO- d_6) δppm 8.52 (d, 1H, J = 6 Hz), 7.44 (s, 1H), 7.32 (d, 2H, J = 6 Hz), 7.19 (d, 1H, J = 12 Hz), 6.04 (br s, 1H), 3.49 (s, 2H); ^{13}C NMR (100 MHz, $CDCl_3$ + DMSO-d_6) δppm 157.9, 154.2, 143.9, 143.7, 135.7, 135.0, 132.4, 131.2, 130.8, 130.5, 128.8, 128.3, 106.4, 36.1; HRMS (ESI) calcd. for $C_{14}H_9Cl_2N_5O_4$ $[M + H]^+$ 382.0104, found 382.0113.

3.4.5. Purification of the compounds by HPLC analysis

Before performing the *in vitro* enzyme activity, cellular activity, MTT assay, morphological analysis and others, all the synthesized compounds were further purified by analytical-HPLC analyses (with a purity level ≥ 94-95%). Prior to the initiation of the purification process, all the compounds were dissolved in 60% MeOH and 40% H_2O, at final concentrations between 1-2 mM, and the resulting solution filtered using Millipore syringe filters (0.22 µm pore size). Two litres of the running buffer, 60% MeOH and 40% H_2O, were also filtered and sonicated for removal of contaminants and air bubbles. Prior to loading the sample, a Hypersil GOLD aQ reverse phase C18 analytical column (Thermo Scientific) was pre-incubated with the running buffer (60% MeOH and 40% H_2O). The UV detectors of Varian # HPLC system was set at 465 nm. The sample's injection volume and flow rate were adjusted to 20 µL and 1 mL/min respectively and the pure compounds peak was eluted after ~7 min. This step was repeated for more than 10-times to get sufficient amount of the pure compounds. All the collected fractions for each compound were dried under reduced pressure and confirmed via mass spectrometry analysis.

3.4.6. Expression and purification of recombinant human IDO1 and TDO enzyme

As described earlier in chapter 2 section 2.4.5.

3.4.7. IDO1 and TDO inhibition assay by spectrophotometric technique

As described earlier in chapter 2 section 2.4.7.3. For the inhibition study, compound concentration was varied from 0.05 to 1 µM for IDO1 and 0.1 to 10 µM for TDO. The IC_{50} values of the compounds were analyzed by repeating this experiments five times. K_i values were also calculated using the measured IC_{50} and K_M values.

3.4.8. IDO1 and TDO inhibition assay by HPLC analysis

As described earlier in chapter 2 section 2.4.7.4. For the inhibition study compound concentration was used 0.05 to 0.1 µM for IDO1 and 10 µM for TDO. The IC_{50} values of the compounds were calculated from the standard curve.

3.4.9. Spectroscopic measurements

As described earlier in chapter 2 section 2.4.7.1. Concentration of IDO1 enzyme and compound used for the study was 5.8 µM and 120 µM, respectively.

3.4.10. Cellular activity assay

MDA-MB-231 breast cancer cells were chosen for the *in vitro* cellular assay. 50000 cells were seeded in each well of a 24-well plate in DMEM/F12 complete media and were allowed to adhere overnight. After that, the cells were treated with human IFN-γ (20 ng/mL) in complete media for a period of 48 h. This treatment is reported to allow over-expression of IDO1 enzyme in MDA-MB-231 cells.[16] Next, the cells were treated with appropriate concentrations of the compounds (20 nM, 50 nM, 100 nM and 500 nM) for a period of 4 h. Following this, 150 μM L-Trp was added and treated for additional period of 5 h. Cells stimulated with IFN-γ alone served as negative control while cells stimulated with IFN-γ and then with 150 μM L-Trp served as positive control. Post treatment phase, the cells were washed with sterile cell-culture grade PBS and were trypsinized and centrifuged at 1000 rpm. The cell pellet was dissolved again in sterile PBS and centrifuged at 1000 rpm as a period of washing. The pellet was hypotonically lysed in 10 mM HEPES buffer by passing through a sterile syringe 10 times. This lysate was used for standard IDO1 assay as mentioned earlier.[2a, 12a, 13a] IC_{50} values were determined for each inhibitor accordingly.

3.4.11. MTT assay and morphological analysis

The dye MTT (3-(4,5-Dimethylthiazol-2-yl)-2,5-Diphenyltetrazolium Bromide) was used to measure cellular viability. 10000 cells were seeded overnight in 96 well plate in total volume of 0.2 mL DMEM/F12 complete medium.[19] The next morning, cells were washed twice with cell culture grade phosphate buffer saline (PBS) and were incubated with the IDO1 inhibitors (at IC_{50} and 2 × IC_{50} values respectively) in 0.2 mL of DMEM/F12 serum free medium (incomplete medium) for 24 h and 48 h. Cells treated with incomplete medium alone were considered as 100% viable. After the treatment period, the cells were washed twice with PBS and taken for morphological analysis via cytell imaging system (GE Healthcare). Images were collected at 10x magnification. After imaging, each well was incubated with 100 μL of MTT (0.5 mg/ml in PBS) for 4h at 37 °C with 5% CO_2. Then, MTT solution was removed and the formazan crystals were dissolved in 100 μL cell culture grade DMSO. The absorbance was determined using a spectrophotometer (SpectraMax M2) at 570nm and 660 nm (to subtract scattering effects of crystals).

3.4.12. Determination of inhibition modes

As described earlier in chapter 2 section 2.4.7.5. The IDO1 activity assay was performed using L-Trp concentrations between 50-150 µM and the inhibitor concentrations between 25-150 nM. The mode of inhibition was determined from the plot of [S]/V against inhibitor concentration [I]. Where, [S] and V represent the L-Trp concentration and initial rate of the enzymatic reaction, respectively.

3.4.13. In-silico molecular docking analysis

Molecular docking studies to understand the probable mode of interaction of the compounds with hIDO1 enzyme (PDB code: 4PK5) was performed using MoleGro Virtual Docker version 6.0 (Molegro ApS, Aarhus, Denmark).[18, 20] To generate apo-protein, the ligands were removed from the co-crystal structures and then were processed by energy minimization. The energy minimized three-dimensional structure of the ligands was prepared by using the GlycoBioChem PRODRG2 server (http://davapc1.bioch.dundee.ac.uk/prodrg/). The occupied position of the ligand PIM (in the crystal structure) was used as the center of docking site (radius: 12 Å; and center: x = 64.3, y = 54.5, z = 19.3). Other parameters were set default during docking analyses. In each docking run, two hundred docked structures were generated for an individual ligand. Energetically favoured docked conformations were evaluated on the basis of the moledock and re-rank scores. The docking poses were exported and examined using PyMOL software (The PyMol Molecular Graphics System, Version 1.0r1, Schrödinger, LLC).

3.5. References

1. (a) Qian, S.; Zhang, M.; Chen, Q.; He, Y.; Wang, W.; Wang, Z., Correction: IDO as a drug target for cancer immunotherapy: recent developments in IDO inhibitors discovery. *RSC Adv.* **2016,** *6* (66), 61267-61267; (b) Mellor, A. L.; Munn, D. H., IDO expression by dendritic cells: tolerance and tryptophan catabolism. *Nat. Rev. Immunol.* **2004,** *4* (10), 762-774; (c) Röhrig, U. F.; Majjigapu, S. R.; Vogel, P.; Zoete, V.; Michielin, O., Challenges in the discovery of indoleamine 2, 3-dioxygenase 1 (IDO1) inhibitors. *J. Med. Chem.* **2015,** *58* (24), 9421-9437; (d) Kershaw, M. H.; Westwood, J. A.; Slaney, C. Y.; Darcy, P. K., Clinical application of genetically modified T cells in cancer therapy. *Clin. Transl. Immunol.* **2014,** *3* (5), e16; (e) Dunn, G. P.; Old, L. J.; Schreiber, R. D., The immunobiology of cancer immunosurveillance and immunoediting.

Immunity **2004,** *21* (2), 137-148; (f) Zou, W., Immunosuppressive networks in the tumour environment and their therapeutic relevance. *Nat. Rev. Cancer* **2005,** *5* (4), 263-274.

2. (a) Takikawa, O.; Yoshida, R.; Kido, R.; Hayaishi, O., Tryptophan degradation in mice initiated by indoleamine 2, 3-dioxygenase. *J. Biol. Chem.* **1986,** *261* (8), 3648-3653; (b) Yamamoto, S.; Hayaishi, O., Tryptophan pyrrolase of rabbit intestine D-and L-tryptophan-cleaving enzyme or enzymes. *J. Biol. Chem.* **1967,** *242* (22), 5260-5266; (c) Uyttenhove, C.; Pilotte, L.; Théate, I.; Stroobant, V.; Colau, D.; Parmentier, N.; Boon, T.; Van den Eynde, B. J., Evidence for a tumoral immune resistance mechanism based on tryptophan degradation by indoleamine 2, 3-dioxygenase. *Nat. Med.* **2003,** *9* (10), 1269-1274; (d) Platten, M.; Wick, W.; Van den Eynde, B. J., Tryptophan catabolism in cancer: beyond IDO and tryptophan depletion. *Cancer Res.* **2012,** *72* (21), 5435-5440.

3. Fallarino, F.; Grohmann, U.; You, S.; McGrath, B. C.; Cavener, D. R.; Vacca, C.; Orabona, C.; Bianchi, R.; Belladonna, M. L.; Volpi, C., The combined effects of tryptophan starvation and tryptophan catabolites down-regulate T cell receptor ζ-chain and induce a regulatory phenotype in naive T cells. *J. Immunol.* **2006,** *176* (11), 6752-6761.

4. (a) Vécsei, L.; Szalárdy, L.; Fülöp, F.; Toldi, J., Kynurenines in the CNS: recent advances and new questions. *Nat. Rev. Drug Discov.* **2013,** *12* (1), 64-82; (b) Croitoru-Lamoury, J.; Lamoury, F. M.; Caristo, M.; Suzuki, K.; Walker, D.; Takikawa, O.; Taylor, R.; Brew, B. J., Interferon-γ regulates the proliferation and differentiation of mesenchymal stem cells via activation of indoleamine 2, 3 dioxygenase (IDO). *PLoS One.* **2011,** *6* (2), e14698.

5. (a) Heyes, M.; Saito, K.; Crowley, J.; Davis, L.; Demitrack, M.; Der, M.; Dilling, L.; Elia, J.; Kruesi, M.; Lackner, A., Quinolinic acid and kynurenine pathway metabolism in inflammatory and non-inflammatory neurological disease. *Brain* **1992,** *115* (5), 1249-1273; (b) Wichers, M. C.; Maes, M., The role of indoleamine 2, 3-dioxygenase (IDO) in the pathophysiology of interferon-α-induced depression. *J. Psychiatry. Neurosci.* **2004,** *29* (1), 11-17; (c) Vazquez, S.; Parker, N. R.; Sheil, M.; Truscott, R. J., Protein-bound kynurenine decreases with the progression of age-related nuclear cataract. *Invest. Ophthalmol. Vis. Sci.* **2004,** *45* (3), 879-883; (d) Sardar, A. M.; Reynolds, G. P., Frontal cortex indoleamine-2, 3-dioxygenase activity is increased in HIV-1-associated dementia. *Neurosci. Lett.* **1995,** *187* (1), 9-12.

6. (a) Muller, A. J.; DuHadaway, J. B.; Donover, P. S.; Sutanto-Ward, E.; Prendergast, G. C., Inhibition of indoleamine 2, 3-dioxygenase, an immunoregulatory

target of the cancer suppression gene Bin1, potentiates cancer chemotherapy. *Nat. Med.* **2005,** *11* (3), 312-319; (b) Hou, D.-Y.; Muller, A. J.; Sharma, M. D.; DuHadaway, J.; Banerjee, T.; Johnson, M.; Mellor, A. L.; Prendergast, G. C.; Munn, D. H., Inhibition of indoleamine 2, 3-dioxygenase in dendritic cells by stereoisomers of 1-methyl-tryptophan correlates with antitumor responses. *Cancer Res.* **2007,** *67* (2), 792-801.

7. (a) Muller, A. J.; Prendergast, G. C., Marrying immunotherapy with chemotherapy: why say IDO? *Cancer Res.* **2005,** *65* (18), 8065-8068; (b) Okamoto, A.; Nikaido, T.; Ochiai, K.; Takakura, S.; Saito, M.; Aoki, Y.; Ishii, N.; Yanaihara, N.; Yamada, K.; Takikawa, O., Indoleamine 2, 3-dioxygenase serves as a marker of poor prognosis in gene expression profiles of serous ovarian cancer cells. *Clin. Cancer Res.* **2005,** *11* (16), 6030-6039.

8. (a) Koblish, H. K.; Hansbury, M. J.; Bowman, K. J.; Yang, G.; Neilan, C. L.; Haley, P. J.; Burn, T. C.; Waeltz, P.; Sparks, R. B.; Yue, E. W., Hydroxyamidine inhibitors of indoleamine-2, 3-dioxygenase potently suppress systemic tryptophan catabolism and the growth of IDO-expressing tumors. *Mol. Cancer Ther.* **2010,** *9* (2), 489-498; (b) Mautino, M. R.; Jaipuri, F. A.; Waldo, J.; Kumar, S.; Adams, J.; Van Allen, C.; Marcinowicz-Flick, A.; Munn, D.; Vahanian, N.; Link, C. J., NLG919, a novel indoleamine-2, 3-dioxygenase (IDO)-pathway inhibitor drug candidate for cancer therapy. *AACR*: **2013**; (c) Malachowski, W. P.; Winters, M.; DuHadaway, J. B.; Lewis-Ballester, A.; Badir, S.; Wai, J.; Rahman, M.; Sheikh, E.; LaLonde, J. M.; Yeh, S.-R., O-alkylhydroxylamines as rationally-designed mechanism-based inhibitors of indoleamine 2, 3-dioxygenase-1. *Eur. J. Med. Chem.* **2016,** *108*, 564-576.

9. Yue, E. W.; Douty, B.; Wayland, B.; Bower, M.; Liu, X.; Leffet, L.; Wang, Q.; Bowman, K. J.; Hansbury, M. J.; Liu, C., Discovery of potent competitive inhibitors of indoleamine 2, 3-dioxygenase with in vivo pharmacodynamic activity and efficacy in a mouse melanoma model. *J. Med. Chem.* **2009,** *52* (23), 7364-7367.

10. Malinen, A. M.; NandyMazumdar, M.; Turtola, M.; Malmi, H.; Grocholski, T.; Artsimovitch, I.; Belogurov, G. A., CBR antimicrobials alter coupling between the bridge helix and the β subunit in RNA polymerase. *Nat. Commun.* **2014,** *5*, 3408.

11. (a) Wang, Y.; Rong, J.; Zhang, B.; Hu, L.; Wang, X.; Zeng, C., Design and synthesis of N-methylpyrimidone derivatives as HIV-1 integrase inhibitors. *Bioorganic Med. Chem.* **2015,** *23* (4), 735-741; (b) Cai, J.; Wei, H.; Hong, K. H.; Wu, X.; Cao, M.; Zong, X.; Li, L.; Sun, C.; Chen, J.; Ji, M., Discovery and preliminary evaluation of 2-aminobenzamide and hydroxamate derivatives containing 1, 2, 4-oxadiazole moiety as

potent histone deacetylase inhibitors. *Eur. J. Med. Chem.* **2015,** *96*, 1-13; (c) Zhuang, Y. D.; Chiang, P. Y.; Wang, C. W.; Tan, K. T., Environment-Sensitive Fluorescent Turn-On Probes Targeting Hydrophobic Ligand-Binding Domains for Selective Protein Detection. *Angew. Chem. Int. Ed.* **2013,** *52* (31), 8124-8128.

12. (a) Röhrig, U. F.; Awad, L.; Grosdidier, A.; Larrieu, P.; Stroobant, V.; Colau, D.; Cerundolo, V.; Simpson, A. J.; Vogel, P.; Van den Eynde, B. t. J., Rational design of indoleamine 2, 3-dioxygenase inhibitors. *J. Med. Chem.* **2010,** *53* (3), 1172-1189; (b) Austin, C. J.; Mizdrak, J.; Matin, A.; Sirijovski, N.; Kosim-Satyaputra, P.; Willows, R. D.; Roberts, T. H.; Truscott, R. J.; Polekhina, G.; Parker, M. W., Optimised expression and purification of recombinant human indoleamine 2, 3-dioxygenase. *Protein Expr. Purif.* **2004,** *37* (2), 392-398; (c) Takikawa, O.; Kuroiwa, T.; Yamazaki, F.; Kido, R., Mechanism of interferon-gamma action. Characterization of indoleamine 2, 3-dioxygenase in cultured human cells induced by interferon-gamma and evaluation of the enzyme-mediated tryptophan degradation in its anticellular activity. *J. Biol. Chem.* **1988,** *263* (4), 2041-2048.

13. (a) Röhrig, U. F.; Majjigapu, S. R.; Grosdidier, A. l.; Bron, S.; Stroobant, V.; Pilotte, L.; Colau, D.; Vogel, P.; Van den Eynde, B. J.; Zoete, V., Rational design of 4-aryl-1, 2, 3-triazoles for indoleamine 2, 3-dioxygenase 1 inhibition. *J. Med. Chem.* **2012,** *55* (11), 5270-5290; (b) Wu, J.-S.; Lin, S.-Y.; Liao, F.-Y.; Hsiao, W.-C.; Lee, L.-C.; Peng, Y.-H.; Hsieh, C.-L.; Wu, M.-H.; Song, J.-S.; Yueh, A., Identification of substituted naphthotriazolediones as novel tryptophan 2, 3-dioxygenase (TDO) inhibitors through structure-based virtual screening. *J. Med. Chem.* **2015,** *58* (19), 7807-7819; (c) Yu, L.-F.; Li, Y.-Y.; Su, M.-B.; Zhang, M.; Zhang, W.; Zhang, L.-N.; Pang, T.; Zhang, R.-T.; Liu, B.; Li, J.-Y., Development of novel alkene oxindole derivatives as orally efficacious AMP-activated protein kinase activators. *ACS Med. Chem. Lett.* **2013,** *4* (5), 475-480.

14. (a) Dawson, J. H.; Andersson, L.; Sono, M., Spectroscopic investigations of ferric cytochrome P-450-CAM ligand complexes. Identification of the ligand trans to cysteinate in the native enzyme. *J. Biol. Chem.* **1982,** *257* (7), 3606-3617; (b) Littlejohn, T. K.; Takikawa, O.; Skylas, D.; Jamie, J. F.; Walker, M. J.; Truscott, R. J., Expression and purification of recombinant human indoleamine 2, 3-dioxygenase. *Protein Expr. Purif.* **2000,** *19* (1), 22-29; (c) Schenkman, J. B.; Sligar, S. G.; Cinti, D. L., Substrate interaction with cytochrome P-450. *Pharmacol. Ther.* **1981,** *12* (1), 43-71.

15. Sugimoto, H.; Oda, S.-i.; Otsuki, T.; Hino, T.; Yoshida, T.; Shiro, Y., Crystal structure of human indoleamine 2, 3-dioxygenase: catalytic mechanism of O_2 incorporation by a heme-containing dioxygenase. *Proc. Natl. Acad. Sci. U.S.A.* **2006,** *103* (8), 2611-2616.

16. Travers, M.; Gow, I. F.; Barber, M.; Thomson, J.; Shennan, D. B., Indoleamine 2, 3-dioxygenase activity and L-tryptophan transport in human breast cancer cells. *Biochim. Biophys. Acta, Biomembr.* **2004,** *1661* (1), 106-112.

17. Yang, S.; Li, X.; Hu, F.; Li, Y.; Yang, Y.; Yan, J.; Kuang, C.; Yang, Q., Discovery of tryptanthrin derivatives as potent inhibitors of indoleamine 2, 3-dioxygenase with therapeutic activity in Lewis lung cancer (LLC) tumor-bearing mice. *J. Med. Chem.* **2013,** *56* (21), 8321-8331.

18. Tojo, S.; Kohno, T.; Tanaka, T.; Kamioka, S.; Ota, Y.; Ishii, T.; Kamimoto, K.; Asano, S.; Isobe, Y., Crystal structures and structure–activity relationships of imidazothiazole derivatives as IDO1 inhibitors. *ACS Med. Chem. Lett.* **2014,** *5* (10), 1119-1123.

19. Kumar, P.; Gorai, S.; Santra, M. K.; Mondal, B.; Manna, D., DNA binding, nuclease activity and cytotoxicity studies of Cu (II) complexes of tridentate ligands. *Dalton Trans.* **2012,** *41* (25), 7573-7581.

20. Mamidi, N.; Borah, R.; Sinha, N.; Jana, C.; Manna, D., Effects of ortho substituent groups of protocatechualdehyde derivatives on binding to the C1 domain of novel protein kinase C. *J. Phys. Chem. B* **2012,** *116* (35), 10684-10692.

3.4.14. NMR spectra of the synthesized compounds

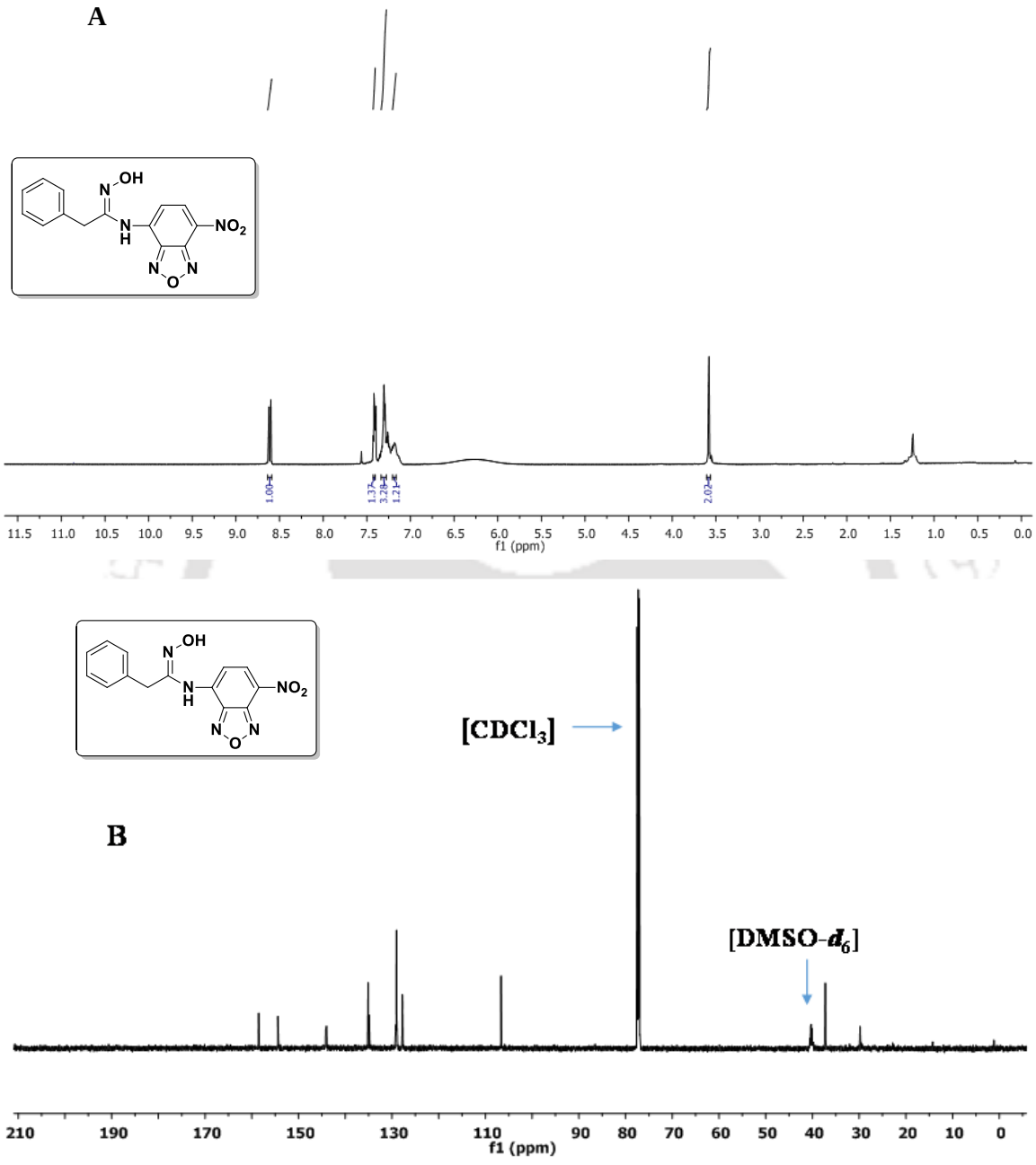

Figure 3.7.1. ^{1}H NMR (**A**) and ^{13}C NMR (**B**) of (Z)-*N'*-hydroxy-*N*-(7-nitrobenzo[c][1,2,5]oxadiazol-4-yl)-2-phenylacetimidamide (**1a**).

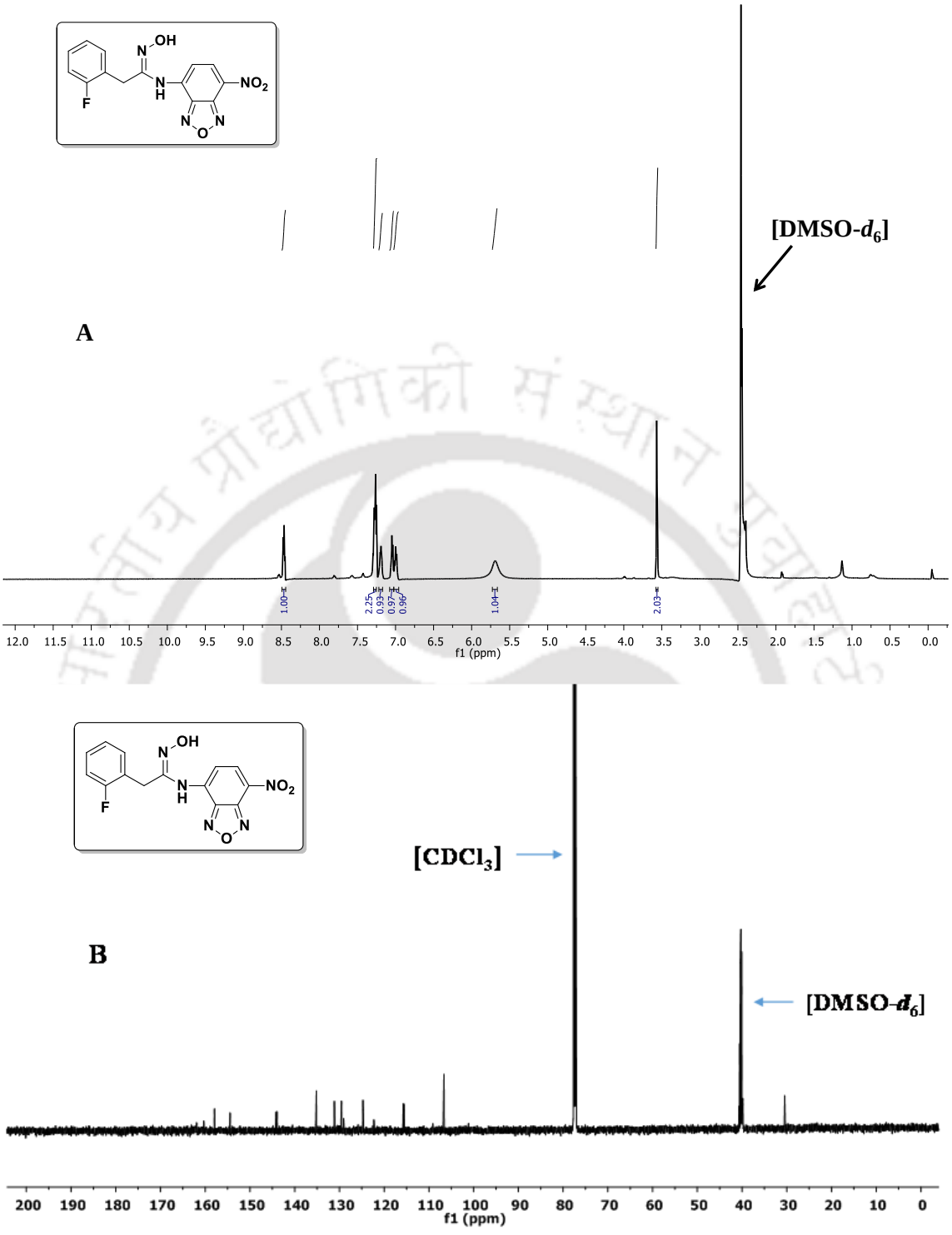

Figure 3.7.2. ^{1}H NMR (**A**) and ^{13}C NMR (**B**) of (Z)-2-(2-fluorophenyl)-*N*′-hydroxy-*N*-(7-nitrobenzo[c][1,2,5]oxadiazol-4-yl)acetimidamide (**1b**).

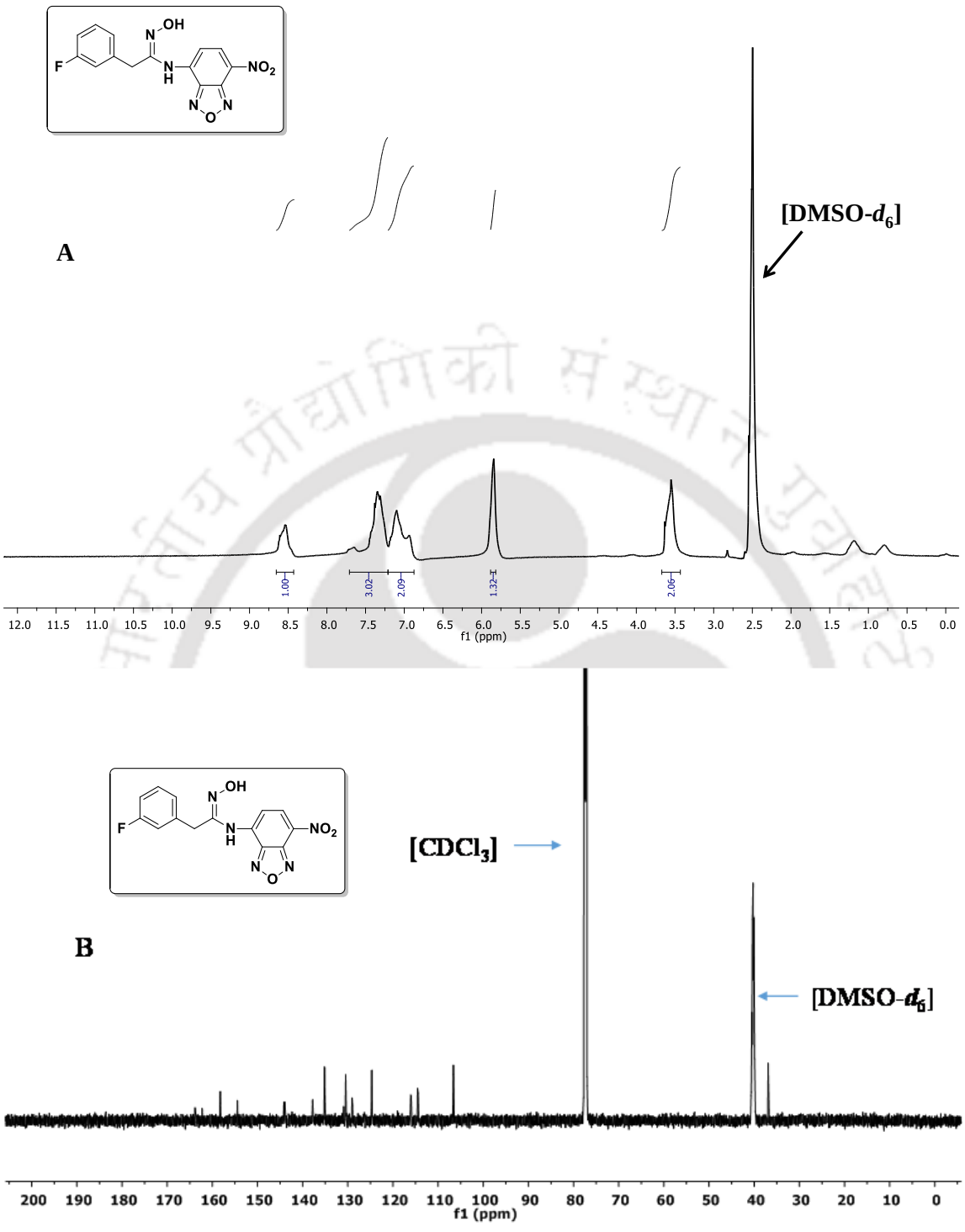

Figure 3.7.3. ^{1}H NMR (**A**) and ^{13}C NMR (**B**) of (Z)-2-(3-fluorophenyl)-*N'*-hydroxy-*N*-(7-nitrobenzo[c][1,2,5]oxadiazol-4-yl)acetimidamide (**1c**).

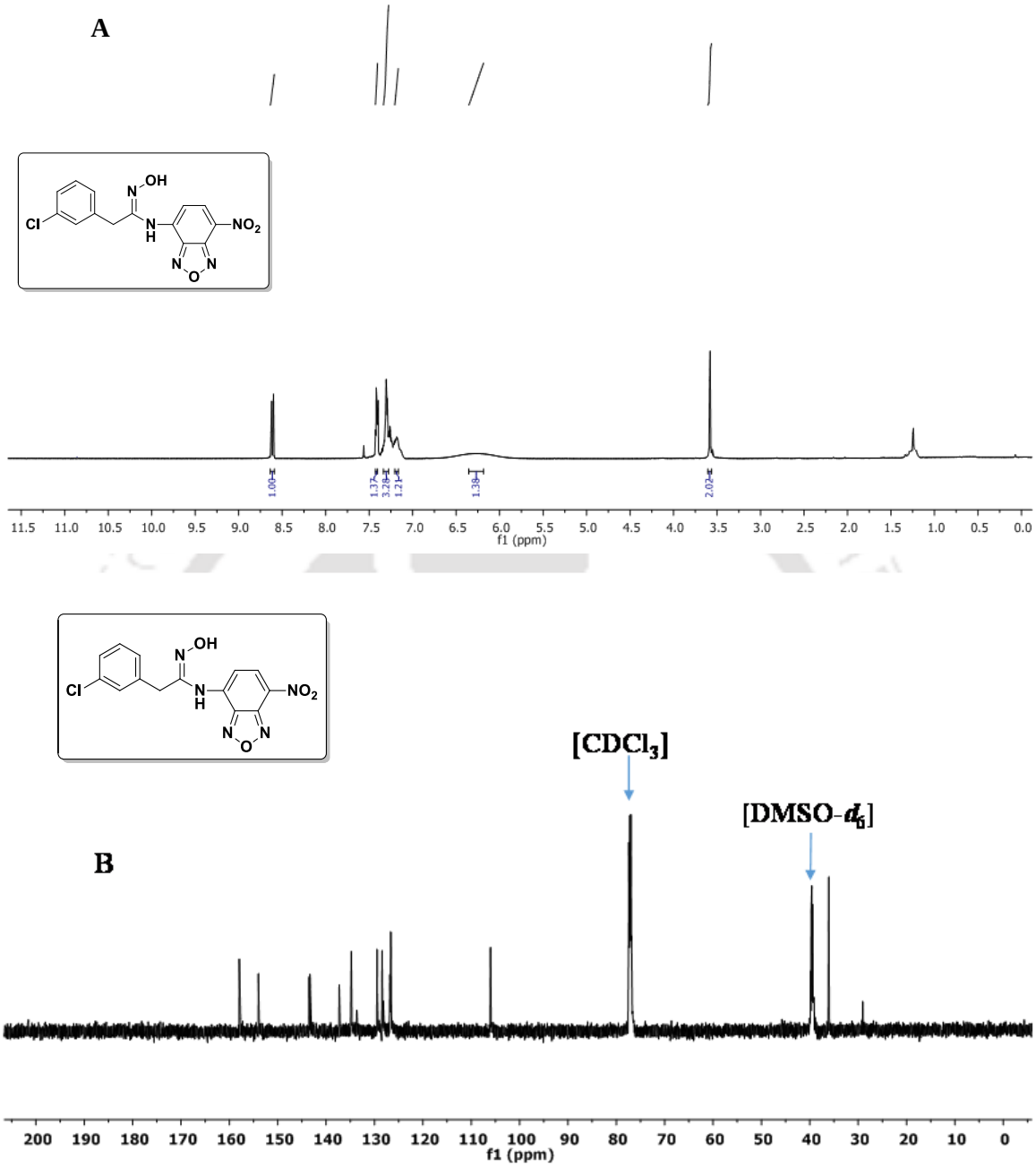

Figure 3.7.4. ^{1}H NMR (**A**) and ^{13}C NMR (**B**) of (Z)-2-(3-chlorophenyl)-*N'*-hydroxy-*N*-(7-nitrobenzo[c][1,2,5]oxadiazol-4-yl)acetimidamide (**1d**).

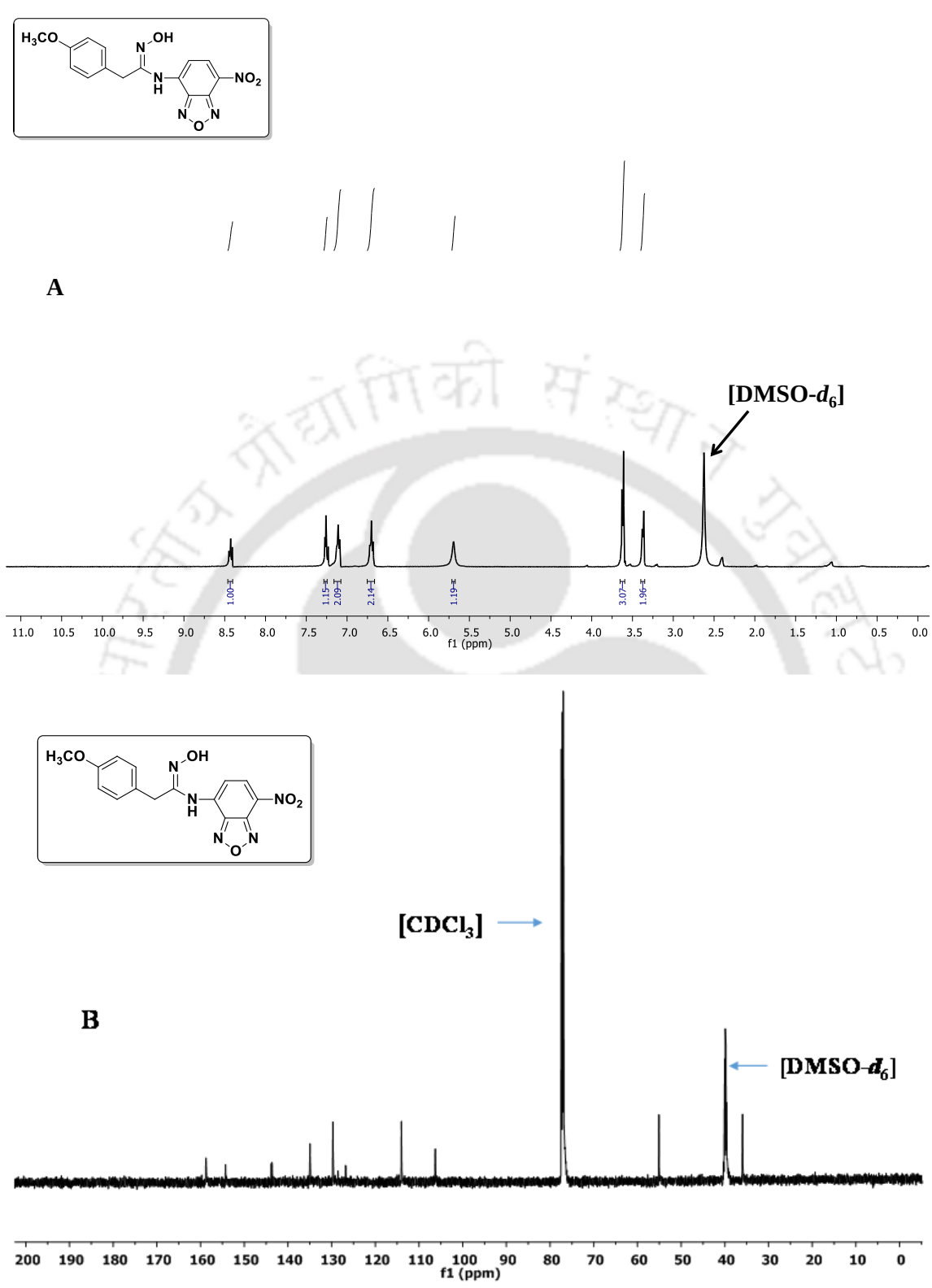

Figure 3.7.5. ^{1}H NMR (**A**) and ^{13}C NMR (**B**) of (Z)-*N'*-hydroxy-2-(4-metoxyphenyl)-*N*-(7-nitrobenzo[c][1,2,5]oxadiazol-4-yl)acetimidamide (**1e**).

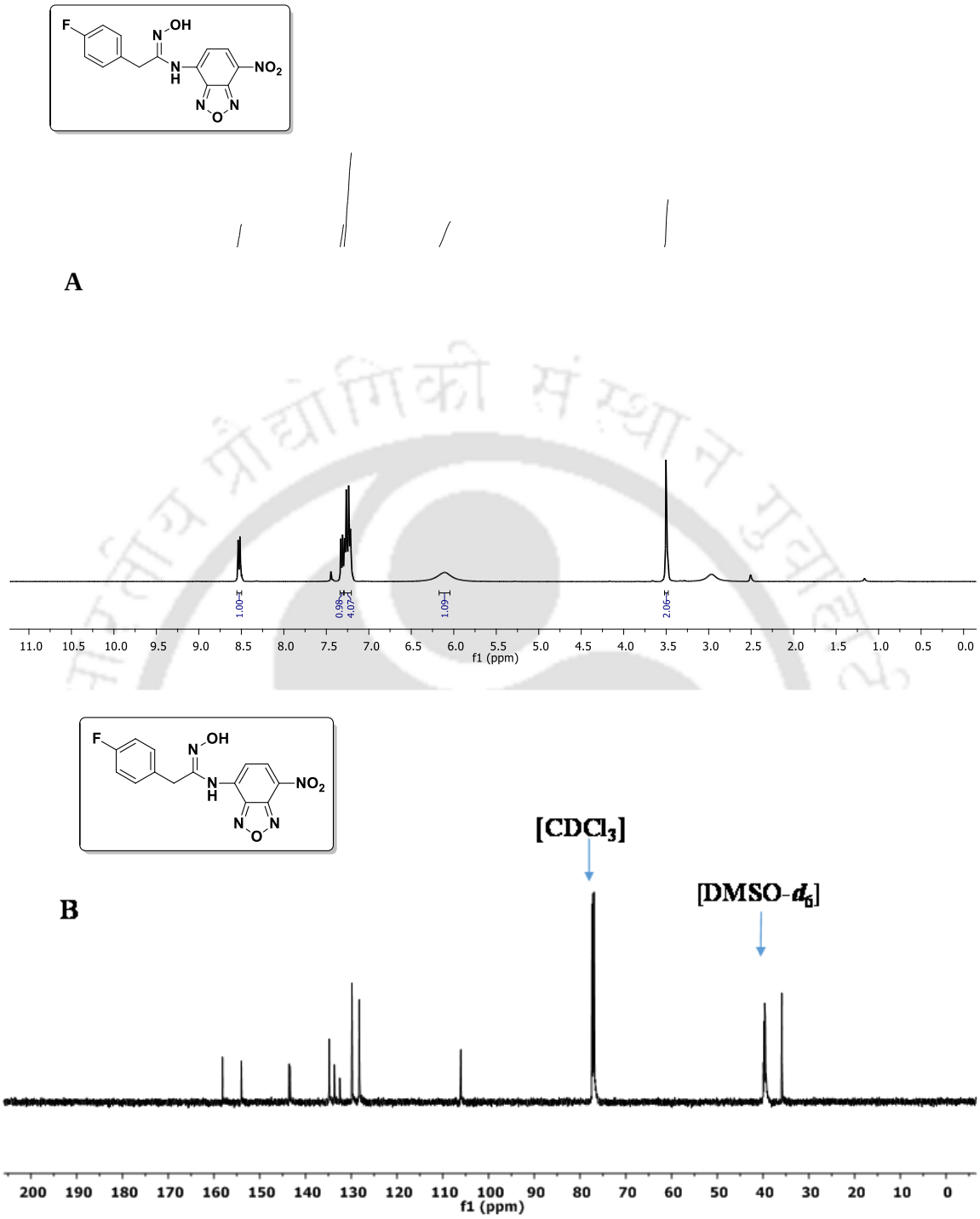

Figure 3.7.6. ^{1}H NMR (**A**) and ^{13}C NMR (**B**) of (Z)-2-(4-fluorophenyl)-*N'*-hydroxy-*N*-(7-nitrobenzo[c][1,2,5]oxadiazol-4-yl)acetimidamide (**1f**).

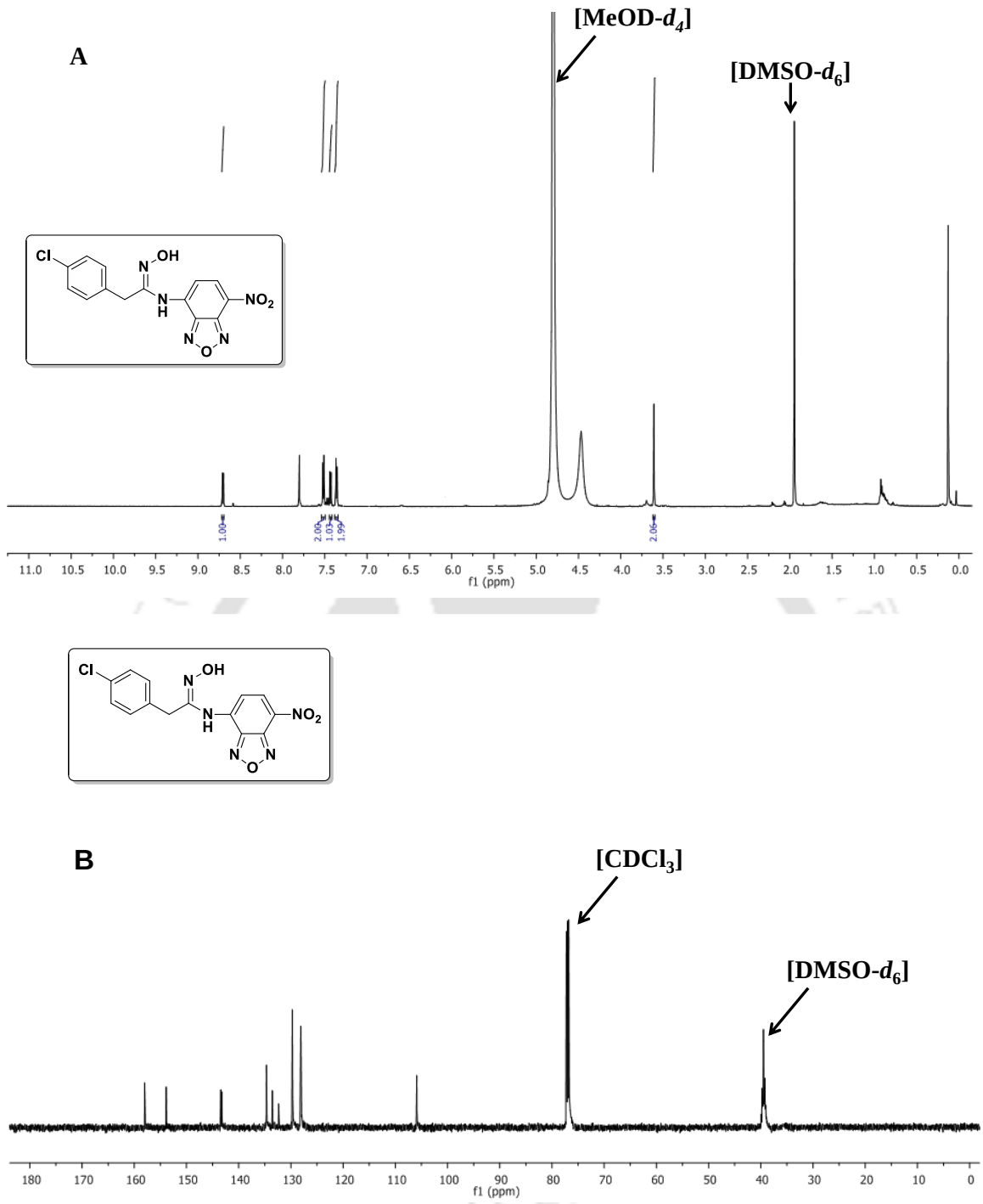

Figure 3.7.7. ^{1}H NMR (**A**) and ^{13}C NMR (**B**) of (Z)-2-(4-chlorophenyl)-*N'*-hydroxy-*N*-(7-nitrobenzo[c][1,2,5]oxadiazol-4-yl)acetimidamide (**1g**).

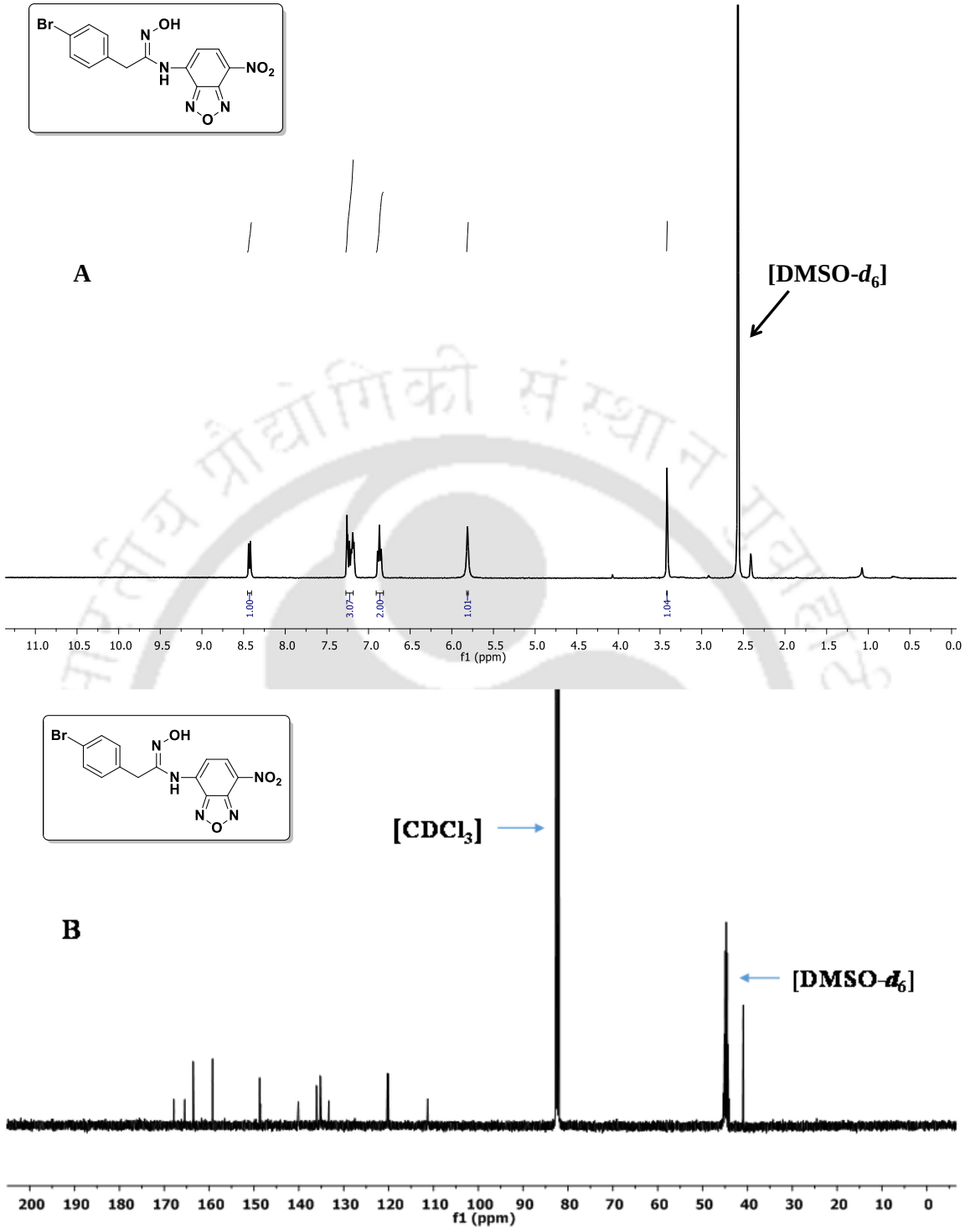

Figure 3.7.8. ^{1}H NMR (**A**) and ^{13}C NMR (**B**) of (Z)-2-(4-bromophenyl)-*N'*-hydroxy-*N*-(7-nitrobenzo[c][1,2,5]oxadiazol-4-yl)acetimidamide (**1h**).

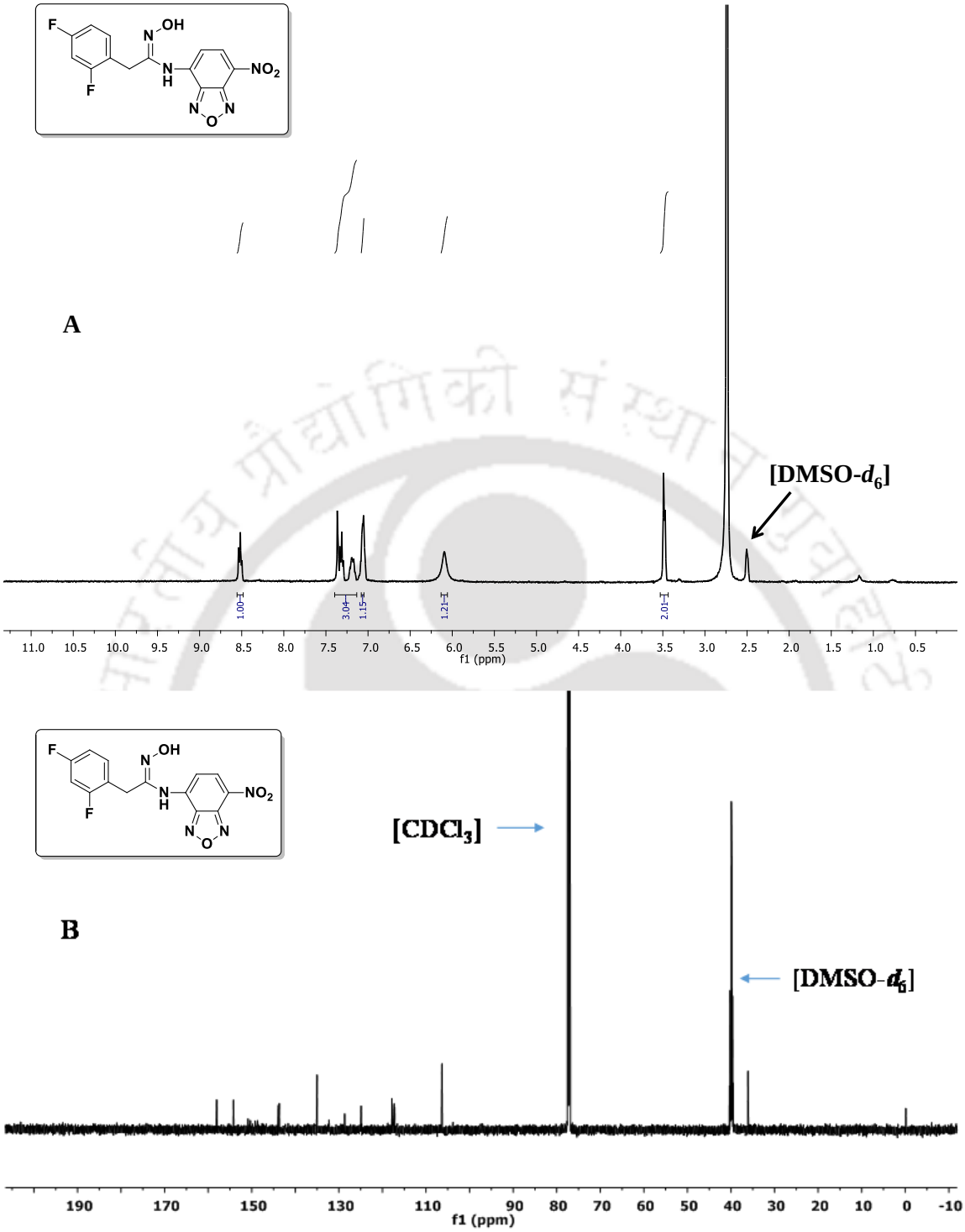

Figure 3.7.9. ^{1}H NMR (**A**) and ^{13}C NMR (**B**) of (Z)-2-(2,4-difluorophenyl)-*N*′-hydroxy-4-methyl-*N*-(7-nitrobenzo[c][1,2,5]oxadiazol-4-yl)acetimidamide (**1i**).

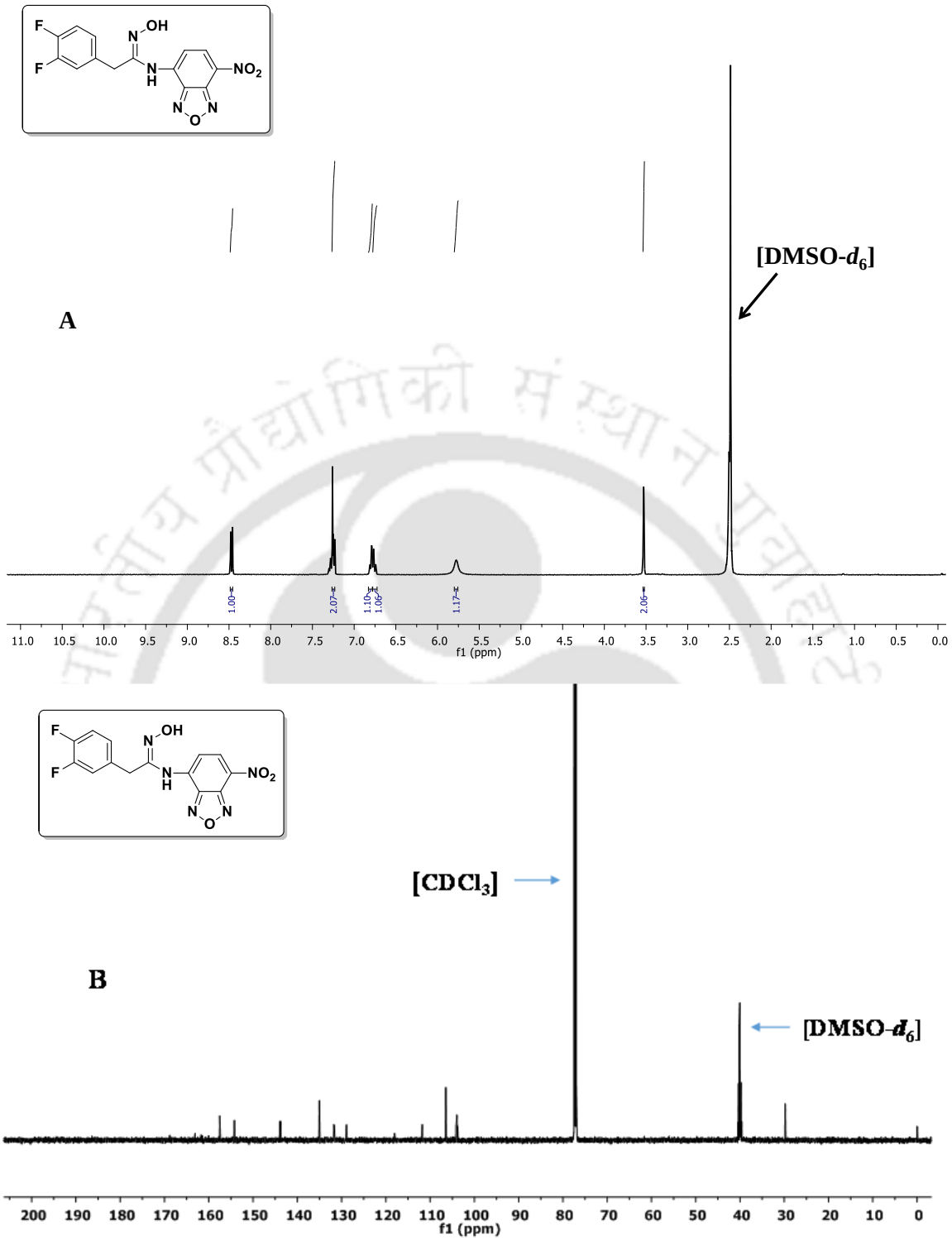

Figure 3.7.10. ^{1}H NMR (**A**) and ^{13}C NMR (**B**) of (Z)-2-(3,4-difluorophenyl)-*N'*-hydroxy-*N*-(7-nitrobenzo[c][1,2,5]oxadiazol-4-yl)acetimidamide (**1j**).

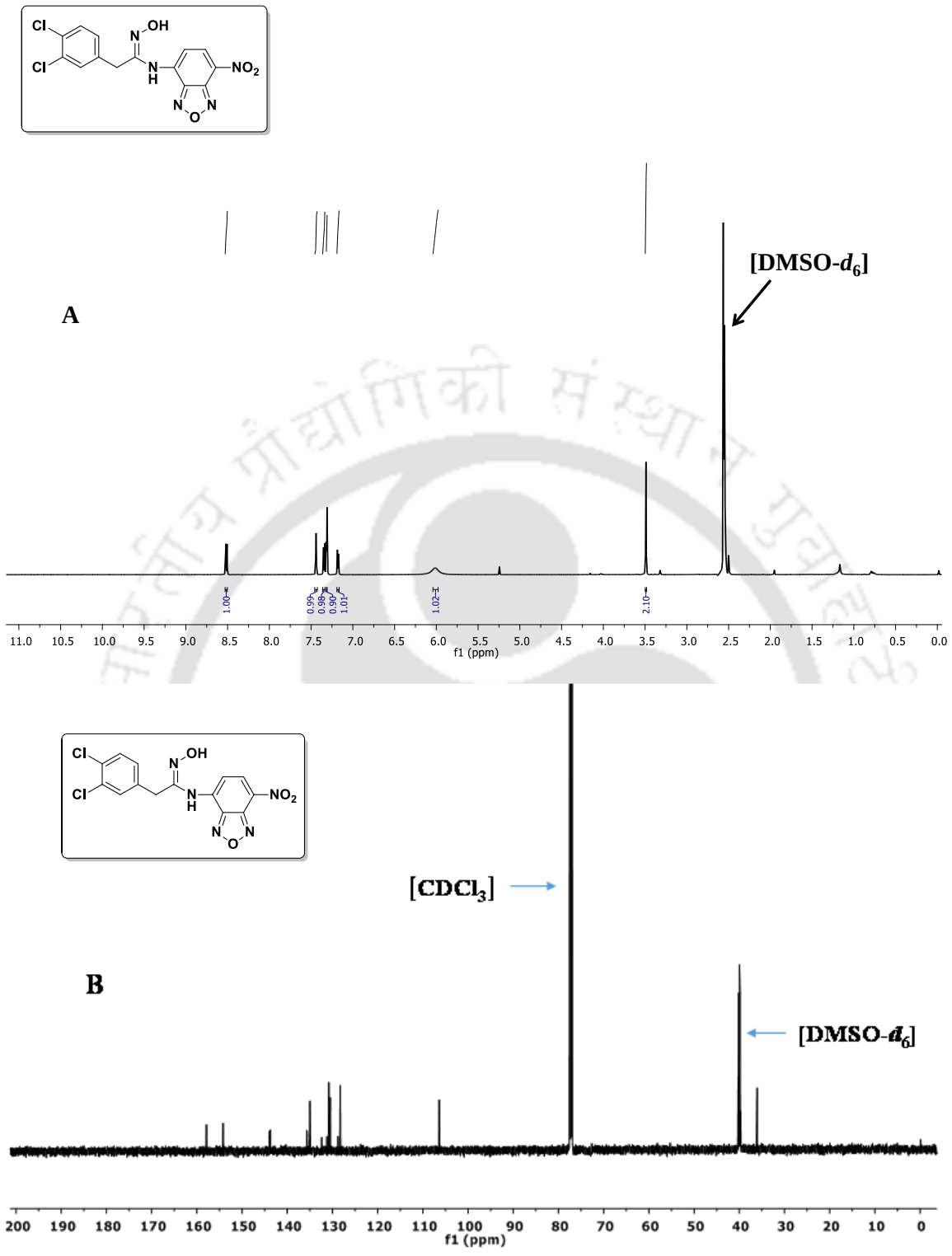

Figure 3.7.11. ^{1}H NMR (**A**) and ^{13}C NMR (**B**) of (Z)-2-(3,4-dichlorophenyl)-*N*'-hydroxy-*N*-(7-nitrobenzo[c][1,2,5]oxadiazol-4-yl)acetimidamide (**1k**).

CHAPTER 4

Development of fused heterocyclic based compounds as IDO1 inhibitors

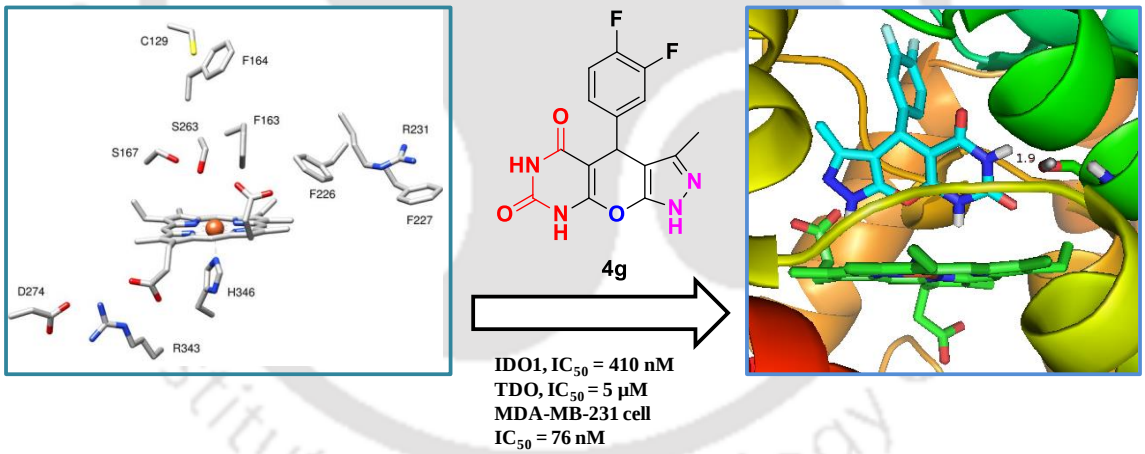

This chapter demonstrates the synthesis of a fused heterocyclic based compounds and their inhibitory activity against purified IDO1 enzyme under both *in vitro* and cellular environment.

4.1. Background and focus of the present work

Cancer immunotherapy by targeting immunosuppressive enzyme indoleamine 2,3-dioxygenase 1 (IDO1) is considered as an exciting approach for drug development.[1] IDO1 mediated depletion of local L-Trp and accumulation of the kynurenine metabolites kynurenine, 3-hydroxy kynurenine, kynurenic acid, excitotoxin quinolinic acid and others are mainly responsible for local immunosuppression.[2]

IDO1 is expressed in several tissues all throughout the body, but over-expressed in a variety of non-hepatic tissues, including lung, epididymis, gut and placenta. Cytokines like interferon-γ are mostly accountable for this over-expression of IDO1 enzyme in non-hepatic tissues. Over-expressed IDO1 defends cancer cells from the attack by the T-cells.[3] IDO1 is also expressed within antigen presenting cells (APC) or accessory cells and boost peripheral tolerance of the tumor associated antigens (TAAs) in tumor-draining lymph nodes. IDO1 induction assists the growth, survival, invasion, and metastasis of malignant cells (MC) expressing TAAs by shielding them from identification and attack by the T-cells.[4] Recent studies with different cancer models suggest that IDO1 assists cancer progression and metastasis.[5]

All these findings draw attention to the significance of IDO1 for cancer immunotherapy, neurological diseases and others. Therefore, systematic blockade of this tumor induced IDO1 activity with small-molecule inhibitors is now an accepted approach for cancer therapy. It has been shown that IDO1 enzyme inhibitors improve the efficacy of therapeutic vaccination, chemotherapeutic and radiotherapeutic treatment of malignant tumors.[2c, 3a, 5]

There are a number of small molecule-based IDO1 inhibitors with different structural classes, including tryptophan, imidazole, triazole, *N*-hydroxyamidine, iminoquinone, and others have been developed through high throughput-screening, structure-based design and natural product screening. Natural products like norharman, β-carboline, benzomalvin, and their derivatives also showed IDO1 inhibitory potencies.[3b, 6] Nevertheless, development of pharmacological inhibitors of IDO1 is quite challenging. Most of the reported IDO1 inhibitors showed low potency or failed *in vivo* assay. Currently, three IDO1 inhibitors, INCB024360 (Epacadostat), GDC-0919 (NLG919) and 1-methyl-L-tryptophan (L-1MT) are under clinical studies for the treatment of cancer and other diseases as a monotherapy or in-combination with traditional cancer chemotherapies or newly developed immune checkpoint inhibitors. A variety of IDO1 inhibitors was also recognized by the several other pharmaceutical companies. Successful exploitation of the

antibody, ipilimumab and nivolumab and recent clinical development of the IDO1 inhibitors is the inspiration of researchers to develop IDO1 inhibitors for cancer immunotherapy.[3b, 7]

For the identification of new structural class of IDO1 inhibitors, we synthesized a series of fused di-and tri-heterocyclic compounds 4-phenyl-1,4-dihydropyridine (**2**), 4-phenyl-2-pyridone (**3**) and 4-phenyl-4*H*-pyran (**4**). To discover the potent inhibitors of IDO1, inhibitory activities of these compounds were studied against purified IDO1 enzyme. Interestingly, the optimizations led to the inhibitory potency of several compounds in the low micromolar-range. The selected compounds also displayed stronger cellular IDO1 enzyme inhibitory activities in MDA-MB-231 cells with insignificant level of cytotoxicity. Additional counter screening test against TDO enzyme revealed that these selected compounds were 13 to 106-fold more selective for IDO1 enzyme. Overall activity suggest the resulting compounds with compelling value for further development as therapeutic agents targeting IDO1 enzyme.

4.2. Result and discussion

4.2.1. Synthesis of fused di- and tri-heterocyclic compounds

The 4-phenyl-1,4-dihydropyridine (**2**), 4-phenyl-2-pyridone (**3**) and 4-phenyl-4*H*-pyran (**4**) derivatives were synthesized according to the reported procedures (Scheme 4.1).[8] For the production of 4-phenyl-4*H*-pyridine derivatives (**2a-i**), the substituted aromatic aldehyde condensed with malononitrile and 6-aminouracil in the presence of K_2CO_3 in EtOH under refluxing condition. To afford 4-phenyl-2-pyridone derivatives (**3a-i**), the substituted aromatic aldehyde was reacted with ethyl cyanoacetate and 6-aminouracil in the presence of K_2CO_3 in EtOH under refluxing condition. The substituted aromatic aldehyde condensed with 5-methyl-2,4-dihydro-3*H*-pyrazole-3-one and 6-aminouracil and yielded 4-phenyl-4*H*-pyran derivatives (**4a-i**) in the presence of K_2CO_3 in EtOH under refluxing condition.

Scheme 4.1. Synthesis of 4-phenyl-1,4-dihydropyridine, 4-phenyl-2-pyridone and 4-phenyl-4*H*-pyran derivatives

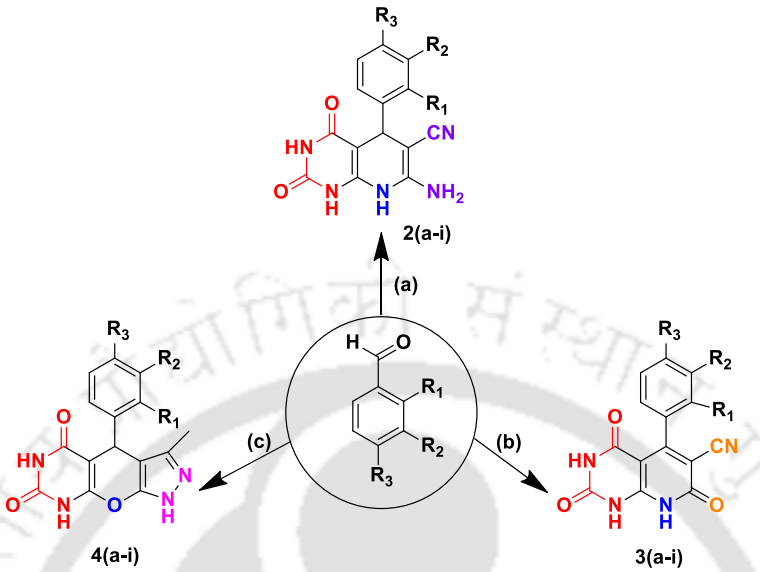

[a]**Reagents and conditions:** (a) malononitrile, 6-aminouracil, K_2CO_3, EtOH, 70 ºC, reflux, 4h. (b) ethyl cyanoacetate, 6-aminouracil, K_2CO_3, EtOH, 70 ºC, reflux, 4h. (c) 5-methyl-2,4-dihydro-3*H*-pyrazole-3-one, 6-aminouracil, K_2CO_3, EtOH, 70 ºC, reflux, 4h.

4.2.2. Inhibitory activities of the fused heterocyclic compounds against purified IDO1 enzyme

The inhibitory activity of the synthesized compounds was investigated using purified IDO1 enzyme by UV-visible spectroscopy as described earlier.[3b, 6a, 9] The enzymatic activity assay was not interfered by the UV-visible spectra of the pure compounds (10 nM to 50 µM). The measured kinetic parameters K_M and k_{cat} values of the purified IDO1 enzyme with respect to L-Trp were 68.9 ± 3.5 µM and 4.2 ± 0.2 s^{-1}, respectively. For the improvement of the efficacy of the fused heterocyclic compounds, we explored two general modifications of the structure of the compounds: alteration of the fused heterocyclic ring and substitution of the phenyl ring.

4.2.2.1. Alteration of the fused heterocyclic ring

The role of fused di- and tri-heterocyclic ring on IDO1 enzyme activity was explored. Compounds **(2-4)** show their inhibitory value against purified IDO1 enzyme in the range 296-3275 nM (Table 4.1). Among those heterocyclic compounds, compound **4a** (IC_{50} = 3275 nM) showed a little lower IDO1 inhibitory efficiency than compound **2a** (IC_{50} =

2784 nM) and **3a** (IC_{50} = 2092 nM). From the IC_{50} values, it is suggested that the presence of di- and tri-heterocyclic ring and their substitution and also their electronic properties are important in IDO1 inhibitory activity.

Table 4.1. Inhibitory activities of the fused heterocyclic compounds against purified IDO1 enzyme

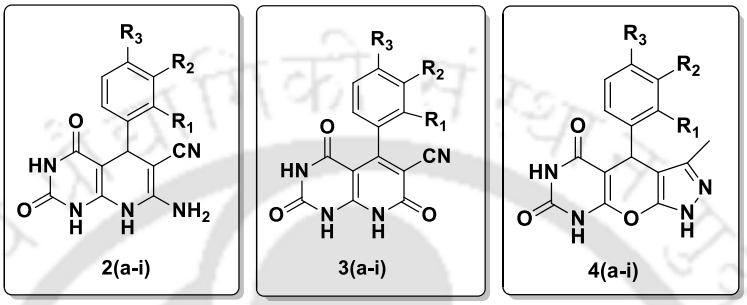

compound	IDO1 inhibition IC_{50} (nM)[a]	compound	IDO1 inhibition IC_{50} (nM)[a]	compound	IDO1 inhibition IC_{50} (nM)[a]
2a; $R_1 = R_2 = R_3 = H$	2784 ± 72	**3a;** $R_1 = R_2 = R_3 = H$	2092 ± 54	**4a;** $R_1 = R_2 = R_3 = H$	3275 ± 96
2b; $R_1 = R_3 = H$, $R_2 = F$	718 ± 19	**3b;** $R_1 = R_3 = H$, $R_2 = F$	383 ± 15	**4b;** $R_1 = R_3 = H$, $R_2 = F$	1347 ± 41
2c; $R_1 = R_3 = H$, $R_2 = Cl$	473 ± 23	**3c;** $R_1 = R_3 = H$, $R_2 = Cl$	296 ± 18	**4c;** $R_1 = R_3 = H$, $R_2 = Cl$	932 ± 39
2d; $R_1 = R_2 = H$, $R_3 = F$	668 ± 30	**3d;** $R_1 = R_2 = H$, $R_3 = F$	1149 ± 41	**4d;** $R_1 = R_2 = H$, $R_3 = F$	571 ± 6
2e; $R_1 = R_2 = H$, $R_3 = Cl$	909 ± 56	**3e;** $R_1 = R_2 = H$, $R_3 = Cl$	1365 ± 47	**4e;** $R_1 = R_2 = H$, $R_3 = Cl$	862 ± 32
2f; $R_1 = R_2 = H$, $R_3 = Br$	942 ± 78	**3f;** $R_1 = R_2 = H$, $R_3 = Br$	790 ± 26	**4f;** $R_1 = R_2 = H$, $R_3 = Br$	969 ± 55
2g; $R_1 = H$, $R_2 = R_3 = F$	680 ± 26	**3g;** $R_1 = H$, $R_2 = R_3 = F$	559 ± 36	**4g;** $R_1 = H$, $R_2 = R_3 = F$	410 ± 24
2h; $R_1 = H$, $R_2 = R_3 = Cl$	577 ± 26	**3h;** $R_1 = H$, $R_2 = R_3 = Cl$	650 ± 35	**4h;** $R_1 = H$, $R_2 = R_3 = Cl$	593 ± 35
2i; $R_1 = H$, $R_2 = Cl$, $R_3 = F$	879 ± 22	**3i;** $R_1 = H$, $R_2 = Cl$, $R_3 = F$	362 ± 15	**4i;** $R_1 = H$, $R_2 = Cl$, $R_3 = F$	438 ± 22

[a] IC_{50} values are the mean of three independent assays.

4.2.2.2. Substitution of the phenyl ring

For further optimization of the efficiency of these fused heterocyclic compounds, the substitution effect of the aryl ring was tested. It was assumed that the importance of the substituted phenyl ring present in the compound's core structural unit to their inhibitory

efficacies is the interactions with the amino acid residues (Y126, C129 and F163) present in the active site of IDO1 enzyme.[6a, 9-10] In the previous work, these interactions and the increased inhibitory potencies of *N′*-hydroxyamidines by the presence of halogen substituted phenyl ring was successfully exploited.[3b] The effect of substituted halogen group at the *meta* and/or *para*-positions of the phenyl ring on their IDO1 inhibitory activity was also observed. Such benefits of halogen substituted phenyl ring on the IDO1 inhibitory efficacies was also described by several reports.[3b, 7a, 9, 11] Substituted halogen groups like chloro, fluoro and bromo to *meta* and/or *para*-positions of the phenyl ring proved to be quite favourable for the fused di- and tri-heterocyclic compounds (Table 4.1). The hydrophobic interactions, pi-stacking interaction with aromatic amino acids or halogen bonding with the Lewis bases present within the active site could play an important role in stronger activity of the halogen substituted compounds.

The halogen substituted pyridopyrimidines and pyrazolopyranopyrimidine **2b-i**, **3b-i** and **4b-i** showed 1.5 to 7.5-fold stronger IDO1 inhibitory activities than the lead compounds **2a, 3a** and **4a** which is in accordance with our hypothesis (Table 4.1). Among these tested compounds, 3-chloro substituted pyridopyrimidines **2c** (IC_{50} = 473 nM) and **3c** (IC_{50} = 296 nM) showed stronger IDO1 inhibitory activity than the other tested pyridopyrimidines. 3-chloro-4-fluoro substituted pyridopyrimidine **3i** showed moderate inhibitory activity with IC_{50} value of 362 nM. However, no considerable preference for IDO1 inhibitory activity of other halogen substitutions at the *meta* and/or *para*-positions was observed in pyridopyrimidines. A considerable preference for the fluoro-substitution at the *meta* and/or *para*-positions of the phenyl ring was observed for the pyrazolopyranopyrimidines. 3,4-di-fluoro and 3-chloro-4-fluoro substituted pyrazolopyranopyrimidines **4g** and **4i** showed stronger IDO1 inhibitory activity with IC_{50} value of 410 nM and 438 nM, respectively. The IC_{50} value of the reported potent compound, 4-amino-*N*-(3-chloro-4-fluorophenyl)-*N′*-hydroxy-1,2,5-oxadiazole-3-carboxymidimade (**5l**) under the experimental conditions was 91 nM, which is in accordance with the reported values.[6c] IDO1 inhibitor L-1MT, which is under clinical trial for the treatment of several types of cancer, showed an IC_{50} value of 385 μM, which is consistent with the reported values.[7b]

4.2.3. Inhibitory activity of heterocyclic compounds against purified IDO1 enzyme by HPLC method

To confirm the inhibition potencies of the selected compounds, IDO1 activity assay was also performed by HPLC analysis. In this assay the extent of kynurenine formed from L-Trp was quantitatively measured to estimate the inhibitory activities of the compounds.[3b] It was shown from the results that the inhibitory concentrations of the compounds are in low micromolar range (Table 4.2) which is consistent with the spectroscopic IC_{50} values. Among the selected compounds, 3,4-difluoro substituted pyrazolopyranopyrimidine compound **4g** exhibited stronger inhibitory activity (IC_{50} = 246 nM). It is assumed that the accuracy of the methylene blue-ascorbate regeneration system to keep IDO1 in its active state (Fe^{2+}) could be the key reason for the differences in the inhibitory activity values between the *p*-DMAB- and HPLC-based methods.[3b, 7a]

Table 4.2. HPLC based IDO1 inhibition assay of the selected compounds

Compound	IDO1 inhibition IC_{50}(nM)[a]
2c	525 ± 16
3c	437 ± 13
4g	246 ± 11
4i	299 ± 19

[a] IC_{50} values calculated by HPLC method are the mean of three independent assays.

Overall, the size and position of the halogen substituent(s) on the phenyl ring senses in the inhibitory efficacy of the fused heterocyclic compounds, possibly due to the restricted space in "pocket A" of the IDO1 enzyme. Stronger inhibitory activities of the 3-chloro substituted pyridopyrimidines **2c** and **3c** could be due to both electronic properties of the fused di-heterocyclic ring and hydrophobic interaction between the halogen substituted phenyl ring and the hydrophobic residues present within the IDO1 binding pocket. Preference for the fluoro-substitution at the *meta* and/or *para*-positions of the phenyl ring of the pyrazolopyranopyrimidine derivatives (**4g** and **4i**) could be due to the pi-stacking interaction with aromatic amino acids (Y126 and F163). Electronic properties of the fused heterocyclic ring and the interactions of the fused heterocyclic ring with the heme-group and polar residues of the IDO1 enzyme also play important role for the inhibitory potencies of the pyrazolopyranopyrimidine derivatives.

4.2.4. Binding analysis of the fused heterocyclic compounds with IDO1 enzyme by spectroscopic measurement

To understand the ligand binding aptitude to the IDO1 enzyme we have performed the UV-visible spectroscopic study as the optical properties of the heme-group are very much sensitive to the local environment.[7a] The inhibition capability of these fused heterocyclic compounds to the IDO1 enzyme fails to provide any direct confirmation of ligand binding to the active site of the enzyme. In this regard, the absorption spectra of ferric-IDO1 and deoxy-ferrous-IDO1 enzyme in the absence and presence of the selected compounds were recorded (Figure 4.1A and 4.1B).[7a] There was no significant shift in the Soret peak (404 nm) of ferric-IDO1 enzyme in the presence of compounds, indicating the trivial binding of the compounds to the ferric-IDO1 enzyme (Figure 4.1A).

In the absence of compounds the deoxy-ferrous-IDO1 enzyme displayed Soret and Q-band at 421 nm, 527 nm and 556 nm, respectively (Figure 4.1B).[7a] Blue shift in the Soret band (417 nm) and appearance of new Q bands around 519/552 nm in the presence of compounds **3c** indicates their probable binding to the Fe^{2+}-IDO1 enzyme (Figure 4.1B). There was no peak of only compounds in this UV-visible spectral region (spectra not shown here). The binding of these compounds to the IDO1 enzyme is clearly supported by these spectral analyses even though additional studies are essential for confirmation.

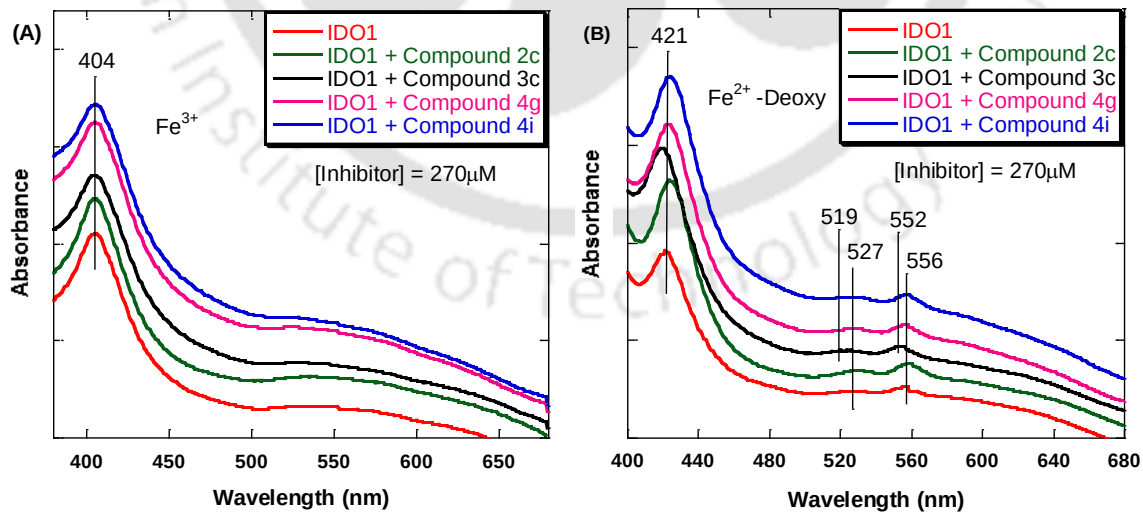

Figure 4.1. Normalized absorption spectra of ferric-IDO1 (A) and deoxy ferrous-IDO1 enzyme (B) in the absence and presence of the 270 μM compounds in 50 mM Tris-HCl buffer at pH 8.0. IDO1 enzyme concentration = 5 μM. Ferrous-deoxy reaction environment was generated by adding $Na_2S_2O_4$ under N_2 atmosphere.

4.2.5. Cellular IDO1 inhibitory activities of the fused heterocyclic compounds

For the investigation of the therapeutic potential of these potent fused heterocyclic compounds, we have performed cellular IDO1 inhibitory activities using MDA-MB-231 breast carcinoma cells. These MDA-MB-231 cells contain mRNA of native IDO1 enzyme and expression of IDO1 enzyme is significantly induced by interferon (IFN)-γ inducer.[3b, 12] In this regard, MDA-MB-231 cells were incubated first with human IFN-γ (20 ng/mL) for 48 h and then in the presence of tested compounds (20 nM to 2 mM) and L-Trp (150 μM) for another 9 h. IDO1 enzyme inhibitory activity was estimated by measuring the formation of L-kynurenine using *p*-DMAB by UV-visible spectroscopy. Compounds show their IDO1 inhibitory efficacy in MDA-MB-231 cells within the range of 75-83 nM (Table 4.3). Control compound, **5l** and **L-1MT** exhibited EC_{50} values of 59 nM and 120 μM, respectively under the similar experimental conditions, which is consistent with the reported value.[6c, 7b] EC_{50} values of the compounds were slightly different from the IC_{50} values due to the trouble in maintaining the IDO1 redox activity and/or environmental effect. In general, a good correlation between these two assays proves the IDO1 inhibition potencies of these fused heterocyclic compounds. It is also assumed that EC_{50} values from the cell-based activity assay of the compounds are lower than the IC_{50} values against purified enzyme due to the same reason.

Table 4.3. EC_{50} values of the selected compounds in MDA-MB-231 cells

Compound	MDA-MB-231 cells[a] EC_{50} (nM)[b]
2c	75 ± 09
3c	52 ± 07
4g	76 ± 11
4i	83 ± 10

[a] IDO1 protein expression in MDA-MB-231 cells was induced by human IFN-γ (20 ng/mL).

[b] EC_{50} values are the mean of three independent assays.

MTT assay of the compounds in MDA-MB-231 cells (concentrations of IC_{50} and 2 × IC_{50} values from the enzymatic assay) also showed insignificant level of cytotoxicity of the compounds under the experimental conditions (Figure 4.2). Data were evaluated by plotting the absorbance at 570 nm due to the different amount of formazan formed against the above mentioned concentrations of the compounds, obtained from three independent experiments. The morphological changes of the cells were studied by treating the MDA-

MB-231 cells with the compounds (concentrations of 2 × IC_{50} values from the enzymatic assay) for 48 h and morphological changes were observed using cytell imaging system (Figure 4.3). Morphological studies showed that after treatment of MDA-MB-231 cells with the potent compounds, the number of cell decreases significantly which indicate the apoptotic cell death. Images were collected from three independent experiments at 10x magnification.

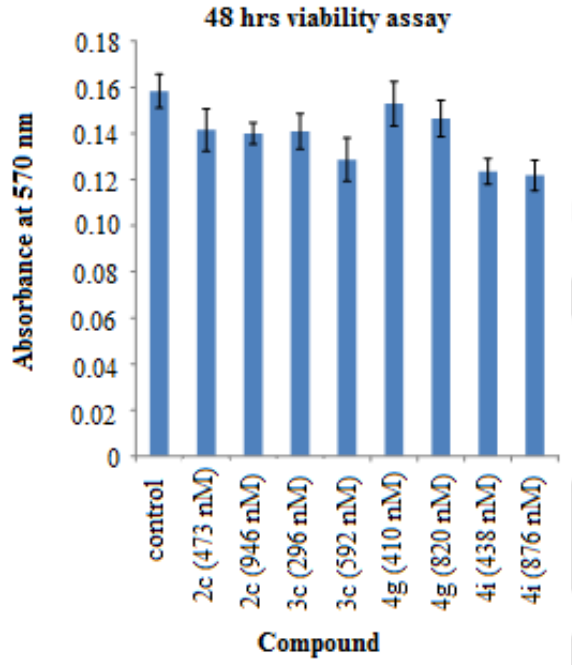

Figure 4.2. Effect of the selected heterocyclic compounds on the viability of MDA-MB-231 cells.

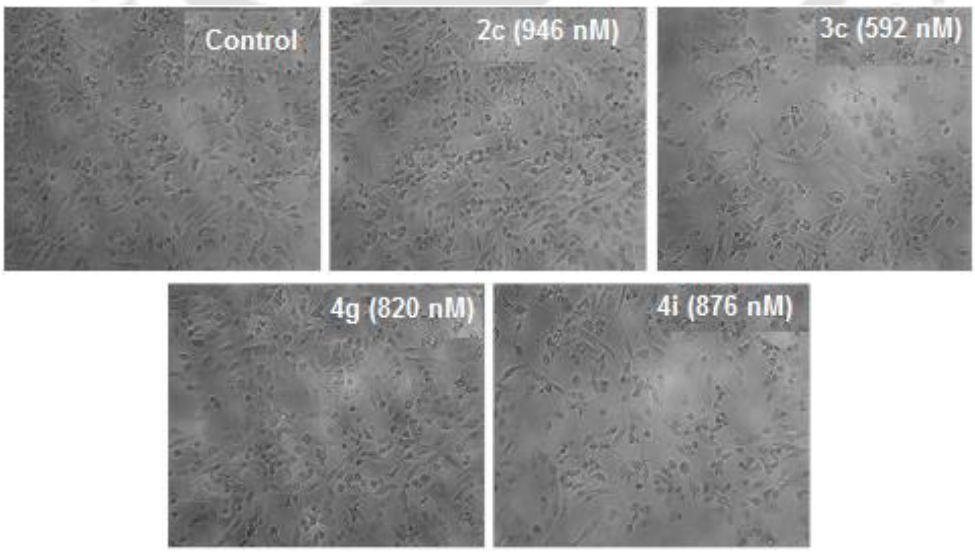

Figure 4.3. Effect of selected heterocyclic compounds on the morphological changes of MDA-MB-231 cells.

4.2.6. Mode of IDO1 enzyme inhibition by the fused heterocyclic compounds

To elucidate the mode of IDO1 inhibition, we performed enzyme kinetics with the variation of compounds concentration (150 nM to 1000 nM) and L-Trp concentration (50 µM to 150 µM). The plots of [S]/V *vs*. inhibitor concentrations ([I]) showed that tested compounds **2c**, **3c** and **4i** followed uncompetitive inhibition, whereas **4g** followed competitive inhibition modes (Figure 4.4). V and [S] represent initial rate of the reaction and the substrate concentration, respectively.[3b, 13] Several uncompetitive and noncompetitive inhibitors of IDO1 enzyme are reported. Although 4-phenylimidazole show noncompetitive mode of IDO1 inhibition, its binding to IDO1 active site by replacing L-Trp is revealed by its crystal structure and enzyme activity studies.[7a, 14] Recently reported compounds, O-alkylhydroxylamines also show uncompetitive mode of IDO1 enzyme inhibition with IC_{50} value in the nanomolar range.[7a] The formation of ferric-superoxide intermediate is the prerequisite for the IDO1 promoted catabolism of L-Trp to *N*-formylkynurenine. Hence, to understand the exact mode of IDO1 enzyme inhibition by these fused heterocyclic compounds further kinetic studies with respect to O_2 are necessary.[3b, 6a, 7a]

4.2.7. Probable mode of interaction of the potent fused heterocyclic compounds with IDO1 enzyme

The strong interaction of the potent fused heterocyclic compounds with the enzyme through its active site was clearly demonstrated by the enzyme inhibition studies. Their binding capabilities with the IDO1 enzyme were also supported by the spectroscopic studies. Therefore, their probable mode of interactions was investigated by performing molecular docking analyses with the IDO1 enzyme (PDB code: 4PK5).[15] It was proposed by the model structures that the potent compounds pyridopyrimidines **2c** and **3c** interacted with the amino acids S167 in the "pocket A" of IDO1 enzyme. A similar mode of interaction for the pyrazolopyranopyrimidines **4g** and **4i** was observed. The halogen substituted phenyl rings of the fused heterocyclic compounds could be involved in interaction with the amino acids residues present in pocket-'A' through pi-stacking and hydrophobic interactions (Figure 4.5).

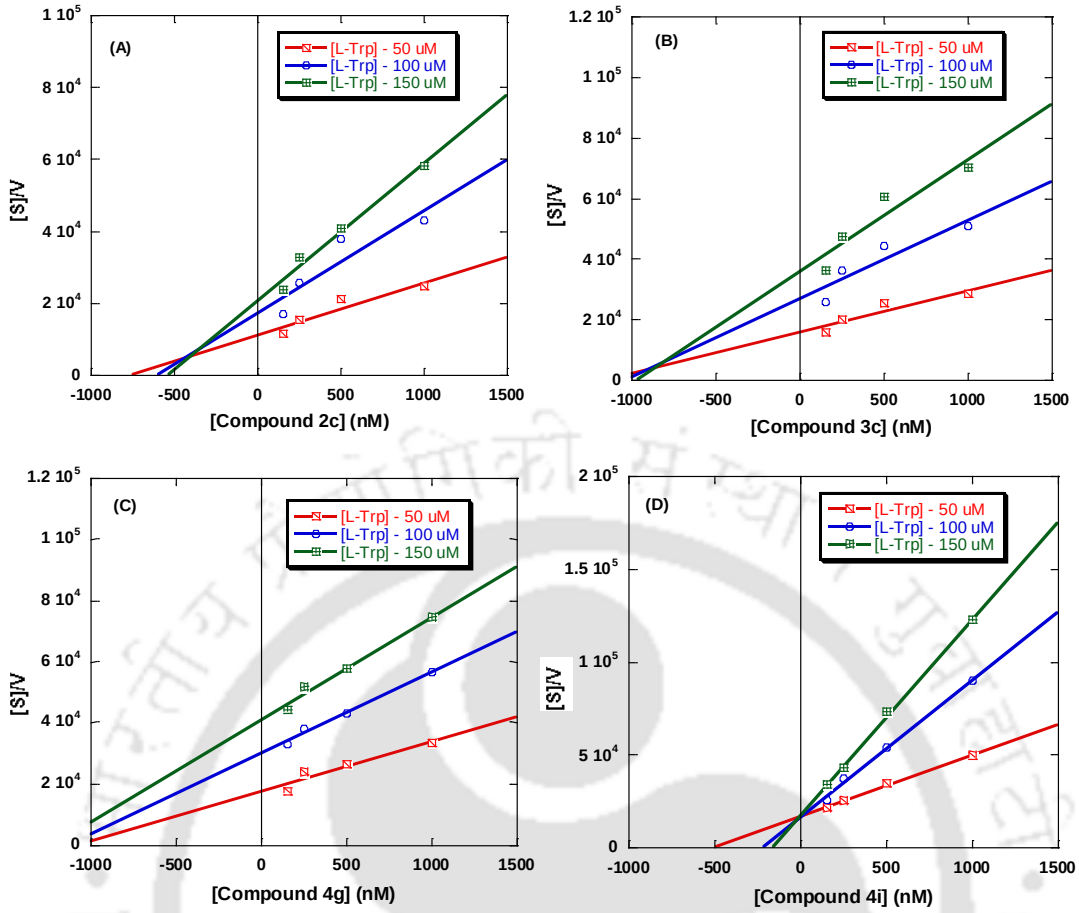

Figure 4.4. Determination of mode of inhibition of the potent compounds. Plot of [S]/V against concentrations of compounds **2c** (A), **3c** (B), **4g** (C) and **4i** (D). Concentration of L-Trp was varied from 50 to 150 µM. The concentrations of compounds were varied from 150 to 1000 nM.

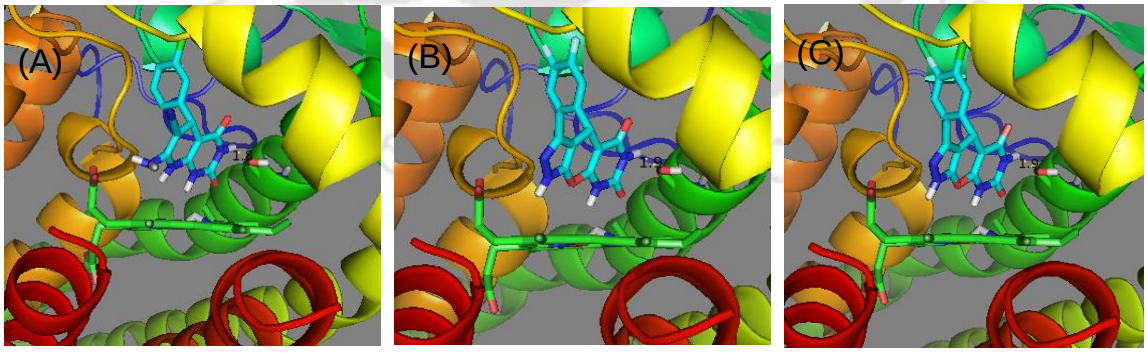

Figure 4.5. Predicted mode of interaction of the compounds, **2c** (A), **4g** (B) and **4i** (C) with the active site of the human IDO1 enzyme (4PK5). The modelled structures were generated using MoleGro Virtual Docker (MVD), version 6.0. The oxygen and nitrogen atoms are shown in red and blue, respectively. Interactions are shown using dashed lines.

Electronic properties of the fused heterocyclic ring and halogen substitution on the phenyl ring also play crucial role in binding of the compounds to the active site of IDO1 enzyme. Thus, hydrogen bonding, pi-stacking and hydrophobic interactions contribute significantly to the stronger binding of the compounds.

4.2.8. Inhibitory activities of the compounds against purified TDO enzyme

The other heme-containing enzyme TDO is also involved in the catabolism of L-Trp through the kynurenine pathway. TDO activity is crucial for the catabolism of L-Trp and regulation of L-Trp level in the liver as TDO is primarily located to the liver. Therefore to verify the selectivity of the potent compounds as IDO1 inhibitors, the inhibitory activities of the compounds against purified TDO enzyme were performed. The results showed the IC_{50} values of the selected compounds within 5 to 31 μM (Table 4.4). Compound **3c** showed higher inhibitory activity for IDO1 (> 100 fold) over TDO enzyme under the similar experimental conditions. The selectivity of the potent compounds as IDO1 inhibitors against TDO enzyme was also confirmed by the HPLC analysis (Table 4.5).

Table 4.4. Inhibitory activity of the selected compounds against purified human IDO1 and TDO enzymes

Compound	IDO1 inhibition IC_{50} (nM)[a]	TDO inhibition IC_{50} (μM)[a]	Selectivity ratio[b]
2c	473 ± 23	29.96 ± 2.12	63
3c	296 ± 18	31.25 ± 3.59	106
4g	410 ± 24	5.21 ± 0.29	13
4i	438 ± 22	10.50 ± 0.76	24

[a] IC_{50} values are the mean of three independent assays against purified enzymes.

[b] Selectivity ratio is calculated as (IC_{50} value of TDO)/(IC_{50} value of IDO1).

Table 4.5. HPLC based IDO1 and TDO inhibition assays of the selected compounds

Compound	IDO1 inhibition IC_{50} (nM)[a]	TDO inhibition IC_{50} (μM)[a]	Selectivity ratio[b]
2c	525 ± 16	2.76 ± 0.09	5
3c	437 ± 13	2.78 ± 0.17	6
4g	246 ± 11	2.71 ± 0.11	11
4i	299 ± 19	4.76 ± 0.19	16

[a] IC_{50} values calculated by HPLC method are the mean of three independent assays.

[b] Selectivity ratio is calculated as (IC_{50} value of TDO)/(IC_{50} value of IDO1).

In this study, fused heterocyclic compounds were designed as IDO1 inhibitors. Subsequent modification of the electronic properties of the fused heterocyclic ring and substitution of the phenyl ring directed to the identification of potent inhibitors with low micromolar IDO1 enzyme inhibitory activities under the *in vitro* conditions. Overall, activity studies showed that pyridopyrimidines and pyrazolopyranopyrimidines moiety and di-halogen substituted phenyl ring could considerably enhance the inhibition potency of these fused heterocyclic compounds. Spectroscopic studies suggest that the pyrazolopyranopyrimidine derivatives preferably interact with the deoxy-ferrous-IDO1 enzyme. Molecular model structure propose that the electronic properties of pyridopyrimidines and pyrazolopyranopyrimidines ring and halogen substituted phenyl ring assist these compounds to interact with the IDO1 through hydrogen bonding, pi-stacking and hydrophobic interactions. Hence, pyridopyrimidines and pyrazolopyranopyrimidines represent a promising class of IDO1 inhibitors. The potent compounds also displayed > 100-fold stronger inhibition for IDO1 enzyme inhibition in comparison with the TDO enzyme. Low cytotoxicity and inactivity for TDO enzyme support further development of fused heterocyclic compounds as inhibitor of IDO1 enzyme.

4.3. Conclusion

To find out potent inhibitors of IDO1 enzyme a series of fused heterocyclic compounds was synthesized. Several of these compounds showed strong inhibitory activity against purified human IDO1 enzyme. The presence of fused di- or tri-heterocyclic moieties and their electronic properties could be the key factor for their strong *in vitro* inhibitory activities. Halogen substitutions in the phenyl ring were effective in improving the potency of these compounds. Spectroscopic measurements supported the interaction of the potent compounds with the heme-group of IDO1 enzyme. IDO1 activity in the interferon-γ induced MDA-MB-231 cells showed that the tested compounds have minimal cytotoxicity and low-nanomolar potencies. These heterocyclic compounds also showed selectivity for IDO1 enzyme over TDO enzyme under the similar experimental conditions. Overall, these observations suggest that these fused heterocyclic compounds are potential inhibitor of IDO1 enzyme and could be of interest as potential drug candidates in cancer and other human diseases.

4.4. Experimental Section

4.4.1. General information

As described in chapter 3 section 3.4.1.

4.4.2. General procedure for the synthesis of 5-methyl-2,4-dihydro-3*H*-pyrazol-3-one

To a stirred solution of hydrazine hydrate (1.2 mmol) and K_2CO_3 (2.5 mmol) in ethanol (20 mL) was added ethyl acetoacetate (1 mmol) and the reaction mixture was heated under reflux at 70 °C for 2 h.[8] The progress of the reaction was monitored by thin layer chromatography (TLC). The reaction mixture was cooled to room temperature and the solid precipitate formed was collected by filtration. It was washed successively with minimum amount of ethanol and water and dried under vacuum to produce the target product in 92% yield.

4.4.3. General procedure for the synthesis of 6-aminouracil

To a stirred solution of hydrazine hydrate (1.2 mmol) and K_2CO_3 (2.5 mmol) in ethanol (20 mL) was added ethyl 3 cyanoacetate (1 mmol) and the reaction mixture was heated under reflux at 70 °C for 2 h.[8] The progress of the reaction was monitored by TLC. The reaction mixture was cooled to room temperature and the solid precipitate formed was collected by filtration. It was washed successively with minimum amount of ethanol and water and dried under vacuum to produce the target product in 88% yield.

4.4.4. General procedure for the synthesis of 4-phenyl-4*H*-pyridine derivatives (2a-i)

To a stirred solution of aromatic aldehyde (1 mmol), malononitrile (1.2 mmol) and K_2CO_3 (2.5 mmol) in 3 ml of ethanol was added 6-amino uracil (1 mmol) and the reaction mixture was heated under reflux at 70 °C for 3 h.[8] The progress of the reaction was monitored by TLC. The reaction mixture was cooled to room temperature and the solid precipitate formed was collected by filtration. It was washed successively with minimum amount of ethanol and water and dried under vacuum to produce the target product in. 82-88% yield.

4.4.5. General procedure for the synthesis of 4-phenyl pyridone derivatives (3a-i)

To a stirred solution of aromatic aldehyde (1 mmol), ethyl cyanoacetate (1.2 mmol) and K_2CO_3 (2.5 mmol) in 3 ml of ethanol was added 6-aminouracil (1 mmol) and the reaction mixture was heated under reflux at 70 °C for 3 h.[8] The progress of the reaction was

monitored by TLC. The reaction mixture was cooled to room temperature and the solid precipitate formed was collected by filtration. It was washed successively with minimum amount of ethanol and water and dried under vacuum to produce the target product in 83-90% yield.

4.4.6. General procedure for the synthesis of 4-phenyl-4*H*-Pyran derivatives (4a-i)

To a stirred solution of aromatic aldehyde (1 mmol), 5-methyl-2,4-dihydro-3*H*-pyrazol-3-one (1.1 mmol) and K_2CO_3 (2.5 mmol) in 3 ml of ethanol was added 6-aminouracil (1.1 mmol) and the reaction mixture was heated under reflux at 70 °C for 3 h.[8] The progress of the reaction was monitored by TLC. The reaction mixture was cooled to room temperature and and the solid precipitate formed was collected by filtration. It was washed successively with minimum amount of ethanol and water and dried under vacuum to produce the target product in 85-90% yield.

4.4.7. Spectroscopic characterization of the synthesized compounds

7-amino-2,4-dioxo-5-phenyl-1,2,3,4,5,8-hexahydropyrido[2,3-d]pyrimidine-6-carbonitrile (2a): As white solid (82% yield; m.p. > 300 °C); ^{1}H NMR (600 MHz, $CDCl_3$ + DMSO-d_6) δppm 7.37-7.35 (m, 2H), 7.19-7.16 (m, 2H), 7.06-7.04 (m, 1H), 4.34 (s, 1H); ^{13}C NMR (151 MHz, $CDCl_3$ + DMSO-d_6) δppm 160.0, 158.8, 137.5, 128.2, 128.0, 127.7, 127.4, 116.2, 82.3, 78.3, 29.4; HRMS (ESI) calcd. for $C_{14}H_{11}N_5O_2$ [M + H]$^+$: 282.0986, found: 282.0982.

7-amino-5-(3-fluorophenyl)-2,4-dioxo-1,2,3,4,5,8-hexahydropyrido[2,3-d]pyrimidine-6-carbonitrile (2b): As white solid (80% yield; m.p. > 300 °C); ^{1}H NMR (600 MHz, DMSO-d_6) δppm 12.14 (br s, 1H), 10.22 (br s, 1H), 7.43.7.36 (m, 1H), 7.20-7.14 (m, 1H), 7.05-7.01 (m, 2H), 4.44 (s, 1H); ^{13}C NMR (151 MHz, DMSO-d_6) δppm 164.3, 160.8, 159.9, 155.9, 152.5, 140.4, 129.5, 123.7, 118.0, 114.4, 93.6, 74.1; HRMS (ESI) calcd. For $C_{14}H_{10}FN_5O_2$ [M + H]$^+$: 300.0852, found: 300.0849.

7-amino-5-(3-chlorophenyl)-2,4-dioxo-1,2,3,4,5,8-hexahydropyrido[2,3-d]pyrimidine-6-carbonitrile (2c): As white solid (85% yield; m.p. > 300 °C); ^{1}H NMR (600 MHz, D_2O + DMSO-d_6) δppm 8.15 (s, 1H), 7.85 (s, 1H), 7.72 (d, J = 12 Hz, 1H), 7.54-7.52 (m, 1H), 7.47-7.43 (m, 1H); ^{13}C NMR (151 MHz, D_2O + DMSO-d_6) δppm

163.6, 160.7, 160.5, 153.8, 134.6, 133.7, 133.2, 131.7, 129.8, 114.2, 85.2, 52.7, 29.8; HRMS (ESI) calcd. for $C_{14}H_{10}ClN_5O_2$ $[M + H]^+$: 316.0596, found: 316.0596.

7-amino-5-(4-fluorophenyl)-2,4-dioxo-1,2,3,4,5,8-hexahydropyrido[2,3-d]pyrimidine-6-carbonitrile (2d): As white solid (80% yield; m.p. > 300 °C); ^{1}H NMR (600 MHz, DMSO-d_6) δppm 7.81-7.78 (m, 2H), 7.56-7.46 (m, 2H), 4.30 (s, 1H); ^{13}C NMR (151 MHz, DMSO-d_6) δppm 164.7, 160.4, 153.9, 134.4, 133.3, 129.5, 129.3, 124.7, 43.2; HRMS (ESI) calcd. for $C_{14}H_{10}FN_5O_2$ $[M + H]^+$: 300.0891, found: 300.0892.

7-amino-5-(4-chlorophenyl)-2,4-dioxo-1,2,3,4,5,8-hexahydropyrido[2,3-d]pyrimidine-6-carbonitrile (2e): As white solid (77% yield; m.p. > 300 °C); ^{1}H NMR (600 MHz, D_2O + DMSO-d_6) δppm 7.78-7.76 (m, 2H), 7.42-7.40 (m, 2H), 3.89 (s, 1H); ^{13}C NMR (151 MHz, D_2O + DMSO-d_6) δppm 170.3, 161.9, 161.2, 153.5, 152.4, 131.6, 119.9, 117.9, 116.0, 114.3; HRMS (ESI) calcd. for $C_{14}H_{10}ClN_5O_2$ $[M + H]^+$: 316.0596, found: 316.0596.

7-amino-5-(4-bromophenyl)-2,4-dioxo-1,2,3,4,5,8-hexahydropyrido[2,3-d]pyrimidine-6-carbonitrile (2f): As white solid (75% yield; m.p. > 300 °C); ^{1}H NMR (600 MHz, D_2O + DMSO-d_6) δppm 7.30 (d, J = 12 Hz, 2H), 6.99 (d, J = 12 Hz), 4.73 (s, 1H); ^{13}C NMR (151 MHz, $CDCl_3$) δppm 166.9, 161.0, 159.7, 132.6, 130.2, 125.9, 115.5, 29.9; HRMS (ESI) calcd. for $C_{14}H_{10}BrN_5O_2$ $[M + H]^+$: 360.0091, found: 360.0085.

7-amino-5-(3,4-difluorophenyl)-2,4-dioxo-1,2,3,4,5,8-hexahydropyrido[2,3-d]pyrimidine-6-carbonitrile (2g): As white solid (88% yield; m.p. > 300 °C); ^{1}H NMR (600 MHz, DMSO-d_6) δppm 6.92-6.85 (m, 2H), 6.76 (s, 1H), 4.17 (s, 1H); ^{13}C NMR (151 MHz, DMSO-d_6) δppm 166.9, 163.1, 161.0, 159.0, 132.6, 130.2, 125.9, 115.5; HRMS (ESI) calcd. for $C_{14}H_9F_2N_5O_2$ $[M + H]^+$: 318.0797, found: 318.0797.

7-amino-5-(3,4-dichlorophenyl)-2,4-dioxo-1,2,3,4,5,8-hexahydropyrido[2,3-d]pyrimidine-6-carbonitrile (2h): As white solid (85% yield; m.p. > 300 °C); ^{1}H NMR (600 MHz, DMSO-d_6) δppm 11.83 (br s, 1H), 9.35 (s, 1H), 7.83-7.78 (m, 1H), 7.31 (s, 1H), 7.17-7.15 (m, 1H), 6.79 (s, 2H), 4.30 (s, 1H); ^{13}C NMR (151 MHz, DMSO-d_6) δppm 164.1, 156.0, 150.3, 148.5, 146.8, 130.8, 128.8, 128.6, 127.3, 119.0, 79.2, 43.2, 37.4; HRMS (ESI) calcd. for $C_{14}H_9Cl_2N_5O_2$ $[M + H]^+$: 350.0206, found: 350.0206.

7-amino-5-(3-chloro-4-fluorophenyl)-2,4-dioxo-1,2,3,4,5,8-hexahydropyrido[2,3-d]pyrimidine-6-carbonitrile (2i): As white solid (88% yield; m.p. > 300 °C); ^{1}H NMR (600 MHz, $CDCl_3$ + DMSO-*d*$_6$) δppm 7.34 (s, 1H), 7.20-7.16 (m, 2H), 4.34 (s, 1H); ^{13}C NMR (151 MHz, $CDCl_3$ + DMSO-*d*$_6$) δppm 162.5, 160.9, 130.1, 128.7, 116.3, 116.1, 36.2, 31.2; HRMS (ESI) calcd. for $C_{14}H_9ClFN_5O_2$ $[M + H]^+$: 334.0502, found: 334.0500.

2,4,7-trioxo-5-phenyl-1,2,3,4,7,8-hexahydropyrido[2,3-d]pyrimidine-6-carbonitrile (3a): As white solid (83% yield; m.p. > 300 °C); ^{1}H NMR (600 MHz, D_2O + DMSO-*d*$_6$) δppm 7.81 (s, 1H), 7.67-7.65 (m, 2H), 7.38-7.31 (m, 3H); ^{13}C NMR (151 MHz, D_2O + DMSO-*d*$_6$) δppm 169.4, 162.6, 153.8, 133.8, 133.7, 131.6, 130.7, 121.1, 110.6; HRMS (ESI) calcd. for $C_{14}H_8N_4O_3$ $[M + H]^+$: 281.0669, found: 281.0671.

5-(3-fluorophenyl)-2,4,7-trioxo-1,2,3,4,7,8-hexahydropyrido[2,3-d]pyrimidine-6-carbonitrile (3b): As white solid (80% yield; m.p. > 300 °C); ^{1}H NMR (600 MHz, D_2O + DMSO-*d*$_6$) δppm 10.02 (br s, 1H), 7.71 (br s, 1H), 7.46-7.43 (m, 1H), 7.24-7.21 (m, 1H), 7.14-7.13 (m, 1H), 7.09-7.07 (m, 1H); ^{13}C NMR (151 MHz, D_2O + DMSO-*d*$_6$) δppm 165.0, 161.3, 157.0, 152.9, 139.8, 130.2, 124.1, 116.0, 115.2, 99.0, 74.5; HRMS (ESI) calcd. for $C_{14}H_7FN_4O_3$ $[M + H]^+$: 299.0536, found: 299.0540.

5-(3-chlorophenyl)-2,4,7-trioxo-1,2,3,4,7,8-hexahydropyrido[2,3-d]pyrimidine-6-carbonitrile (3c): As white solid (83% yield; m.p. > 300 °C); ^{1}H NMR (600 MHz, D_2O + DMSO-*d*$_6$) δppm 8.14 (s, 1H), 7.87 (s, 1H), 7.77-7.76 (m, 1H), 7.53-7.52 (m, 1H), 7.48-7.46 (m, 1H); ^{13}C NMR (151 MHz, D_2O + DMSO-*d*$_6$) δppm 163.4, 159.8, 153.6, 134.5, 133.7, 133.2, 131.6, 129.9, 129.8, 124.8, 116.2, 106.6; HRMS (ESI) calcd. for $C_{14}H_7ClN_4O_3$ $[M + H]^+$: 315.0279, found: 315.0280.

5-(4-fluorophenyl)-2,4,7-trioxo-1,2,3,4,7,8-hexahydropyrido[2,3-d]pyrimidine-6-carbonitrile (3d): As white solid (78% yield; m.p. > 300 °C); ^{1}H NMR (600 MHz, D_2O + DMSO-*d*$_6$) δppm 7.86-7.69 (m, 4H); ^{13}C NMR (151 MHz, D2O + DMSO-*d*$_6$) δppm 165.7, 162.4, 161.9, 153.1, 134.1, 132.8, 121.0, 119.1, 117.2; HRMS (ESI) calcd. for $C_{14}H_7FN_4O_3$ $[M + H]^+$: 299.0575, found: 299.0570.

5-(4-chlorophenyl)-2,4,7-trioxo-1,2,3,4,7,8-hexahydropyrido[2,3-d]pyrimidine-6-carbonitrile (3e): As white solid (75% yield; m.p. > 300 °C); ^{1}H NMR (600 MHz, DMSO-*d*$_6$) δppm 7.87-7.86 (m, 2H), 7.56-7.54 (m, 2H); ^{13}C NMR (151 MHz, DMSO-*d*$_6$) δppm 161.8, 145.0, 134.8, 132.5, 130.8, 129.0, 119.3, 115.5; HRMS (ESI) calcd. for $C_{14}H_7ClN_4O_3$ $[M + H]^+$: 315.0279, found: 315.0277.

5-(4-bromophenyl)-2,4,7-trioxo-1,2,3,4,7,8-hexahydropyrido[2,3-d]pyrimidine-6-carbonitrile (3f): As white solid (65% yield; m.p. > 300 °C); ^{1}H NMR (600 MHz, D_2O + DMSO-*d*$_6$) δppm 7.90 (d, 2H, J = 18 Hz), 7.46 (d, 2H, J = 12 Hz); ^{13}C NMR (151 MHz, D_2O + DMSO-*d*$_6$) δppm 172.1, 165.8, 160, 159.5, 158.8, 138.8, 131.7, 130.6, 122.1, 120.1, 97.8, 96.1; HRMS (ESI) calcd. for $C_{14}H_7BrN_4O_3$ $[M + H]^+$: 358.9774, found: 358.9775.

5-(3,4-difluorophenyl)-2,4,7-trioxo-1,2,3,4,7,8-hexahydropyrido[2,3-d]pyrimidine-6-carbonitrile (3g): As white solid (70% yield; m.p. > 300 °C); ^{1}H NMR (600 MHz, D_2O + DMSO-*d*$_6$) δppm 8.11 (s, 1H), 7.82-7.81 (m, 1H), 7.65 (s, 1H), 7.37-7.34 (m, 1H); ^{13}C NMR (151 MHz, D_2O + DMSO-*d*$_6$) δppm 164.5, 161.3, 161.0, 154.0, 130.1, 125.6, 120.0, 119.7, 118.1, 116.8, 116.1, 114.2; HRMS (ESI) calcd. for $C_{14}H_6F_2N_4O_3$ $[M + H]^+$: 317.0481, found: 317.0481.

5-(3,4-dichlorophenyl)-2,4,7-trioxo-1,2,3,4,7,8-hexahydropyrido[2,3-d]pyrimidine-6-carbonitrile (3h): As white solid (68% yield; m.p. > 300 °C); ^{1}H NMR (600 MHz, D_2O + DMSO-*d*$_6$) δppm 8.15 (s, 1H), 8.04 (s, 1H), 7.78-7.76 (m, 1H), 7.64-7.62 (m, 1H); ^{13}C NMR (151 MHz, D_2O + DMSO-*d*$_6$) δppm 165.7, 162.1, 161.9, 154.7, 153.1, 135.0, 134.1, 133.9, 132.8, 121.0, 119.1, 117.2, 115.3; HRMS (ESI) calcd. for $C_{14}H_6Cl_2N_4O_3$ $[M + H]^+$: 348.9890, found: 348.9885.

5-(3-chloro-4-fluorophenyl)-2,4,7-trioxo-1,2,3,4,7,8-hexahydropyrido[2,3-d]pyrimidine-6-carbonitrile (3i): As white solid (70% yield; m.p. > 300 °C); ^{1}H NMR (600 MHz, D_2O + DMSO-*d*$_6$) δppm 9.69 (s, 1H), 7.84-7.68 (m, 2H), 7.23 (s, 1H); ^{13}C NMR (151 MHz, D_2O + DMSO-*d*$_6$) δppm 163.9, 150.6, 133.3, 133.2, 131.2, 119.4, 118.9, 118.8, 111.9; HRMS (ESI) calcd. for $C_{14}H_6FClN_4O_3$ $[M + H]^+$: 333.0185, found: 333.0190.

3-methyl-4-phenyl-4,8-dihydropyrazolo[4',3':5,6]pyrano[2,3-d]pyrimidine-5,7(1H,6H)-dione (4a): As white solid (65% yield; m.p. > 300 °C); ^{1}H NMR (600 MHz, D_2O) δppm 7.33-7.03 (m, 5H), 5.30 (s, 1H), 2.10 (s, 3H); ^{13}C NMR (151 MHz, D_2O) δppm 166.5, 165.7, 153.8, 135.3, 129.9, 128.3, 126.6, 77.6, 31.7, 9.4; HRMS (ESI) calcd. for $C_{15}H_{12}N_4O_3$ $[M + H]^+$: 297.0982, found: 297.0975.

4-(3-fluorophenyl)-3-methyl-4,8-dihydropyrazolo[4',3':5,6]pyrano[2,3-d]pyrimidine-5,7(1H,6H)-dione (4b): As white solid (65% yield; m.p. > 300 °C); ^{1}H NMR (600 MHz, DMSO-*d*$_6$) δppm 7.31–7.28 (m, 1H), 7.15–6.95 (m, 3H), 4.78 (s, 1H), 1.95 (s, 3H); ^{13}C NMR (151 MHz, DMSO-*d*$_6$) δppm 168.1, 165.4, 163.8, 161.3, 142.4, 129.7, 125.4, 123.7, 114.9, 111.4, 35.2, 13.4; HRMS (ESI) calcd. for $C_{15}H_{11}FN_4O_3$ $[M + H]^+$: 315.0849, found: 315.0852.

4-(3-chlorophenyl)-3-methyl-4,8-dihydropyrazolo[4',3':5,6]pyrano[2,3-d]pyrimidine-5,7(1H,6H)-dione (4c): As white solid (75% yield; m.p. > 300 °C); ^{1}H NMR (600 MHz, D_2O + DMSO-*d*$_6$) δppm 9.87 (br s, 1H), 7.98 (s, 1H), 7.87-7.76 (m, 1H), 7.54-7.49 (m, 1H), 7.38-7.32 (m, 1H), 3.55 (s, 1H), 1.09 (s, 3H); ^{13}C NMR (151 MHz, D_2O + DMSO-*d*$_6$) δppm 168.6, 167.0, 152.8, 144.1, 132.7, 132.3, 130.8, 130.0, 129.7, 129.3, 93.1, 32.6, 11.5; HRMS (ESI) calcd. for $C_{15}H_{11}ClN_4O_3$ $[M + H]^+$: 331.0592, found: 331.0592.

4-(4-fluorophenyl)-3-methyl-4,8-dihydropyrazolo[4',3':5,6]pyrano[2,3-d]pyrimidine-5,7(1H,6H)-dione (4d): As white solid (68% yield; m.p. > 300 °C); ^{1}H NMR (600 MHz, DMSO-*d*$_6$) δppm 7.29-7.26 (m, 2H), 7.17-7.14 (m, 2H), 4.44 (s, 1H), 1.99 (s, 3H); ^{13}C NMR (151 MHz, DMSO-*d*$_6$) δppm 165.7, 164.8, 163.2, 151.4, 142.0, 132.3, 130.0, 125.1, 116.7, 42.1, 10.6; HRMS (ESI) calcd. for $C_{15}H_{11}FN_4O_3$ $[M + H]^+$: 315.0888, found: 315.0885.

4-(4-chlorophenyl)-3-methyl-4,8-dihydropyrazolo[4',3':5,6]pyrano[2,3-d]pyrimidine-5,7(1H,6H)-dione (4e): As white solid (75% yield; m.p. > 300 °C); ^{1}H NMR (600 MHz, DMSO-*d*$_6$) δppm 8.97 (br s, 1H), 7.75 (d, 2H, J = 18 Hz), 7.05 (d, 2H, J = 18 Hz), 5.35 (s, 1H), 2.14 (s, 3H); ^{13}C NMR (151 MHz, D_2O) δppm 168.5, 166.7, 154.1, 152.5, 141.2, 140.4, 130.9, 128.4, 128.2, 103.9, 93.2, 31.6, 9.6; HRMS (ESI) calcd. for $C_{15}H_{11}ClN_4O_3$ $[M + H]^+$: 331.0592, found: 331.0590.

4-(4-bromophenyl)-3-methyl-4,8-dihydropyrazolo[4',3':5,6]pyrano[2,3-d]pyrimidine-5,7(1H,6H)-dione (4f): As white solid (85% yield; m.p. > 300 °C); ^{1}H NMR (600 MHz, DMSO-*d*$_6$) δppm 7.80-7.67 (m, 4H), 3.48 (s, 1H), 2.13 (s, 3H); ^{13}C NMR (151 MHz, DMSO-*d*$_6$) δppm 176.8, 168.0, 162.2, 160.6, 154.2, 131.7, 131.5, 130.1, 79.5, 25.3, 16.5; HRMS (ESI) calcd. for $C_{15}H_{11}BrN_4O_3$ $[M + H]^+$: 375.0087, found: 375.0085.

4-(3,4-difluorophenyl)-3-methyl-4,8-dihydropyrazolo[4',3':5,6]pyrano[2,3-d]pyrimidine-5,7(1H,6H)-dione (4g): As white solid (90% yield; m.p. > 300 °C); ^{1}H NMR (600 MHz, D_2O + DMSO-*d*$_6$) δppm 7.44-7.39 (m, 3H), 5.48 (s, 1H), 2.32 (s, 3H); ^{13}C NMR (151 MHz, D2O + DMSO-*d*$_6$) δppm 170.0, 168.4, 157.3, 154.9, 143.2, 133.9, 131.0, 129.6, 121.7, 116.0, 94.7, 33.6, 13.4; HRMS (ESI) calcd. for $C_{15}H_{10}F_2N_4O_3$ $[M + H]^+$: 333.0794, found: 333.0790.

4-(3,4-dichlorophenyl)-3-methyl-4,8-dihydropyrazolo[4',3':5,6]pyrano[2,3-d]pyrimidine-5,7(1H,6H)-dione (4h): As white solid (89% yield; m.p. > 300 °C); ^{1}H NMR (600 MHz, D_2O + DMSO-*d*$_6$) δppm 7.35 (s, 1H), 7.00-6.97 (m, 2H), 5.21 (s, 1H), 2.04 (s, 3H); ^{13}C NMR (151 MHz, D_2O + DMSO-*d*$_6$) δppm 164.7, 163.1, 153.4, 140.1, 131.8, 128.6, 126.2, 120.8, 118.4, 43.1, 11.7; HRMS (ESI) calcd. for $C_{15}H_{10}Cl_2N_4O_3$ $[M + H]^+$: 365.0203, found: 365.0205.

4-(3-chloro-4-fluorophenyl)-3-methyl-4,8-dihydropyrazolo[4',3':5,6]pyrano[2,3-d]pyrimidine-5,7(1H,6H)-dione (4i): As white solid (91% yield; m.p. > 300 °C); ^{1}H NMR (600 MHz, DMSO-*d*$_6$) δppm 9.37 (br s, 1H), 7.15-7.12 (m, 1H), 7.09-7.08 (m, 1H), 7.00 (s, 1H), 5.26 (s, 1H), 2.06 (s, 3H); ^{13}C NMR (151 MHz, DMSO-*d*$_6$) δppm 168.6, 167.0, 152.8, 143.6, 132.7, 130.8, 130.0, 129.7, 129.3, 32.7, 12.1; HRMS (ESI) calcd. for $C_{15}H_{10}FClN_4O_3$ $[M + H]^+$: 349.0498, found: 349.0499.

4.4.8. Purification of the compounds by HPLC analysis

Before performing the *in vitro* enzyme activity, cellular activity, MTT assay, morphological analysis and others, all the synthesized compounds were further purified by analytical-HPLC analyses (with a purity level ≥ 94-95%). Prior to the initiation of the purification process, all the compounds were dissolved in 60% MeOH and 40% H_2O, at final concentrations between 1-2 mM, and the resulting solution filtered using Millipore

syringe filters (0.22 µm pore size). Two litres of the running buffer, 60% MeOH and 40% H_2O, were also filtered and sonicated for removal of contaminants and air bubbles. Prior to loading the sample, an Ascentis® Express reverse phase C18, 2.7 µm analytical HPLC column was pre-incubated with the running buffer (60% MeOH and 40% H_2O). The UV detectors of Waters 600E HPLC system were set at 280 nm and 350 nm as the compounds have a strong absorption at this region. The sample's injection volume and flow rate were adjusted to 20 µL and 0.5 mL/min respectively and the pure compounds peak was eluted after ~7 min. This step was repeated for more than 10- times to get sufficient amount of the pure compounds. All the collected fractions for each compound were dried under reduced pressure and confirmed via mass spectrometry analysis.

4.4.9. Expression and purification of recombinant human IDO1 and TDO enzyme

As described earlier in chapter 2 section 2.4.5.

4.4.10. IDO1 and TDO inhibition assay by spectrophotometric method

As described earlier in chapter 2 section 2.4.7.3. The IC_{50} values were calculated in triplicate using ten different inhibitor concentrations (0.01-50 µM for IDO1 and 0.01-100 µM for TDO). Data were analyzed with the GraphPadPrism Software (GraphPadPrism. Version 5.01 program).

4.4.11. IDO1 and TDO inhibition assay by HPLC method

As described earlier in chapter 2 section 2.4.7.4. The concentrations of inhibitors were varied from 50 nM to 50 µM. The IC_{50} values of the compounds were analyzed using the GraphPad Prism software (GraphPad Prism. Version 5.01 program).

4.4.12. Spectroscopic measurements

As described earlier in chapter 2 section 2.4.7.1. The concentration of IDO1 enzyme and compounds, used for this study were 5 µM and 270 µM, respectively.

4.4.13. Cellular activity assay

As described earlier in chapter 3 section 3.4.10. Compound concentrations were varied from 20 nM to 1 mM.

4.4.14. Cell viability and morphological analysis

As described earlier in chapter 3 section 3.4.11.

4.4.15. Determination of modes of enzyme inhibition by the compounds

As described earlier in chapter 2 section 2.4.7.5. Compound concentrations were varied from 150 nM to 1000 nM.

4.4.16. Molecular docking analysis

As described earlier in chapter 3 section 3.4.13.

4.5. References

1. (a) Greco, F. A.; Bournique, A.; Coletti, A.; Custodi, C.; Dolciami, D.; Carotti, A.; Macchiarulo, A., Docking studies and molecular dynamic simulations reveal different features of IDO1 structure. *Mol. Inform.* **2016,** *35* (8-9), 449-459; (b) Austin, C. J.; Rendina, L. M., Targeting key dioxygenases in tryptophan–kynurenine metabolism for immunomodulation and cancer chemotherapy. Drug Discov. Today**2015,** *20* (5), 609-617; (c) Prendergast, G. C.; Smith, C.; Thomas, S.; Mandik-Nayak, L.; Laury-Kleintop, L.; Metz, R.; Muller, A. J., Indoleamine 2, 3-dioxygenase pathways of pathogenic inflammation and immune escape in cancer. Cancer Im*munol. Immunother.* **2014,** *63* (7), 721-735; (d) Mellor, A. L.; Munn, D. H., IDO expression by dendritic cells: tolerance and tryptophan catabolism. *Nat. Rev. Immunol.* **2004,** *4* (10), 762-774.

2. (a) Munn, D. H.; Mellor, A. L., Indoleamine 2, 3-dioxygenase and tumor-induced tolerance. *J. Clin. Investig.* **2007,** *117* (5), 1147-1154; (b) Okamoto, A.; Nikaido, T.; Ochiai, K.; Takakura, S.; Saito, M.; Aoki, Y.; Ishii, N.; Yanaihara, N.; Yamada, K.; Takikawa, O., Indoleamine 2, 3-dioxygenase serves as a marker of poor prognosis in gene expression profiles of serous ovarian cancer cells. *Clin. Cancer Res.* **2005,** *11* (16), 6030-6039; (c) Uyttenhove, C.; Pilotte, L.; Théate, I.; Stroobant, V.; Colau, D.; Parmentier, N.; Boon, T.; Van den Eynde, B. J., Evidence for a tumoral immune resistance mechanism based on tryptophan degradation by indoleamine 2, 3-dioxygenase. *Nat. Med.* **2003,** *9* (10), 1269-1274.

3. (a) Wichers, M. C.; Maes, M., The role of indoleamine 2, 3-dioxygenase (IDO) in the pathophysiology of interferon-α-induced depression. *J. Psychiatry Neurosci.* **2004,** *29* (1), 11-17; (b) Paul, S.; Roy, A.; Deka, S. J.; Panda, S.; Trivedi, V.; Manna, D.,

Nitrobenzofurazan derivatives of *N′*-hydroxyamidines as potent inhibitors of indoleamine-2, 3-dioxygenase 1. *Eur. J. Med. Chem.* **2016,** *121*, 364-375.

4. Zou, W., Immunosuppressive networks in the tumour environment and their therapeutic relevance. *Nat. Rev. Cancer* **2005,** *5* (4), 263-274.

5. (a) Hou, D.-Y.; Muller, A. J.; Sharma, M. D.; DuHadaway, J.; Banerjee, T.; Johnson, M.; Mellor, A. L.; Prendergast, G. C.; Munn, D. H., Inhibition of indoleamine 2, 3-dioxygenase in dendritic cells by stereoisomers of 1-methyl-tryptophan correlates with antitumor responses. *Cancer Res.* **2007,** *67* (2), 792-801; (b) Muller, A. J.; DuHadaway, J. B.; Donover, P. S.; Sutanto-Ward, E.; Prendergast, G. C., Inhibition of indoleamine 2, 3-dioxygenase, an immunoregulatory target of the cancer suppression gene Bin1, potentiates cancer chemotherapy. *Nat. Med.* **2005,** *11* (3), 312-319.

6. (a) Röhrig, U. F.; Majjigapu, S. R.; Vogel, P.; Zoete, V.; Michielin, O., Challenges in the discovery of indoleamine 2, 3-dioxygenase 1 (IDO1) inhibitors. *J. Med. Chem.* **2015,** *58* (24), 9421-9437; (b) Yu, L.-F.; Li, Y.-Y.; Su, M.-B.; Zhang, M.; Zhang, W.; Zhang, L.-N.; Pang, T.; Zhang, R.-T.; Liu, B.; Li, J.-Y., Development of novel alkene oxindole derivatives as orally efficacious AMP-activated protein kinase activators. *ACS Med. Chem. Lett.* **2013,** *4* (5), 475-480; (c) Yue, E. W.; Douty, B.; Wayland, B.; Bower, M.; Liu, X.; Leffet, L.; Wang, Q.; Bowman, K. J.; Hansbury, M. J.; Liu, C., Discovery of potent competitive inhibitors of indoleamine 2, 3-dioxygenase with in vivo pharmacodynamic activity and efficacy in a mouse melanoma model. *J. Med. Chem.* **2009,** *52* (23), 7364-7367.

7. (a) Malachowski, W. P.; Winters, M.; DuHadaway, J. B.; Lewis-Ballester, A.; Badir, S.; Wai, J.; Rahman, M.; Sheikh, E.; LaLonde, J. M.; Yeh, S.-R., O-alkylhydroxylamines as rationally-designed mechanism-based inhibitors of indoleamine 2, 3-dioxygenase-1. *Eur. J. Med. Chem.* **2016,** *108*, 564-576; (b) Huang, Q.; Zheng, M.; Yang, S.; Kuang, C.; Yu, C.; Yang, Q., Structure–activity relationship and enzyme kinetic studies on 4-aryl-1*H*-1, 2, 3-triazoles as indoleamine 2, 3-dioxygenase (IDO) inhibitors. *Eur. J. Med. Chem.* **2011,** *46* (11), 5680-5687.

8. Fadda, A. A.; El-Mekabaty, A.; Elattar, K. M., Chemistry of Enaminonitriles of Pyrano [2, 3-c] pyrazole and Related Compounds. *Synth. Commun.* **2013,** *43* (20), 2685-2719.

9. Röhrig, U. F.; Majjigapu, S. R.; Grosdidier, A. l.; Bron, S.; Stroobant, V.; Pilotte, L.; Colau, D.; Vogel, P.; Van den Eynde, B. J.; Zoete, V., Rational design of 4-aryl-1, 2,

3-triazoles for indoleamine 2, 3-dioxygenase 1 inhibition. *J. Med. Chem.* **2012,** *55* (11), 5270-5290.

10. Röhrig, U. F.; Awad, L.; Grosdidier, A.; Larrieu, P.; Stroobant, V.; Colau, D.; Cerundolo, V.; Simpson, A. J.; Vogel, P.; Van den Eynde, B. t. J., Rational design of indoleamine 2, 3-dioxygenase inhibitors. *J. Med. Chem.* **2010,** *53* (3), 1172-1189.

11. Matsuno, K.; Takai, K.; Isaka, Y.; Unno, Y.; Sato, M.; Takikawa, O.; Asai, A., S-Benzylisothiourea derivatives as small-molecule inhibitors of indoleamine-2, 3-dioxygenase. *Bioorganic Med. Chem. Lett.* **2010,** *20* (17), 5126-5129.

12. Travers, M.; Gow, I. F.; Barber, M.; Thomson, J.; Shennan, D. B., Indoleamine 2, 3-dioxygenase activity and L-tryptophan transport in human breast cancer cells. *Biochim. Biophys. Acta, Biomembr.* **2004,** *1661* (1), 106-112.

13. Yang, S.; Li, X.; Hu, F.; Li, Y.; Yang, Y.; Yan, J.; Kuang, C.; Yang, Q., Discovery of tryptanthrin derivatives as potent inhibitors of indoleamine 2, 3-dioxygenase with therapeutic activity in Lewis lung cancer (LLC) tumor-bearing mice. *J. Med. Chem.* **2013,** *56* (21), 8321-8331.

14. Kumar, S.; Jaller, D.; Patel, B.; LaLonde, J. M.; DuHadaway, J. B.; Malachowski, W. P.; Prendergast, G. C.; Muller, A. J., Structure based development of phenylimidazole-derived inhibitors of indoleamine 2, 3-dioxygenase. *J. Med. Chem.* **2008,** *51* (16), 4968-4977.

15. Tojo, S.; Kohno, T.; Tanaka, T.; Kamioka, S.; Ota, Y.; Ishii, T.; Kamimoto, K.; Asano, S.; Isobe, Y., Crystal structures and structure–activity relationships of imidazothiazole derivatives as IDO1 inhibitors. *ACS Med. Chem. Lett.* **2014,** *5* (10), 1119-1123.

4.4.17. NMR spectra of the synthesized compounds

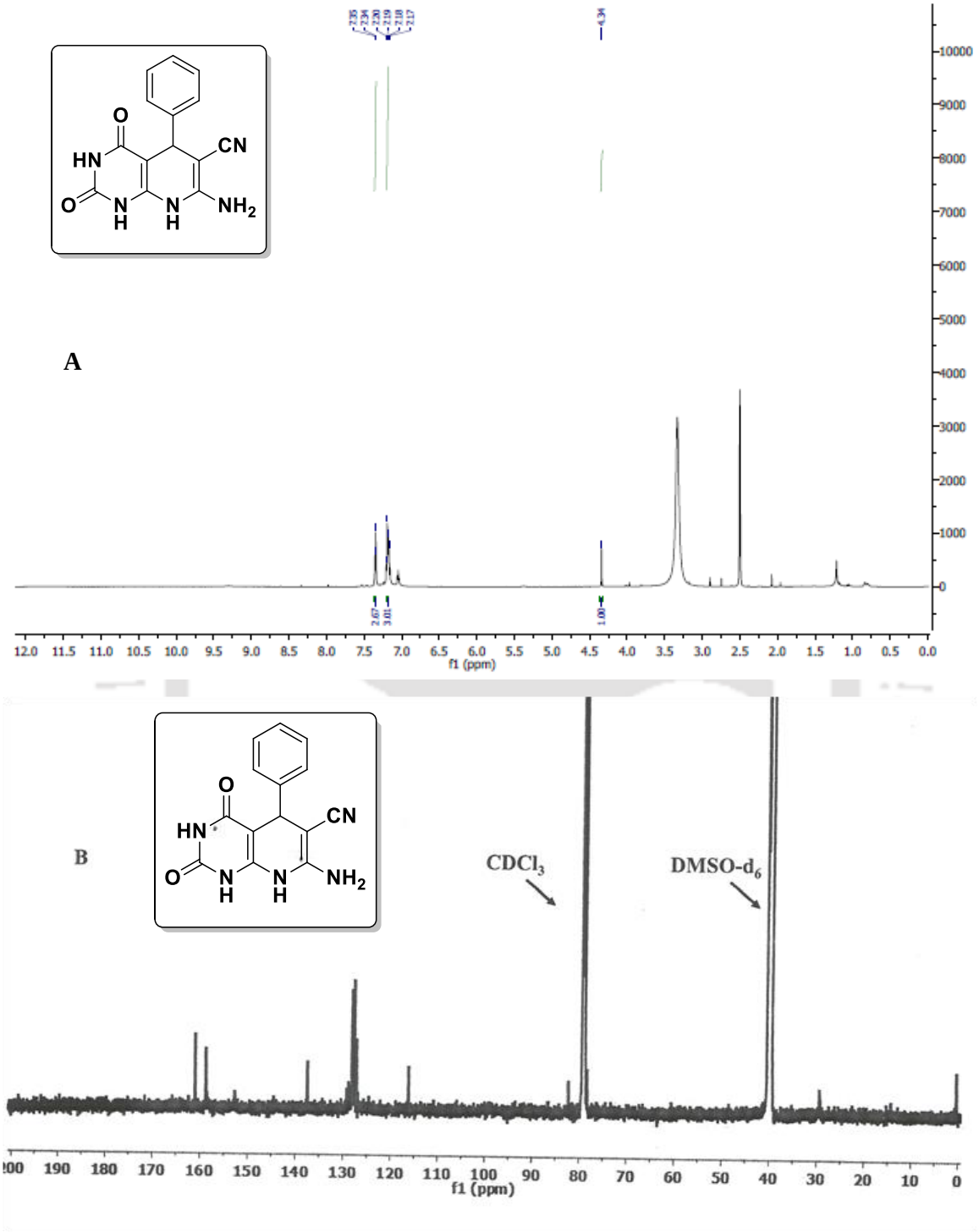

Figure 4.6.1. ^{1}H NMR (A) and ^{13}C NMR (B) of 7-amino-2,4-dioxo-5-phenyl-1,2,3,4,5,8-hexahydropyrido[2,3-d]pyrimidine-6-carbonitrile (**2a**).

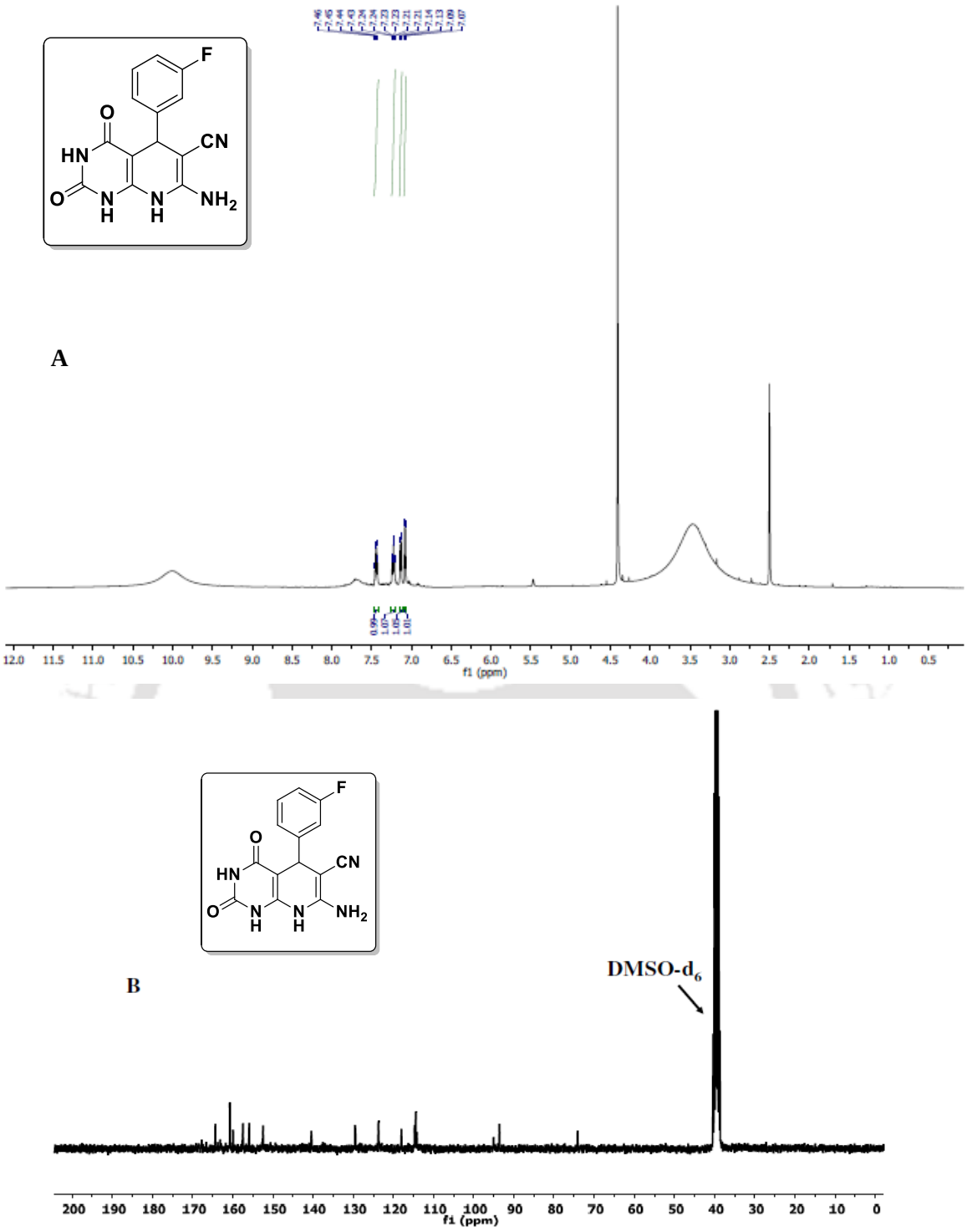

Figure 4.6.2. ^{1}H NMR (A) and ^{13}C NMR (B) of 7-amino-5-(3-fluorophenyl)-2,4-dioxo-1,2,3,4,5,8-hexahydropyrido[2,3-d]pyrimidine-6-carbonitrile (**2b**).

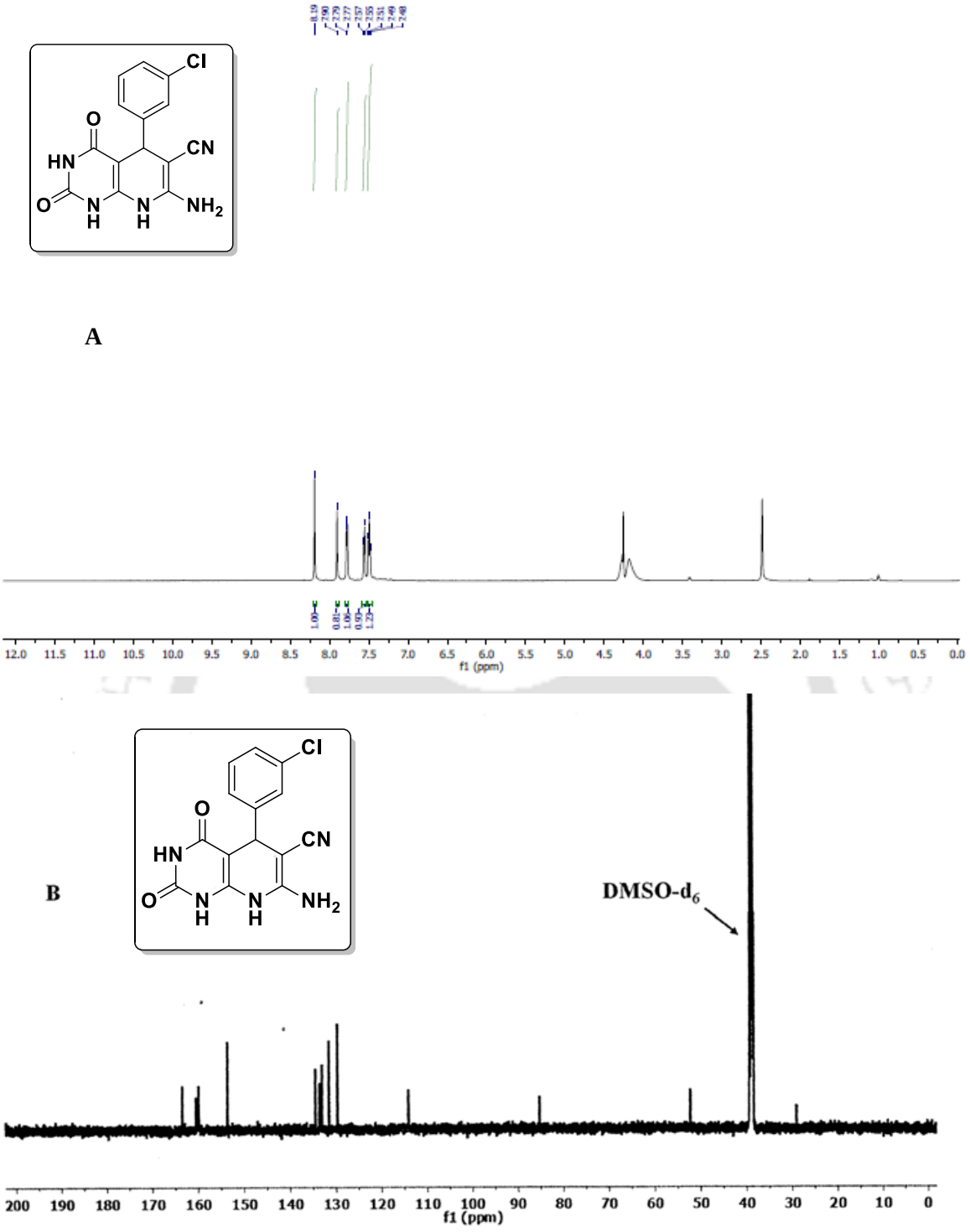

Figure 4.6.3. ^{1}H NMR (A) and ^{13}C NMR (B) of 7-amino-5-(3-chlorophenyl)-2,4-dioxo-1,2,3,4,5,8-hexahydropyrido[2,3-d]pyrimidine-6-carbonitrile (**2c**).

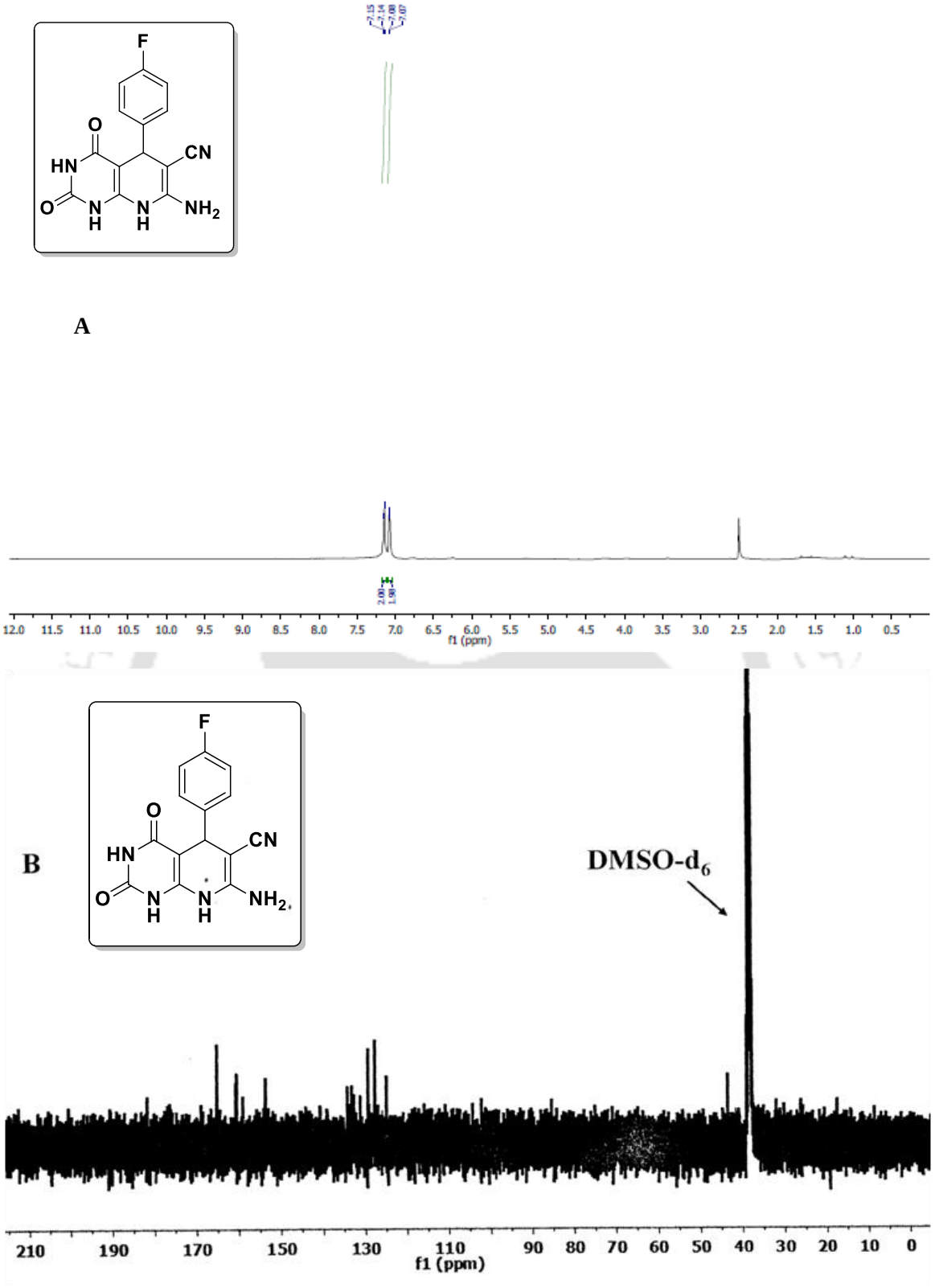

Figure 4.6.4. ^{1}H NMR (A) and ^{13}C NMR (B) of 7-amino-5-(4-fluorophenyl)-2,4-dioxo-1,2,3,4,5,8-hexahydropyrido[2,3-d]pyrimidine-6-carbonitrile (**2d**).

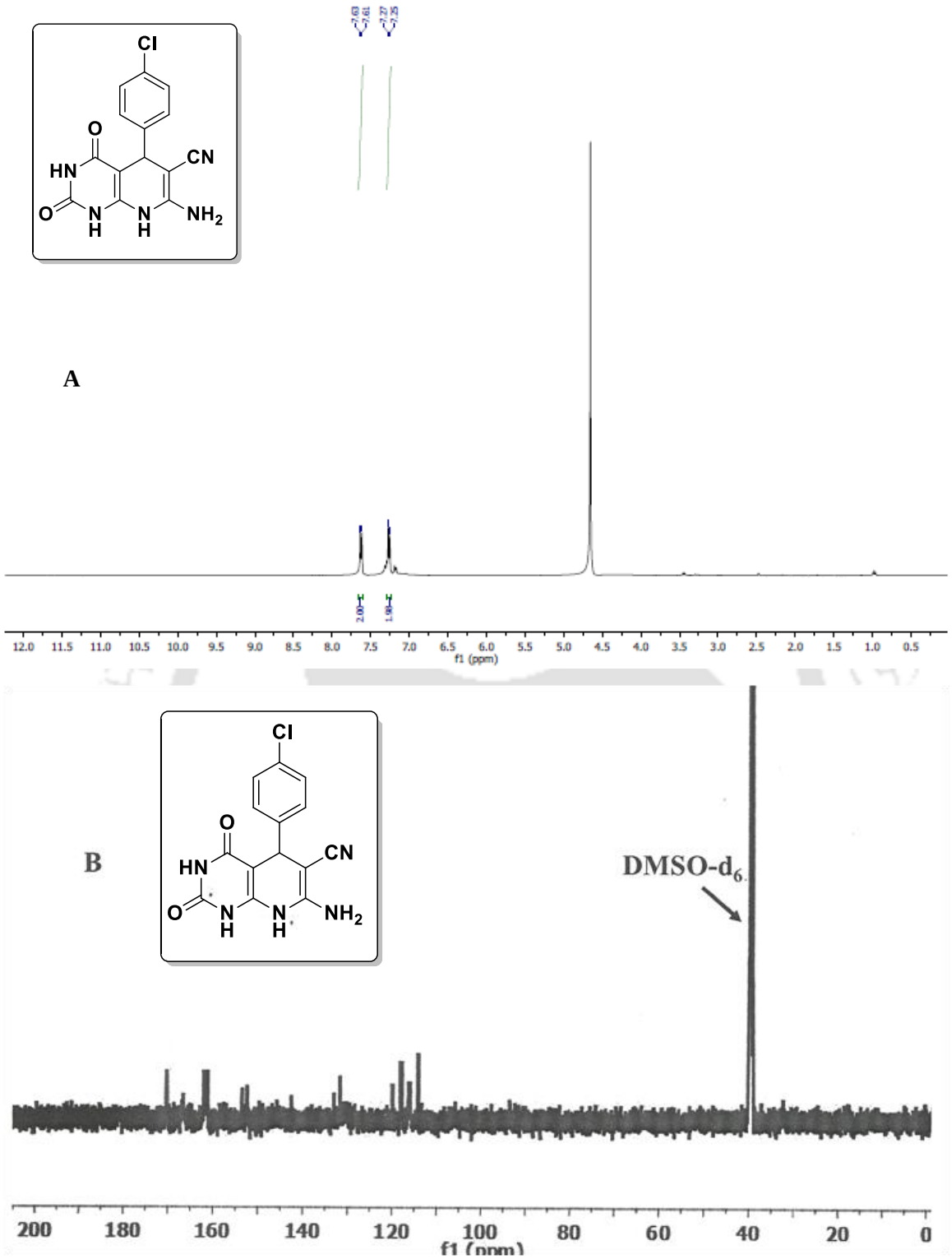

Figure 4.6.5. ^{1}H NMR (A) and ^{13}C NMR (B) of 7-amino-5-(4-chlorophenyl)-2,4-dioxo-1,2,3,4,5,8-hexahydropyrido[2,3-d]pyrimidine-6-carbonitrile (**2e**).

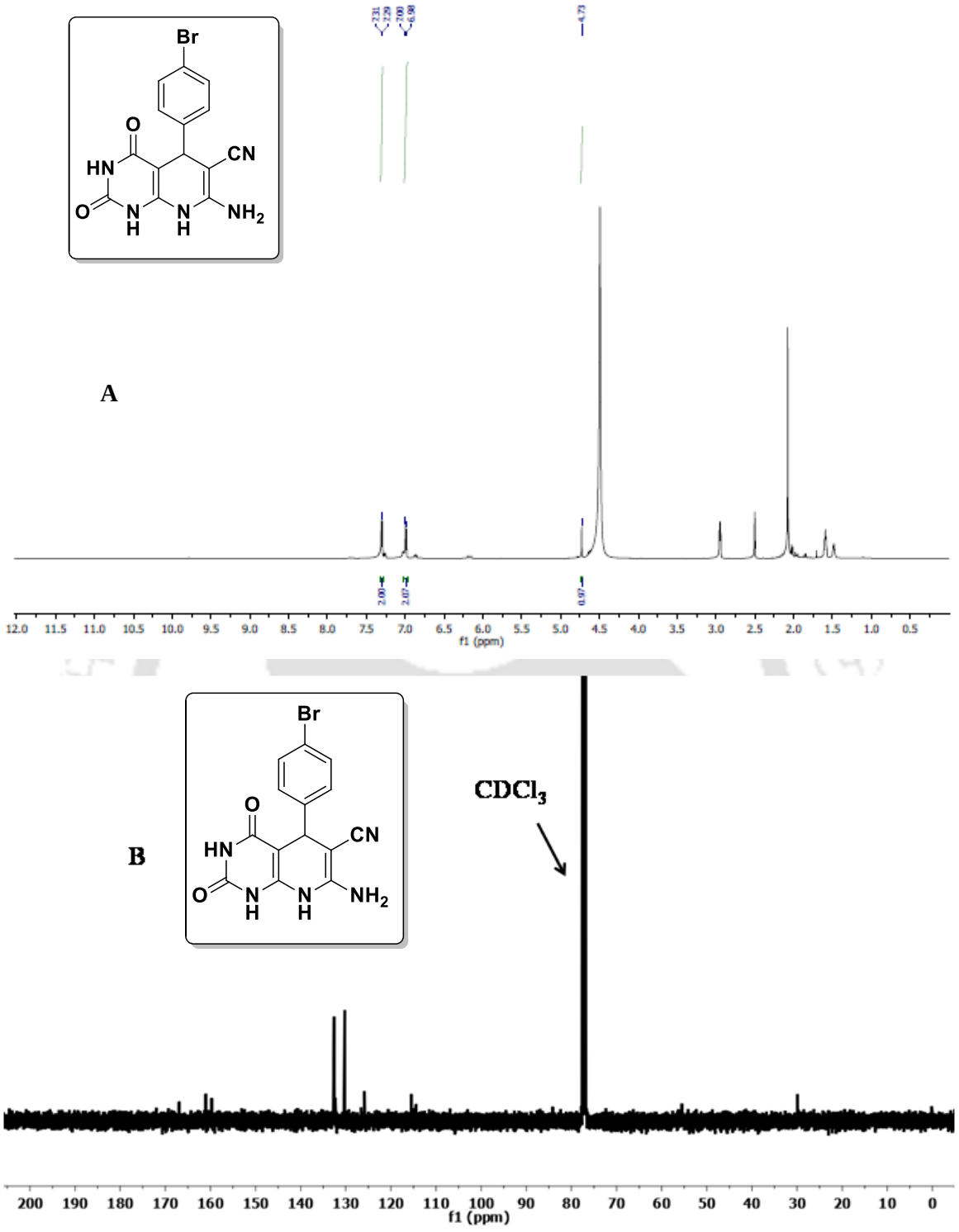

Figure 4.6.6. ^{1}H NMR (A) and ^{13}C NMR (B) of 7-amino-5-(4-bromophenyl)-2,4-dioxo-1,2,3,4,5,8-hexahydropyrido[2,3-d]pyrimidine-6-carbonitrile (**2f**).

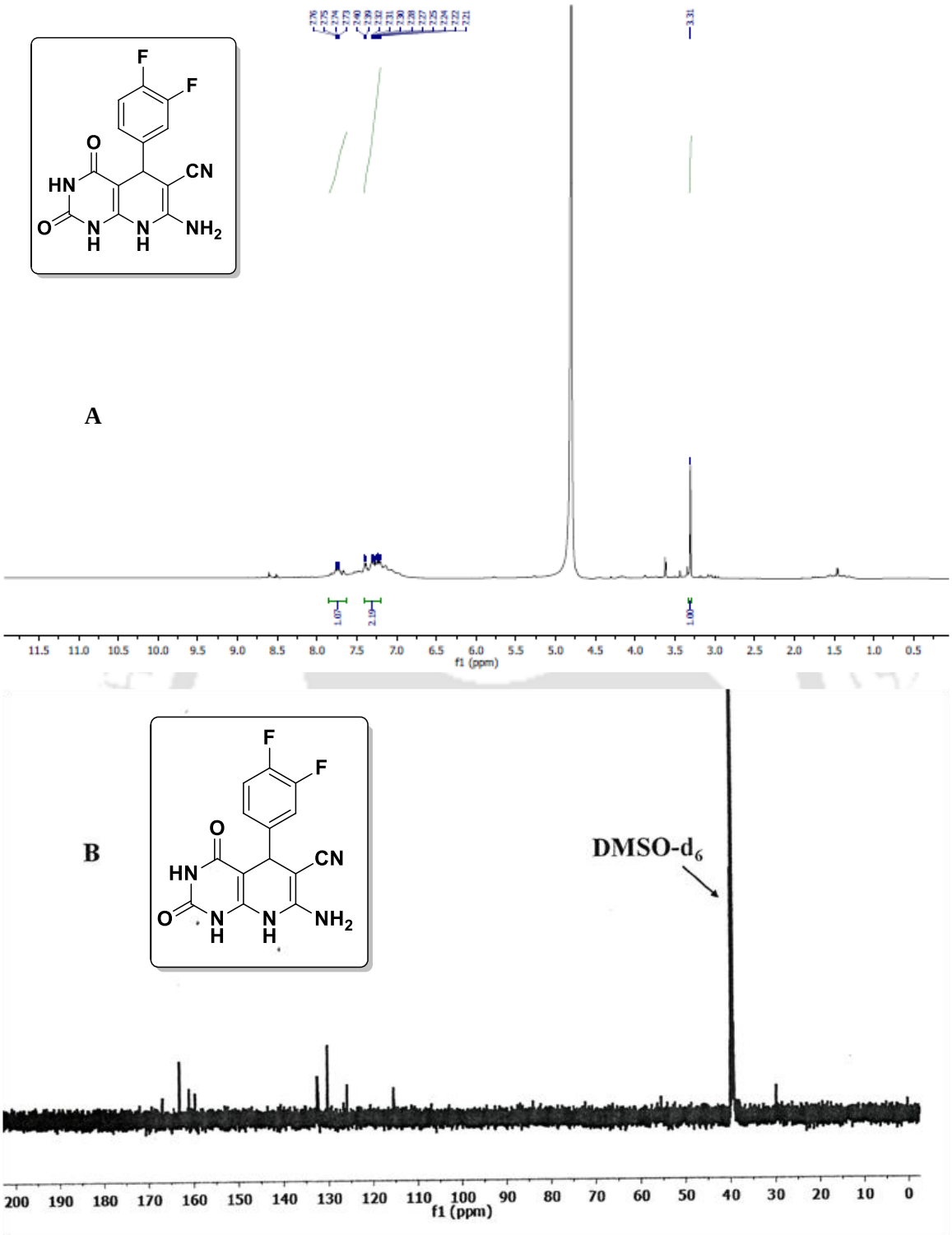

Figure 4.6.7. ^{1}H NMR (A) and ^{13}C NMR (B) of 7-amino-5-(3,4-difluorophenyl)-2,4-dioxo-1,2,3,4,5,8-hexahydropyrido[2,3-d]pyrimidine-6-carbonitrile (**2g**).

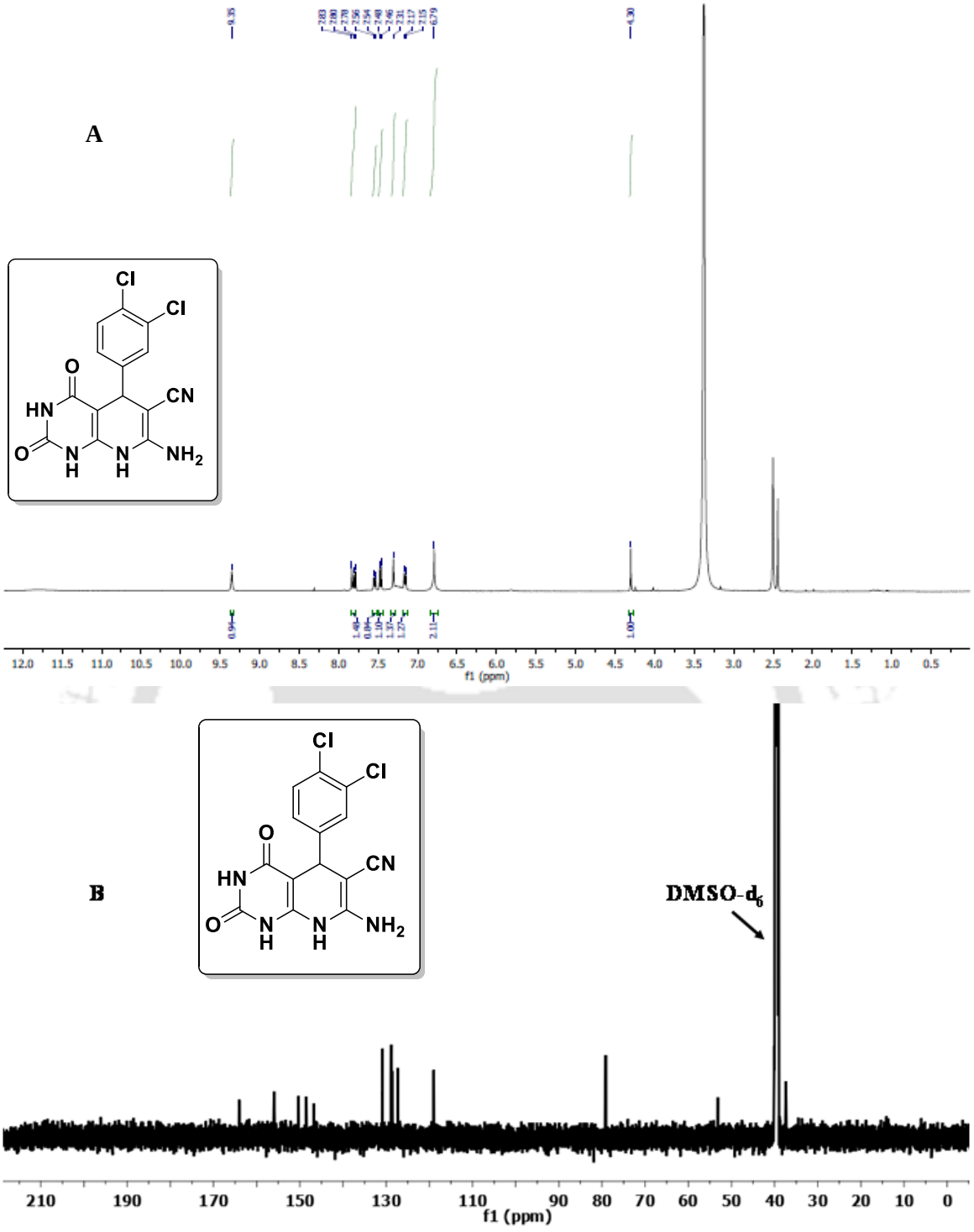

Figure 4.6.8. ^{1}H NMR (A) and ^{13}C NMR (B) of 7-amino-5-(3,4-dichlorophenyl)-2,4-dioxo-1,2,3,4,5,8-hexahydropyrido[2,3-d]pyrimidine-6-carbonitrile (**2h**).

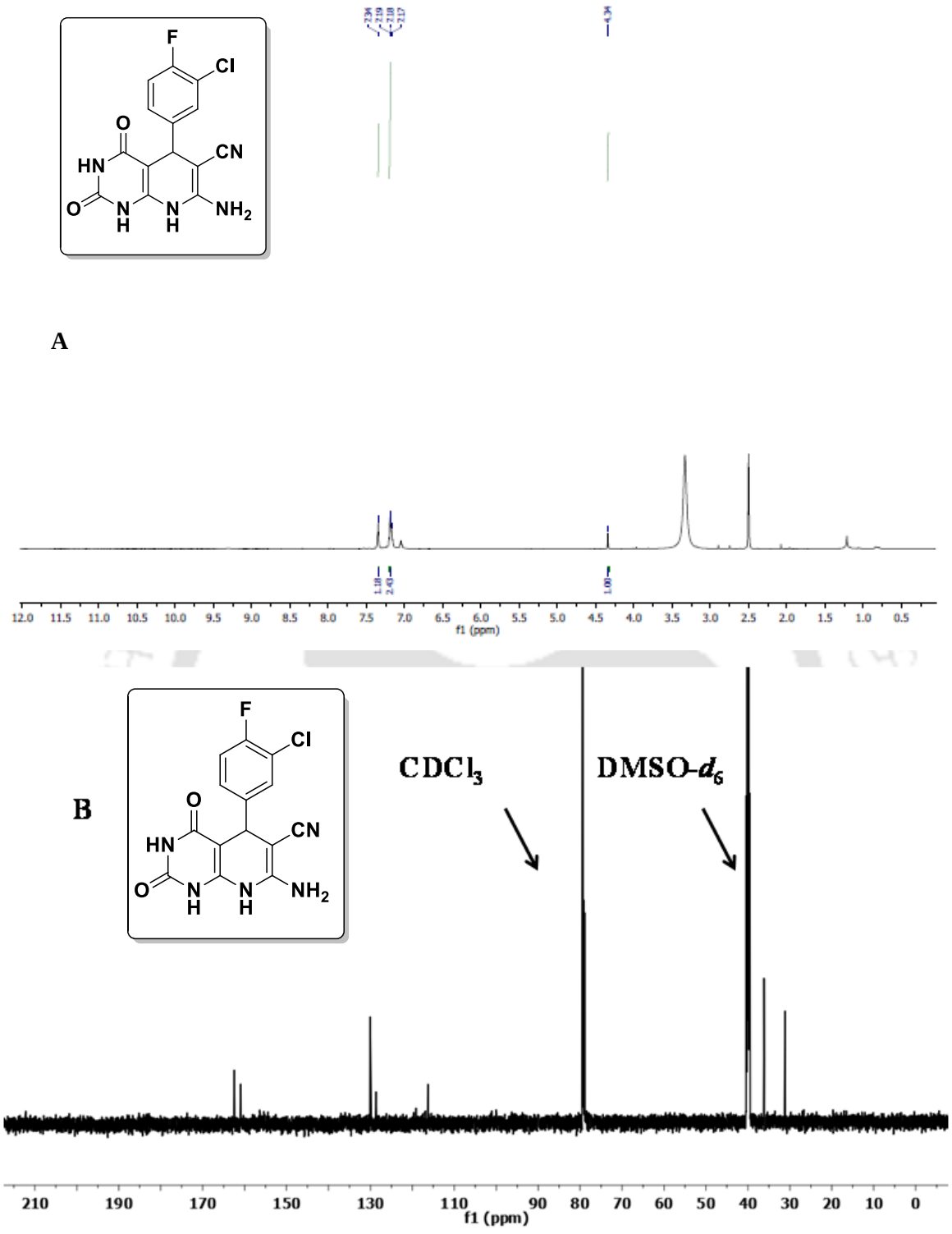

Figure 4.6.9. ^{1}H NMR (A) and ^{13}C NMR (B) of 7-amino-5-(3-chloro-4-fluorophenyl)-2,4-dioxo-1,2,3,4,5,8-hexahydropyrido[2,3-d]pyrimidine-6-carbonitrile (**2i**).

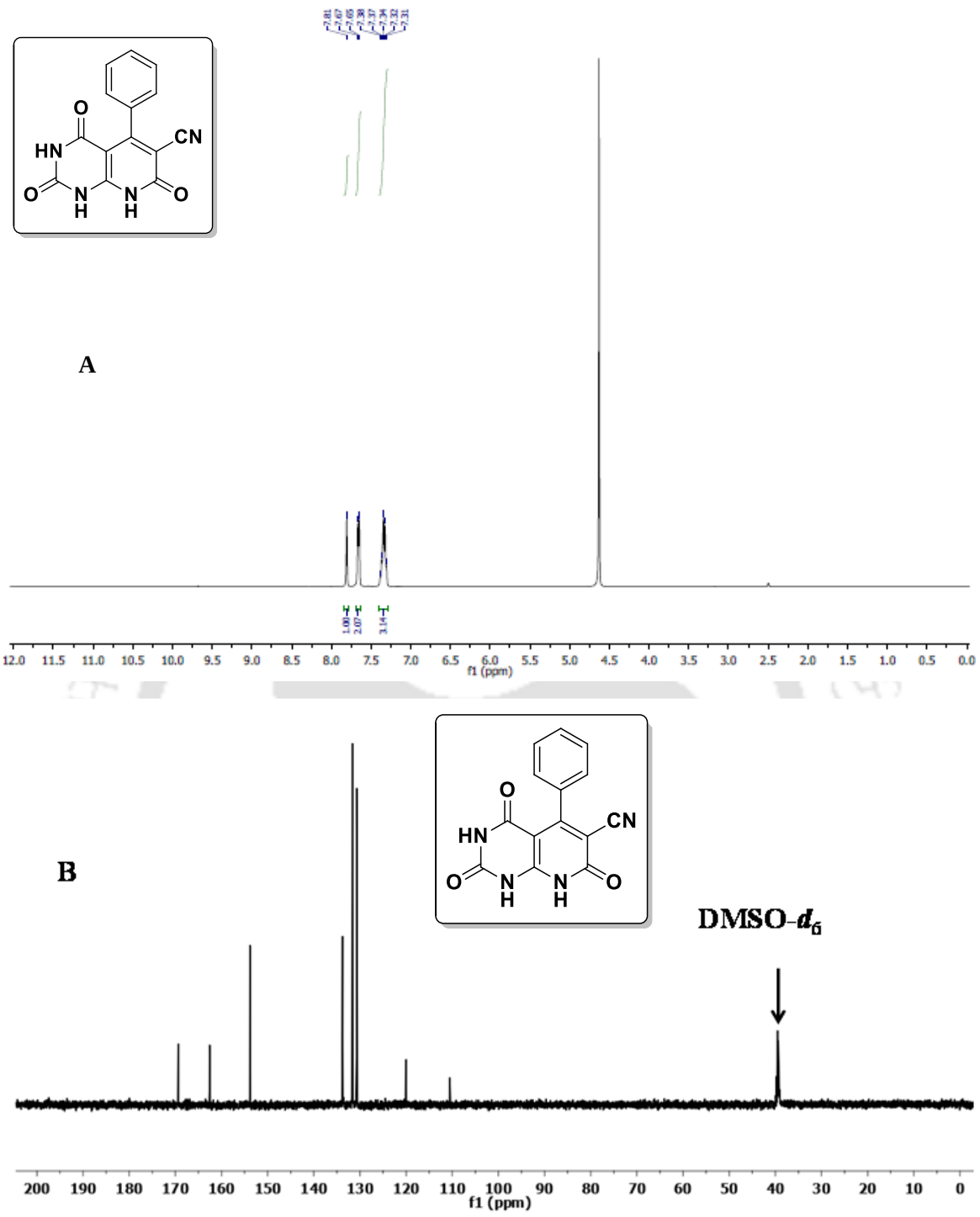

Figure 4.7.1. ^{1}H NMR (A) and ^{13}C NMR (B) of 2,4,7-trioxo-5-phenyl-1,2,3,4,7,8-hexahydropyrido[2,3-d]pyrimidine-6-carbonitrile (**3a**).

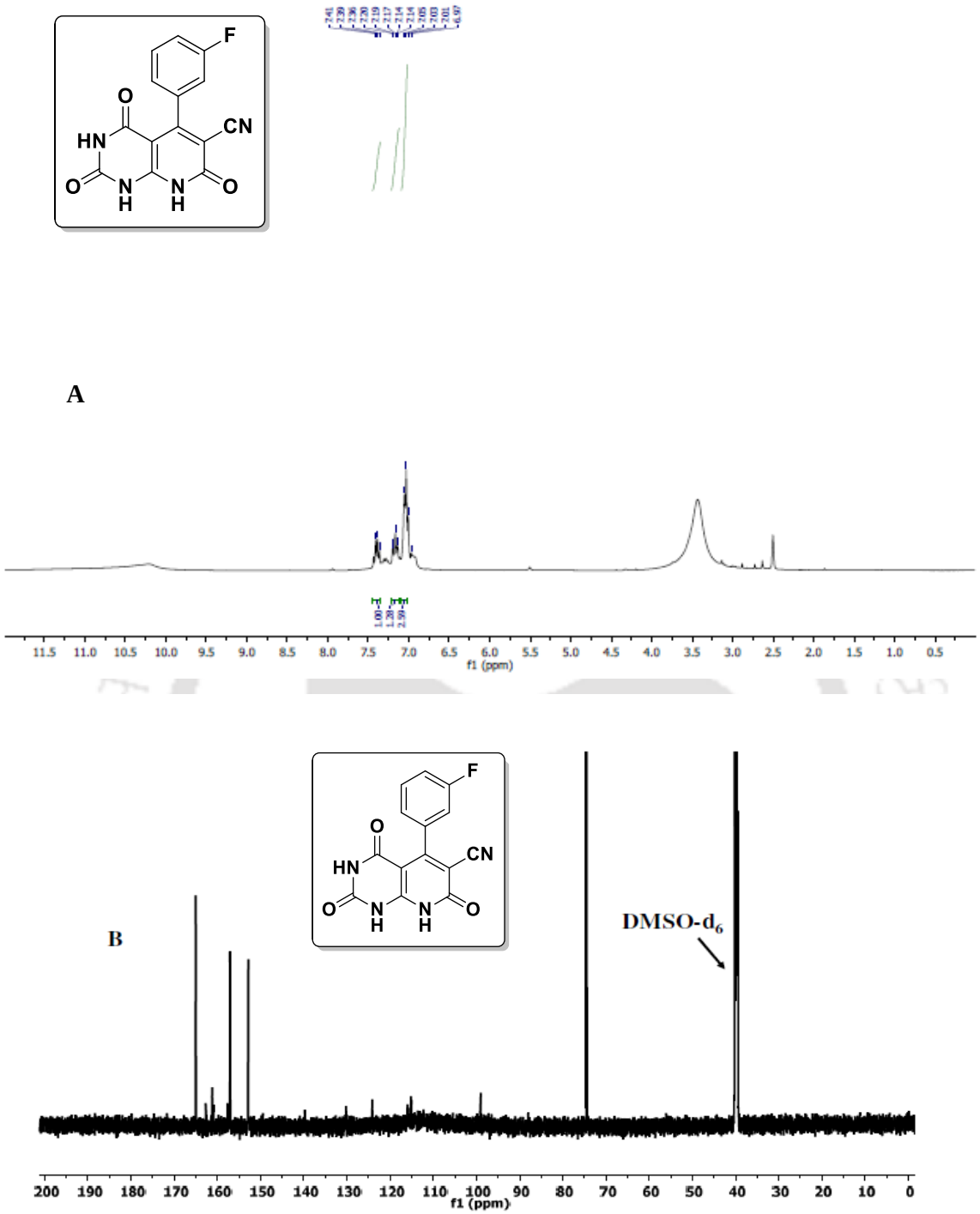

Figure 4.7.2. ^{1}H NMR (A) and ^{13}C NMR (B) of 5-(3-fluorophenyl)-2,4,7-trioxo-1,2,3,4,7,8-hexahydropyrido[2,3-d]pyrimidine-6-carbonitrile (**3b**).

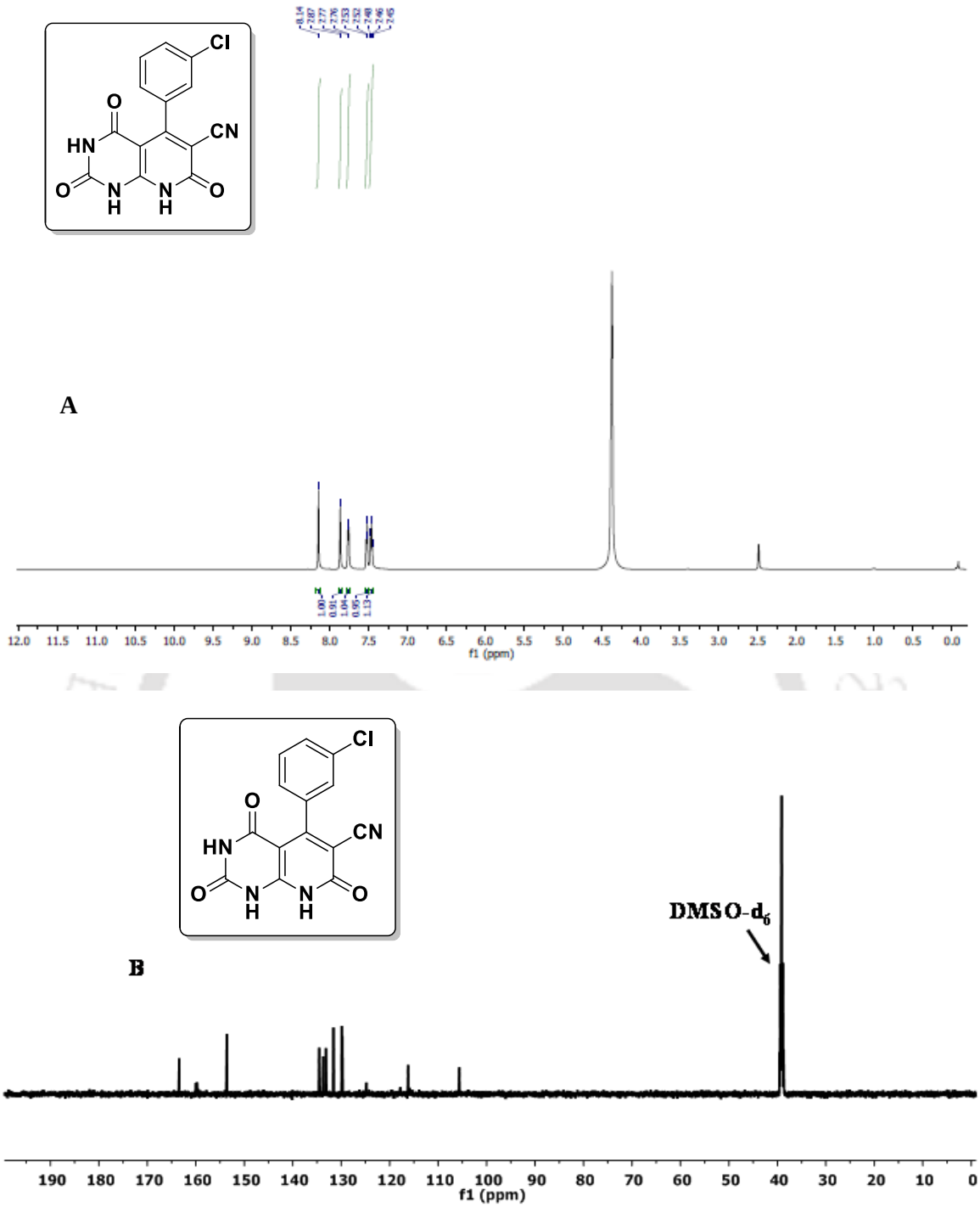

Figure 4.7.3. ^{1}H NMR (A) and ^{13}C NMR (B) of 5-(3-chlorophenyl)-2,4,7-trioxo-1,2,3,4,7,8-hexahydropyrido[2,3-d]pyrimidine-6-carbonitrile (**3c**).

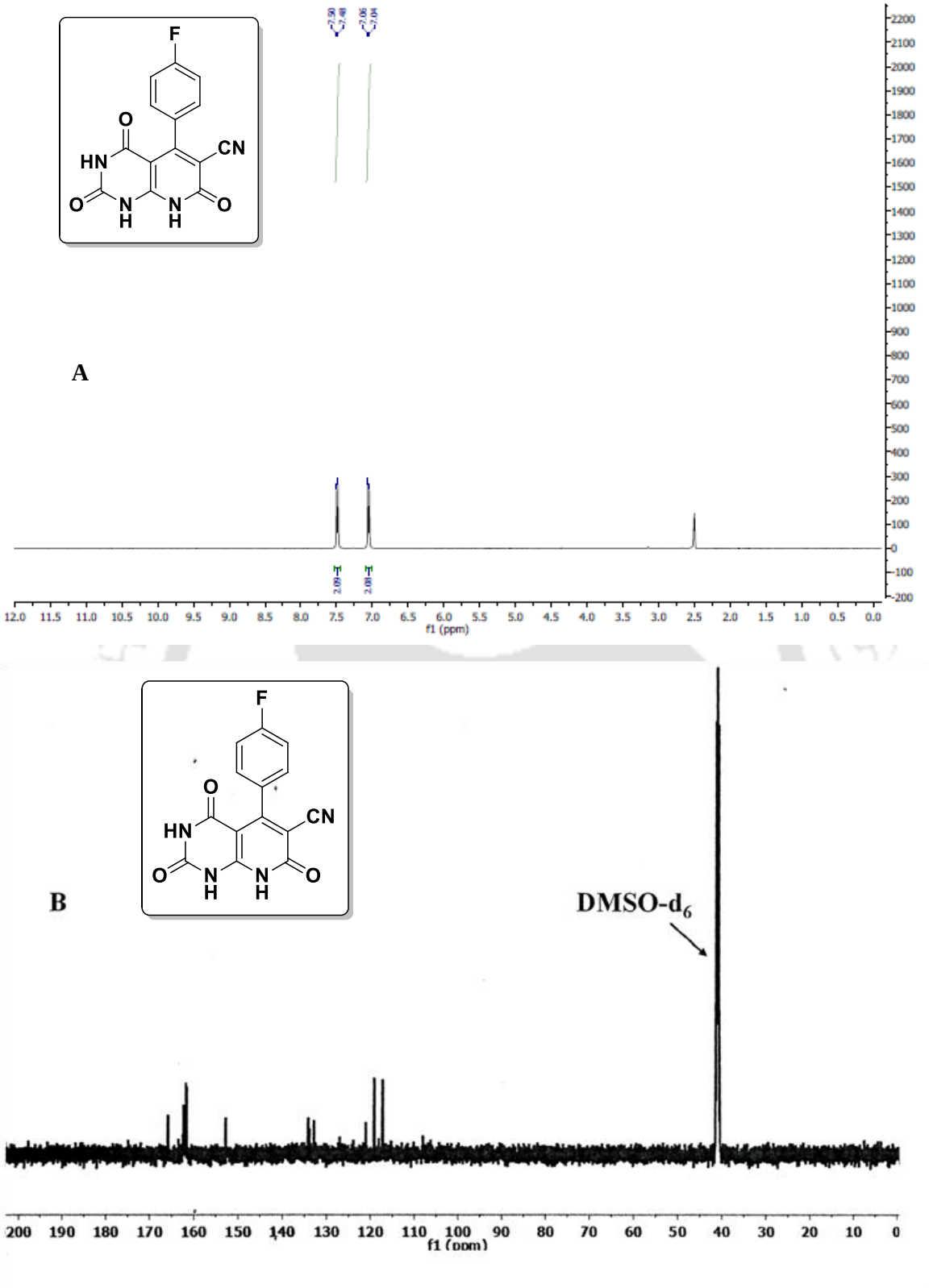

Figure 4.7.4. ^{1}H NMR (A) and ^{13}C NMR (B) of 5-(4-fluorophenyl)-2,4,7-trioxo-1,2,3,4,7,8-hexahydropyrido[2,3-d]pyrimidine-6-carbonitrile (**3d**).

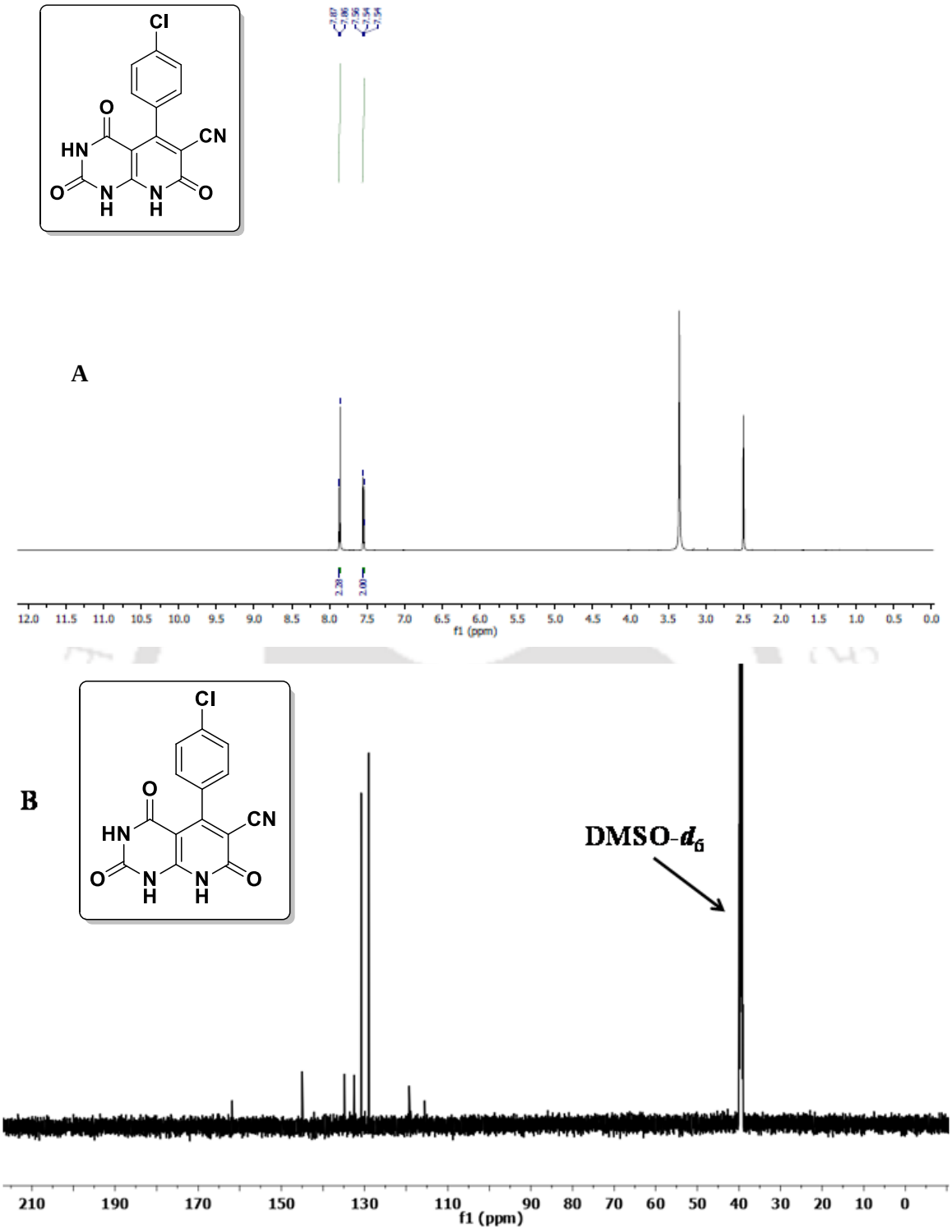

Figure 4.7.5. ^{1}H NMR (A) and ^{13}C NMR (B) of 5-(4-chlorophenyl)-2,4,7-trioxo-1,2,3,4,7,8-hexahydropyrido[2,3-d]pyrimidine-6-carbonitrile (**3e**).

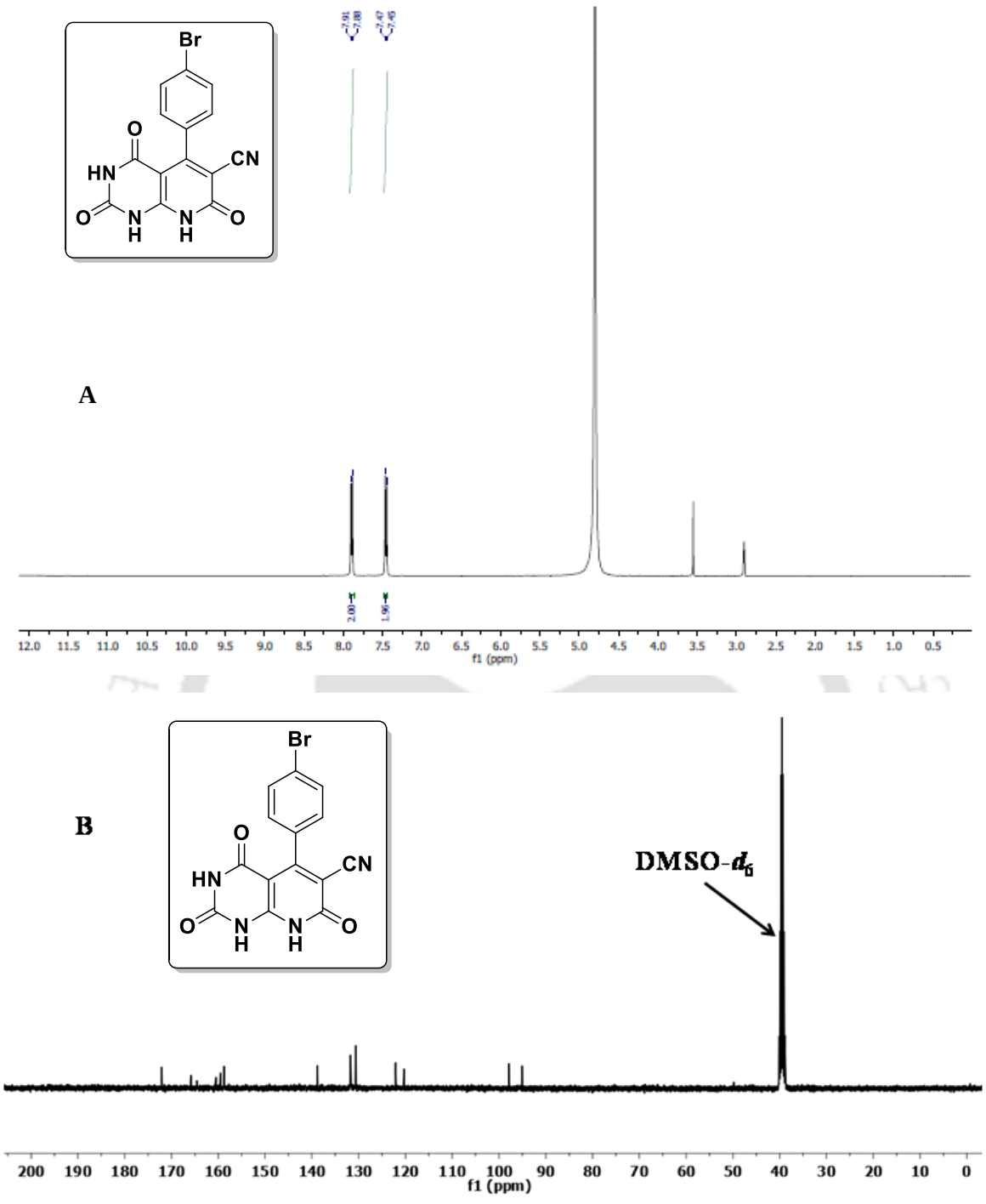

Figure 4.7.6. ^{1}H NMR (A) and ^{13}C NMR (B) of 5-(4-bromophenyl)-2,4,7-trioxo-1,2,3,4,7,8-hexahydropyrido[2,3-d]pyrimidine-6-carbonitrile (**3f**).

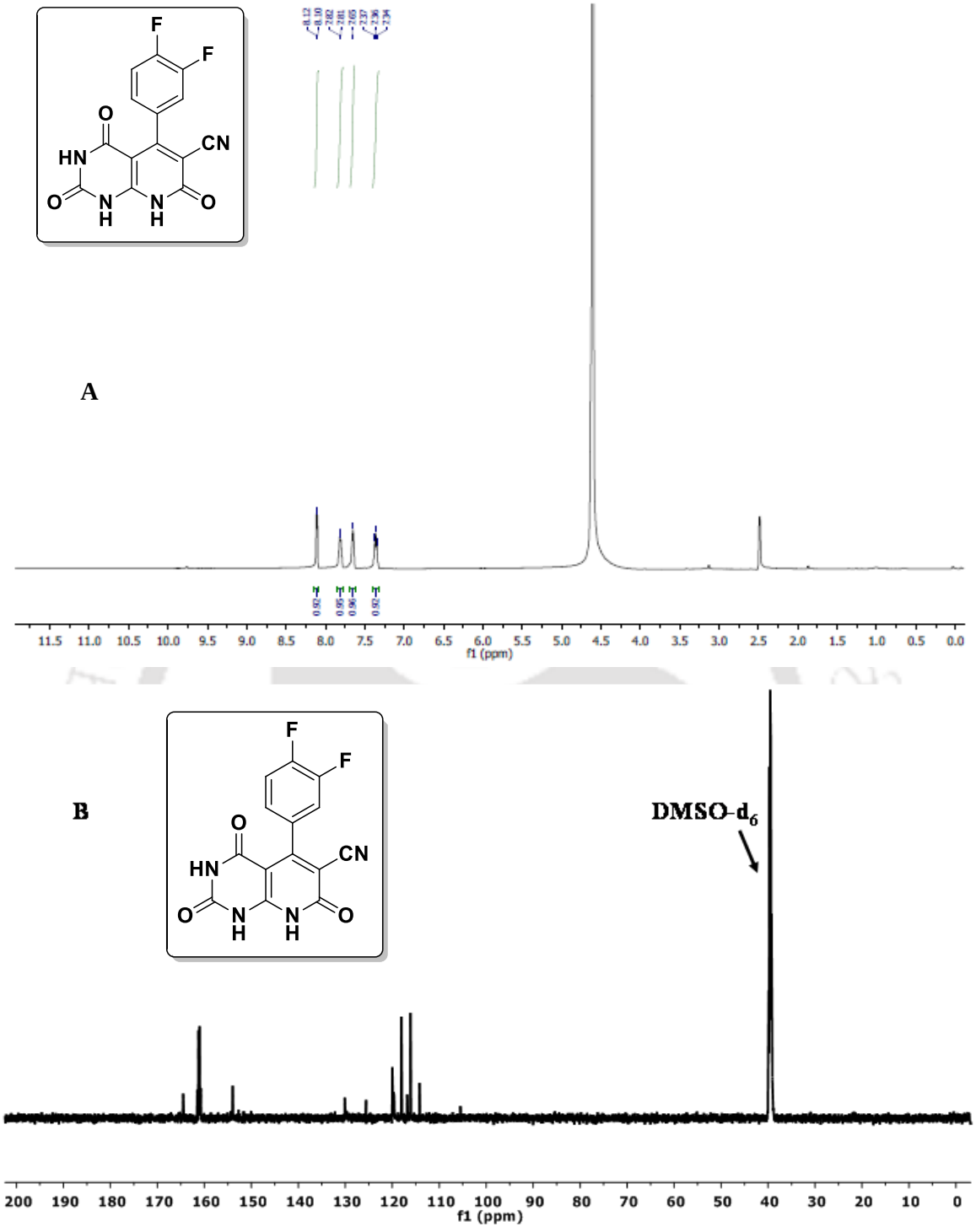

Figure 4.7.7. ^{1}H NMR (A) and ^{13}C NMR (B) of 5-(3,4-difluorophenyl)-2,4,7-trioxo-1,2,3,4,7,8-hexahydropyrido[2,3-d]pyrimidine-6-carbonitrile (**3g**).

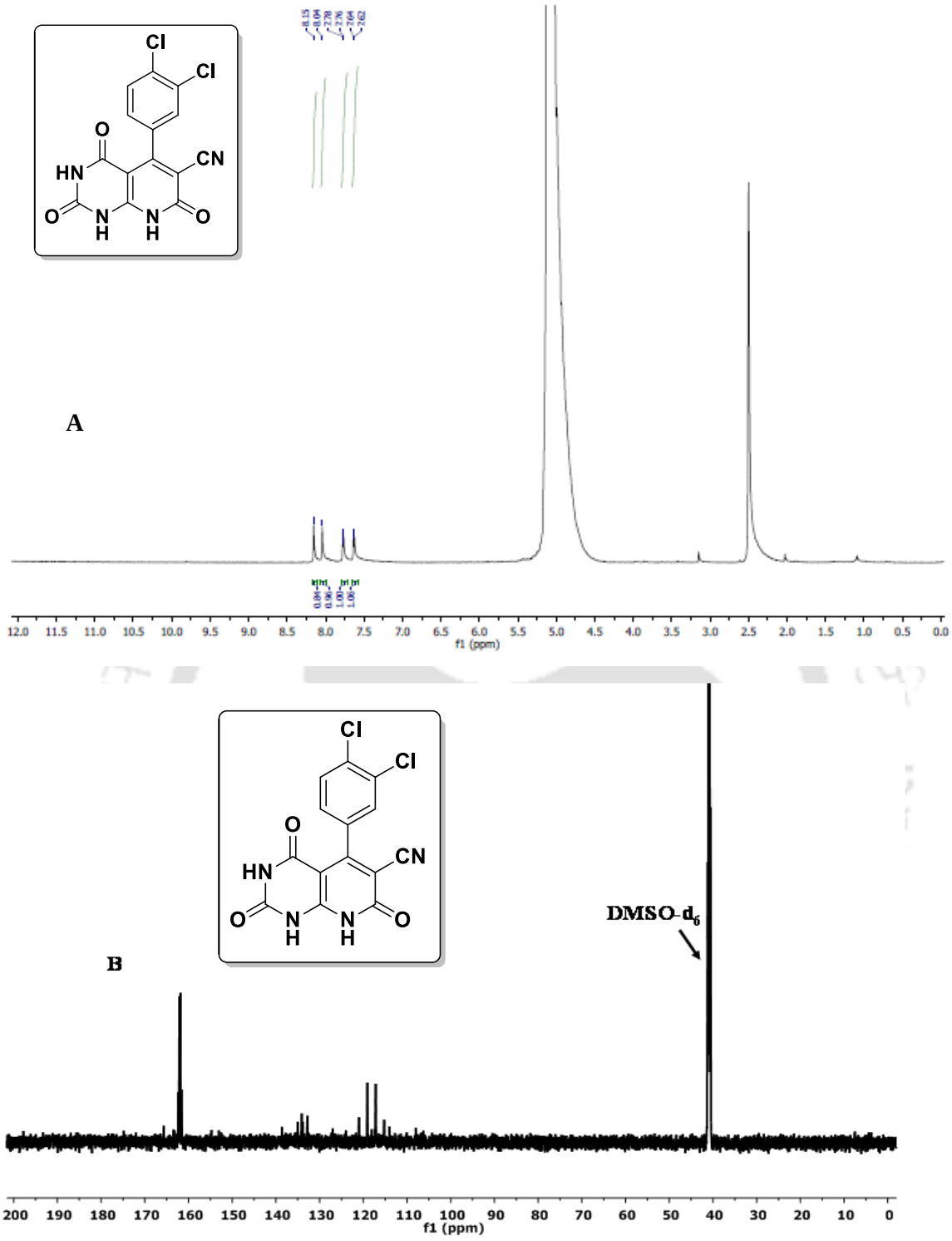

Figure 4.7.8. ^{1}H NMR (A) and ^{13}C NMR (B) of 5-(3,4-dichlorophenyl)-2,4,7-trioxo-1,2,3,4,7,8-hexahydropyrido[2,3-d]pyrimidine-6-carbonitrile (**3h**).

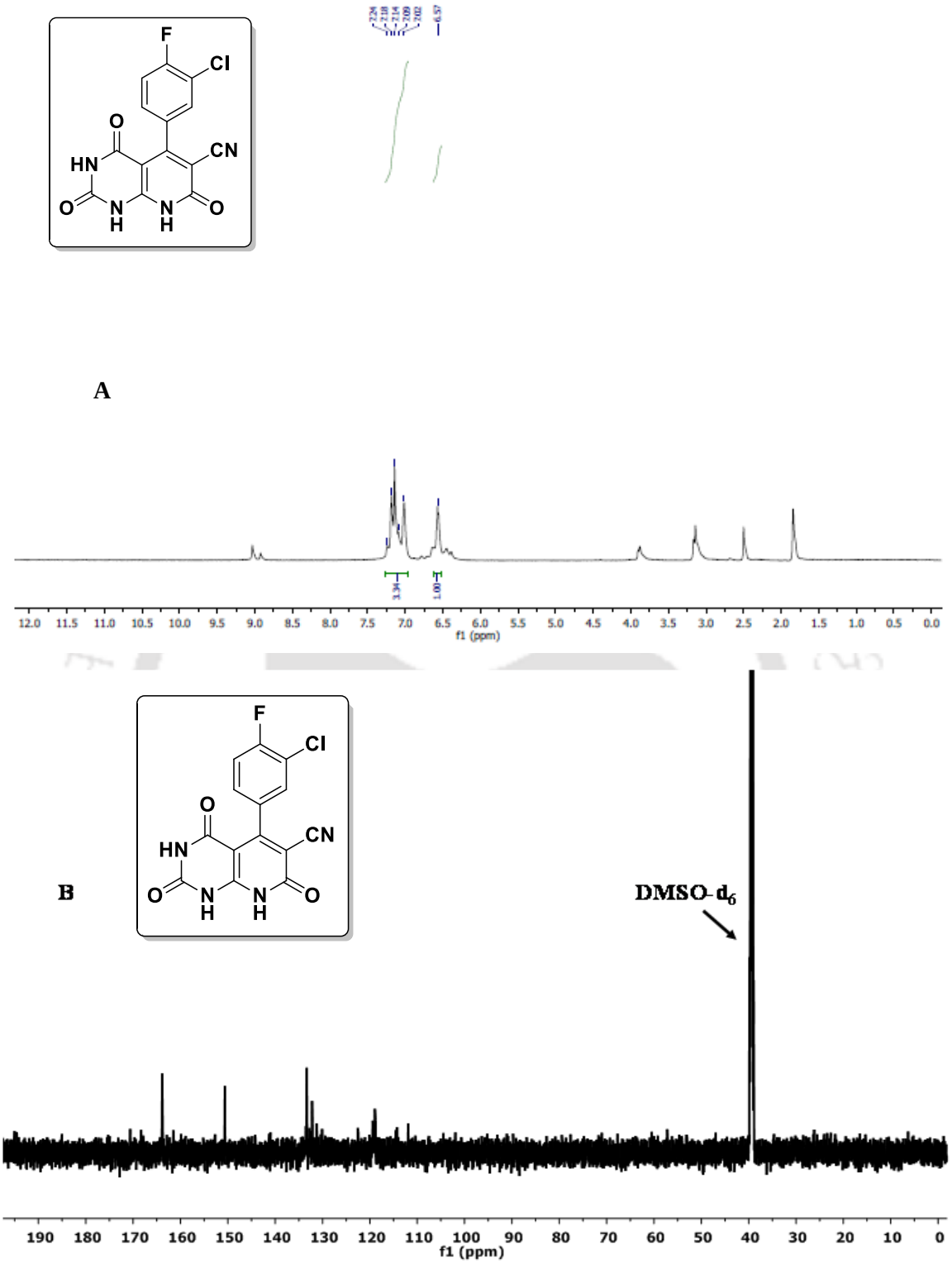

Figure 4.7.9. ^{1}H NMR (A) and ^{13}C NMR (B) of 5-(3-chloro-4-fluorophenyl)-2,4,7-trioxo-1,2,3,4,7,8-hexahydropyrido[2,3-d]pyrimidine-6-carbonitrile (**3i**).

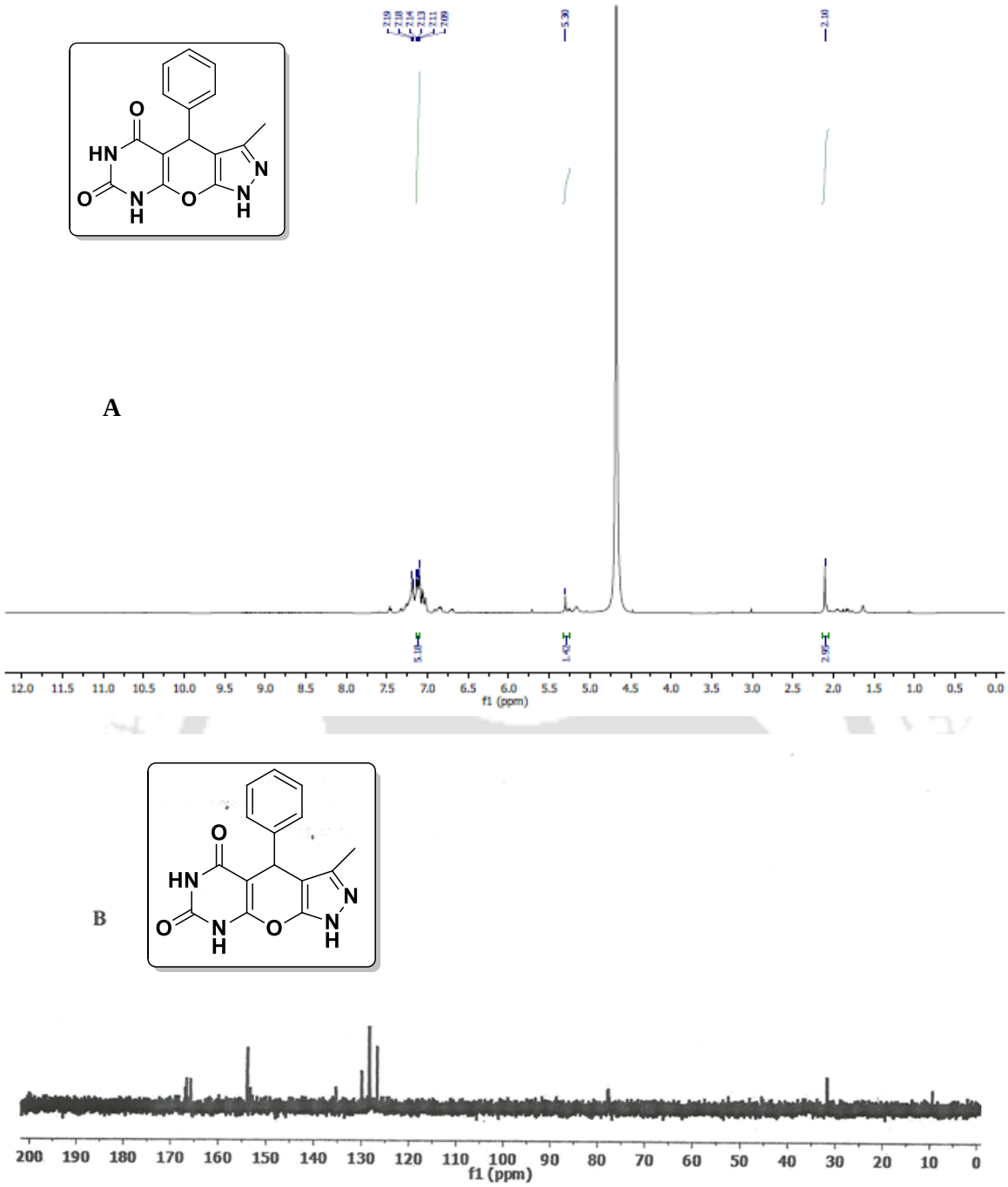

Figure 4.8.1. ^{1}H NMR (A) and ^{13}C NMR (B) of 3-methyl-4-phenyl-4,8-dihydropyrazolo[4',3':5,6]pyrano[2,3-d]pyrimidine-5,7(1H,6H)-dione (**4a**).

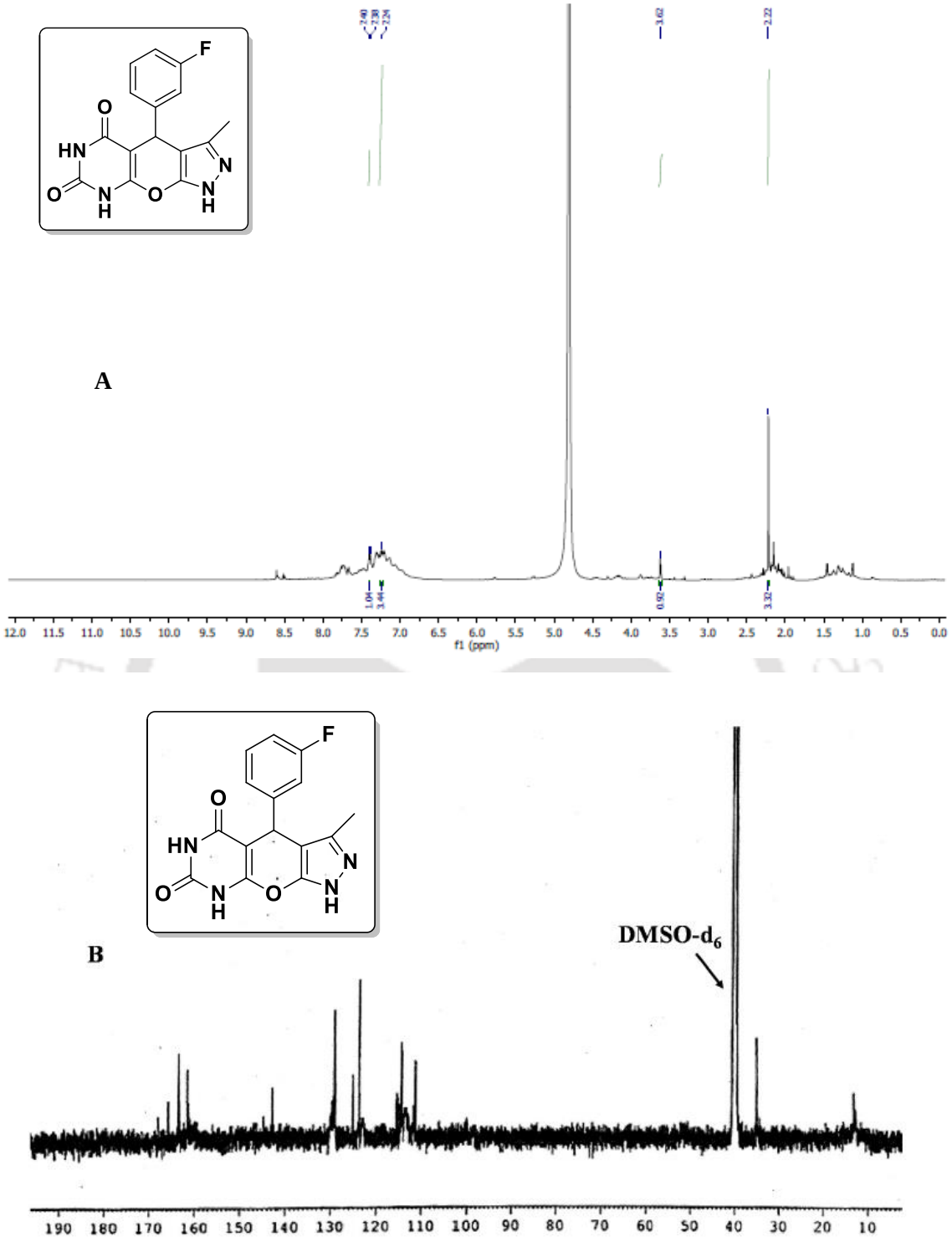

Figure 4.8.2. ^{1}H NMR (A) and ^{13}C NMR (B) of 4-(3-fluorophenyl)-3-methyl-4,8-dihydropyrazolo[4',3':5,6]pyrano[2,3-d]pyrimidine-5,7(1H,6H)-dione (**4b**).

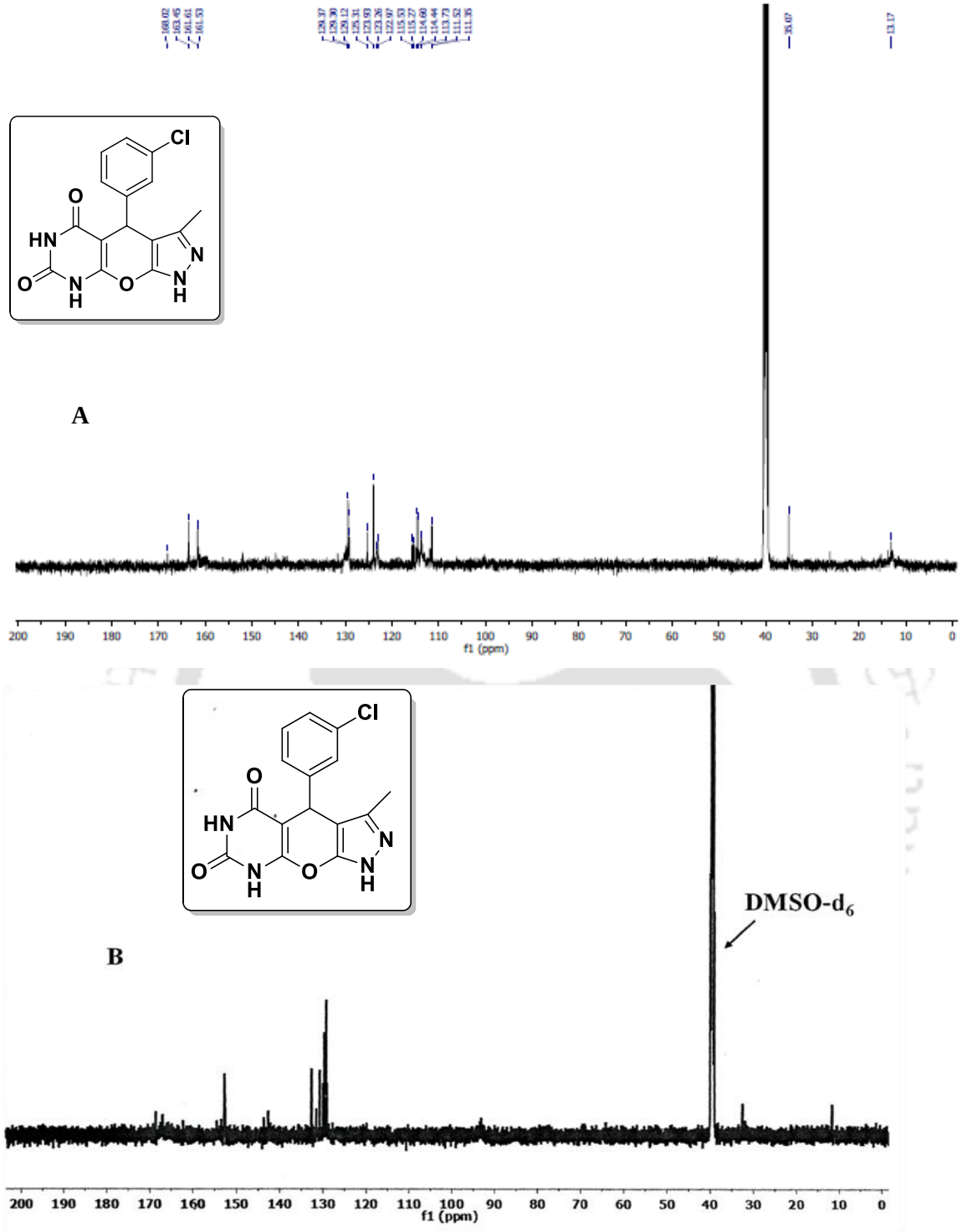

Figure 4.8.3. ^{1}H NMR (A) and ^{13}C NMR (B) of 4-(3-chlorophenyl)-3-methyl-4,8-dihydropyrazolo[4',3':5,6]pyrano[2,3-d]pyrimidine-5,7(1H,6H)-dione (**4c**).

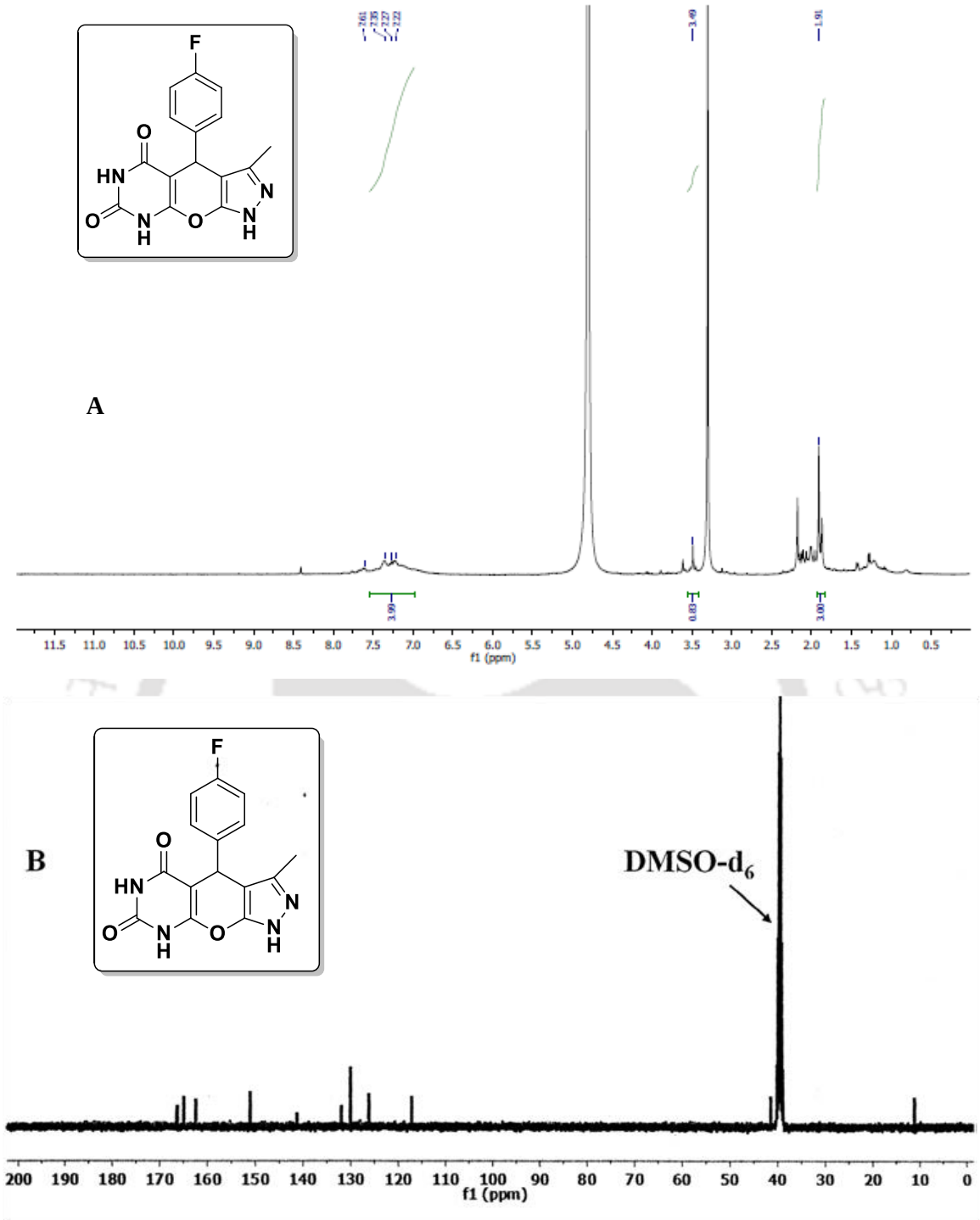

Figure 4.8.4. ^{1}H NMR (A) and ^{13}C NMR (B) of 4-(4-fluorophenyl)-3-methyl-4,8-dihydropyrazolo[4',3':5,6]pyrano[2,3-d]pyrimidine-5,7(1H,6H)-dione (**4d**).

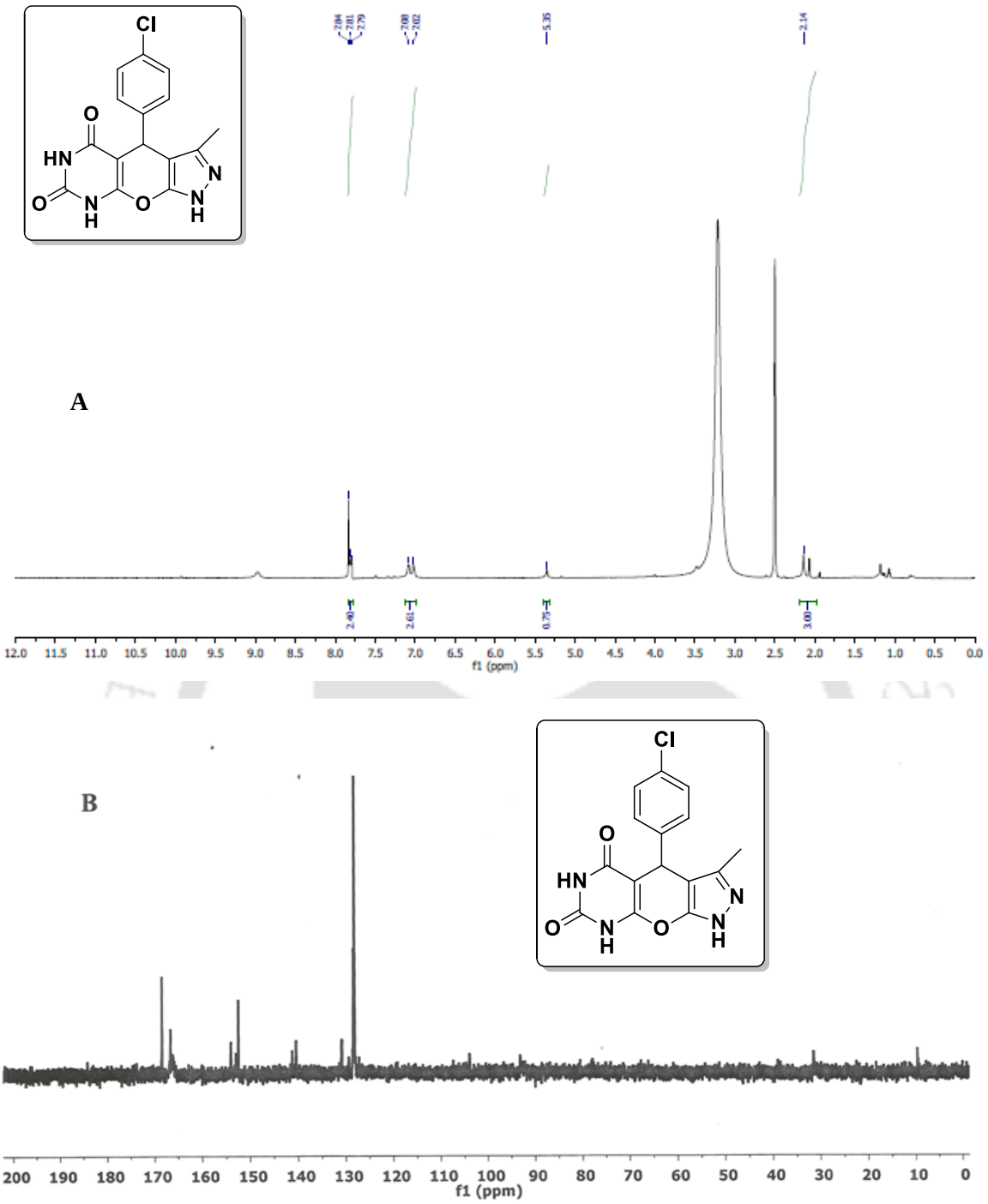

Figure 4.8.5. ^{1}H NMR (A) and ^{13}C NMR (B) of 4-(4-chlorophenyl)-3-methyl-4,8-dihydropyrazolo[4',3':5,6]pyrano[2,3-d]pyrimidine-5,7(1H,6H)-dione (**4e**).

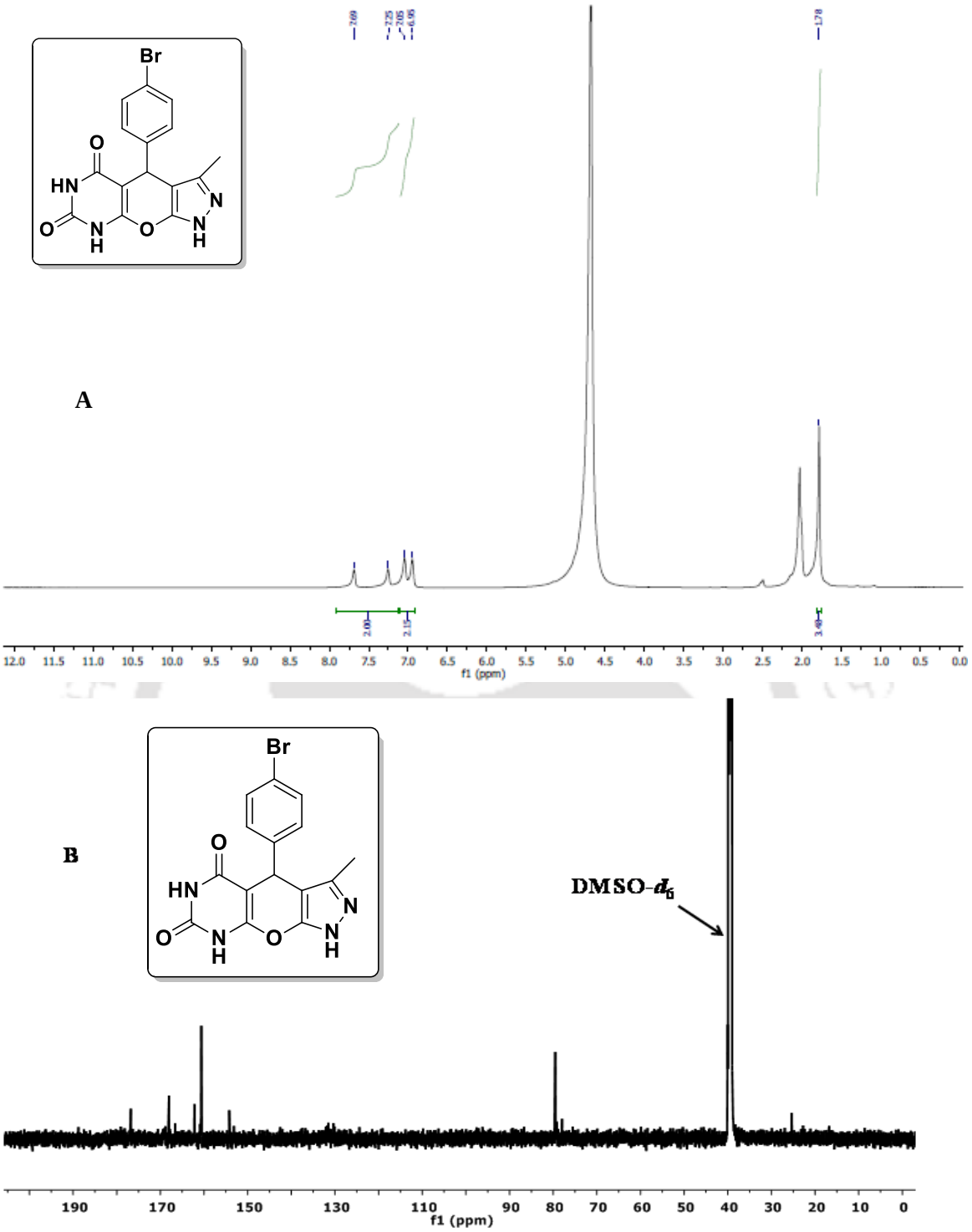

Figure 4.8.6. ^{1}H NMR (A) and ^{13}C NMR (B) of 4-(4-bromophenyl)-3-methyl-4,8-dihydropyrazolo[4',3':5,6]pyrano[2,3-d]pyrimidine-5,7(1H,6H)-dione (**4f**).

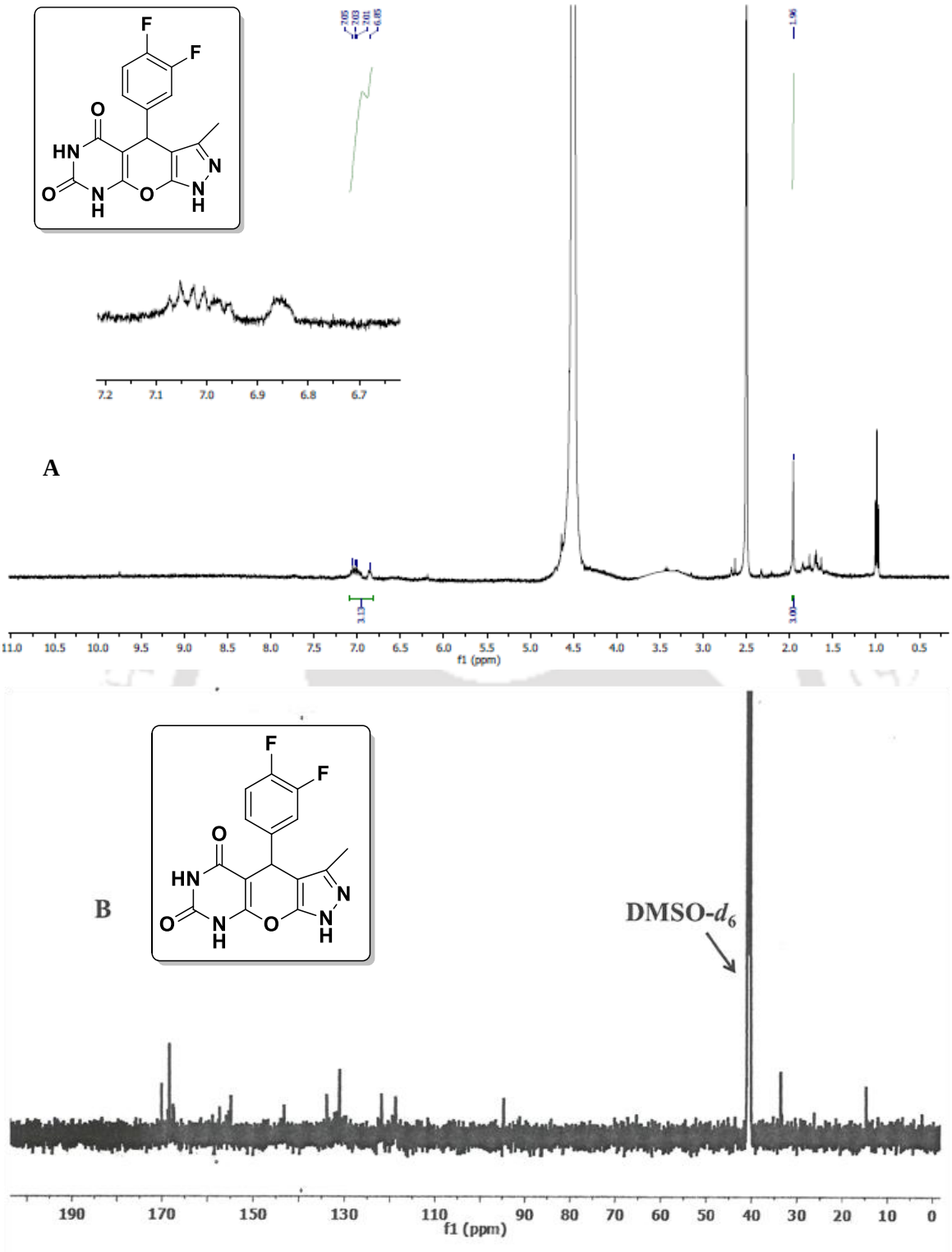

Figure 4.8.7. ^{1}H NMR (A) and ^{13}C NMR (B) of 4-(3,4-difluorophenyl)-3-methyl-4,8-dihydropyrazolo[4',3':5,6]pyrano[2,3-d]pyrimidine-5,7(1H,6H)-dione (**4g**).

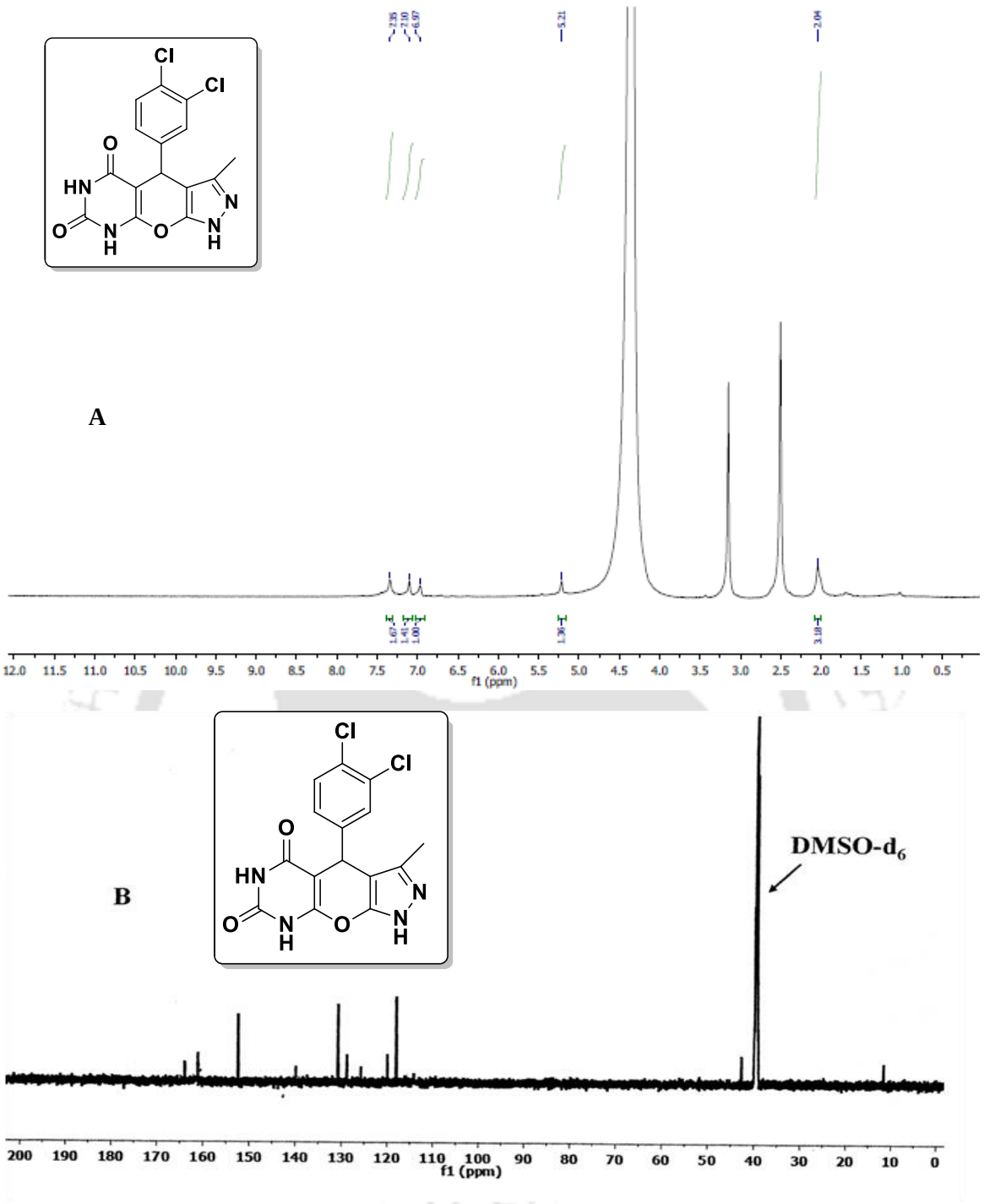

Figure 4.8.8. ^{1}H NMR (A) and ^{13}C NMR (B) of 4-(3,4-dichlorophenyl)-3-methyl-4,8-dihydropyrazolo[4',3':5,6]pyrano[2,3-d]pyrimidine-5,7(1H,6H)-dione (**4h**).

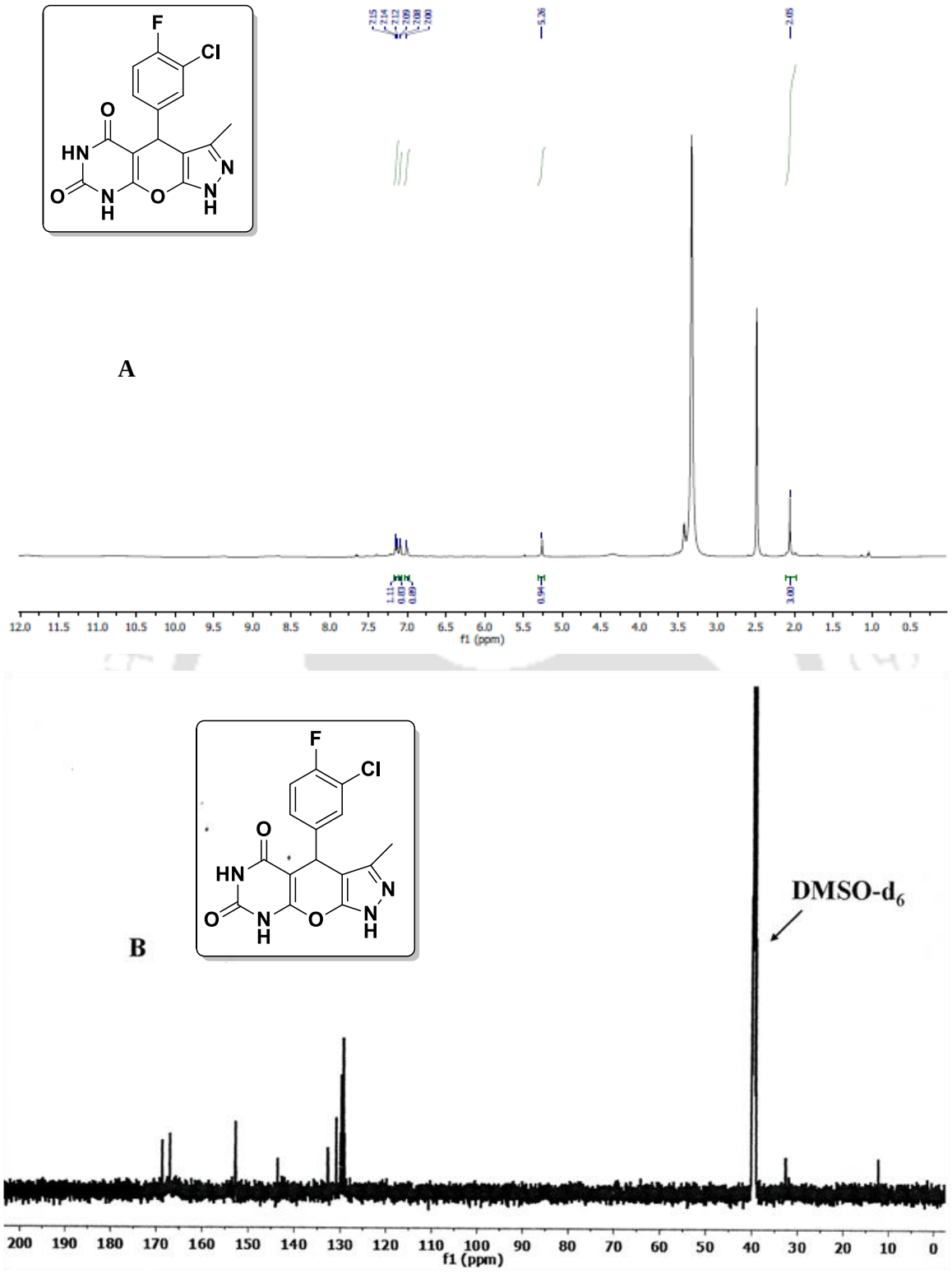

Figure 4.8.9. ^{1}H NMR (A) and ^{13}C NMR (B) of 4-(3-chloro-4-fluorophenyl)-3-methyl-4,8-dihydropyrazolo[4',3':5,6]pyrano[2,3-d]pyrimidine-5,7(1H,6H)-dione (**4i**).

CHAPTER 5

Molecular crowding effect on the activity and stability of IDO1 enzyme

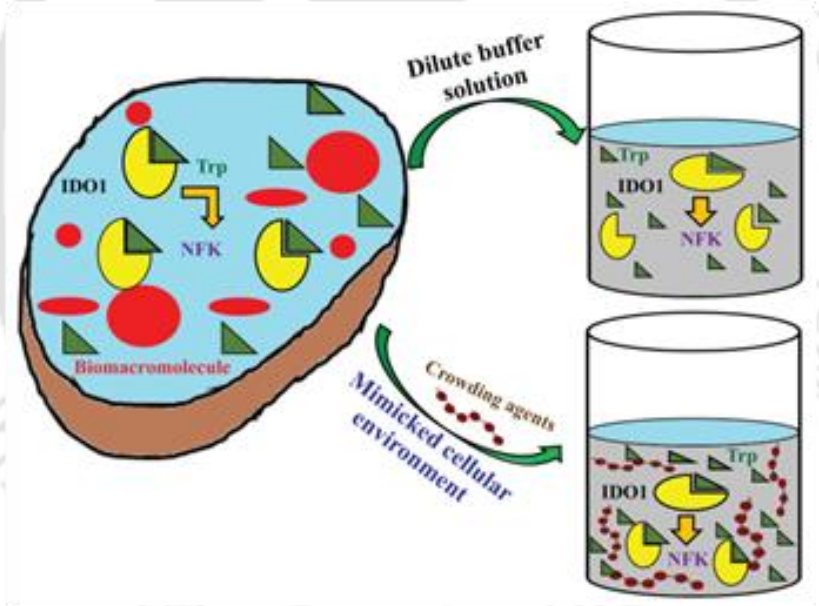

This chapter describes the effect of molecular crowding agents on the kinetic parameters, inhibitory activity and stability of IDO1 enzyme.

5.1. Background and focus of the present work

Uncontrolled metabolism of L-tryptophan (L-Trp) in the immune system has been recognized as a critical cellular process in immune tolerance.[1] Indoleamine 2,3-dioxygenase 1 (IDO1) enzyme plays pivotal role in the metabolism of a local L-Trp through the kynurenine pathway in the immune systems.[2] Under pathophysiological conditions the expression of IDO1 enzyme from its mRNA gets highly up-regulated in response to inflammatory signals (like interferon-γ) within the immune system.[3] Up-regulation of the IDO1 enzyme is directly related with several immunosuppressive diseases including cancer, neurodegenerative disorders such as Alzheimer's disease, bacterial and viral infections, meningitis, transient cerebral ischemia, schizophrenia, depression, age-related cataract, and HIV-1 encephalitis.[2d, 4] Recent *in vivo* studies established that IDO1 promotes a tolerogenic state in the tumor cells and its lymph nodes by suppressing the T cells and enhancing the local regulatory T cells under various physiological and pathophysiological conditions, including pregnancy, tumor resistance, atherosclerosis, obesity, autoimmunity, tuberculosis, influenza, chronic inflammation, and chronic infections.[2c, 5] Ongoing preclinical and clinical studies with different cancer models suggest that IDO1 assists cancer progression and metastasis.[6] Studies also demonstrated the role of IDO1 in maintaining the maternal immune tolerance under normal physiological conditions.[3b, 7] All these findings demonstrate the immunosuppressive role of IDO1 enzyme. Therefore, key challenges in advancing immunotherapies are the development of specific IDO1 inhibitors, exploration of their mechanism of action and optimization of various assay parameters.

1-Methyl-D-tryptophan (D-1MT, indoximod), *N*-hydroxyamidine INCB024360 (epacadostat), imidazole GDC-0919 (navoximod), PF-0684003 (EOS-200271), BMS-986205 (ONO-7701) are the only five small-molecule based IDO1 inhibitors that are now under clinical trials either alone or in combination with other antibodies.[7-8] A wide range of heterocyclic moieties have emerged as excellent IDO1 inhibitors in our on-going drug discovery programme. Novel classes of indazole, tryptophan, oxindoles, triazoles, *N*-hydroxyamidines and several other moieties have come forward as potent IDO1 inhibitors through the structure based drug designing approach.[9] Other research groups also reported several novel classes of compounds.[1a, 1c, 10] Despite having outstanding activity under the *in vitro* assay conditions these developed inhibitors often show poor results in clinical trials. The use of idealized dilute buffer solution conditions during the screening and optimization of inhibitors could be one of the reasons for their failure in clinical trials.

The idealized buffer solution does not reflect the complexity of the environment as present inside the biological cell, where diverse unaccounted biological parameters come into play.[11] Performance of compound screening and other pre-clinical studies under cellular conditions are expensive, extremely time-consuming and cannot be used to screen a high number of compounds at the same time. Investigation of IDO1 enzyme kinetics parameters and inhibitory activity in the presence of synthetic crowding agents could be an alternative approach in mimicking the cellular environment that may leads to better insight into the IDO1 activities in real systems. Hence, understanding of the effect of molecular crowding on the enzyme activities is becoming an important research area in the fields of biochemical, medical, and pharmaceutical sciences.

In the present study, we investigated the efficacy of external crowding agents in mimicking the cell like environment for IDO1 enzyme. The IDO1 enzyme kinetics parameters (K_M, k_{cat} and V_{max}) and IDO1 inhibitory activity were evaluated and compared under these externally manipulated crowded environments. For the inhibitory studies *N*′-hydroxyamidine and aryl-substituted pyran scaffolds-based potent compounds were selected from our previously developed compound library. Crowding agents of various sizes and volumes were used to optimise the experimental conditions in achieving the ideal cell-like conditions. All the IDO1 enzymatic parameters were also compared in the presence of cell lysate. IDO1 inhibitory activities of these selected potent compounds showed stronger potency both in the presence of crowding agent and cell lysate. The thermal stability, catalytic efficiency and secondary structural contents of the IDO1 enzyme under the selected experimental condition were also investigated to understand the therapeutic applicability of the selected crowding agents as well as the inhibitors.

5.2. Result and discussion

5.2.1. Chemistry

It is well documented that cytoplasm has restricted free space because of the presence of biomacromolecules such as proteins, lipids, nucleic acids, ribonucleoproteins and polysaccharides. These biomacromolecules make the intracellular environment highly crowded.[12] However, during drug development process idealized dilute buffer solutions are used for enzymatic studies, which fail to mimic the intracellular environment precisely.[11b, 13] Comprehensive enzyme-kinetic models of metabolism are generally built on enzyme-kinetic data measured under environments that do not resemble the intracellular environment leading to discrepancies between these theoretical models and

the experimental data.[12b, 12c] Several attempts has been made to construct an assay medium that should resemble the intracellular environment as closely as practically possible and simple enough to be applied under *in vitro* condition. To mimic the intracellular environment under *in vitro* condition nonreactive biopolymers are often used as molecular crowding agents and their effect on activity and reaction kinetics of enzymes have been described systematically.[12b, 14] These studies described that the presence of macromolecular crowding agent enhance the reaction rates, reduce the activity and causes negligible changes in the structure of the enzymes.[15] Few studies explored the effect of molecular crowding on enzyme kinetics by considering the effect of volume exclusion, protein association and diffusion and others.[16] However, still a lot remains to be explored and hence a comprehensive study of the underlying mechanisms is attractive and demanding. Therefore, a thorough understanding of the effects of molecular crowding on the enzyme activity is an important research topic in the fields of biochemical, medical, and pharmaceutical sciences. This report describes the activity studies of immunosuppressive enzyme IDO1 in the presence of molecular crowding agents of varied molecular weight and size (Table 5.1).

Efficient evaluation of the effect of macromolecular crowding agent on the kinetic parameters of an enzymatic reaction requires the reaction of interest to have a well-established kinetic behavior and the effect could be only considered with respect to the size and concentration of the crowding agent. IDO1 metabolized the L-Trp to *N*-formylkynurenine through kynurenine pathway. The initial rate of formation of *N*-formylkynurenine can easily be monitored spectrophotometrically (Table 5.1). The use of chemically inert, non-charged, hydrophilic synthetic polymers is equally important. Synthetic polymers, polyethylene glycol (PEG) and ficoll were selected as crowding agents for the present study as these are flexible, neutral, hydrophilic in nature**,** they exert minimum interaction with proteins and various lengths of these polymers are available.[14b]

There are several reports on enzyme kinetics models of IDO1 to calculate the kinetics parameters.[10d, 17] This complexity is due to the inherent properties of IDO1, which is a bi-substrate dependent enzyme. For this reason, different K_M, k_{cat}, V_{max} and k_{cat}/K_M values were reported for IDO1. The kinetics of oxidoreductase enzyme IDO1 depends on both local concentration of O_2 and L-Trp. In our assay system, we only varied the L-Trp concentration and measured the activity under open system, assuming that the O_2 concentration remained constant. Michielin and coworkers suggested this assay conditions which have recently been used widely in IDO1 based drug discovery.[1a]

5.2.2. IDO1 enzyme activity in presence of crowding agents

First, the IDO1 enzyme kinetic parameters including K_M, k_{cat} and V_{max} were measured from time-dependent experiments at different L-Trp concentrations using the Michaelis-Menten equation and their values are listed in Table 5.1 and Figure 5.1. An initial increase in the value of K_M at low concentration [upto 10% (w/v)] of crowding agent was observed followed by a gradual decrease as the environment became increasingly crowded. The value of K_M also showed an increasing trend with the increase in the size of PEG. This high value of K_M is indicative of decreased substrate affinity of the enzyme and hence possibility of less favorable formation of the product. On the other hand, the values of V_{max} increase with both size and concentration of the crowding agent. The change in k_{cat} values is in good correlation with the V_{max} values. For the crowding agent ficoll 400, the change in V_{max} values are smaller with an increase in concentration and are in fact close to the value obtained in non-ideal diluted buffer solution. These findings suggest the consequences of the excluded volume effect, which accounts for the increase in effective enzyme and substrate concentration.[12c] The decrease in randomness of the particles within the crowded solutions causes a noticeable reduction in the entropy of the solution. Formation of the product (*N*-formylkynurenine) from enzyme-substrate complex leads to the generation of free enzyme and product, which is likely to increase the entropy of such a crowded system and therefore, may be a considerably unfavourable process. The decease of K_M value or increase of V_{max} or k_{cat} value at high concentration of a particular crowding agent indicates the prospect of the cage effect produced by the highly crowded environment. We hypothesize that the crowding effect or excluded volume effect is to some extent compensated by the cage effect within this restricted environment.[12b] An increase in the V_{max} values with an increase in the size of the crowding agents supports this observation. The increase in k_{cat}/K_M and V_{max} values with the increase in concentration of the crowding agent implies a diffusion controlled enzyme-substrate complex formation model, which indicates more favorable formation of product under such highly viscous crowded solution. The restricted environment imposed by the crowding agent could alter the reactivity of the substrate and increase the activity coefficient ratio between the free enzyme and the enzyme-substrate complex that might be responsible for this reduction in K_M values with increase in crowding agent concentration. The results also showed that the large decrease in K_M values but similar k_{cat} values with increase in concentration of a particular crowding agent results in the observed overall increase in catalytic efficiency (k_{cat}/K_M) of IDO1 enzyme.

Besides external crowding environment, imposed by large macromolecules; enzyme kinetic reactions are also found to be modified by co-solutes of comparatively smaller size. To investigate the effect of small molecular co-solute on IDO1 enzyme kinetics, glycerol was used as co-solute. The K_M values increased noticeably in presence of these co-solutes, which may be due to chemical interaction between the substrate and co-solutes. Decrease in K_M value with the higher concentration of co-solute suggests the importance of cage effects on the IDO1 enzyme kinetics.

The change in kinetic parameters (k_{cat} and V_{max} values) under the crowded environment was supported by the *in vitro* cellular experiment using cell lysate. Interestingly, the calculated k_{cat} values under the PEG 1000 and PEG 200 medium are very close to that of cell lysate at 10% (w/v) concentration. An increase in V_{max} value under the crowded conditions is generally explained by the excluded volume effect, which increases the effective enzyme concentration and the decrease in V_{max} value is explained by the activation control of enzymatic reaction. The reduction in k_{cat} value are usually explained by a conformational changes in the active site of the enzyme due to the surrounding environment.[15d] There were several reports on decrease in V_{max} in various molecular weights of crowding agents.[12b] The observed rate was found to be in accordance with the reported ones.

The initial lower substrate affinity of the enzyme could be the consequences of excluded volume effect.[15d, 18] However, at higher concentration of the crowding agent the cage effect predominates and as a result V_{max} value increases with increasing size of crowding agents. The increase of V_{max} value with increasing size of crowding agent and increase of k_{cat}/K_M ratio with increase in concentration of the crowding agent (implying diffusion-control mechanism) is well-documented and are in-fact indicative of the fact that not all size and concentration of the crowding agents would mimic cellular environment.[16c, 19] In our case, the 10% (w/v) of PEG 1000 and PEG 200 showed catalytic efficiency 0.036 which was very close to the value obtained for 10% cell-lysate (0.037). For this reason additional activity studies of IDO1 enzyme were performed in the presence of 10% PEG 1000 and PEG 200 in the buffer system.

Table 5.1. Michaelis-Menten reaction parameters in various crowding agents

Media	Weight % (w/v)	K_M (μM)[a]	k_{cat} (s^{-1})[a]	V_{max} (μM/min)[a]	k_{cat}/K_M ($\mu M^{-1}s^{-1}$)
Buffer	-	88.80 ± 7.44	7.30 ± 0.34	17.52 ± 0.81	0.082
PEG 8000	10	697.52 ± 12.49	22.11 ± 0.76	53.06 ± 1.83	0.032
	20	393.24 ± 2.93	26.58 ± 0.61	63.80 ± 1.48	0.068
	30	366.10 ± 2.98	28.95 ± 0.90	69.48 ± 2.17	0.079
PEG 1000	10	564.03 ± 18.15	20.28 ± 1.78	48.67 ± 4.28	0.036
	20	412.64 ± 16.55	21.50 ± 0.32	51.61 ± 0.76	0.052
	30	304.02 ± 16.02	24.07 ± 0.44	57.78 ± 1.07	0.079
PEG 400	10	277.72 ± 1.90	8.71 ± 0.25	20.92 ± 0.59	0.031
	20	129.19 ± 9.76	14.52 ± 1.04	34.86 ± 2.49	0.112
	30	111.21 ± 3.94	15.38 ± 1.06	36.92 ± 3.19	0.138
PEG 200	10	234.50 ± 1.68	8.43 ± 0.12	20.24 ± 0.29	0.036
	20	107.46 ± 3.45	11.45 ± 0.93	27.48 ± 2.24	0.107
	30	72.16 ± 2.05	11.56 ± 0.68	27.74 ± 1.63	0.160
Ficoll 400	10	257.37 ± 6.76	7.43 ± 0.14	17.83 ± 0.34	0.029
	20	111.85 ± 3.91	7.75 ± 0.76	18.61 ± 0.47	0.069
	30	104.89 ± 4.48	9.03 ± 0.65	21.67 ± 1.56	0.086
Glycerol	10	148.24 ± 4.39	4.18 ± 0.03	10.03 ± 0.07	0.028
	20	110.94 ± 10.60	5.89 ± 0.32	14.15 ± 0.76	0.053
	30	87.97 ± 7.51	6.30 ± 0.56	15.13 ± 0.81	0.072
Cell lysate	10	71.45 ± 4.63	2.64 ± 0.22	6.34 ± 0.61	0.037
	20	159.15 ± 7.24	7.66 ± 0.71	18.38 ± 0.94	0.048
	30	174.24 ± 2.98	9.57 ± 1.06	22.97 ± 2.54	0.055

[a] All the values are average of three independent measurements.

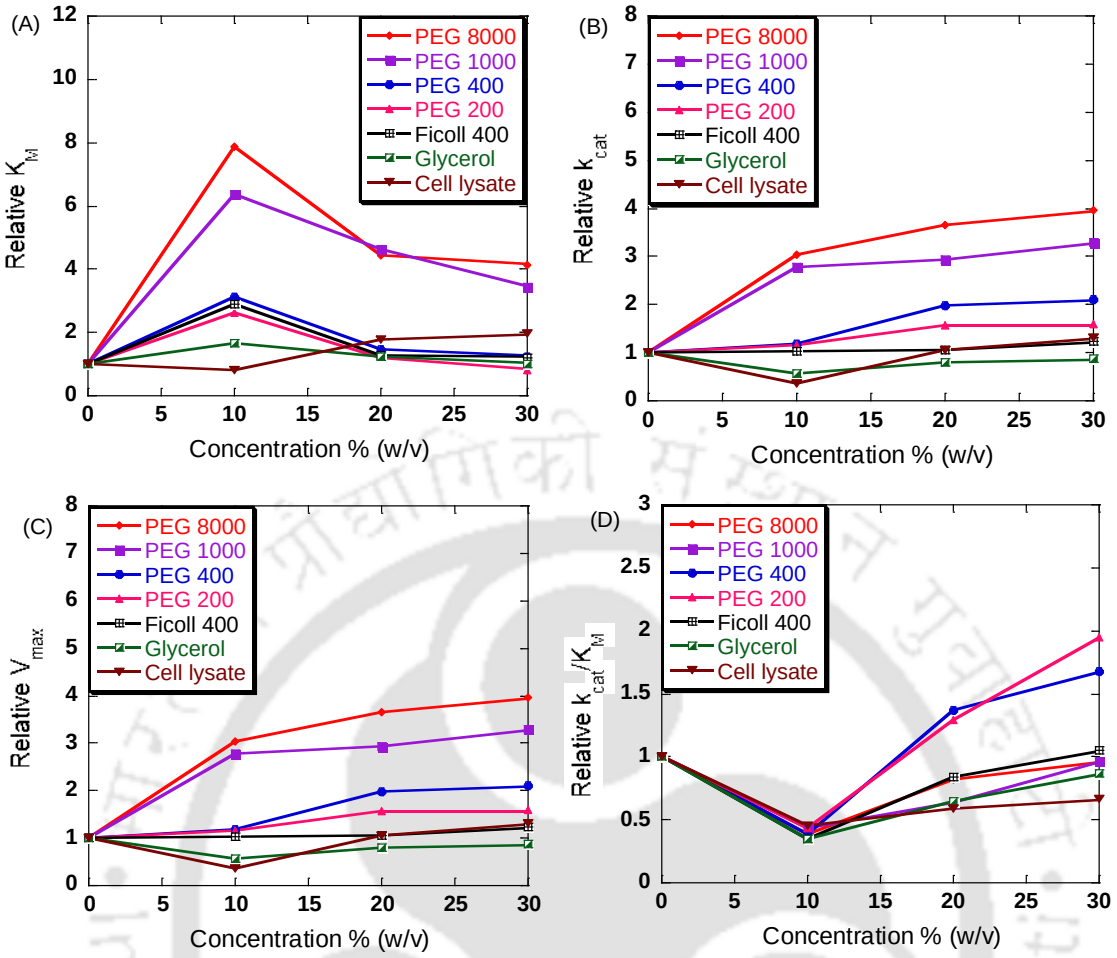

Figure 5.1. Dependence of IDO1 enzymatic activity on the concentration of crowding agents. Relative K_M (A), k_{cat} (B), V_{max} (C) and catalytic efficiency (k_{cat}/K_M) versus % (w/v) crowding agents (D). All data normalized to 1 for buffer conditions and average of three independent measurements.

5.2.3. IDO1 inhibitory activities of selected compounds in presence of crowding agents

IDO1 is an attractive drug target for cancer immunotherapy and development of its inhibitors are highly demanding. Hence, to investigate the crowding effect on the inhibitory activity of IDO1 enzyme, the activity assay was performed in the presence of few known potent compounds including, *N'*-hydroxyamidine, 4-phenyl-4*H*-pyran derivatives, 4-amino-*N*-(3-chloro-4-fluorophenyl)-*N'*-hydroxy-1,2,5-oxadiazole-3-carboxymidimade (**5l**) and **L-1-MT** (Figure 5.2). Earlier, reported results showed that the compounds (**1-4**) have stronger IDO1 inhibitory activity with IC_{50} values in the range of 39-437 nM against purified IDO1 enzyme in the presence of only buffer.[9a, 9b] The other reported compounds **5l** and **L-1-MT** also showed IDO1 inhibitory activity with IC_{50}

values of 91 nM and 385 µM, respectively under the similar assay conditions (buffer only).[10a, 10c] In the presence of crowding agents, PEG 1000 (10% w/v) and PEG 200 (10% w/v) these selected potent compounds (**1-4**) and **5l** showed IC_{50} values in the range of 12-294 nM and 58-563 nM, respectively while **L-1-MT** showed IC_{50} values of 154 µM and 465 µM, respectively (Table 5.2).

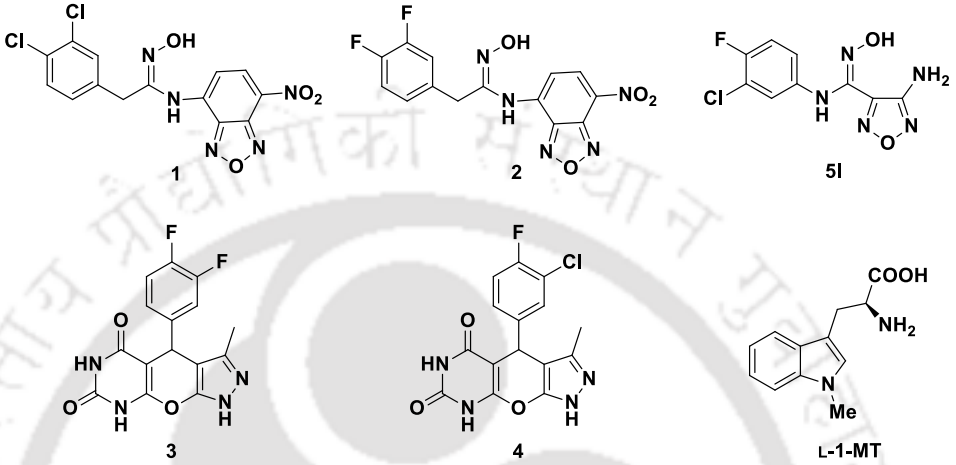

Figure 5.2. Structure of the known inhibitors including, *N'*-hydroxyamidine (**1**, **2** and **5l**), 4-phenyl-4*H*-pyrans (**3** and **4**) and **L-1-MT** were used to measure their IDO1 inhibitory efficacies under this optimized assay conditions.

Table 5.2. Inhibitory activity of *N'*-hydroxyamidine and 4-phenyl-4*H*-pyran based and reported compounds against purified IDO1 enzyme

	IDO1 inhibition IC_{50} (nM)[a]				
Compound	Buffer	PEG 1000	PEG 200	Cell lysate	Cellular assay
1	39 ± 1	12 ± 1	58 ± 1	8 ± 1	71 ± 10
2	59 ± 5	27 ± 2	67 ± 2	33 ± 1	50 ± 8
5l[b]	91 ± 2	41 ± 2	59 ± 2	56 ± 1	59 ± 4
3	410 ± 24	206 ± 13	517 ± 14	156 ± 11	76 ± 11
4	438 ± 22	294 ± 16	563 ± 22	315 ± 19	83 ± 10
L-1-MT[b]	385000 ± 35000	166000 ± 4000	468000 ± 9000	175000 ± 10000	120000 ± 11000

[a] IC_{50} values are the mean of three independent assays.

[b] Reported compound.

The deviation in IC_{50} values of the compounds between the buffer only assay conditions and crowding assay conditions could be due to the presence of crowding agents within the assay system. However, the IC_{50} values of the compounds are in good correlation with that measured under *in vitro* cellular environment (IC_{50} value 8-315 nM for compounds, **1-4** and **5l** and IC_{50} value 175 µM for **L-1-MT**) (Table 5.2). The difference observed between the IC_{50} values of compound **3** and **4** under *in vitro* crowded environment and *in vitro* cellular assay is likely a result of the entropy pressure imposed by the macromolecular crowding agents, which induces some conformational changes in the enzyme to reduce the excluded volume.[16b]

In addition, the enzyme kinetic studies of IDO1 enzyme with these selective potent compounds **1** and **3** in presence of crowding agent show no significant change in their mode of IDO1 inhibition (Figure 5.3 and 5.4). The changes in enzyme-kinetic parameters (K_M, k_{cat} and V_{max}) follow a similar pattern as their inhibitory activity (Table 5.3).

Table 5.3. Michaelis-Menten reaction parameters of selected compounds in presence of crowding agents

Compound	Media	Weight % (w/v)	K_M (µM)[a]	k_{cat} (s^{-1})[a]	V_{max} (µM s^{-1})[a]	k_{cat}/K_M (μM^{-1} s^{-1})
1	Buffer	-	36.76 ± 3.66	5.57 ± 0.13	0.25 ± 0.01	0.15
1	PEG 1000	10	16.83 ± 0.93	5.93 ± 0.53	0.25 ± 0.02	0.35
1	PEG 200	10	43.22 ± 2.19	6.30 ± 0.10	0.25 ± 0.01	0.15
1	Cell lysate	10	12.58 ± 1.01	5.59 ± 0.11	0.22 ± 0.01	0.44
3	Buffer	-	40.08 ± 2.96	5.96 ± 0.48	0.21 ± 0.01	0.15
3	PEG 1000	10	17.77 ± 1.72	3.44 ± 0.08	0.13 ± 0.01	0.19
3	PEG 200	10	37.41 ± 3.04	8.52 ± 0.46	0.30 ± 0.01	0.23
3	Cell lysate	10	22.12 ± 1.82	5.33 ± 0.98	0.20 ± 0.01	0.24

[a] All the values are average of three independent measurements.

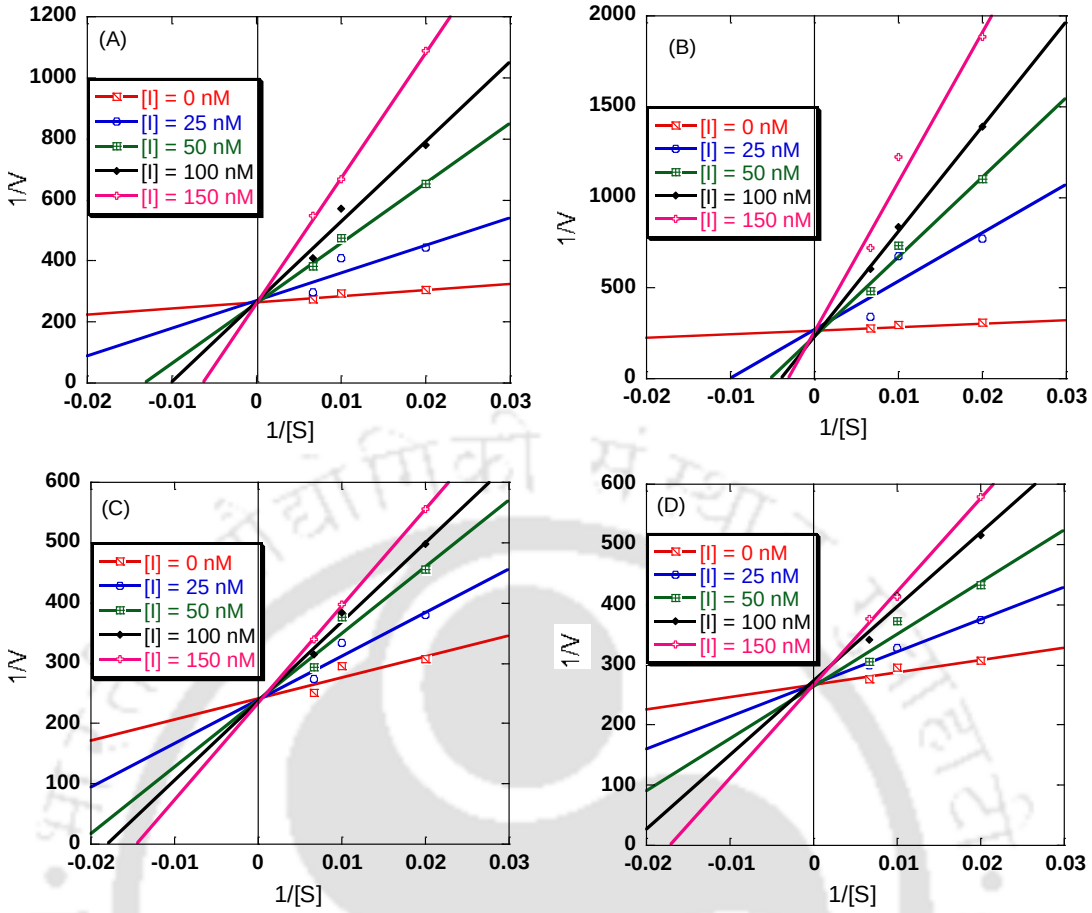

Figure 5.3. Determination of mode of inhibition of the selected compound **1**. 1/V *vs*.1/[S] plot (**A-D**) of compound **1** in presence of buffer, PEG 1000, PEG 200 and cell lysate, respectively. Concentration of L-Trp and compounds were varied from 50 to 150 µM and 25 to 150 nM, respectively.

5.2.4. Effect of crowding agents on the secondary structure of IDO1 enzyme

To explore the possibility that changes in enzyme-kinetics parameter and their inhibitory activity due to the change in native-enzyme conformation, an extensive circular dichroism (CD) analysis in the presence and absence of the crowding agents were performed. Several reports also mentioned the changes in native-state structure of some proteins in presence of crowding agents.[15a, 15d, 16b, 20] The far-UV CD measurement of IDO1 enzyme showed almost no change in the average secondary structure content of the IDO1 enzyme in the presence of different crowding agents, indicating no correlation with their concentration and/or size (Table 5.4 and Figure 5.5A and 5.5B). Undoubtedly the figure confirms no notable change in the CD spectra, but its negative minimum at 222 nm rises along with slight blue-shift (from 222 to 219 nm) as the molecular weight of the crowding agents (PEG 200 to 8000) increases. These shifts in CD spectra are in good correlation

with the change in K_M values in the presence of these crowding agents (Table 5.1).[16a] However, in the presence of glycerol and ficoll the CD spectra remain nearly unchanged.

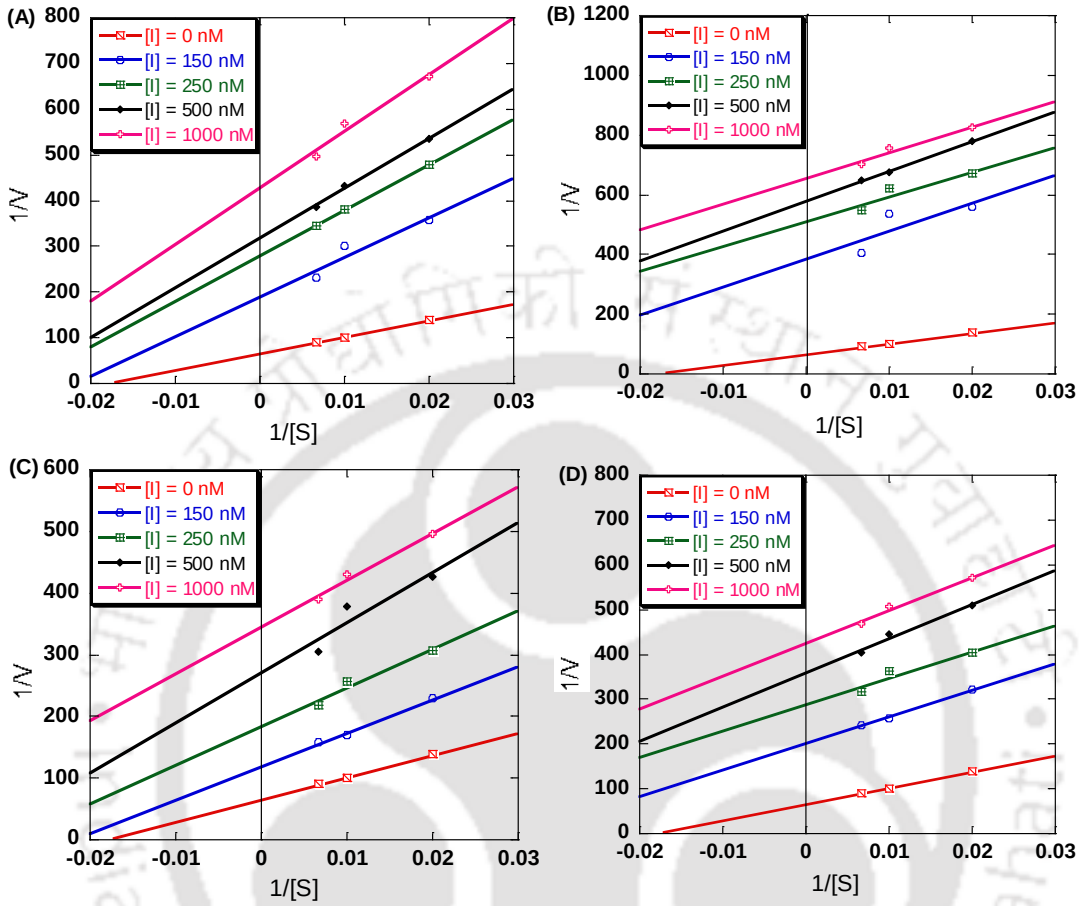

Figure 5.4. Determination of mode of inhibition of the selected compound **3**. 1/V *vs*.1/[S] plot (**A-D**) of compound **3** in presence of buffer, PEG 1000, PEG 200 and cell lysate, respectively. Concentration of L-Trp and compounds were varied from 50 to 150 µM and 150 to 1000 nM, respectively.

Near-UV CD measurements also showed no change in the tertiary structure of IDO1 enzyme in the presence of these crowding agents (Figure 5.5C). To investigate whether the crowding agents have any role on the thermal stability of the IDO1 enzyme, temperature-dependent CD measurements were performed. The results show that the presence of 10% crowding agent increases the thermal perturbation temperature of IDO1 enzyme (T_m value 55 °C in buffer solution) by 5-10 °C (Figure 5.5D) indicating the better stability of the IDO1 enzyme under this crowded environment. Presence of co-solute, glycerol also increases the thermal stability of the IDO1 enzyme.

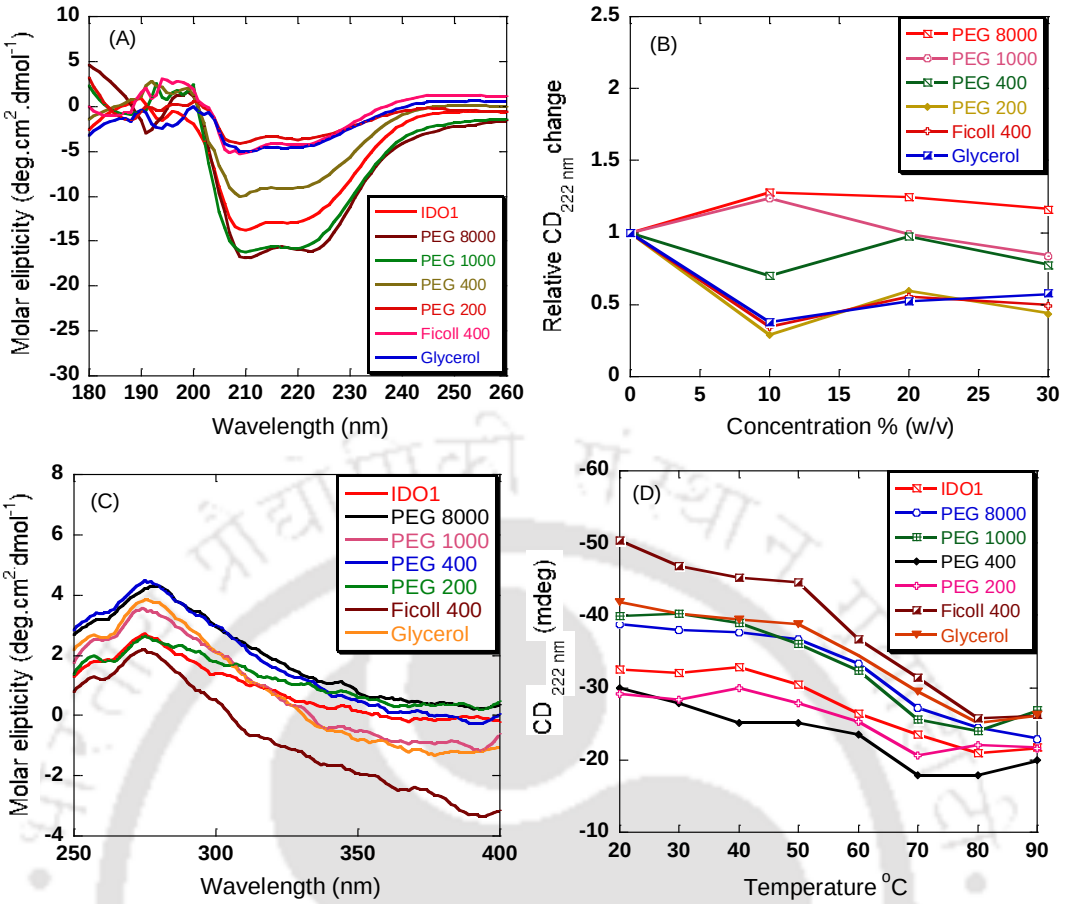

Figure 5.5. Effect of crowding agents on IDO1 secondary structure. (A) Far-UV CD spectra of IDO1 in absence and presence of various crowding agents at 10% (w/v). (B) Relative CD signal at 222 nm as a function of % (w/v) crowding agents. (C) Near-UV CD spectra of IDO1 in absence and presence of various crowding agents at 10% (w/v). (D) Thermal perturbation of IDO1 at various crowding agents as probed by changes in CD $_{222}$ nm.

It is important to mention that k_{cat} and K_M values for IDO1 enzyme behave differently under this crowded environment. A decrease in apparent K_M (stronger binding) value could be due to the excluded volume effect of crowding agents. The high concentration of crowding agents increases the effective concentration of the enzyme and the substrate. Also an increase in k_{cat} values with higher concentration of molecular crowding agents was observed. Therefore, the excluded volume between the enzyme and substrate is directly associated with the inherent properties and molecular weight of the crowding agents, which affect the assay conditions and/or reduction in iron-site reorganization energy of the enzyme (by affecting solvent dynamics) upon redox change.[21] Accordingly, crowding agents can change the internal protein dynamics as well

as increase the thermal stability for IDO1, as observed here. It is well documented that the side chain and backbone of IDO1 enzyme is flexible which causes different conformations for pocket-A and different shapes and sizes of the pocket-B within the active site.[1a]

Table 5.4. IDO1 secondary structure contents in presence of crowding agents

Media	Weight % (w/v)	α-helix	β-sheet	β-turn	Random coil
Buffer	-	0.0	0.0	0.0	100.0
IDO1 in buffer	-	27.7	8.6	27.4	36.3
PEG 8000	10	24.3	17.6	24.5	33.6
	20	30.2	15.1	22.7	32.0
	30	31.0	14.6	21.8	32.6
PEG 1000	10	23.7	13.4	28.8	34.1
	20	29.3	11.2	27.7	31.8
	30	30.6	9.4	28.8	31.2
PEG 400	10	22.7	11.4	27.1	38.8
	20	27.2	8.3	26.6	37.9
	30	29.4	5.6	30.2	34.8
PEG 200	10	22.3	7.1	31.5	39.1
	20	25.6	6.9	31.4	36.1
	30	27.1	5.1	28.8	39.0
Ficoll 400	10	24.5	6.1	31.4	38.0
	20	26.1	7.9	28.8	37.2
	30	28.3	7.1	24.7	39.9
Glycerol	10	24.5	14.1	28.9	32.5
	20	31.7	11.8	29.0	27.5
	30	31.4	10.2	28.1	30.3

5.3. Conclusions

In summary, IDO1 enzyme activity under *in vitro* crowded media produced by PEG and ficoll of different concentrations and sizes has been studied. Our results illustrate a non-linear response of the effect of molecular crowding agent on IDO1 enzyme activity under *in vitro* crowded conditions. The excluded volume effect plays an important role in formation of IDO1-substrate complex. The results also indicate that the activities of IDO1 enzyme in the presence of selected molecular crowding agents could be very similar to that of under cellular conditions. These observations are highly relevant for the intracellular cytosolic IDO1 enzyme as its environment is highly crowded. The cellular environment is a heterogeneous media because of the presence of a range of biomacromolecules which generated disparities in local concentration, viscosities, and

diffusional properties and excluded volume level. Overall our findings suggest that IDO1 enzyme activity under *in vitro* crowding environments will be helpful in understanding its enzymatic activity under complex media such as biological fluids. Additional studies of IDO1 enzyme activities in the presence of mixed crowding agents are also required to understand their effect of IDO1 activity under *in vitro* conditions.

5.4. Experimental section

5.4.1. General information

As described in chapter 2 section 2.4.1.

5.4.2. Expression and purification of recombinant human IDO1 enzyme

As described in chapter 2 section 2.4.5.1.

5.4.3. IDO1 enzyme kinetic study

IDO1 enzyme activity assay was performed as previously described in chapter 2 section 2.4.7.5 with 0 to 30% (w/v) of crowding reagent (polyethylene glycol, ficoll and glycerol).

5.4.4. IDO1 inhibitory activity

IDO1 enzyme inhibition assay was performed as previously described in chapter 2 section 2.4.7.3 with and without inhibitors (32 nM-1 mM) and crowding agent (PEG 1000 and PEG 200) 10% (w/v). The IC_{50} values of the compounds were analyzed using the Graph Pad Prism software (Graph Pad Prism. Version 5.01 program).

5.4.5. Determination of IDO1 inhibition modes

The mode of IDO1 enzyme inhibition by the selected compounds was investigated as previously described in chapter 3 and 4 section 3.4.13 and 4.4.15 with compounds (25-1000 nM) and crowding agent (10%) at 37 ºC for 30 min.

5.4.6. Determination of secondary structure and thermal stability of IDO1 enzyme

The far-UV, near-UV circular dichroism (CD) and thermal stability measurements of IDO1 enzyme was performed as previously described in chapter 2 sections 2.4.7.2 with 0 to 30% (w/v) of the crowding agents.

5.5. References

1. (a) Röhrig, U. F.; Majjigapu, S. R.; Vogel, P.; Zoete, V.; Michielin, O., Challenges in the discovery of indoleamine 2, 3-dioxygenase 1 (IDO1) inhibitors. *J. Med. Chem.* **2015,** *58* (24), 9421-9437; (b) Kershaw, M. H.; Westwood, J. A.; Slaney, C. Y.; Darcy, P. K., Clinical application of genetically modified T cells in cancer therapy. *Clin. Transl. Immunology* **2014,** *3* (5) e16; (c) Qian, S.; Zhang, M.; Chen, Q.; He, Y.; Wang, W.; Wang, Z., IDO as a drug target for cancer immunotherapy: recent developments in IDO inhibitors discovery. *RSC Adv.* **2016,** *6* (9), 7575-7581; (d) Dunn, G. P.; Old, L. J.; Schreiber, R. D., The immunobiology of cancer immunosurveillance and immunoediting. *Immunity* **2004,** *21* (2), 137-148.

2. (a) Munn, D. H.; Mellor, A. L., Indoleamine 2, 3-dioxygenase and tumor-induced tolerance. *J. Clin. Investig.* **2007,** *117* (5), 1147-1154; (b) Platten, M.; Wick, W.; Van den Eynde, B. J., Tryptophan catabolism in cancer: beyond IDO and tryptophan depletion. *Cancer Res.* **2012,** *72* (21), 5435-5440; (c) Uyttenhove, C.; Pilotte, L.; Théate, I.; Stroobant, V.; Colau, D.; Parmentier, N.; Boon, T.; Van den Eynde, B. J., Evidence for a tumoral immune resistance mechanism based on tryptophan degradation by indoleamine 2, 3-dioxygenase. Nat. Med. **2003,** *9* (10), 1269-1274; (d) Fujigaki, H.; Yamamoto, Y.; Saito, K., L-Tryptophan-kynurenine pathway enzymes are therapeutic target for neuropsychiatric diseases: focus on cell type differences. *Neuropharmacology* **2017,** *112*, 264-274; (e) Munn, D. H.; Mellor, A. L., Indoleamine 2, 3 dioxygenase and metabolic control of immune responses. *Trends Immunol.* **2013,** *34* (3), 137-143.

3. (a) Croitoru-Lamoury, J.; Lamoury, F. M.; Caristo, M.; Suzuki, K.; Walker, D.; Takikawa, O.; Taylor, R.; Brew, B. J., Interferon-γ regulates the proliferation and differentiation of mesenchymal stem cells via activation of indoleamine 2, 3 dioxygenase (IDO). *PloS one* **2011,** *6* (2), e14698; (b) Greco, F. A.; Coletti, A.; Camaioni, E.; Carotti, A.; Marinozzi, M.; Gioiello, A.; Macchiarulo, A., The Janus-faced nature of IDO1 in infectious diseases: challenges and therapeutic opportunities. Future Med. Chem. **2016,** *8* (1), 39-54.

4. (a) Vazquez, S.; Parker, N. R.; Sheil, M.; Truscott, R. J., Protein-bound kynurenine decreases with the progression of age-related nuclear cataract. Invest. Ophthalmol. Vis. Sci. **2004,** *45* (3), 879-883; (b) Wichers, M. C.; Maes, M., The role of indoleamine 2, 3-dioxygenase (IDO) in the pathophysiology of interferon-α-induced

depression. *J. Psychiatry Neurosci.* **2004,** *29* (1), 11-16; (c) Heyes, M.; Saito, K.; Crowley, J.; Davis, L.; Demitrack, M.; Der, M.; Dilling, L.; Elia, J.; Kruesi, M.; Lackner, A., Quinolinic acid and kynurenine pathway metabolism in inflammatory and non-inflammatory neurological disease. *Brain* **1992,** *115* (5), 1249-1273.

5. (a) Hornyák, L.; Dobos, N.; Koncz, G.; Karányi, Z.; Páll, D.; Szabó, Z.; Halmos, G.; Székvölgyi, L., The role of indoleamine-2, 3-dioxygenase (IDO) in cancer development, diagnostics, and therapy. *Front Immunol.* **2018,** *9*, 151; (b) Fallarino, F.; Grohmann, U.; You, S.; McGrath, B. C.; Cavener, D. R.; Vacca, C.; Orabona, C.; Bianchi, R.; Belladonna, M. L.; Volpi, C., The combined effects of tryptophan starvation and tryptophan catabolites down-regulate T cell receptor ζ-chain and induce a regulatory phenotype in naive T cells. *J. Immunol.* **2006,** *176* (11), 6752-6761.

6. (a) Okamoto, A.; Nikaido, T.; Ochiai, K.; Takakura, S.; Saito, M.; Aoki, Y.; Ishii, N.; Yanaihara, N.; Yamada, K.; Takikawa, O., Indoleamine 2, 3-dioxygenase serves as a marker of poor prognosis in gene expression profiles of serous ovarian cancer cells. *Clin. Cancer Res.* **2005,** *11* (16), 6030-6039; (b) Godin-Ethier, J.; Hanafi, L.-A.; Piccirillo, C. A.; Lapointe, R., Indoleamine 2, 3-dioxygenase expression in human cancers: clinical and immunologic perspectives. *Clin. Cancer Res.* **2011,** *17* (22), 6985-6991.

7. Coletti, A.; Greco, F. A.; Dolciami, D.; Camaioni, E.; Sardella, R.; Pallotta, M. T.; Volpi, C.; Orabona, C.; Grohmann, U.; Macchiarulo, A., Advances in indoleamine 2, 3-dioxygenase 1 medicinal chemistry. *Med. Chem. Comm.* **2017,** *8* (7), 1378-1392.

8. (a) Weng, T.; Qiu, X.; Wang, J.; Li, Z.; Bian, J., Recent discovery of indoleamine-2, 3-dioxygenase 1 inhibitors targeting cancer immunotherapy. *Eur. J. Med. Chem.* **2017**, 143 (6) 656-669; (b) Prendergast, G. C.; Malachowski, W. P.; DuHadaway, J. B.; Muller, A. J., Discovery of IDO1 inhibitors: from bench to bedside. *Cancer Res.* **2017,***77* (24), 6795-6811.

9. (a) Paul, S.; Roy, A.; Deka, S. J.; Panda, S.; Trivedi, V.; Manna, D., Nitrobenzofurazan derivatives of *N*′-hydroxyamidines as potent inhibitors of indoleamine-2, 3-dioxygenase 1. *Eur. J. Med. Chem.* **2016,** *121*, 364-375; (b) Panda, S.; Roy, A.; Deka, S. J.; Trivedi, V.; Manna, D., Fused Heterocyclic Compounds as Potent Indoleamine-2, 3-dioxygenase 1 Inhibitors. *ACS Med. Chem. Lett.* **2016,** *7* (12), 1167-1172; (c) Pradhan, N.; Paul, S.; Deka, S. J.; Roy, A.; Trivedi, V.; Manna, D., Identification of Substituted 1H- Indazoles as Potent Inhibitors for Immunosuppressive

Enzyme Indoleamine 2, 3- Dioxygenase 1. *Chemistry Select* **2017,** *2* (20), 5511-5517; (d) Paul, S.; Roy, A.; Deka, S. J.; Panda, S.; Srivastava, G. N.; Trivedi, V.; Manna, D., Synthesis and evaluation of oxindoles as promising inhibitors of the immunosuppressive enzyme indoleamine 2, 3-dioxygenase 1. *Med. Chem. Comm.* **2017,** *8* (8), 1640-1654.

10. (a) Yang, S.; Li, X.; Hu, F.; Li, Y.; Yang, Y.; Yan, J.; Kuang, C.; Yang, Q., Discovery of tryptanthrin derivatives as potent inhibitors of indoleamine 2, 3-dioxygenase with therapeutic activity in Lewis lung cancer (LLC) tumor-bearing mice. J. Med. Chem. **2013,** *56* (21), 8321-8331; (b) Koblish, H. K.; Hansbury, M. J.; Bowman, K. J.; Yang, G.; Neilan, C. L.; Haley, P. J.; Burn, T. C.; Waeltz, P.; Sparks, R. B.; Yue, E. W., Hydroxyamidine inhibitors of indoleamine-2, 3-dioxygenase potently suppress systemic tryptophan catabolism and the growth of IDO-expressing tumors. *Mol. Cancer Ther.* **2010,** *9* (2), 489-498; (c) Yue, E. W.; Douty, B.; Wayland, B.; Bower, M.; Liu, X.; Leffet, L.; Wang, Q.; Bowman, K. J.; Hansbury, M. J.; Liu, C., Discovery of potent competitive inhibitors of indoleamine 2, 3-dioxygenase with in vivo pharmacodynamic activity and efficacy in a mouse melanoma model. *J. Med. Chem.* **2009,** *52* (23), 7364-7367; (d) Sono, M.; Cady, S. G., Enzyme kinetic and spectroscopic studies of inhibitor and effector interactions with indoleamine 2, 3-dioxygenase. 1. Norharman and 4-phenylimidazole binding to the enzyme as inhibitors and heme ligands. *Biochemistry* **1989,** *28* (13), 5392-5399; (e) Röhrig, U. F.; Majjigapu, S. R.; Grosdidier, A. l.; Bron, S.; Stroobant, V.; Pilotte, L.; Colau, D.; Vogel, P.; Van den Eynde, B. J.; Zoete, V., Rational design of 4-aryl-1, 2, 3-triazoles for indoleamine 2, 3-dioxygenase 1 inhibition. *J. Med. Chem.* **2012,** *55* (11), 5270-5290; (f) Dolušić, E.; Larrieu, P.; Blanc, S.; Sapunaric, F.; Pouyez, J.; Moineaux, L.; Colette, D.; Stroobant, V.; Pilotte, L.; Colau, D., Discovery and preliminary SARs of keto-indoles as novel indoleamine 2, 3-dioxygenase (IDO) inhibitors. *Eur. J. Med. Chem.* **2011,** *46* (7), 3058-3065; (g) Serra, S.; Moineaux, L.; Vancraeynest, C.; Masereel, B.; Wouters, J.; Pochet, L.; Frédérick, R., Thiosemicarbazide, a fragment with promising indolamine-2, 3-dioxygenase (IDO) inhibition properties. *Eur. J. Med. Chem.* **2014,** *82*, 96-105.

11. (a) Zhou, H.-X.; Rivas, G.; Minton, A. P., Macromolecular crowding and confinement: biochemical, biophysical, and potential physiological consequences. *Annu. Rev. Biophys.* **2008,** *37*, 375-397; (b) Minton, A. P., The influence of macromolecular crowding and macromolecular confinement on biochemical reactions in physiological media. *J. Biol. Chem.* **2001,** *276* (14), 10577-10580; (c) Aumiller Jr, W. M.; Davis, B.

W.; Hatzakis, E.; Keating, C. D., Interactions of macromolecular crowding agents and cosolutes with small-molecule substrates: effect on horseradish peroxidase activity with two different substrates. J. Phys. Chem. B**2014,** *118* (36), 10624-10632.

12. (a) Ellis, R. J., Macromolecular crowding: obvious but underappreciated. *Trends Biochem. Sci.* **2001,** *26* (10), 597-604; (b) Balcells, C.; Pastor, I.; Vilaseca, E.; Madurga, S.; Cascante, M.; Mas, F., Macromolecular crowding effect upon in vitro enzyme kinetics: mixed activation–diffusion control of the oxidation of NADH by pyruvate catalyzed by lactate dehydrogenase. *J. Phys. Chem. B* **2014,** *118* (15), 4062-4068; (c) Balcells, C.; Pastor, I.; Pitulice, L.; Hernández, C.; Via, M.; Garcés, J. L.; Madurga, S.; Vilaseca, E.; Isvoran, A.; Cascante, M., Macromolecular Crowding upon *in-vivo*-Like Enzyme-Kinetics: Effect of Enzyme-Obstacle Size Ratio. *New Front. Chem.* **2015,** *24* (1), 3.

13. Kuznetsova, I. M.; Turoverov, K. K.; Uversky, V. N., What macromolecular crowding can do to a protein. *Int. J. Mol. Sci.* **2014,** *15* (12), 23090-23140.

14. (a) Laurent, T. C., Enzyme reactions in polymer media. *FEBS J.* **1971,** *21* (4), 498-506; (b) Ellis, R. J.; Minton, A. P., Cell biology: join the crowd. *Nature* **2003,** *425* (6953), 27; (c) Kuznetsova, I. M.; Zaslavsky, B. Y.; Breydo, L.; Turoverov, K. K.; Uversky, V. N., Beyond the excluded volume effects: mechanistic complexity of the crowded milieu. *Molecules* **2015,** *20* (1), 1377-1409.

15. (a) Totani, K.; Ihara, Y.; Matsuo, I.; Ito, Y., Effects of macromolecular crowding on glycoprotein processing enzymes. J. Am. *Chem. Soc.* **2008,** *130* (6), 2101-2107; (b) Norris, M. G.; Malys, N., What is the true enzyme kinetics in the biological system? An investigation of macromolecular crowding effect upon enzyme kinetics of glucose-6-phosphate dehydrogenase. *Biochem. Biophys. Res. Commun.* **2011,** *405* (3), 388-392; (c) Pastor, I.; Vilaseca, E.; Madurga, S.; Garcés, J. L.; Cascante, M.; Mas, F., Effect of Crowding by Dextrans on the Hydrolysis of N-Succinyl-l-phenyl-Ala-p-nitroanilide Catalyzed by α-Chymotrypsin. *J. Phys. Chem. B* **2010,** *115* (5), 1115-1121; (d) Pozdnyakova, I.; Wittung-Stafshede, P., Non-linear effects of macromolecular crowding on enzymatic activity of multi-copper oxidase. *Biochim. Biophys. Acta* **2010,** *1804* (4), 740-744; (e) Pastor, I.; Pitulice, L.; Balcells, C.; Vilaseca, E.; Madurga, S.; Isvoran, A.; Cascante, M.; Mas, F., Effect of crowding by Dextrans in enzymatic reactions. *Biophys. Chem.* **2014,** *185*, 8-13.

16. (a) Dix, J. A.; Verkman, A., Crowding effects on diffusion in solutions and cells. *Annu. Rev. Biophys.* **2008,** *37*, 247-263; (b) Jiang, M.; Guo, Z., Effects of macromolecular crowding on the intrinsic catalytic efficiency and structure of enterobactin-specific isochorismate synthase. J. Am. Chem. Soc. **2007,** *129* (4), 730-731; (c) Homchaudhuri, L.; Sarma, N.; Swaminathan, R., Effect of crowding by dextrans and Ficolls on the rate of alkaline phosphatase–catalyzed hydrolysis: A size- dependent investigation. *Biopolymers* **2006,** *83* (5), 477-486; (d) Minton, A. P., Influence of macromolecular crowding upon the stability and state of association of proteins: predictions and observations. *J. Pharm. Sci.* **2005,** *94* (8), 1668-1675.

17. (a) Terentis, A. C.; Freewan, M.; Sempértegui Plaza, T. S.; Raftery, M. J.; Stocker, R.; Thomas, S. R., The selenazal drug ebselen potently inhibits indoleamine 2, 3-dioxygenase by targeting enzyme cysteine residues. *Biochemistry* **2009,** *49* (3), 591-600; (b) Lu, C.; Lin, Y.; Yeh, S.-R., Spectroscopic studies of ligand and substrate binding to human indoleamine 2, 3-dioxygenase. *Biochemistry* **2010,** *49* (24), 5028-5034; (c) Huang, Q.; Zheng, M.; Yang, S.; Kuang, C.; Yu, C.; Yang, Q., Structure–activity relationship and enzyme kinetic studies on 4-aryl-1H-1, 2, 3-triazoles as indoleamine 2, 3-dioxygenase (IDO) inhibitors. *Eur. J. Med. Chem.* **2011,** *46* (11), 5680-5687.

18. Jiang, M.; Guo, Z., Effects of macromolecular crowding on the intrinsic catalytic efficiency and structure of enterobactin-specific isochorismate synthase. J. Am. Chem. Soc. **2007,** *129* (4), 730-731.

19. Pastor, I.; Vilaseca, E.; Madurga, S.; Garcés, J. L.; Cascante, M.; Mas, F., Diffusion of α-chymotrypsin in solution-crowded media. A fluorescence recovery after photobleaching study. *J. Phys. Chem. B* **2010,** *114* (11), 4028-4034.

20. Homouz, D.; Perham, M.; Samiotakis, A.; Cheung, M. S.; Wittung-Stafshede, P., Crowded, cell-like environment induces shape changes in aspherical protein. *Proc. Natl. Acad. Sci. U.S.A.* **2008,** *105* (33), 11754-11759.

21. (a) Charlton, L. M.; Barnes, C. O.; Li, C.; Orans, J.; Young, G. B.; Pielak, G. J., Residue-level interrogation of macromolecular crowding effects on protein stability. *J. Am. Chem. Soc.* **2008,** *130* (21), 6826-6830; (b) Minh, D. D.; Chang, C.-e.; Trylska, J.; Tozzini, V.; McCammon, J. A., The influence of macromolecular crowding on HIV-1 protease internal dynamics. *J. Am. Chem. Soc.* **2006,** *128* (18), 6006-6007.

Conclusion and Future Perspective

Indoleamine 2,3-dioxygenase 1 (IDO1) is an immunosuppressive enzyme which catalyses the first and rate limiting step of the kynurenine pathway for L-Trp metabolism. Under pathophysiological condition, IDO1 is over-expressed by most human tumours. Increased level of IDO1 is correlated with poor prognosis in cancer patients. IDO1 inhibitors are under investigation to enhance endogenous anticancer immunosurveillance. Hence, IDO1 is a potentially valuable therapeutic target for cancer treatment. IDO1 mediated immunotherapy may provide improved effects in combination with other therapies, such as chemotherapy and small molecule therapy. So far several classes of compounds have been reported as IDO1 inhibitors, but most of the scaffolds have never been used after their initial studies due to their inconsistent results or unconfirmed activity and /or specificity. Hence, there is a demand for the development of novel molecules which can actively and selectively inhibits the IDO1 enzyme in comparison with the other heme-containing enzymes.

Prior to the development of IDO1 inhibitor, an expression and purification system that produces enzymatically active human IDO1 needed to be developed. For that purpose, an expression and purification system was optimized in our laboratory conditions, which is described in **Chapter 2**. Characterization of the recombinant IDO1 showed the identity of native human IDO1 enzyme in terms of spectroscopic properties and enzyme activity. This optimized conditions provided us a reliable source of functional human IDO1. Availability of this purified enzyme assisted us in screening the potencies of the synthesized compounds, which helped us in synthesizing compounds through our ligand-based approach.

IDO1 enzyme inhibition activity studies of our synthesized compounds showed the inhibitory potency of the hydroxyamidines in the nanomolar range. The hydroxyamidine based compound epacadostat is currently under clinical trial for the treatment of cancer and other diseases. The synthesis and IDO1 inhibitory activity studies of the hydroxyamidines are described in the **Chapter 3**. The experimental results suggested that the presence of both phenylacetimidamide as well as, the nitrobenzofurazan moiety plays a significant role in achieving the better inhibitory capabilities of the compounds. The *in vitro* cellular IDO1 activity studies showed that these hydroxyamidines have no/ negligible level of toxicity and stronger potencies. The

stronger IDO1 selectivity of these compounds was confirmed by the activity assay with another heme-containing enzyme TDO. The structure activity relationship (SAR) was obtained by systematically substituting the *N'*-hydroxyphenylacetimidamide moiety with halogen and methoxy group which showed that there was a significant contribution of the halogen substitution (preferably chloro- and fluoro-derivatives) towards the enhancement of the overall inhibitory potencies as compared to that of the lead compound.

The **Chapter 4** described the investigation of SAR of the fused heterocyclic compounds against IDO1 enzyme. Subsequent modification of the electronic properties of the fused heterocyclic ring and substitution of the phenyl ring directed to the identification of potent inhibitors with low micromolar IDO1 enzyme inhibitory activities under the *in vitro* conditions. Overall, activity studies showed that pyridopyrimidines and pyrazolopyranopyrimidines moiety and di-halogen substituted phenyl ring could considerably enhance the inhibition potency of these fused heterocyclic compounds. Spectroscopic studies suggested that the pyrazolopyranopyrimidine derivatives preferably interact with the deoxy-ferrous-IDO1 enzyme. Molecular model structure proposed that the electronic properties of pyridopyrimidines and pyrazolopyranopyrimidines ring and halogen substituted phenyl ring assist these compounds to interact with the IDO1 through hydrogen bonding, pi-stacking and hydrophobic interactions. Hence, pyridopyrimidines and pyrazolopyranopyrimidines represent a promising class of IDO1 inhibitors. The potent compounds also displayed > 100-fold stronger inhibition for IDO1 enzyme inhibition in comparison with the TDO enzyme. Low cytotoxicity and inactivity for TDO enzyme supported further development of fused heterocyclic compounds as inhibitor of IDO1 enzyme and would provide IDO1 inhibitors with much improved potencies.

IDO1-based drug development has been hindered due to the use of idealized dilute buffer solution conditions during the screening and optimization of inhibitors, which do not reflect the highly crowded intracellular environment. In **Chapter 5**, IDO1 enzyme inhibitory activity of few potent compounds of *N*-hydroxyamidine and aryl substituted pyran scaffolds were investigated under macromolecularly crowded *in vitro* environments. The synthetic crowding agents were used to generate a cellular mimetic condition and these inhibitors were found to retain their promising IDO1 inhibitory activity. A non-linear relationship between the size and volume of the crowding agent with enzyme kinetics parameters was observed. The excluded volume effect plays an important role in formation of IDO1-substrate complex. The results suggest that judicious use of size and volume of the crowding agent could provide cellular mimetic

environment. A very similar catalytic efficiency, inhibitory activity along with preservation of secondary structural content of IDO1 enzyme under the selected crowded media makes these crowding agents appropriate for further therapeutic application. The cellular environment is a heterogeneous media because of the presence of a range of biomacromolecules which generated disparities in local concentration, viscosities, and diffusional properties and excluded volume level. Overall our findings suggest that IDO1 enzyme activity under *in vitro* crowding environments will be helpful in understanding its enzymatic activity under complex media such as biological fluids.

We identified two different classes of compounds *N*-hydroxyamidine and fused heterocyclic based compounds which can be further developed to design potent compounds. We also developed an assay system which will be highly beneficial for screening of the synthesized compounds. This assay system can give much better results and much close to the cellular environment. So, this study will be helpful for further IDO1 based drug development. Hence, structural simplicity and low-micromolar/nanomolar IDO1 inhibition potencies, no/negligible level of toxicity, similar IDO1 inhibition potencies under selected crowding conditions of the synthesized compounds makes them quite attractive and potential drug target for further investigation of IDO1 function and immunotherapeutic applications.

List of Publications

1. Panda, S.; Pradhan, N.; Morla, S.; Saha, A.; **Roy, A**.; Kumar, S.; Manna, D. Development of 2*H*-triazole scaffold-based potent inhibitors for indoleamine 2,3-dioxygenase 1 enzyme. (Manuscript under preparation).

2. **Roy, A**.; Das, S.; Manna, D. Effect of molecular crowding agents on the activity and stability of immunosuppressive enzyme indoleamine 2,3-dioxygenase 1. *Chem. Select* **2018**, *3* (16), 6294-6301.

3. Deka, S. J.; **Roy, A**.; Manna. D.; Trivedi. V. Integrating virtual screening and biochemical experimental approach to identify potential anti-cancer agents from drug databank. *J. Bioinform. Comput. Biol.* **2018,** *16* (3), 1850002.

4. Pradhan, N.; Paul, S.; Deka, S. J.; **Roy, A.**;Trivedi, V.; Manna, D. Identification of substituted 1*H*-indazoles as potent inhibitors for immunosuppressive enzyme indoleamine 2,3-dioxygenase 1. *Chem. Select* **2017**, *2* (20), 5511-5517.

5. Paul, S.; **Roy, A.**; Deka, S. J.; Panda, S.; Srivastava, G. N.; Trivedi, V.; Manna, D. Synthesis and evaluation of oxindoles as promising inhibitors tothe immunosuppressive enzyme indoleamine 2,3-dioxygenase 1. *Med. Chem. Commun.* **2017**, *8* (8), 1640-1654.

6. Deka, S. J., **Roy, A**.; Ramakrishnan, V.; Manna, D.; Trivedi, V. Danazol has potential to cause PKC translocation, cell cycle dysregulation, and apoptosis in breast cancer cells.

7. Panda, S.; **Roy, A.**; Deka, S. J.; Trivedi, V.; Manna, D. Fused heterocyclic compounds as potent indoleamine 2,3-dioxygenase 1 inhibitors. *ACS Med. Chem. Lett.* **2016**, *7* (12), 1167-1172.

8. Paul, S.; **Roy, A.**; Deka, S. J.; Panda, S.; Trivedi, V.; Manna. D. Nitrobenzofurazan derivatives of *N'*-hydroxyamidines as potentinhibitors of indoleamine 2,3-dioxygenase 1. *Eur. J. Med. Chem.* **2016**, *121*, 364-375.